An analysis of the dynamics of protective immune responses in human populations with endemic schistosome infection

Kate Margaret Mitchell

Doctor of Philosophy
University of Edinburgh
2010

Declaration

I declare that this thesis has been composed by myself, that the work presented here is my own unless stated otherwise, and that this work has not been submitted for any other degree or professional qualification.

Kate Mitchell
July 2010

Acknowledgements

The work described here would not have been possible without the help of a great many people.

I would like to thank my supervisors Mark Woolhouse, Francisca Mutapi and Nick Savill for all of their help, support and guidance over the course of my PhD, for their enthusiasm and their encouragement when the going got tough. I would also like to thank my colleagues in both the Epigroup and the Parasite Immunoepidemiology Group for stimulating discussions about my work and practical help and advice. Particular thanks to Richard Howey and Brajendra Singh for help with programming and Eric Fèvre for assistance with analysing mapping data. I am grateful for the extensive use I have been able to make of the ECDF computing cluster at Edinburgh University, which saved me many months of computing time. I am also grateful to the attendees at the IIIR lab meetings who were able to bring a different perspective to some of the questions I have explored here, with particular thanks due to David Gray and Matt Taylor for helpful and enlightening discussions about B cell dynamics and immunosuppression respectively. I would also like to thank our collaborators in Zimbabwe and members of the field team who collected the Murehwa infection data and enabled the collection of the mapping and questionnaire data analysed here. Thanks to everyone who waded through earlier drafts of this thesis and made helpful comments and suggestions.

I would also like to thank my flatmates, friends and family who have supported me over the last few years, providing encouragement and tea whenever it was needed, and particularly my parents, who convinced me to keep going.

Finally I would like to thank the MRC for funding my studentship, and the RAPIDD consortium for providing additional funds to allow me to carry out the analysis of long-term treatment.

Abstract

Urinary schistosomiasis, which is caused by the blood fluke *Schistosoma haematobium*, is a tropical disease infecting over 100 million people in sub-Saharan Africa. Infection typically involves repeated re-infection with long-lived parasites, and field studies have demonstrated that protective immunity takes many years to develop in humans. In communities with endemic schistosomiasis, distinctive patterns of infection and schistosome-specific antibody responses are seen, including a peaked age-infection curve, a highly aggregated distribution of infection intensities among individuals, and an age-related switch in the subclasses of antibody produced. The antibody switch, which occurs naturally in older children, is also seen in younger children following treatment with the antihelminthic drug praziquantel, which kills adult worms.

This study aimed to identify the important mechanisms underlying the slow development of protective immunity, using a mathematical modelling approach. Deterministic population-level and stochastic individual-based models were developed that describe how levels of infection and antibody change with age for individuals living in endemic communities. These models were used to explore different hypotheses for the slow development of protective immunity: (1) that schistosome parasites actively suppress protective immune responses; (2) that dying worms provide the main antigenic stimulus for protective immunity and (3) that a threshold level of antigen must be experienced before a protective immune response is initiated. Models were assessed for their ability to simultaneously reproduce different robust patterns of infection and antibody responses identified in cross-sectional and post-treatment field data from Zimbabwe.

It was found that significant immunosuppression by schistosomes was not consistent with population-level patterns of infection intensity, including the peaked age-infection curve. In order to explain both age-related and post-treatment changes in infection intensity and antibody responses, including the antibody switch, protective antibody responses had to be stimulated by antigens from dying worms. Additionally, it was shown that these protective responses reduced worm fecundity rather than reducing rates of re-infection. An antigen threshold was found to be consistent with observed field patterns, but was not necessary to explain them.

From a large number of possible models that were considered, a single model structure and a subset of parameter combinations were identified that were consistent with field data. This model was used to predict the longer-term impact of mass-treatment programmes upon the development of protective immunity, and the consequent effects on infection levels.

Contents

Chapter 1

Introduction

Schistosomiasis is a tropical disease of major public health importance, with an estimated 200 million people worldwide infected with the causative trematode parasites (Gryseels *et al.* 2006; Mascie-Taylor & Karim 2003). It is largely a disease of rural poverty, persisting in communities without access to safe water supplies or proper sanitation, and is responsible for a considerable burden of pathology. Control efforts are currently focussed upon vaccine development and mass chemotherapy, with the principal aim of reducing pathology rather than eliminating infection (Capron *et al.* 2005; Fenwick *et al.* 2009; WHO 2001). No vaccines have yet been licensed for use in humans, and an increased understanding of natural immunity is highly desirable in order to identify the relevant antigens, targets and immune pathways involved in protective immune responses, which can be exploited by a successful vaccine. In common with other parasitic infections, protective immunity against schistosomes takes a long time to develop (Yazdanbakhsh & Sacks 2010), in contrast with the strong and long-lasting protective immunity which rapidly develops following an initial encounter with many viral and bacterial pathogens. The reasons for this slow development of protective immunity are still not fully understood. Chemotherapy has been shown to alter the nature of the schistosome-specific immune responses, with the data suggesting that it may have an immunizing effect (Mutapi *et al.* 1998), although the long-term impact of chemotherapy upon protective immunity has not yet been assessed. Studies of the dynamics of schistosome infection and schistosome-specific immune responses in humans have mainly relied upon large cross-sectional and treatment-reinfection surveys in populations with endemic infection, and mathematical models have played an important role in interpreting these immunoepidemiological studies (Hellriegel 2001).

In this thesis, mathematical models are used to explore a number of hypotheses which have been put forward to explain the slow development of protective immunity, and the models are tested for their ability to reproduce a variety of robust patterns seen in both infection and antibody data in population-based surveys. Models are also used to predict the long-term impact of mass chemotherapy programmes upon the development of protective immunity. This thesis focuses upon infection with *Schistosoma haematobium*, which causes urinary schistosomiasis. In this introductory chapter, the basic biology and epidemiology of *S. haematobium* infection is reviewed, with an overview of past and current control methods. The current state of knowledge about protective immunity in humans is discussed, and different hypotheses for the slow development of protective immunity are put forward. Previous approaches to modelling schistosome transmission, immunity and control are reviewed, and

the aims of this thesis are outlined. While the focus throughout is upon *S. haematobium*, findings for other schistosome species are mentioned where relevant.

1.1 *S. haematobium* biology, life-cycle and disease

Humans are natural hosts for the schistosome species *Schistosoma mansoni*, *S. haematobium*, *S. japonicum*, *S. intercalatum* and *S. mekongi*. The schistosome life cycle includes an intermediate freshwater snail host, and the distribution of each schistosome species is related to the distribution of its respective snail host species (Gryseels & Nkulikyinka 1988).

S. haematobium, which causes urinary schistosomiasis, has as its intermediate host the *Bulinus* snail species, and occurs in Africa and the Arabian Peninsula (Gryseels *et al.* 2006). Over 100 million people are infected in sub-Saharan Africa (van der Werf *et al.* 2003). Infection occurs through contact with water containing the infective stages (figure 1.1). The life cycle for *S. haematobium* is shown in figure 1.2. The water-borne infective stages (cercariae) penetrate the human skin and transform into schistosomulae, which enter the bloodstream and are carried via the lungs to the liver, where they mature into adult worms. Worms of opposite sexes pair up and migrate to the vesical veins surrounding the bladder. Eggs produced by mated female worms penetrate the blood vessel wall, and exit the body in urine. Upon contact with fresh water, eggs hatch to release miracidia, which infect the snail host. Following asexual reproduction within the snail, infective cercariae are released into the water (Jordan *et al.* 1993).

The different stages of the life cycle have different life expectancies: eggs can remain viable for up to 7 days, miracidia for 4–16 hours, and cercariae for up to 72 hours (Anderson & May 1991*a*; Gryseels *et al.* 2006). The within-snail stages and the schistosomulae stage each last for around 4-6 weeks (Gryseels *et al.* 2006). In contrast, adult worms can live for years within their human hosts, with their mean life span estimated at 3–10 years (Fulford *et al.* 1995; Wilkins *et al.* 1984).

More than 50% of eggs become trapped in the tissues of the bladder and surrounding region, and pathology results from the immune reaction to these trapped eggs (King 2001*b*). Morbidity ranges from anaemia and haematuria to long-term kidney and bladder damage, with an estimated 6–13.5 million disability-adjusted life years (DALYs) lost globally to infections with all schistosome species (Bergquist *et al.* 2005; King *et al.* 2005). *S. haematobium* is estimated to cause 150 000 deaths every year due to kidney failure (WHO 2006) with an overall mortality rate of 2 per 1000 infected persons per year (Fenwick *et al.* 2003). Disease severity has been shown to be related to the duration and intensity of infection in some studies (Koukounari *et al.* 2007; Mahmoud 2001; Ndamba *et al.* 1991). However, other studies suggest that morbidity is related to infection status rather than intensity (King 2007), with the severity of disease being related to the location of the eggs, host and parasite genetics, and the type of immune response that is mounted (Brouwer *et al.* 2003; de Vlas 1996; King 2001*b*; Quinnell 2003; Remoué *et al.* 2001). The less severe morbidities are reversible by chemotherapy (Magnussen 2003).

Figure 1.1: Water contact in rural Zimbabwe. (a) washing (b) laundry

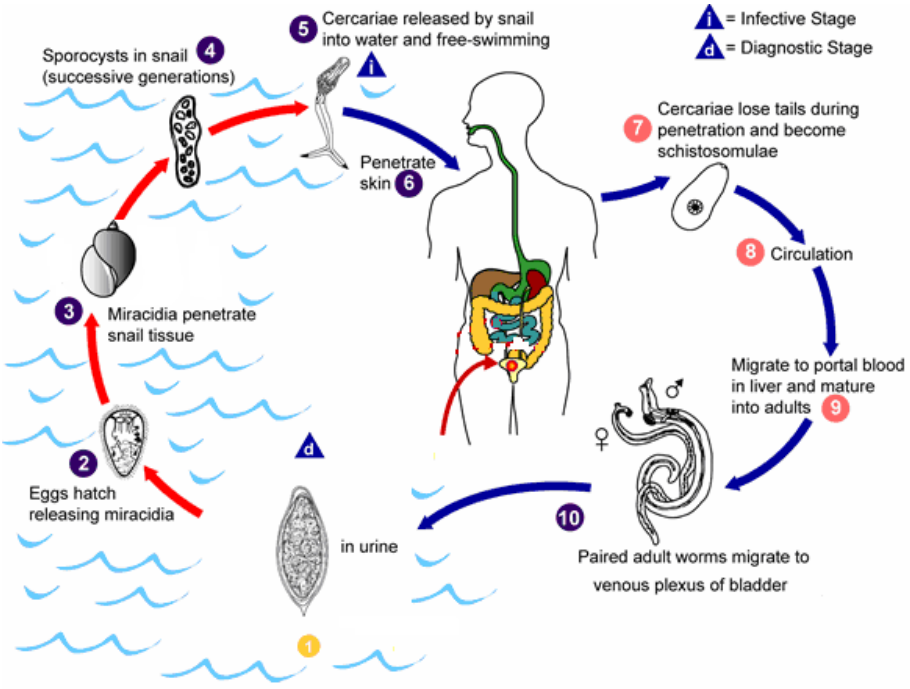

Figure 1.2: Life cycle for *S. haematobium*, adapted from the CDC website http://www.dpd.cdc.gov/dpdx/HTML/Schistosomiasis.htm

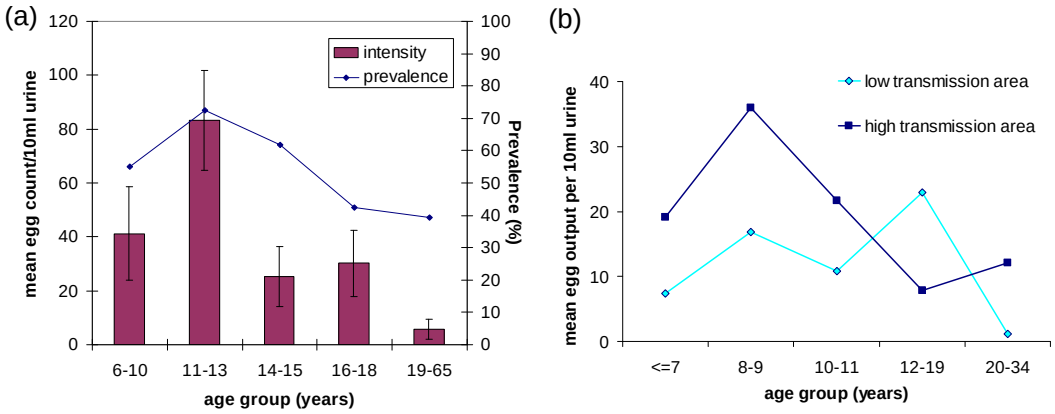

Figure 1.3: Intensity peak and peak shift. (a) Mean intensity and prevalence of infection with age in a population in Northern Zimbabwe (based on data from Mutapi *et al.* (2007)). (b) Intensity of infection (mean number of eggs/10 ml urine) in two areas of Eastern Zimbabwe with high and low transmission as marked (based on data from Mutapi *et al.* (1997)).

1.2 Epidemiology and patterns of infection

Schistosomiasis shows strong spatial clustering, related to patterns of snail distribution and human water contact (Clennon *et al.* 2004; Gryseels *et al.* 2006; Woolhouse *et al.* 1998). A characteristic age-intensity pattern is seen in endemically infected populations, with infection intensity rising rapidly through the childhood years to peak at around 8–15 years of age, then falling again, with a slight rise sometimes observed in much older age groups (figure 1.3a) (Fisher 1934; King 2001*a*). Prevalence also tends to peak in children and decline in older individuals, but usually more gradually than infection intensity (figure 1.3a). The peak in infection intensity is higher and occurs at a younger age in populations with higher overall infection prevalence, a phenomenon termed the peak shift (figure 1.3b) (Woolhouse 1998).

Schistosomes, like many other helminths, are highly aggregated in human populations, with a few individuals harbouring the majority of parasites (figure 1.4), so that the population variance in infection intensity greatly exceeds the mean (Woolhouse *et al.* 1994). The extent of aggregation has been reported to change with age, either decreasing or displaying an inverse-convex pattern (Chan *et al.* 2000; Fulford *et al.* 1992; Woolhouse *et al.* 1994). This aggregated distribution has important consequences for schistosome transmission and for intervention programmes (Galvani 2003; Woolhouse *et al.* 1998).

Following chemotherapy, infection levels are greatly reduced, with mean infection intensity being reduced by a greater proportion than prevalence (egg reduction rates are consistently higher than cure rates, section 1.4.1). Infection levels subsequently increase again, with substantially higher rates of re-infection being consistently observed in younger children when compared with older children or adults, which cannot entirely be explained by differences in exposure levels (Etard *et al.* 1995; Hagan *et al.* 1991; Kabatereine *et al.* 1999; Wilkins *et al.* 1987). Several studies have also reported pre-disposition, with post-treatment levels of re-infection being positively correlated with pre-treatment infection intensity for both *S. mansoni* and *S. haematobium* (Bensted-Smith *et al.* 1987; Etard *et al.* 1995; Tingley *et al.* 1988). This pre-disposition is stronger in younger individuals than in older people (Bensted-Smith *et al.* 1987; Tingley *et al.* 1988).

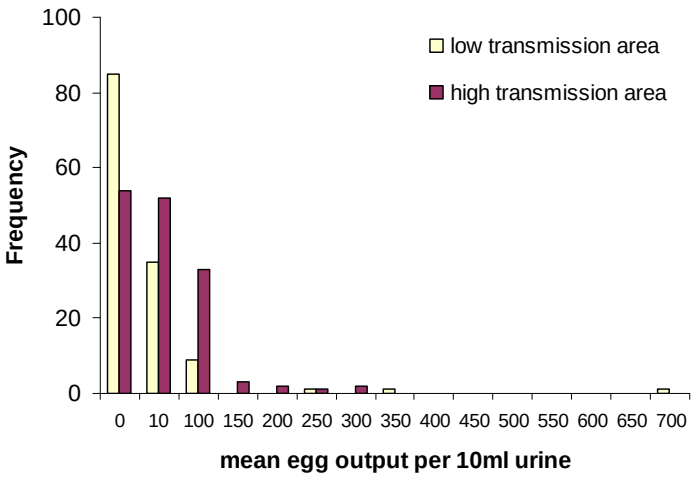

Figure 1.4: Parasite aggregation. Distribution of egg counts in 10ml urine from individuals for the two areas in Eastern Zimbabwe shown in Figure 1.3b. (Based on data from Mutapi *et al.* (1997)).

1.3 Measuring infection levels

Both prevalence and infection intensity of schistosomiasis in populations are routinely measured using parasitological methods, which are regarded as the gold-standard of detection for urinary schistosomiasis. Two or three urine samples are collected on consecutive days from each individual, and examined microscopically following filtration (Mott 1983). Egg counts are recorded as the mean number of eggs in a fixed volume of urine (usually 10ml). Whilst this method is nearly 100% specific, the sensitivity varies, depending upon observer skill, urine sample size and infection intensity. It cannot detect single-sex infections, since eggs are only produced by mated females. Egg counts vary throughout the day, peaking at around midday (Doehring *et al.* 1983). There are also fluctuations in day-to-day urine egg counts, with zero counts increasingly likely in lightly infected individuals (Doehring *et al.* 1983; Savioli *et al.* 1990; van Etten *et al.* 1997; Warren *et al.* 1978). False negatives may lead to significant under-estimation of prevalence and over-estimation of reinfection rates (de Vlas 1996). Studies on *S. mansoni* egg counts from stool samples also reveal considerable variation in intra-individual egg counts, following a negative binomial distribution (de Vlas *et al.* 1992). For *S. mansoni*, the variation in intra-individual egg counts was found to be constant for different populations provided the sampling interval was the same, and did not change significantly with infection intensity (de Vlas 1996). Negative and positive predictive values of tests are affected by infection prevalence as well as by test accuracy. Population-level infection intensity may be reported as the arithmetic or geometric mean of individual mean egg counts, or as the arithmetic mean of ln(egg count + 1) (related to the geometric mean). Some studies report means for positive individuals only, others for the whole population. Use of different types of mean (arithmetic or geometric) can affect the apparent age-intensity pattern (Fulford 1994; Mutapi *et al.* 2003*a*).

A more direct measure of worm burden sometimes used in epidemiological studies is the detection of circulating (gut-associated) anodic and cathodic antigens (CAA and CCA), which can be detected in the blood or urine, and correlate well with worm burden (Agnew *et al.* 1995).

Serum CAA levels correlate well with egg output for both *S. haematobium* and *S. mansoni* (Ndhlovu *et al.* 1996*a*; Polman *et al.* 1998), and can identify low level infections in some egg-negative individuals (Ndhlovu *et al.* 1996*a*). Serum CAA levels show lower fluctuation than egg output (Polman *et al.* 1998).

The relationship between egg counts and worm burdens is difficult to quantify. Estimates for the number of eggs produced per mated *S. haematobium* female vary considerably. One study of 7 human patients undergoing bladder surgery suggested that an average 200 eggs per mated female were passed in urine per day (range 3–560) (Cheever *et al.* 1975). Another study looking at the number of adult *S. haematobium* worms and eggs in cadavers in Egypt found an average of 1.28 viable eggs per 10ml urine per female worm in the genito-urinary tract (Cheever *et al.* 1977). Data from this autopsy study suggests that there is lower egg production per worm in higher density *S. haematobium* infections (Cheever *et al.* 1977; Woolhouse 1994*a*), and there is evidence for reduced worm fecundity in older human hosts, from comparing levels of CCA or CAA with egg output (Agnew *et al.* 1996; Ndhlovu *et al.* 1996*a*). For *S. mansoni*, egg production and worm burden are linearly related regardless of host age or worm density (Agnew *et al.* 1996; Wertheimer *et al.* 1987).

1.4 Control

Amidst increasing recognition of the severe burden of disease which schistosomiasis causes, control efforts are being stepped up, with an emphasis upon widespread drug treatment and vaccine development (Capron *et al.* 2005; Fenwick *et al.* 2009; WHO 2001). There has been a switch in focus from transmission control targeted at the snail intermediate host, which was expensive and raised environmental concerns, to morbidity control through large-scale chemotherapy programmes, as effective drugs, particularly praziquantel, have become affordable (Brooker *et al.* 2004*b*; Gryseels *et al.* 2006). Concerns have been raised about the sustainability of this approach, which will require ongoing drug treatments to have long-term benefits (Utzinger *et al.* 2003*a*). It is important that control programmes are well-monitored for ongoing prevalence and intensity of infection and morbidity markers, and to detect any development of drug resistance (King *et al.* 2000).

1.4.1 Chemotherapy

Currently, treatment for schistosomiasis mainly relies upon praziquantel. This has been in use for around 30 years, and has proved to be safe and effective against all the human schistosomes (McMahon & Kolstrup 1979; WHO 2005). The precise mechanism of action for praziquantel is unknown, but it alters worm calcium transport, causing paralysis following muscular contraction, and also causes severe damage to the tegument, working in synergy with the host immune system (Harnett 1988; Nyazema *et al.* 1995; Utzinger *et al.* 2003*b*). Praziquantel has little effect on eggs and immature worms, and cure rates for *S. mansoni* may be improved by administering a second dose a few weeks later to kill worms which were immature at the time of the initial treatment (Picquet *et al.* 1998). Oxamniquine may be used as a second-line drug in areas where praziquantel has a low cure rate, but is effective only against *S. mansoni* (Stelma *et al.* 1997). Metrifonate, which is effective against *S. haematobium*, was used extensively until the 1990s, but has since been withdrawn from the WHO Model List of

Essential Medicines (Danso-Appiah *et al.* 2008). Metrifonate treatment has to be given in three doses over a six week period, making it less amenable for use in mass drug administration (MDA) programmes than praziquantel, for which a single dose is effective (Danso-Appiah *et al.* 2008). Another potential anti-schistosome drug is artemisinin, which acts against schistosomulae, and works well in combination with praziquantel (Utzinger *et al.* 2003*b*); however, it cannot be used in malarial regions, since it is also an anti-malarial and may induce resistance in malaria parasites (WHO 2005).

As well as being made available to infected individuals through primary health care systems, praziquantel has been increasingly used in MDA programmes (Brooker *et al.* 2004*a*; Gryseels *et al.* 2006). In these preventive chemotherapy programmes, praziquantel is given at a dose of 40mg/kg bodyweight, and is currently mainly targeted at school-age children (Fenwick *et al.* 2009; WHO 2006). The recommended frequency of treatment depends upon the prevalence of schistosome infection found in children in sentinel primary schools. Yearly treatment of all school-age children is recommended for areas with high prevalence (more than 50% prevalence in sentinel primary schools as assessed by parasitological methods). Biannual treatment of all school-age children is recommended for areas with moderate prevalence (10–50% prevalence in sentinel primary schools) and treatment of all school-age children twice during their time at primary school for areas with low prevalence (<10% prevalence in sentinel primary schools) (WHO 2006). In areas of moderate and high prevalence, adults from high-risk groups (pregnant and lactating women, occupationally exposed groups including fishermen and farmers, or entire communities living in endemic areas) should also be treated (WHO 2006). Strategic timing of treatment to coincide with low or absent transmission, either following molluscicide to remove snails, or in seasons when snail populations are reduced or absent, can increase the impact upon prevalence.

Cure rates for *S. mansoni* with a single dose of praziquantel are usually over 70%, although rather lower rates have been reported in a recently established focus of infection in Senegal (Picquet *et al.* 1998; Stelma *et al.* 1997; Tchuem Tchuente *et al.* 2001). Variable cure rates have been reported for *S. haematobium* following praziquantel treatment, between 50 and 90% (De Clercq *et al.* 2002; Midzi *et al.* 2008; Saathoff *et al.* 2004; Sissoko *et al.* 2009; Tchuem Tchuente *et al.* 2004), but reductions in egg output are consistently high, ranging between 83–99.9% (Danso-Appiah *et al.* 2008; De Clercq *et al.* 2002; King *et al.* 2000; Midzi *et al.* 2008; Saathoff *et al.* 2004; Sissoko *et al.* 2009; Tchuem Tchuente *et al.* 2004). There is some evidence that eggs continue to be released from the tissues for a few weeks following the death of adult worms, which may lead to an underestimate of the cure rate, depending upon when post-treatment infection levels are assessed (De Clercq *et al.* 2002; Picquet *et al.* 1998; Tchuem Tchuente *et al.* 2004).

Praziquantel tolerance can be selected for in animal schistosome infections (Fallon & Doenhoff 1994), but, despite variation in cure rates in humans, there is no firm evidence to date that resistance is developing (King *et al.* 2000).

1.4.2 Vaccination

Despite extensive research into vaccine candidates for schistosomiasis, none have yet been approved for use in humans (McManus & Loukas 2008). Although irradiated cercariae can give up to 70% protection against re-infection in murine studies (Anderson *et al.* 1999; Hsu *et al.*

1981), no vaccine candidate antigen has yet consistently given more than 50% protection against infection in mice (Bergquist *et al.* 2005). The main aim of vaccination is shifting from reducing infection towards reducing fecundity or pathology, as the focus of schistosomiasis control in general is moving towards controlling morbidity. Sh28GST has entered Phase III clinical trials as an anti-fecundity vaccine, and Sm14 has entered Phase I clinical trials (WHO 2005; Wilson & Coulson 2006). Six other vaccine candidates have been identified in animal models (Bergquist *et al.* 2005), and genome mapping and other genetic analysis has enabled new structural proteins and antigens to be identified (Wilson *et al.* 2007). Mathematical modelling has suggested that a vaccine will need to induce long-lived protection as well as a high degree of protection to have a significant long-term impact upon infection levels (Chan *et al.* 1997).

1.4.3 Other control measures

In the past, snail control was a major focus of control efforts, with molluscicides widely used. A three year molluscicide campaign in St. Lucia gave significant reductions in prevalence and infection intensity (Goddard & Jordan 1980). However, this is now less popular, due to the toxic effects on fish (Gryseels *et al.* 2006). Biological control and habitat alteration (such as weed removal at water contact sites) are alternative ways of controlling snail numbers. Changing peoples' water contact habits should enable the elimination of schistosomiasis, but in practice this is very hard to do, particularly for children who are responsible for the bulk of transmission. Provision of safe water supplies, latrines and good health education is essential (Gryseels *et al.* 2006; Utzinger *et al.* 2003*a*).

1.5 Immune responses

Immune responses to schistosomes have been extensively studied both in animal models and in human populations. There has been considerable debate about the extent to which humans develop protective immunity against schistosome infection (section 1.5.1), and the mechanisms which might underlie such protection are still not fully understood. Animal models have severe limitations in seeking to understand the role and development of protective immunity in human schistosome infection. Mice, the most frequently used model, cannot be used to identify relevant immune correlates of protection, owing to fundamental physiological and immunological differences between mice and humans (Capron *et al.* 1999; Wilson 1990). The pathways of IgE antibody production (known to be important in human infection) are quite different between the two species, and IgG isotypes are not homologous between them (Mestas & Hughes 2004). Anatomical changes in the liver following primary infection can greatly alter the course of further infection in mice (Wilson 1990). Rats, while good models for the IgE response, are non-permissive hosts, meaning that worms are not able to reach sexual maturity, or lay eggs, so that the influence of these stages on host immunity cannot be assessed (Capron & Capron 1986). Infections of baboons with schistosomes appear to mirror human infection much more closely, although *S. haematobium* infections differ in terms of the anatomical location of adult worms (Nyindo & Farah 1999). Because of these limitations, the following summary focuses upon human population studies, citing animal and in vitro studies only where the mechanisms in question cannot be measured in humans.

1.5.1 Evidence for development of protective immunity in humans

Reduced levels of infection in adults, and the even more striking reduced re-infection rates in adults after treatment (compared with children) suggest that adults may develop acquired protective immune responses against schistosomes. In endemic areas, where prevalence has been constant over a long period of time, the effects of age and previous exposure to infection (which will affect the development of protective immunity) are difficult to dissociate. Age-related changes in water contact, although these do often decline in adults, are not sufficient to explain the disparity in re-infection rates (Hagan *et al.* 1991; Kabatereine *et al.* 1999; Wilkins *et al.* 1987), but other age-related factors (such as hormonal changes or changes in skin composition) could be responsible for these observations (Gryseels 1994). In areas with recently-established foci of infection, or endemic areas with a recent immigrant population, the exposure time is known and independent of host age, so the effects of exposure history and age can be distinguished (Naus *et al.* 1999; Ouma *et al.* 1998; Talla *et al.* 1992; Webster *et al.* 1998). Alternatively, the effects of age and infection history can be distinguished by comparing areas with different levels of endemic infection (Mutapi *et al.* 1997).

Some studies support the idea that age itself is important: immigrants who moved into an endemic area in Burundi showed the same peaked age-intensity profile and age-dependent reinfection rates as long term residents within a few years of their arrival, and similar patterns were seen in Senegal, in a recently established focus of infection (Gryseels 1994). The difference in levels of infection seen between adults and adolescents in the epidemic focus in Senegal, who had all been exposed to infection for the same length of time, could not be explained by differences in water contact (Scott *et al.* 2003). On the other hand, peak shifts between endemic areas with different levels of infection strongly suggest that acquired immunity is acting as a function of cumulative exposure rather than of age (Mutapi *et al.* 1997; Woolhouse 1992*b*, 1998). Several immune correlates of protection have been identified from re-infection studies (see section 1.5.4), and there is evidence of earlier changes in the balance of antibodies in more intensely infected populations (Mutapi *et al.* 1997), supporting the idea of immune involvement. This protective immunity appears to develop slowly, as in communities with endemic infection susceptibility only decreases in older children or adults, despite evidence that individuals are repeatedly exposed and infected from a young age (Woolhouse *et al.* 2000).

1.5.2 The immune interaction with different life cycle stages

The human host encounters four distinct stages of the schistosome life cycle: cercaria, schistosomulum, adult worm and egg, and each stage interacts differently with the immune system (Dunne & Cooke 2005; Jenkins *et al.* 2005). These stages differ in their life span (section 1.1) and gene expression (Jolly *et al.* 2007). Detecting these distinct interactions is complicated by the frequent presence within the host of more than one parasite life stage, and by antigens shared between different schistosome stages (Curwen *et al.* 2004). These antigens may be somatic, surface or excretory.

In common with other helminth infections, immune responses to schistosomes are dominated by Th2 responses (Maizels *et al.* 1993). These are associated with the Th2 subset of differentiated T helper cells, which tend to be stimulated by extracellular antigens, and are characterised by the cytokines they secrete (cytokines are proteins secreted by immune cells which affect the behaviour of other cells). Th2 cells secrete the cytokines interleukin (IL)-4,

IL-5, IL-10 and IL-13, and stimulate B cells to produce antibody (Janeway *et al.* 2001; Maizels *et al.* 1993). Eggs are potent inducers of Th2 responses (Pearce 2005), while adult worms are thought to reduce their stimulation of the immune response through reduced surface antigen expression and adsorption of host molecules (Skelly & Wilson 2006; Smithers *et al.* 1969). Cercariae can stimulate local inflammatory responses in the skin (Jenkins *et al.* 2005).

1.5.3 What is the target of protective immunity against schistosomes?

Possible outcomes of protective immune responses are killing of cercariae or immature schistosomulae, killing of mature adult worms, or reduced adult worm fecundity. Human re-infection studies cannot distinguish which stage of the schistosome life cycle is being targeted by protective immune responses, since they only look at egg output, which would be reduced by all three outcomes. There is evidence of all of these being targets of the protective immune response, from animal, human or in vitro studies, although this varies by schistosome species. Results for *S. mansoni* and *S. haematobium* are discussed below.

Killing of cercariae or schistosomulae

Antibody-dependent cell-mediated cytotoxicity (ADCC) has been identified as a major human immune effector mechanism against both *S. mansoni* and *S. haematobium* schistosomulae in vitro, with eosinophils the main cell type involved (Butterworth *et al.* 1975, 1974; Hagan *et al.* 1985). Several in vitro and murine studies have shown that *S. mansoni* schistosomulae become less susceptible to immune-mediated killing (including oxidative killing and ADCC) as they mature (Ahmed *et al.* 1997; Mkoji *et al.* 1988; Moser *et al.* 1980).

Killing of adult worms

Studies of *S. mansoni* have demonstrated that adult schistosomes develop a tough outer membrane which can be rapidly repaired, reduce their surface expression of antigens and adsorb host molecules onto their surface, as well as producing immune evasion molecules which protect against oxidative killing by phagocytes (Carvalho-Queiroz *et al.* 2004; Dunne & Cooke 2005; Sher & Moser 1981; Skelly & Wilson 2006; Smithers *et al.* 1969). Significant killing of adult worms has been shown in infections of cattle with their natural pathogens *S. bovis* and *S. matthei* (both closely related to *S. haematobium*), and in *S. bovis* infection in mice (Agnew *et al.* 1993; Bushara *et al.* 1983, 1980; Saad *et al.* 1980). However, no immune-mediated killing of *S. mansoni* or *S. haematobium* was seen in murine infections (Agnew *et al.* 1993).

Reduced worm fecundity

Suppression of egg production has been shown in cattle infections with *S. bovis* and *S. matthei*, and in *S. haematobium* infections in mice (Agnew *et al.* 1993; Bushara *et al.* 1983, 1980; Saad *et al.* 1980). Transfer of *S. haematobium* worms from infected to naïve baboons gave rise to an increase in worm fecundity, which suggested that anti-fecundity immune responses were acting (Webbe *et al.* 1976). In contrast, murine infections with *S. mansoni* showed no evidence of immune-mediated reduction in fecundity, and transfer of *S. mansoni* worms from infected to naïve baboons did not affect their egg output (Damian *et al.* 1986).

In vitro studies have demonstrated that IgA antibodies against the *S. mansoni* antigen Sm28GST from infected human subjects reduce both worm fecundity and egg hatching capability (Grzych *et al.* 1993). In human population studies, some evidence has been found for reduced worm fecundity in infections with *S. haematobium* but not *S. mansoni*. Comparisons of egg output with levels of circulating cathodic antigen (CAA) (a more direct measure of worm burden) show that worm fecundity is reduced in older hosts for *S. haematobium* but not *S. mansoni* infections (Agnew *et al.* 1996). Additionally, autopsy studies looking at *S. haematobium* indicated reduced fecundity in more heavily infected patients, although this could be due to other (non-immune) density dependent mechanisms (Cheever *et al.* 1977; Woolhouse 1994*a*).

1.5.4 Immune responses associated with protection or susceptibility

IgG1, IgG3 and IgE antibodies are able to mediate a killing effect of *S. mansoni* schistosomulae by eosinophils in vitro (Gounni *et al.* 1994; Khalife *et al.* 1989). Blocking of the IgG1 and IgG3-mediated ADCC responses by IgG4, IgG2 and IgM has been reported (Khalife *et al.* 1986, 1989).

High pre-treatment eosinophilia is associated with protection against reinfection with *S. mansoni* (Ganley-Leal *et al.* 2006; Sturrock *et al.* 1983) and *S. haematobium* (Hagan *et al.* 1985). High post-treatment IgE (specific for larval or adult worm antigens) has been associated with protection against reinfection in a number of human studies for both *S. mansoni* and *S. haematobium*, independently of host age (Butterworth *et al.* 1996; Demeure *et al.* 1993; Dunne *et al.* 1992*a*; Hagan *et al.* 1991; Rihet *et al.* 1991). Dunne *et al.* (1992*b*) found that individuals with higher levels of post-treatment IgE against a 22kDa antigen in the worm tegument were highly protected against reinfection. IgE responses to egg antigens give a more mixed picture, being apparently protective for *S. haematobium* (Hagan 1992) but associated with reinfection for *S. mansoni* (Dunne *et al.* 1992*b*). B cells bearing the low-affinity IgE receptor (CD23) have been associated with protection against re-infection with *S. mansoni* (Mwinzi *et al.* 2009). Worm-specific IgG1 has also been associated with protection against *S. mansoni* re-infection (Satti *et al.* 1996). IgA against the Sm28GST molecule was found to be protective against reinfection with *S. mansoni* in a Kenyan population (Grzych *et al.* 1993).

Several antibody isotypes have been found to be positively associated with reinfection levels following chemotherapy, including IgM and IgG2 directed against *S. mansoni* egg antigens (Butterworth *et al.* 1988), IgG2 and IgG4 directed against larval *S. mansoni* antigens (Demeure *et al.* 1993) and IgG4 directed against *S. mansoni* and *S. haematobium* worm and egg antigens (Hagan *et al.* 1991; Rihet *et al.* 1992). While these isotypes demonstrate blocking activity in vitro, competing for the same binding sites on eosinophils as the protective isotypes, the immunoepidemiological evidence for blocking activity in vivo is less convincing (Woolhouse 1994*b*). The observed patterns of correlation of blocking isotypes with reinfection, blocking responses peaking earlier than protective responses, and increasing ratios of protective:blocking antibodies with host age can all be explained if these 'blocking' isotypes are in fact neutral but have a shorter immunological memory than protective antibody responses (Woolhouse 1994*b*).

Th2 cytokines have also been associated with protection. Pre-treatment IL-5 was inversely correlated with subsequent reinfection level in one reinfection study with *S. mansoni* (Roberts *et al.* 1993). In another study, levels of IL-4 and IL-5 were both negatively correlated with

reinfection following treatment for *S. haematobium* (Medhat *et al.* 1998), and pre-treatment *S. mansoni*-specific IL-5 has been shown to be strongly related to post-treatment IgE levels (Walter *et al.* 2006). Low IL-10 and high IFN-γ (associated with Th1 responses, which are antagonistic to Th2) have also been associated with becoming reinfected (Mduluza *et al.* 2003; Medhat *et al.* 1998).

1.5.5 Population-level patterns of schistosome-specific antibody and cytokine responses

Studies in human populations have demonstrated that schistosomes induce a wide range of antibody and cellular responses, with considerable heterogeneity seen between individuals in terms of the magnitude of particular responses (Mutapi & Roddam 2002), although the extent of this heterogeneity has not been previously quantified. It should be remembered that specific humoral or cellular responses to schistosome antigens may represent protective responses (reducing reinfection, reducing worm fecundity or killing adult worms directly); they may simply be markers of infection (having no impact upon the pathogen) or they may control or reduce the impact of other protective responses (for example, suppressive cytokines or blocking antibodies). Depending upon the longevity of the immune memory of individual responses, they may correlate with current infection levels or with cumulative exposure to infection. Long-lasting responses will also tend to increase with host age.

As well as variation in individual responses, variability is seen in the types of schistosome-specific responses made at a population level. One cross-sectional population study of *S. haematobium* adult worm-specific cytokine responses suggested that suppressive immune responses (with high IL-10) were gradually surpassed by Th2 responses (with increased IL-4 and IL-5) with increasing age, as shown in figure 1.5a (Mutapi *et al.* 2007). Another study reported no age-related changes in levels of *S. haematobium* egg antigen specific IL-4, IL-5, IL-10 or IFN-γ (Scott *et al.* 2001). Several studies have shown levels of worm or egg-specific IgE increasing with age in endemic communities (Butterworth *et al.* 1996; Dunne *et al.* 1992*a*; Hagan *et al.* 1991; Mutapi *et al.* 1997; Ndhlovu *et al.* 1996*b*). Different studies have shown schistosome-specific IgG1 and IgG4 responses either increasing or decreasing with age (Butterworth *et al.* 1996; Mutapi *et al.* 1997; Ndhlovu *et al.* 1996*b*). Worm-specific IgM has often been reported to decline with age (Mutapi *et al.* 1997; Ndhlovu *et al.* 1996*b*), but egg-specific IgM has been reported to increase or decrease with age in different studies (Mutapi *et al.* 1997; Ndhlovu *et al.* 1996*b*). One striking pattern reported for *S. haematobium* was a very rapid switch with age from an IgA to an IgG1 response (figure 1.5b), which was characterised by a strong negative correlation between the two responses at the population level (Mutapi 1997; Mutapi *et al.* 1998). This antibody 'switch' occurred earlier in a more heavily infected population (Mutapi *et al.* 1997). Negative correlations between different isotypes in a separate study suggest that a similar switch occurs (Ndhlovu *et al.* 1996*b*), but this type of pattern has rarely been looked for or reported in other studies of schistosome-specific antibodies.

1.5.6 Effects of treatment on immunity

In vitro and murine studies have demonstrated that praziquantel treatment exposes previously hidden antigens following drug-induced worm death (Harnett & Kusel 1986; Redman *et al.* 1996). Human studies have shown that praziquantel and artemisinin treatments can both

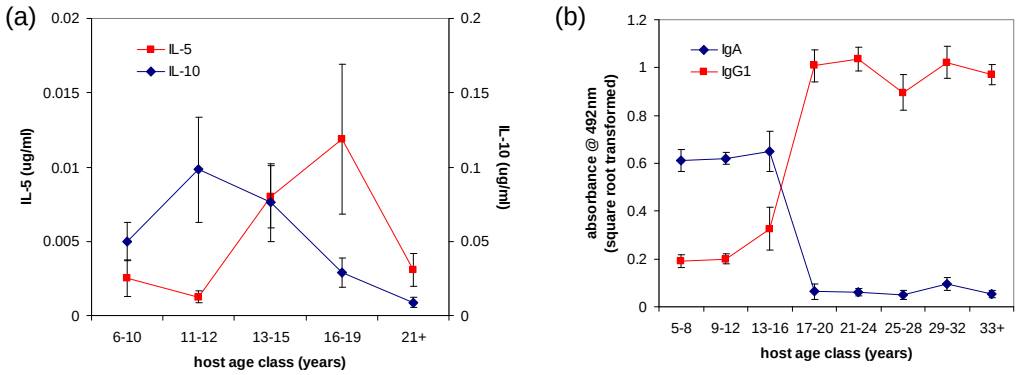

Figure 1.5: Age-profiles of *S. haematobium*-specific immune responses. (a) IL-10 and IL-5 cytokines against whole worm antigen (b) IgA and IgG1 antibodies against egg antigen. Note that these data come from 2 different studies in Zimbabwe, (a) from Mutoko-Rusike, adapted from Mutapi *et al.* (2007), (b) from the Burma Valley, taken from Mutapi *et al.* (1998).

alter host immune responses (Bergquist *et al.* 2004; Mutapi *et al.* 2005, 1998). An array of changes in antibody responses to adult and/or egg antigens have been reported following chemotherapy, varying with time after treatment, age, and study location (Corrêa-Oliveira *et al.* 2000; Fitzsimmons *et al.* 2004; Mutapi 2001). While studies often show marked alteration in antibody isotypes following treatment, the actual isotypes involved vary widely between studies. Several studies, though not all, report increased levels of anti-egg and/or anti-worm IgE following treatment, for *S. haematobium* and *S. mansoni* (Butterworth *et al.* 1996; Fitzsimmons *et al.* 2004; Gomes *et al.* 2002; Grogan *et al.* 1996; Mutapi *et al.* 1998). Levels of IgG subtypes and IgA may increase or decrease following treatment (Mutapi 2001; Mutapi *et al.* 2003*b*). Responses to egg and adult antigens do not always correlate with each other, and antibody levels change with time after treatment (Mutapi *et al.* 2003*b*). One study showed a sustained switch following chemotherapy in children from a predominant IgA-response to *S. haematobium* eggs and adult worms to a predominant IgG1 response, which also occurred more slowly with age in the same population (figures 1.5b and 1.6) (Mutapi 2001; Mutapi *et al.* 1998). A separate study showed that the increase in IgE and IgG3 levels seen at 18 weeks post-treatment was proportional to pre-treatment egg counts (Mutapi *et al.* 2003*b*). The magnitude of the increase in antibody level may reflect previous immunity as well as pre-treatment worm burden, as significantly increased responses to the Sm22.6 antigen are seen in adults with low *S. mansoni* egg counts as well as in heavily infected adolescents, suggesting that in adults a memory response to previous infection is boosted by treatment (Fitzsimmons *et al.* 2007). Another study found that protective IgE responses against *S. mansoni* post-treatment were associated with high IL-5 levels pre-treatment, suggesting that a pre-existing Th2 environment was required for protective antibody responses to be developed (Walter *et al.* 2006).

Treatment has also been reported to boost levels of schistosome-specific Th2 cytokine responses. Levels of *S. haematobium* egg and worm-specific IL-4 were increased 5 weeks after praziquantel treatment (Grogan *et al.* 1996). Levels of *S. mansoni* adult worm-specific Th2 cytokines IL-4, IL-5, IL-13 and IL-10 were significantly raised seven weeks after treatment in one study (Joseph *et al.* 2004*b*). In another study, *S. mansoni* increases in adult worm-specific IL-5, IL-4, IL-13 and IL-10 and TGF-β were seen 21 days after treatment (Fitzsimmons *et al.* 2004). In the same study, eosinophil numbers and worm-specific IL-5, IL-13 and IL-10 were

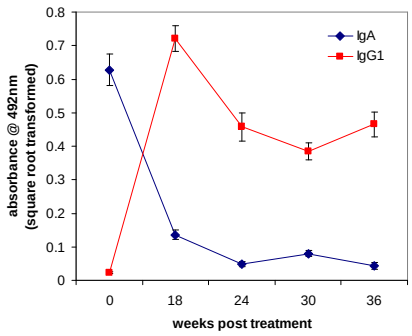

Figure 1.6: Levels of *S. haematobium* egg antigen-specific IgA and IgG1 in a cohort of 6–15 year olds before treatment, and 18, 24, 30 and 36 weeks post treatment with praziquantel. Data taken from Mutapi *et al.* (1998).

transiently decreased one day after treatment, associated with a rapid rise in plasma IL-5 a day after treatment. As well as striking changes in the antibody isotypes produced after treatment, changes are seen in the antigens recognised by sera from infected individuals following treatment (Mutapi *et al.* 2005). Drug-induced anti-schistosome responses do differ from naturally-acquired responses, due to the different patterns of antigen exposure involved (Corrêa-Oliveira *et al.* 2000; Mutapi *et al.* 2005). Cluster analysis of population antibody responses suggests that in natural infection, a modified Th2 response (dominated by IgG1, IgM and IgG4) is developed, while following treatment, individuals gain a balanced Th1/Th2/Treg profile, with high levels of IgG1, IgM and IgE (Maizels & Yazdanbakhsh 2003; Mutapi *et al.* 2005).

1.6 Measuring immune markers

Antibody and cytokine levels are both measured by enzyme linked immuno-sorbent assay (ELISA). Levels of non-specific cytokines are measured directly in blood samples (Milner *et al.* 2010), and antigen-specific cytokine responses are assessed by measuring cytokine levels in the supernatants from whole blood re-stimulations with schistosome antigens (Joseph *et al.* 2004*a*; Mutapi *et al.* 2007). Cytokine concentrations in the blood or supernatant are calculated by interpolation from a standard curve which is constructed using cytokine samples of known concentration. Concentrations of total antibody isotypes can be calculated in a similar way. Levels of specific antibody may be measured directly in the blood using an ELISA with the antigen of interest, but these are reported as optical densities (relative measures of intensity from the ELISA) rather than absolute concentrations, since there is no straightforward way to calculate concentrations of antigen-specific antibodies. These optical densities are not directly comparable between different studies, due to a lack of standardisation of laboratory protocols (Mutapi 1997).

1.7 Hypotheses for the slow development of protective immunity in human schistosomiasis

Several different hypotheses have been put forward to explain why protective immunity develops slowly in human schistosome infection. These are outlined below. The first three are explored further in this thesis.

1.7.1 Parasite-induced immunosuppression

There is growing evidence that schistosomes are able to modulate the host immune response, suppressing non-specific responses to bystander antigens and other pathogens as well as specific responses to schistosomes (reviewed by Maizels & Yazdanbakhsh (2003)). In the mouse model of *S. mansoni* infection, suppression of immunopathological responses to trapped eggs in chronic infection has been clearly shown (King 2001*c*), and suppressor activity has been transferred from chronically to acutely infected mice by adoptive transfer of spleen cells (Weinstock & Boros 1981). In humans, experiments using peripheral blood mononuclear cells from chronically infected individuals have shown that schistosome antigen-specific proliferation and cytokine production are reduced in chronic infection (Araújo *et al.* 1996; Colley *et al.* 1986; de Jesus *et al.* 1993; Grogan *et al.* 1998*a*; King *et al.* 1996; Viana *et al.* 1994). This does not appear to be due to tolerance (deletion of antigen-reactive T cells), since antigen-specific responses can be restored in vitro, either by neutralization of interleukin (IL)-10 or by culture with dendritic-like cells (which improve antigen presentation by unelucidated contact-dependent and -independent mechanisms) (Araújo *et al.* 1996; Corrêa-Oliveira *et al.* 1998; Grogan *et al.* 1998*b*; King *et al.* 1996; van den Biggelaar *et al.* 2000). Antigen-specific proliferation and interferon-γ production in chronically infected individuals are inversely correlated with infection intensity (de Jesus *et al.* 1993; Grogan *et al.* 1998*a*), and schistosome antigen-specific IL-10 – a possible marker for suppression – has been found in some studies to be positively correlated with infection intensity (Mutapi *et al.* 2007; Reimert *et al.* 2006). This suggests that the degree of suppression is related to infection intensity (as estimated from egg counts in urine or faeces). Schistosome-specific IL-10 has also been associated with the suppression of non-specific cell proliferation and responses to bystander allergen antigens in humans (Grogan *et al.* 1998*a*; van den Biggelaar *et al.* 2000). Proliferative and cytokine responses to schistosome antigens are restored by praziquantel treatment, which kills adult worms (Grogan *et al.* 1996; van den Biggelaar *et al.* 2004), implying that suppression is induced by worms.

There is also evidence that cercariae can downregulate host immune responses (Jenkins *et al.* 2005). Murine studies have shown that IL-10 is induced soon after exposure to schistosome cercariae (He *et al.* 2002; Kumar & Ramaswamy 1999; Ramaswamy *et al.* 2000). The presence of IL-10 enhances cercarial migration through the skin (Ramaswamy *et al.* 2000). Cercarial excretory/secretory products and molecules in the cercarial glycocalyx have both been shown to enhance cercarial survival at local skin sites (Fallon *et al.* 1996; Harn *et al.* 1989). Recent studies have suggested that cercariae can also have systemic immunomodulatory effects, affecting distant skin sites and responses to schistosome eggs in the mesenteric lymph node (A.M. Mountford, pers. comm.).

1.7.2 Dying worms

Praziquantel kills adult worms, exposing the immune system to previously hidden antigens (Harnett & Kusel 1986; Redman *et al.* 1996), and enhancing immune recognition of specific antigens (Mutapi *et al.* 2005). The antibody 'switch' observed in children following treatment mimics changes which occur naturally with age in endemic populations (Grogan *et al.* 1996; Mutapi *et al.* 1998), suggesting that in the absence of chemotherapy, these changes are triggered by natural worm death (Mutapi *et al.* 1998; Woolhouse & Hagan 1999). If dying worms are the main trigger for protective responses, then in natural infections the necessary exposure to dying worms might be expected to be delayed for several years after initial infection, due to the long schistosome adult worm life span (Woolhouse & Hagan 1999). If the protective response stimulated by this release of antigens from dying worms reduces subsequent re-infection, it is proposed that the protective response targets shared epitopes on invading cercariae. In this scenario, it is suggested that the immune system has insufficient exposure to these antigens to stimulate a protective response following cercarial exposure alone, either due to reduced expression levels on cercariae or short exposure time (Fitzsimmons *et al.* 2007; Woolhouse & Hagan 1999). In *S. mansoni*, one candidate antigen for this type of immune mechanism is Sm22.6, which is expressed at high levels by adult *S. mansoni* worms, at much lower levels on cercariae and not at all by the egg stage. The IgE response to Sm22.6 is strongly boosted by treatment of infection, and has been shown to be associated with protection against re-infection (Fitzsimmons *et al.* 2007; Webster *et al.* 1996). If, on the other hand, responses generated by these previously hidden adult antigens are assumed to affect the adult stage, either leading to the killing of adult worms or reduced fecundity, then it might again be assumed that surface expression of these antigens is too low to trigger a protective response.

Both the mean worm life span and the distribution of worm survival times are expected to affect the timing of exposure to antigen from dying worms. Maximum life spans of up to 30 years have been reported for *S. mansoni* and *S. haematobium* (Berberian *et al.* 1953; Christopherson 1924; Fairley 1931; Harris *et al.* 1984), but this should not be confused with the average worm life span, which is considerably shorter. The mean life span of adult schistosomes in their human hosts has been estimated at between 3 and 10 years from studies with interrupted transmission (Goddard & Jordan 1980; Vermund *et al.* 1983; Warren *et al.* 1974; Wilkins *et al.* 1984). There is little data available to determine the distribution of worm survival times. In studies with interrupted transmission, it has not been possible to estimate the shape of the worm survival curve due to egg output variability and insufficient follow-up times, and survival has been assumed to be exponentially distributed. However, one study did report *S. mansoni* egg output declining more rapidly with time after the cessation of transmission, suggesting non-exponential worm survival (Goddard & Jordan 1980). Data on *S. haematobium* survival in experimental animal hosts is limited; data from some studies appears to be consistent with exponential worm decay (Cheever *et al.* 1988, 1974), whilst other studies suggest that worm burdens decline more slowly initially (Webbe *et al.* 1974).

1.7.3 Antigen threshold

It has been proposed that individuals must be exposed to a certain threshold level of schistosome antigens before they begin to mount a protective immune response (Mutapi *et al.* 2008; Woolhouse & Hagan 1999). This is implicit in the dying worms hypothesis (with the assumption

that low levels on cercariae or on the surface of living worms are insufficient to trigger a protective response), but is explored explicitly in this hypothesis. This antigen threshold might be supposed to rely upon current levels of antigen or cumulative exposure to antigen. Mutapi *et al.* (2008) showed that groups of people from areas with endemic *S. haematobium* infection recognise more schistosome antigens, and produce higher levels of IgG directed against them, with increasing age or infection level. This is consistent with the hypothesis that these different antigens need to be experienced at certain threshold levels before they trigger an antibody response, since these people are all likely to have been regularly exposed to infection from a very early age. In malaria, class switching in antibody responses against malarial merozoite-associated antigens has been shown to be associated with cumulative exposure to infection (Tongren *et al.* 2006), hinting at a similar mechanism.

At a cellular level both B and T cells require minimum threshold levels of receptor binding in order to be activated (Carter & Fearon 1992; Viola & Lanzavecchia 1996), which could explain how a threshold based upon current levels of antigen might work. A requirement for a threshold level of cumulative antigen exposure could represent a succession of cellular activation and expansion events that are required upstream of antibody production, particularly for antibody class switching. This could include repeated T cell activation and accumulation of a polarised T cell response leading to a change in the cytokine environment, which is a strong determinant of antibody class switching. The Th2 cytokines IL-4 and IL-13 induce IgG4 or IgE class switching by B cells (Capron *et al.* 1992; Jeannin *et al.* 1998), and the Th1 cytokine interferon-γ inhibits IgE production (Capron *et al.* 1992). The regulatory cytokine IL-10 inhibits class switching to IgE, and can induce IgA, IgG4 or IgG1 production, depending upon which other cytokines are present (Beniguel *et al.* 2003; Jeannin *et al.* 1998). There is antagonism between different cytokine responses, and the interactions between cytokines have highly nonlinear dynamics (Abbas *et al.* 1996; Callard *et al.* 1999). Due to these non-linear interactions, mathematical models have predicted that with repeated antigen exposure, it is possible to see a delayed but rapid change in the cytokine balance over time (Schweitzer & Anderson 1992*a*).

1.7.4 Multiple strains

Theoretical work has suggested that responses must be generated against several different schistosome strains to gain full protection, taking time to develop as individuals are exposed to successive strains (Galvani 2005). A high degree of genetic variability has been demonstrated within *S. haematobium* populations, from both snail and human hosts (Brouwer *et al.* 2001; Davies *et al.* 1999), but antigenic differences have not yet been studied. Since this hypothesis already has a good theoretical basis, and there is no available data on antigenically-distinct strains with which to test it, it is not further considered in this thesis.

1.8 Mathematical modelling of helminth infections

Mathematical modelling is a valuable tool in studying complex host-pathogen interactions such as human schistosomiasis. To be useful and relevant, models should make use of as much field and laboratory data as possible "otherwise, theory soars free of the constraints of data and experiment and field measurement simply contribute to an ever expanding sea of descriptive detail" (Anderson 1998). Many different types of mathematical models have been used to

aid understanding of schistosome infection and other helminths. The structure and type of model used depends upon the type of questions that are being asked, and the data available to parameterise or validate them.

In deterministic models, there is no allowance for chance events, so that there is only one possible outcome for a particular set of parameters and starting conditions (Garnett 2002). Deterministic models composed of coupled differential equations can provide good approximations to disease dynamics in large populations (Anderson & May 1991*a*; Chan *et al.* 1999). Chance is taken into account in stochastic models, so that a range of different possible outcomes can occur for a single set of parameters (Garnett 2002). Individual based models (IBMs) are fully stochastic models which simulate the behaviour of individuals. In infectious disease modelling, they can track individual births and deaths and infection events for hosts, and even for individual parasites (Habbema *et al.* 1996). IBMs allow large amounts of variability to be taken into account, but are much more computationally intensive than deterministic models (requiring multiple repeated simulations for each parameter set), and are harder to analyse mathematically (Chan *et al.* 2000). However, increasing computing speed and power has allowed much more widespread use of stochastic models (Garnett 2002), and they have a valuable role to play in the modelling of helminth infections, where the distribution of infection (and antibody) between individuals is of interest.

1.8.1 Modelling of transmission

A number of models of schistosome transmission have been developed which track the mean number of schistosomes worms per person and the prevalence of patent snail infection (Barbour 1996; MacDonald 1965; Woolhouse 1991). Further additions to these transmission models have included that of a pre-patent period for snails, density dependence within the human host, explicit modelling of snail and larval population dynamics, and worm mating probabilities (Barbour 1996; Woolhouse 1991). The basic reproductive rate, R_0, is defined for macroparasites (pathogens which do not undergo direct replication within their primary host) as the average number of mature female offspring produced by a single mated female worm over her reproductive life span, in the absence of any density dependent constraints (Halloran 2001). R_0 determines whether or not a pathogen can become endemic in a particular setting (it must exceed 1 for this to occur), and also determines the magnitude of the control effort which is required to eradicate it (Halloran 2001). Transmission models have been used to give an estimate of 4–5 for R_0 for *S. haematobium* (Woolhouse *et al.* 1996). Models including heterogeneities in water contacts both between individuals and between sites have shown that R_0 may be even larger than these earlier estimates (Woolhouse *et al.* 1998). It has generally been assumed in previous models that individuals retain a set level of exposure for life relative to others (Chan & Isham 1998; Woolhouse *et al.* 1998). However, other models have demonstrated that the extent of prediposition can have a substantial impact upon the population-level distribution of infection, (Quinnell *et al.* 1995), and in seeking to account for observed levels of infection aggregation, it will be important to take this into account.

Other models focussing upon explaining patterns of infection in human populations with endemic infection have assumed that infection rates remain constant over time, rather than model transmission explicitly (Duerr *et al.* 2003*a*; Woolhouse 1992*b*). Similar models have been developed which describe prevalence rather than mean infection intensity (Woolhouse 1998).

1.8.2 Models including acquired immunity

In models of schistosomiasis and helminth infections

Immunity has frequently been modelled as a single parameter, related to cumulative worm burden, with protection being either life-long or decaying over time. A successful approach has been to adapt the basic immigration death model to include acquired immunity as a density dependent process with memory (Anderson & May 1985; Roberts & Grenfell 1991; Woolhouse 1994*a*). As well as tracking worm burden with age, 'experience of infection' (related to cumulative exposure with some immune attrition over time) is modelled, and resistance is related to this experience level (Woolhouse 1992*b*). A limitation of this approach is relating these mathematical variables to real immunological responses. It is suggested that 'experience of infection' may be correlated with the number of specific memory cells, while 'resistance' is correlated with levels of protective antibodies or eosinophilia (Woolhouse 1994*a*). Different schistosome stages can trigger the immune response in these models, by relating infection experience to cumulative exposure to larvae, adult worms or eggs (Woolhouse 1994*a*). Resistance may be modelled as reducing susceptibility, increasing worm death rates or reducing worm fecundity. When eggs are included in the model, egg output has been assumed to be proportional to worm burden (Chan *et al.* 2000; Woolhouse 1994*a*). This approach has been adapted for stochastic models, with immunity modelled as a discrete variable (Chan *et al.* 2000). Galvani (2005) modelled strong immunity developing against numerous individual strains to generate a similar overall age-related pattern of infection burden.

Despite the simplicity with which the immune responses are represented in these models, they have been able to elegantly demonstrate several phenomena, including peak shifts, the expected changes with age in the correlation of a protective response with egg counts, and the inconsistency of population-level data with the blocking antibody hypothesis (Woolhouse 1992*b*, 1994*b*).

A different approach has been modelling specific within-host immune mechanisms. A subsection of the immune responses, including T cell and cytokine dynamics, have been explicitly modelled along with host parasite burden (Austin & Anderson 1996). This approach has been used to look at the effects of epitope variation on immunodominance (Austin & Anderson 1996), and at the complex relationships between parasite level, T cell proliferation and cytokine production (Schweitzer & Anderson 1992*b*). However, these models have become outdated as understanding of the immune responses involved has changed over recent years, and currently there is a lack of within-host data from humans with which to test this type of model.

In models of other infectious diseases

Immune responses have been included in a large number of different models of both within-host and population-level dynamics of other infectious diseases. The level of immune detail included in these models has been partly driven by the data available, the research question being asked, and how well the immune response to a given infection has been characterised. In population-level models of viral or bacterial epidemics, immunity is often included as a compartment of 'recovered' or immune individuals, whose immunity is either lifelong or wanes over time (Earn *et al.* 2000; Grassly *et al.* 2005). In macroparasite models of infection intensity, immunity is more usually included as an additional compartment describing a level of partial immunity (Anderson & May 1985), as described in the previous section on helminth models.

Within-host models including CD4+ and CD8+ T cells have been used to further the understanding of the dynamics of a range of viruses, including hepatitis B and C, CMV, HTLV, SIV, and particularly HIV (Asquith *et al.* 2009; Perelson 2002; Ribeiro 2007). These models rely upon detailed data on infection and T cells over time within the same individuals or use data from in vivo T cell labelling. Some models have also included B cell kinetics and isotype class-switching in response to viral infections (Funk *et al.* 1998). For malaria, where the immune markers of protection are less well characterised (similar to the current situation for schistosomiasis), within-host models have tended to include more general representations of immune responses. Multi-strain models fit to time-series parasitaemia data have included variant-specific and variant-transcending responses (Molineaux *et al.* 2001; Paget-McNicol *et al.* 2002), or specific antibody responses (with a threshold parasite load required to trigger them)(Paget-McNicol *et al.* 2002). Recent models incorporating immunity to malaria into population-level transmission models have included immune responses in a phenomenological way, related to cumulative exposure or age (Filipe *et al.* 2007; Maire *et al.* 2006). These models were fit to infection prevalence data, not to data on immune markers.

Data on within-host T or B cell dynamics are not available for schistosome infection, so detailed within-host models cannot currently be fitted to data; however, cross-sectional data on antibody responses are available. In this thesis, B cells rather than generic immune responses are modelled, and models are tested for their ability to reproduce qualitative patterns seen across different specific antibody responses (which could not be done in models with only generic representations of immune responses).

1.8.3 Models incorporating control measures

A number of models have been used to assess the effects of control measures (Woolhouse 1992*a*). Models can assess how hard eradication would be to achieve, by looking at the effect on R_0. Alternatively, models may assess the rate of return to endemic levels following the intervention. Such models can be used for cost-benefit analysis, to advise local policy makers (Woolhouse 1992*a*).

A number of models have looked at the effects of chemotherapy, either modelling it as an increased worm death rate (assuming frequent treatment) or as discrete reductions in worm burden (Anderson & May 1985; Chan *et al.* 1996, 1999; de Vlas *et al.* 1996). Two very different simulation approaches which have been used to predict the effects of chemotherapy in specific populations are the EpiSchisto and Schistosim programmes (Chan *et al.* 1999; de Vlas *et al.* 1996). The EpiSchisto model used a deterministic framework to predict the prevalence of infection following treatment, and was validated using data from Zanzibar. The model only required data on initial conditions, and was able to predict post-treatment prevalence well, especially on larger population scales, although it performed less well at higher infection prevalence (Chan *et al.* 1999). Schistosim is a fully stochastic microsimulation model, requiring a large number of parameters to be estimated. It was used to make predictions about the effects of chemotherapy in Burundi, and was able to predict short term effects very well, but not long term effects (de Vlas *et al.* 1996). This lack of ability to predict long-term effects may have arisen from changes in transmission following treatment or ageing of the sampled population (neither of which which were taken into account by the model), or because the effects of treatment on immune responses were not correctly modelled (de Vlas *et al.* 1996). These are all factors which

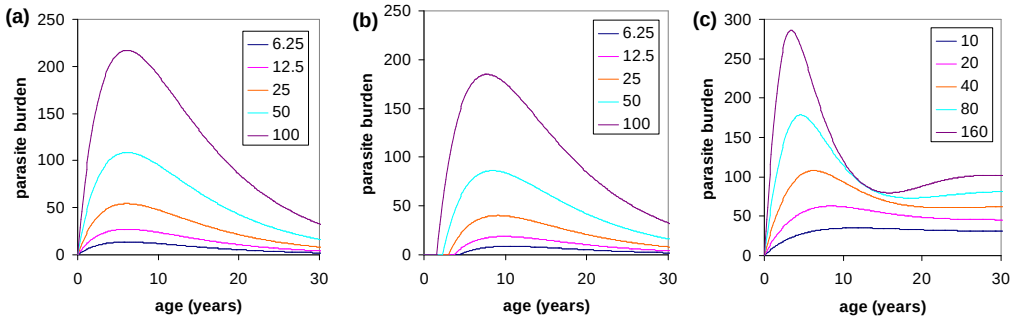

Figure 1.7: Output from an immigration-death model, showing changing parasite burden with age: (a) with infection rate declining exponentially with age starting at level indicated, no immunity (after Woolhouse (1992*b*) (b) as (a), with age at first exposure inversely related to infection rate (as in Fulford *et al.* (1992)) (c) with constant infection rates as indicated, with immunity included (after Woolhouse (1992*b*)

should be considered in future modelling of treatment of schistosomiasis.

Assumptions about immunity can make a big difference to such models. One model showed a progressively shorter and slighter impact of treatment with stronger and longer-lived immunity (Chan *et al.* 1996). This was because, to keep prevalence constant in the model, increased immunity had to be balanced by a higher value for R_0. If chemotherapy is assumed to be removing the stimulus for protective immunity, then it can lead to transient increases (or 'overshoots') in infection above pre-treatment levels after treatment ceases (Chan *et al.* 1996). This model assumed that the antigens stimulating protective immunity came from live adult worms, which are removed by treatment. However, if this antigen is assumed to come from dying worms (section 1.7.2), then treatment is expected to boost protective immunity, and different long-term effects on infection may be seen. This has not been modelled previously.

Several models have assessed the hypothetical effects of schistosome vaccination (Chan *et al.* 1997; Woolhouse 1995). Assumptions about both natural and vaccine-induced immunity are crucial for these models, and will need to be reassessed as the biological understanding of immunity develops. However, these models are able to make several solid predictions. They show that the type of vaccine-induced protection (reducing susceptibility or egg output) may not make much difference to population level effects, in terms of subsequent infection intensity, and age of peak intensity (Chan *et al.* 1997). The models also demonstrate that increasing the duration of protection will have a greater impact than increasing the degree of protection, and that using vaccination in combination with chemotherapy will have the greatest impact upon worm burdens both short-term and long-term (Chan *et al.* 1997).

1.8.4 Taking helminth models to data

Different approaches have been taken to challenging these models with data. A number of studies have attempted to reproduce qualitative patterns seen in field data (Chan *et al.* 2000; Duerr *et al.* 2003*a*; Fulford *et al.* 1992; Galvani 2003; Woolhouse 1992*b*). These studies have usually only attempted to reproduce one or two patterns at a time. Such patterns can often be reproduced by several different models which imply different underlying mechanisms (Duerr *et al.* 2003*a*). A case in point is the peaked age-intensity curve seen in populations with endemic schistosome infection. This can be reproduced by permitting the rate of infection to decline

exponentially with age, or to vary with age as a convex pattern (based on observed water contact rates), by including host heterogeneity coupled with parasite-induced host mortality, or with the inclusion of an acquired immunity process related to cumulative worm burden (even with age-constant exposure) (Duerr *et al.* 2003*a*; Fulford *et al.* 1992; Woolhouse 1992*b*; Woolhouse *et al.* 1994). Requiring models to also reproduce additional patterns can distinguish between some of these possibilities. Models with declining rates of infection with age cannot reproduce the peak shift unless the age at first exposure also varies with the infection prevalence (figure 1.7 (a) and (b)); (Fulford *et al.* 1992; Woolhouse 1992*b*). Models with acquired immunity can also reproduce the peak shift (Woolhouse 1992*b*) (figure 1.7c).

Aggregated infection can be generated by including variability in host susceptibility or exposure, or if infection is modelled as a 'clumped' process, where there is aggregation in the number of worms acquired per contact (Duerr *et al.* 2003*a*). Density-dependent processes, including acquired immunity related to previous exposure, reduce infection aggregation (Duerr *et al.* 2003*a*; Galvani 2003). Immune responses targeting re-infection have been shown to reduce aggregation to a greater extent than anti-fecundity responses (Galvani 2003), and models have been used to show that aggregated host exposure is much more able to explain observed levels of infection aggregation than heterogeneity in individual immune responses (Chan & Isham 1998).

Other studies have assessed the ability of models to reproduce more quantitative patterns, based on large data sets for particular populations. De Vlas *et al.* (1996) assessed the ability of their model to reproduce population prevalence of infection, and of different levels of infection at multiple time points after treatment. Chan *et al.* (1999) assessed the ability of their model to reproduce school- and district-level prevalence measured at five different time points after treatment using likelihood methods. Another approach that has been taken is formal fitting of a model to population data (Woolhouse *et al.* 1996).

A different approach which has not yet been used for helminth modelling but which could be a useful tool for distinguishing between different mechanisms giving rise to observed patterns is pattern-oriented modelling (POM). This has been developed in ecology for agent (or individual)-based simulation models (Grimm *et al.* 2005). In this approach, models are identified which can reproduce multiple patterns observed in real systems at different levels or scales. This can guide the design of model structure and aid parameter estimation. In very different settings, POM has been used to discriminate between different possible model structures and to vastly narrow down potential parameter ranges and combinations (Janssen *et al.* 2009; Rossmanith *et al.* 2007; Swanack *et al.* 2009; Wiegand *et al.* 2008). This approach allows both quantitative and qualitative patterns to be considered, and the use of multiple different patterns makes it less likely that models including different biological processes will be able to reproduce all of these patterns. The pattern-oriented approach used in this thesis is outlined in appendix A.

Previous modelling work has generally focussed upon reproducing patterns of infection intensity rather than markers of the immune response (an exception being Woolhouse (1992*b*), who looked at correlations between infection and antibody). With increasing amounts of data available on patterns of schistosome-specific immune markers (section 1.5.5), it is of interest to investigate whether models can also reproduce these patterns.

1.9 Aims

The aims of this study were:

1. To characterise and quantify robust patterns of infection and specific antibody responses in populations with endemic *S. haematobium* infection which could be used to test mathematical models. In particular, to identify quantitative limits for infection patterns which have previously been used for qualitative modelling, and to characterise antibody patterns which have not been used in modelling studies before, including the antibody switch.

2. To develop mathematical models of specific immune responses to schistosomes which could be used to predict population-level patterns of infection and antibody, building upon earlier model frameworks for helminth immunoepidemiological models to incorporate explicit immune pathways and allow different distributions of worm survival.

3. To use these models in a pattern-oriented modelling approach (outlined in appendix A) to formally test for the first time whether the following hypotheses for the slow development of protective immunity against schistosomes were consistent with population-level patterns of infection and antibody:

    - Worm-induced immunosuppression/immunomodulation of protective host responses will delay the development of protective responses
    - Exposure to dying worms is necessary for the development of protective immunity
    - A threshold level of antigen exposure must be exceeded before a protective immune response can be mounted

4. To use models in which dying worms stimulate protective immune responses to predict the impact of mass treatment programmes upon the development of natural protective immunity, and subsequent effects upon infection levels in treated populations during and after treatment programmes

1.10 Thesis outline

In chapter 2, patterns in field data for both infection intensity and schistosome-specific antibody responses are analysed in more detail to draw up a set of robust criteria against which models can be tested.

In chapter 3, deterministic models including a single protective antibody response are used to explore the ability of models including suppression, dying worms or an antigen threshold to delay the development of protective immunity and reproduce peaked infection curves and a peak shift.

In chapter 4, deterministic models are used to identify the mechanisms capable of explaining the antibody switch as well as the peaked age-intensity curve and the peak shift. Models with two antibody responses are used to systematically explore the potential role of different life cycle stages providing antigen for the two responses, cross-regulation between the two antibody responses and an antigen threshold.

In chapter 5, stochastic individual based models with cross-regulation or an antigen threshold are used to further discriminate the ability of selected models which were successful in the deterministic model analysis to reproduce observed aggregation of infection and antibody co-distributions, and observed patterns of antibody after treatment.

In chapter 6, model structures and parameter combinations for which all of the patterns of infection and antibody were reproduced are used to make predictions about the impact of large-scale treatment programmes upon the development of protective immunity and subsequent impact upon infection levels, both during these treatment programmes and after their cessation.

Chapter 2

Patterns in field data

2.1 Introduction

In using mathematical models to understand the development of protective immunity in human schistosomiasis, it is important to first characterize the key patterns of infection and immune markers seen in field data, which must be replicated by a successful model. Previous helminth modelling work has mainly focussed on reproducing patterns of infection intensity, including age-related changes in both mean levels of infection and the distribution of infection (Anderson & May 1985; Chan & Isham 1998; Fulford *et al.* 1992; Woolhouse *et al.* 1994). Correlations between infection intensity and antibody have also been studied (Woolhouse 1992*b*). In addition to looking at distributions of infection, my analysis will also attempt to reproduce patterns of antibody distribution and correlations between different antibody responses.

A wide range of immune cells and molecules have been measured with the aim of identifying immune correlates for protection in schistosomiasis, including antibody isotypes (both antigen-specific and total levels), cytokines (background levels in sera, or levels produced after re-stimulation of whole blood or peripheral blood mononuclear cells with specific antigens), as well as numbers of different cell types (such as eosinophils and T cell subtypes) (Butterworth *et al.* 1996; Demeure *et al.* 1993; Hagan *et al.* 1985; Medhat *et al.* 1998; Mutapi *et al.* 2007). As several different responses have been associated with reduced re-infection rates after treatment, it seems unwise to attempt to fit models to a single immune variable. I have chosen instead to develop models which replicate qualitative and semi-quantitative patterns seen in the field data.

Of the data available to me (on antibody responses, cytokines and some eosinophil data), I have decided to focus upon antibody responses. These have been well characterised in the literature and have a clearly defined cellular source. From a modelling perspective, the B cell maturation pathways and production of antibody are much more clearly defined than those leading to production of cytokine (which can come from a variety of cellular sources) and so can be more confidently represented in some detail. Additionally, antigen-specific antibody can be directly detected in sera. Measures of antigen-specific cytokine levels use an indirect assay where cells are re-stimulated ex vivo, meaning that these represent a potential cellular response to a particular antigen preparation rather than directly corresponding to an actual cytokine response made in vivo. Background cytokine levels in sera are generally very low and are not specific for schistosomes but could be stimulated by any other pathogens present

in the host. The main drawbacks of using antigen-specific antibody data are that, firstly, it is not possible to measure actual concentrations, and the optical densities which are reported are not directly comparable between different studies in which different protocols are used, and secondly, there is some uncertainty surrounding where negative cutoff values lie (i.e. at what level of measurement there is actually no antibody being made – this is also an issue for cytokine data (Uh *et al.* 2008)). There are seven main secreted human antibody isotypes (IgA, IgE, IgM, IgG1, IgG2, IgG3 and IgG4), which have been measured for a number of different schistosome antigens and antigen mixtures. None of these isotypes have as yet been exclusively associated with protection against schistosomiasis and there is not an easy way to amalgamate the different isotype data into a single variable. Therefore, rather than characterise specific isotype responses, my aim here is to identify broad patterns in the antibody data which can be replicated by a model.

In this chapter, I have reviewed the established patterns for infection and antibody which have been published by other authors (section 2.1.1), and then carried out additional analysis of infection and antibody data for endemic *Schistosoma haematobium*, with the aim of quantitatively characterizing features of the age-intensity profile (section 2.3.1), age-related distributions of both infection and antibody (sections 2.3.2 and 2.3.3), and the post-treatment antibody switch (section 2.3.4).

2.1.1 Previously identified patterns for infection and antibody

Cross-sectional studies in populations with endemic infection of all of the major human schistosome species consistently show that mean levels of infection (estimated from egg output in stool or urine) follow a convex or 'peaked' curve with host age, with peak levels of infection intensity occurring in childhood and lower levels of infection found in adults (Clarke 1966; Fisher 1934; Fulford *et al.* 1992). Prevalence of infection also tends to follow a peaked curve with host age but does not decline as rapidly as infection intensity in older individuals (Mutapi *et al.* 2007).

Mathematical models predict that if acquired immunity with memory of previous pathogen exposure is acting to reduce levels of schistosome infection, then in areas with higher rates of infection, the peak level of infection will occur at a higher level and at a younger age than in areas with lower infection rates, a phenomenon termed the 'peak shift' (Woolhouse 1998). This has been demonstrated for infection curves for *S. mansoni* in Kenya (Fulford *et al.* 1992) and for prevalence curves for *S. haematobium* in Zimbabwe (Woolhouse *et al.* 1991).

Schistosomes are not equally distributed between their hosts: within an endemic population, a few individuals will carry the majority of parasites, with most people having very light or no infection at a given moment in time (Chandiwana *et al.* 1991; Guyatt *et al.* 1994; Mutapi *et al.* 1997). This is called an aggregated or overdispersed distribution, and has also been reported for a range of other parasitic species (Basáñez & Boussinesq 1999; Bundy *et al.* 1988). Chan & Isham (1998) concluded from their modelling work that this aggregation can mostly be explained by differences in infection rates, and other modelling exercises have also tended to assume this as the main source of aggregation in infection levels (Galvani 2003; Woolhouse *et al.* 1994).

Age profiles of schistosome-specific antibodies vary somewhat between different studies. Antibody levels also tend to be aggregated between individuals (Mutapi & Roddam (2002),

section 2.3.3) and different isotypes are often highly correlated. One pattern to emerge in two separate studies of *S. haematobium* in Zimbabwe is the clustering of different isotypic responses into two different age-related patterns – one group increasing with age (including IgE against adult worm antigen) and another group declining with age (Mutapi *et al.* 1997; Ndhlovu *et al.* 1996*b*).

Another pattern previously reported for schistosome-specific antibody is a 'switch' from an IgA to an IgG1 response directed against schistosome egg and adult worm antigen preparations at both a population and an individual level, occurring around age 14-16 (Mutapi *et al.* 1998). This switch (from egg-specific IgA to IgG1) was also reported to occur in younger individuals following praziquantel treatment (Mutapi *et al.* 1998).

2.1.2 Additional patterns and parameters to be identified

The convex age-intensity curve is always seen for *S. haematobium* in endemic populations, and can be qualitatively reproduced in models through a variety of mechanisms (Fulford *et al.* 1992; Woolhouse 1992*b*). For more quantitative analysis, I wanted to determine the age-range over which the peak in infection intensity occurs, and to what extent infection is reduced in adults relative to the peak level seen.

I also wanted to get an estimate of typical levels of aggregation in both infection and antibody, and see how this varied with host age. I looked at patterns of co-distribution for different antibody isotypes, to determine how widespread the antibody switch pattern is (referred to in section 2.1.1), using correlation and percentile cutoffs as alternative ways of characterizing these patterns. Finally, I quantified the extent and longevity of the reported antibody switch following praziquantel treatment.

Analysis framework for chapter 2

- The aim of the analysis in this chapter is to
  - Identify robust patterns in field data on infection intensity and antibody
  - Determine upper and lower bounds on quantitative patterns
  - Use these patterns to draw up criteria
- In subsequent chapters, models will be tested against these criteria, using the pattern-oriented modelling approach (see appendix A)
- Data used is for *S. haematobium* from studies in Zimbabwe and other published studies from Africa
- Patterns analysed:
  - shape of age intensity curve (age and relative height of peak)
  - aggregation in infection
  - aggregation in antibody responses
  - dichotomous relationship between antibody responses
  - changes in antibody levels after treatment
- Even qualitative criteria, or criteria with large uncertainty, can be powerful in discriminating between different models, particularly when a number of different criteria are used together.

2.2 Data sources and methods

2.2.1 Field data

Data on *S. haematobium* infection intensity was taken from (pre-treatment) baseline studies of six Zimbabwean populations from three different field studies: Valhalla and Kaswa were both part of the Burma Valley study conducted in 1994 (Mutapi *et al.* 1997); the Mutoko-Rusike study was conducted in 2003 (Mutapi *et al.* 2007), and Magaya, Chipinda and Chitate were all part of the Murehwa study conducted in 2008/2009 (unpublished data). These were all school-based studies, with additional participation of adults from the local community. There was additional recruitment of pre-school children with their parents in the Chitate population. Infection intensities were calculated using the arithmetic mean egg count from two or three 10ml urine samples collected on consecutive days, processed using the urine filtration method (Mott 1983). Antibody data for the main analysis came from the Burma Valley study (Valhalla and Kaswa), with some additionally coming from the Mutoko-Rusike study. Antibody data for the post-treatment switch came from the Burma Valley study. Antibodies specific for different crude homogenates (whole worm homogenate (WWH), schistosome egg antigen (SEA) or cercarial antigen preparation (CAP)) were measured by ELISA, quantified as optical densities (OD) read at 492nm (Mutapi *et al.* 1997).

2.2.2 Data from the literature

A survey of the wider literature was undertaken to pinpoint the age of the peak level of infection and any trends in the relationship between infection levels in adults and the peak level of infection. To be included, studies had to measure infection intensities of endemic *S. haematobium*, had to include both children and adult subjects (over the age of 20), and had to give infection levels for at least four different age groups. Adult age groups were chosen to be as close to that used in the data analysis as possible (24-34 years old). Data was taken from results tables where given, otherwise it was extracted from graphs using the software application Datathief III version 1.5.

Data on water contact for the Burma Valley area, which had been collected by direct observation of water contact sites, was taken from figure 1 in Chan *et al.* (2000) using Datathief.

2.2.3 Statistical analysis

Infection and antibody data were grouped by age to plot age profiles, with five age groups chosen to give roughly equal numbers of individuals in each group for the Burma Valley populations (age groups: $\leq$8, 9-10, 11-12, 13-23, 24-34 years old). Standardized variances were calculated for both infection and antibody, for the whole population and in two age groups (0-14, 15-34 years old), in order to have sufficiently large group sizes to give stable variance estimates. The two age groups were chosen to coincide with the sudden change (or 'switch') in antibody isotypes seen in the Burma Valley populations.

Standardized variance was defined as:

$$SV = \frac{\sigma^2}{\overline{x}}$$

Correlations between infection and antibody levels were calculated using a two-tailed

Spearman's rank correlation coefficient (this was preferred to parametric methods since the data are highly skewed). All tests used a significance cut-off level of 1%. The age-contact curve was fitted to the data points by least squares, using the solver function in Microsoft Excel 2003. Statistical analyses were performed using SPSS version 15.

2.3 Results

2.3.1 Age-infection profile

Age infection profiles for six Zimbabwean communities with endemic *S. haematobium* infection are shown in figure 2.1. The key parameters of interest (age and level of peak infection, and ratio between adult and peak infection levels) for these populations are given in table 2.1. Note that data was only included for individuals up to the age of 34, because data on water contacts for the Burma Valley populations showed that this remained fairly stable for adults up to this age, although they declined at older ages (figure 2.2). Table 2.1 also includes information on the infection peak and its relationship to infection in adults for a number of studies of endemic schistosomiasis taken from the literature, which give mean infection intensities by age group, and cover a sufficiently wide age range to capture both the peak and adult levels. For *S. haematobium*, the peak infection intensity in these studies was recorded between the ages of 6 and 18 years old (cf. 12–25 years old for *S. mansoni*, Fulford *et al.* (1992)). Adult age groups for comparison were chosen to be as close to the range used in the analysis in figure 2.1 as possible. Results from studies giving means of log-transformed egg counts were back-transformed to give geometric means. It is difficult to compare these studies or use all of the estimates for the ratio between adult and peak levels of infection since the different studies use a range of types of means (arithmetic or geometric mean, including the whole population or only those with infection), which give very different answers. From the studies which use arithmetic means for *S. haematobium* infections, the ratio of final:peak infection level is 0.5–26%. It should be noted that most of the additional populations in this analysis come from Clarke (1966), who did not use fixed volumes of urine for egg counts. No clear relationship could be seen between the age of the peak and the level of reduction. Using different age groupings for the populations shown in figure 2.1 changed the ratio of final:peak infection level substantially for some of the populations (Valhalla - ratio up to 34%, Chipinda - ratio up to 30%), indicating that this metric is not stable for these populations.

2.3.2 Infection distributions

Figure 2.3 shows the distributions of infection for the Burma Valley populations (Kaswa and Valhalla), by two age groups. The age groups were chosen to coincide with the sudden change in antibody isotypes seen in the Burma Valley populations. Standardized variances ($\sigma^2/\overline{x}^2$) are given in the figure. Mean infection intensity and standardized variance for infection were calculated for all of the populations in figure 2.1, for the whole population (up to age 34) and subdivided into two age groups. Figure 2.4 shows the infection intensity and standardized variance for each of the villages by age group. Both infection intensity and the standardized variance varied considerably across the different villages, and while infection intensity decreased in the older group for all of the villages apart from Chitate, the standardized variance varied substantially with age, increasing or decreasing with age for different populations. Overall prevalence of infection in these populations (up to age 34) varied from 9.8% in Chitate up to 67.6% in Valhalla (data not shown).

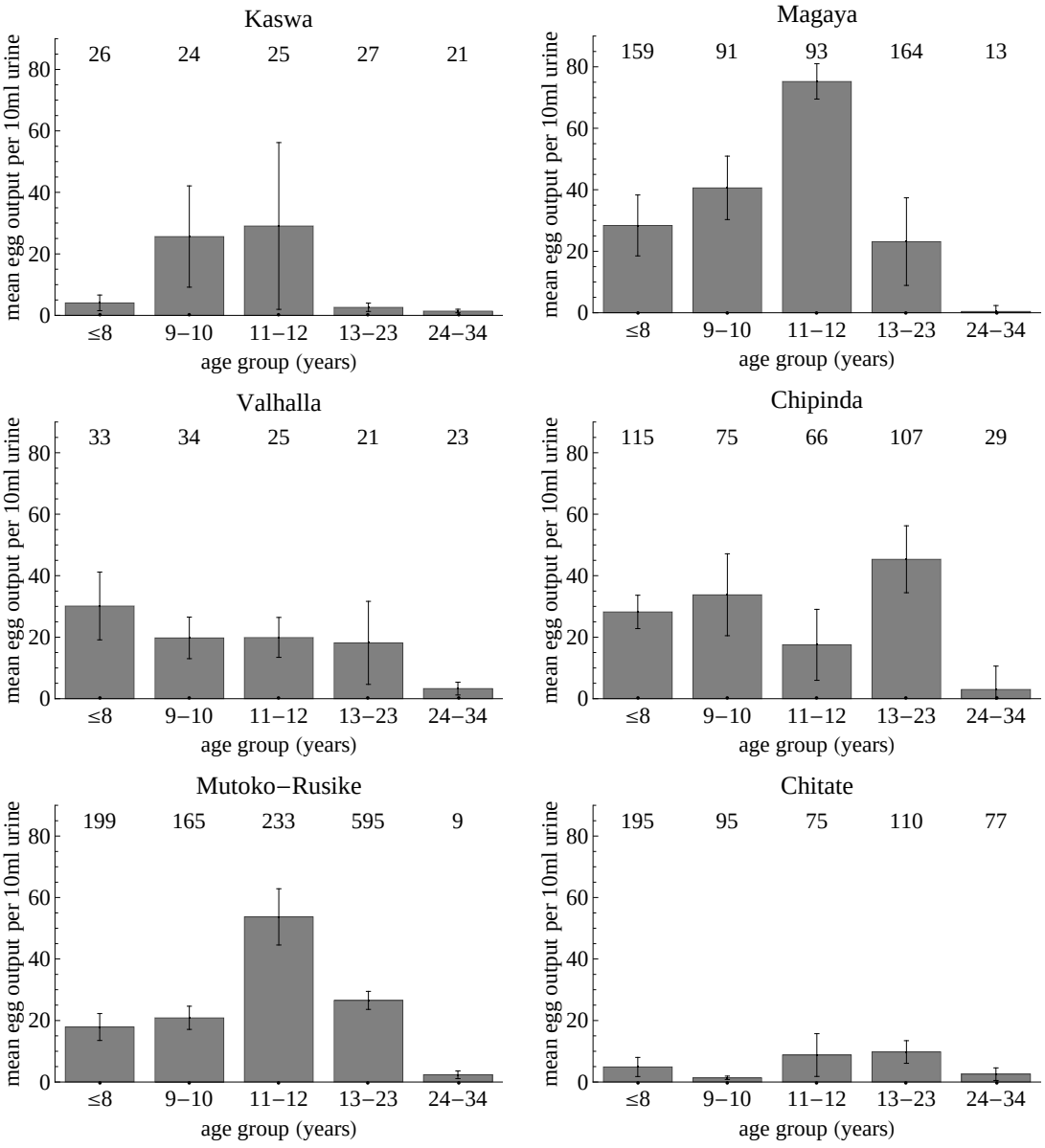

Figure 2.1: Age-intensity graphs for six Zimbabwean populations with endemic *S. haematobium*. Grey bars represent arithmetic mean egg counts per 10ml urine for the five age-groups shown, error bars represent standard error of the mean. The numbers at the top of each graph show the sample size for that age group.

Table 2.1: Summary of age-intensity profiles for *S. haematobium*

Reference	Country	Mean	Peak age	Peak level	Adult age	Adult level	% Adult/Peak
Kaswa (Mutapi *et al.* 1997)	Zimbabwe	arithmetic	11–12	29.1	24–34	1.4	4.9
Valhalla (Mutapi *et al.* 1997)	Zimbabwe	arithmetic	5–8	30.2	24–34	3.3	10.9
Mutoko-Rusike	Zimbabwe	arithmetic	11–12	53.7	24–34	2.3	4.3
Magaya	Zimbabwe	arithmetic	11–12	75.3	24–34	0.4	0.5
Chipinda	Zimbabwe	arithmetic	13–23	45.4	24–34	3.0	6.6
Chitate	Zimbabwe	arithmetic	13–23	9.8	24–34	2.5	26.0
Bradley & McCullough (1973)	Tanzania	arithmetic	9	311.0	33–34	35.0	11.3
Clarke (1966)	Zimbabwe	arithmetic	10–12	3405.6	21–40	428.0	12.6
Clarke (1966)	Zimbabwe	arithmetic	7–9	853.4	21–40	20.7	2.4
Clarke (1966)	Zimbabwe	arithmetic	10–12	922.3	21–40	55.9	6.1
Clarke (1966)	Zimbabwe	arithmetic	7–9	688.3	21–40	18.2	2.6
Clarke (1966)	Zimbabwe	arithmetic	10–12	373.7	21–40	43.0	11.5
Agnew *et al.* (1996)	Kenya	geometric (all)	11–15	25.2	31–40	3.8	15.0
Useh & Ejezie (1999)	Nigeria	geometric (all)	10–14	11.6	30–39	7.4	64.2
Wilkins *et al.* (1984)	Gambia	geometric (all)	8–12	326.0	25–39	1.9	0.6
Wilkins *et al.* (1984)	Gambia	geometric (all)	8–12	170.0	25–39	1.8	1.1
Wilkins *et al.* (1987)	Gambia	geometric (all)	5–9	108.6	15+	11.0	10.1
Chandiwana *et al.* (1988)	Zimbabwe	geometric (positives)	16–20	234.7	31–50	32.4	13.8
Chandiwana *et al.* (1988)	Zimbabwe	geometric (positives)	7–9	116.3	31–40	11.1	9.5
Ndhlovu *et al.* (1996*b*)	Zimbabwe	geometric (positives)	10–14	31.0	25–44	4.3	14.0
King *et al.* (1992)	Kenya	geometric (unspecified)	12–15	34.9	adults	6.0	17.1

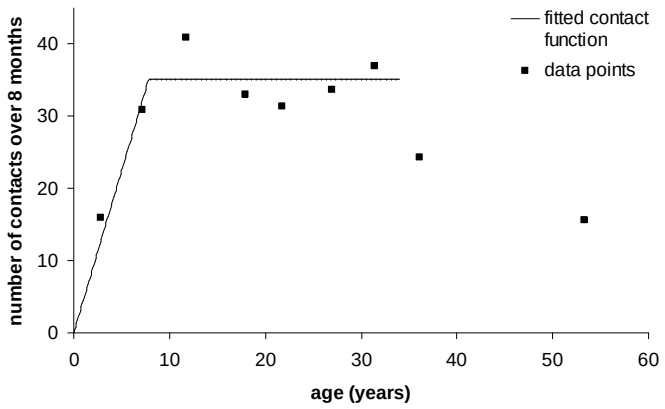

Figure 2.2: Age-related water contact frequency. Data is for the Burma Valley region in Zimbabwe, with data points extracted from figure 1 in Chan *et al.* (2000). The two-part linear function was fitted using least squares.

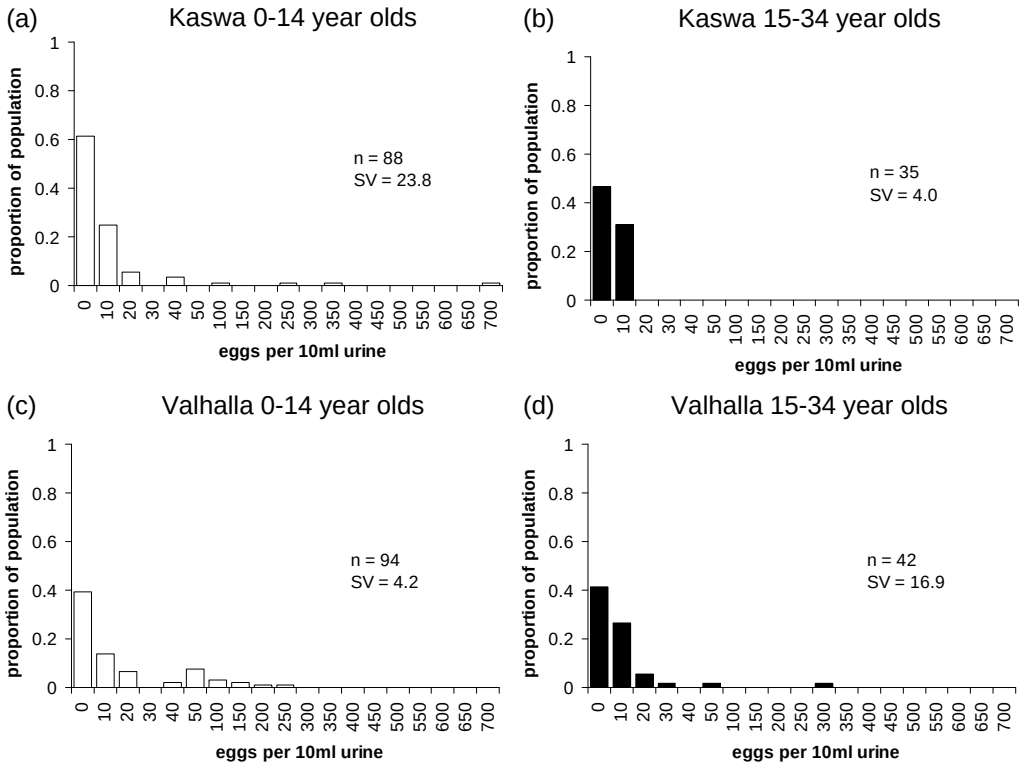

Figure 2.3: Infection intensity distributions for the Burma Valley populations divided into two age groups. (a) Kaswa, age 0–14, (b) Kaswa, aged 15–34 (c) Valhalla, aged 0–14 and (d) Valhalla, aged 15–34 years old. SV = standardized variance ($\sigma^2/\overline{x}^2$). Note that the intervals for different egg counts on the x-axis are uneven in size.

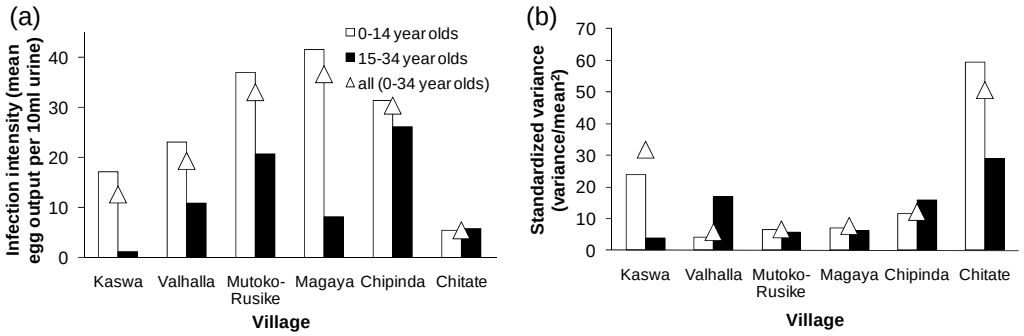

Figure 2.4: (a) Mean intensity and (b) standardized variance for infection levels for each of the six populations by two age groups and all together.

2.3.3 Antibody distributions

Mutapi *et al.* (1998), using the same dataset from the Burma Valley populations, showed that there is a switch from IgA production in children to IgG1 production in adults against SEA antigen. They used partial correlation analysis to demonstrate a consistent significant negative correlation between IgA and IgG1 directed against SEA for both populations and across two age groups, and also between IgA and IgG1 directed against WWH antigen for adults in Valhalla (Mutapi 1997). I wanted to see whether this striking change (or 'switch') in the antibody response was limited to the IgA and IgG1 responses in these particular populations, or whether it was a more widespread phenomenon across different isotypes and in different population settings. I first of all looked for significant negative correlations between different antibody isotypes across the full population age range (using an age range of 0-34 as with my previous analyses), and found that this was able to discriminate well the dichotomous antibody relationship that I was trying to detect. In the Burma Valley populations, these negative correlations all occurred between isotypes which change significantly with age in opposite directions – i.e. one of the pair increased with age and the other decreased (as assessed by one-way ANOVA or the equivalent non-parametric Kruskal Wallis test, using age as a categorical variable in the five age groups used for the infection profiles). In Kaswa, significant negative correlations were found between the IgG4 and IgA anti-SEA responses, IgG1 and IgA anti-WWH responses and the IgM and IgG1 anti-WWH responses as well as the SEA IgA and IgG1 antibodies (figure 2.5). In Valhalla, all of these correlations were also seen, and additionally a negative correlation between IgA and IgM SEA antibodies (figure 2.6). For the negative correlations which were significant at the 1% level, the correlation coefficient varied between -0.662 and -0.247.

Since this antibody dichotomy (or 'L-shaped' relationship) is not technically a negative correlation, I also tried to characterize the relationship by looking at each pair of antibody isotypes in turn to identify combinations for which no individuals ever make high levels of both isotypes, using different percentile cutoff levels (calculated separately for each isotype across the whole population), using a range of percentiles from 50%-85%. For the Burma Valley populations, I found that the SEA IgA-IgG1 dichotomy could be detected at the 70^{th} percentile for both populations (i.e. both antibodies being produced above the 70^{th} percentile by any one individual is never observed). The 85^{th} percentile was not sufficiently discriminatory in Valhalla, but the 80^{th} percentile was able to pick out responses which looked dichotomous

(these were all also identified by correlation analysis apart from the SEA IgA-IgE switch suggested for Valhalla) (figures 2.5 and 2.6). It should be noted that with the population sizes used for this analysis (around 100 individuals each for Kaswa and Valhalla), you would expect by chance to only see four individuals simultaneously exceed the 80^{th} percentile for two independent antibody responses – only 2.25 people for the 85^{th} percentile and 9 people for the 70^{th} percentile. When the dichotomous relationships identified by correlation analysis were plotted by age group, a clear change was seen ocurring with age in both the individual antibody distributions (distributions plotted in appendix B, standardized variances plotted in figure 2.7), and in their co-distributions (figure 2.8). For these responses in the Burma Valley populations, antibodies which increased with host age all demonstrated a decrease in their standardized variance in the older age group, with the reverse being observed for antibodies which decrease with host age (figure 2.7). The marked change in the co-distribution showed that the switch not only happened very rapidly on an individual scale (as nobody was found producing high levels of both isotypes), but also over a relatively short period at a population level, with only a few individuals falling outside the majority response for their age group (figure 2.8).

In Mutoko-Rusike, there were no significant negative correlations between different isotypes directed at the same antigen preparation (for cercarial, egg or adult worm antigen preparations). Most antibodies were significantly positively correlated with each other (data not shown), and no responses showed a dichotomy for the percentile levels tested, up to and including the 85^{th} percentile.

Correlations between antibody responses and infection levels were also looked at (figures 2.5 and 2.6). Negative correlations were seen between SEA IgG1 and infection level for Valhalla. No antibody-infection relationships were identified using percentile cutoffs. Positive correlations between infection intensity and antibody levels were seen for a range of isotypes in all four populations, including SEA IgA (for Valhalla) and SEA IgG4 (Valhalla and Mutoko-Rusike).

2.3.4 The post-treatment antibody switch

I wanted to quantify both the extent of the switch and the length of time over which the antibody responses remained switched. Data was available from a subset of the Burma Valley population aged 6–15 years old for whom SEA IgA and IgG1 were measured pre-treatment and at 18, 24, 30 and 36 weeks after praziquantel treatment. Data on other isotype responses (measured at 18 and 36 weeks) were not used for quantifying the post-treatment antibody switch due to small sample sizes at 36 weeks (Mutapi *et al.* 1998). The data used is shown in figure 2.9. IgG1 showed a substantial increase after treatment, and IgA a very rapid drop. A conservative limit for identifying such a switch in model outputs (substantially exceeded in this data set) was set as a doubling in the response which increases naturally with age, and a halving of the response which decreases naturally with age. This was exceeded at all time points post treatment, and so the criterion applies to the first and last of these, at 18 and 36 weeks post treatment.

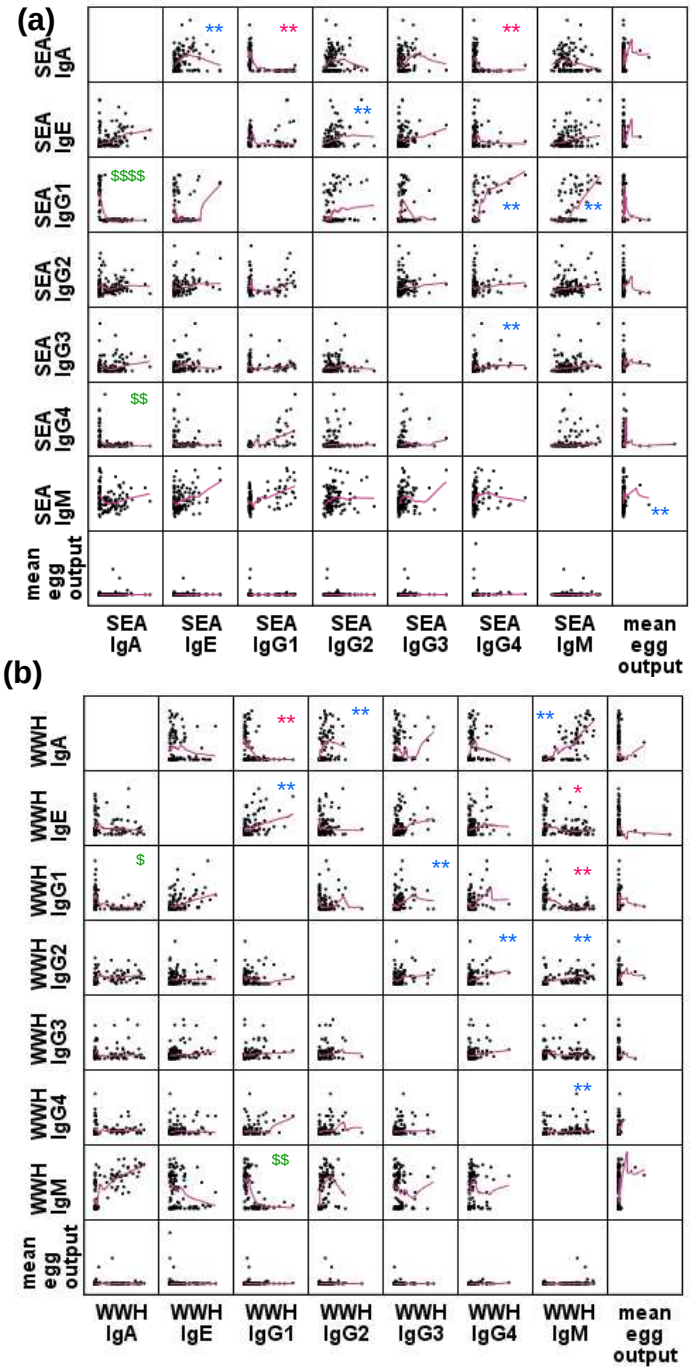

Figure 2.5: Co-distributions between different antibody isotypes directed against (a) SEA antigen (b) WWH antigen for Kaswa. Co-distribution of each antibody response with mean *S. haematobium* egg output is also shown. Upper-right half of graph: significant correlations marked. * $p < 0.05$, ** $p < 0.01$; red = negative correlation, blue = positive correlation. Lower-left half of graph: percentile cutoffs marked. Percentile: \$\$\$\$\$ = 65th, \$\$\$\$ = 70th, \$\$\$ = 75th, \$\$ = 80th, \$ = 85th. Pink lines are Loess lines fitted in SPSS, using 50% of points and an Epanechnikov kernel.

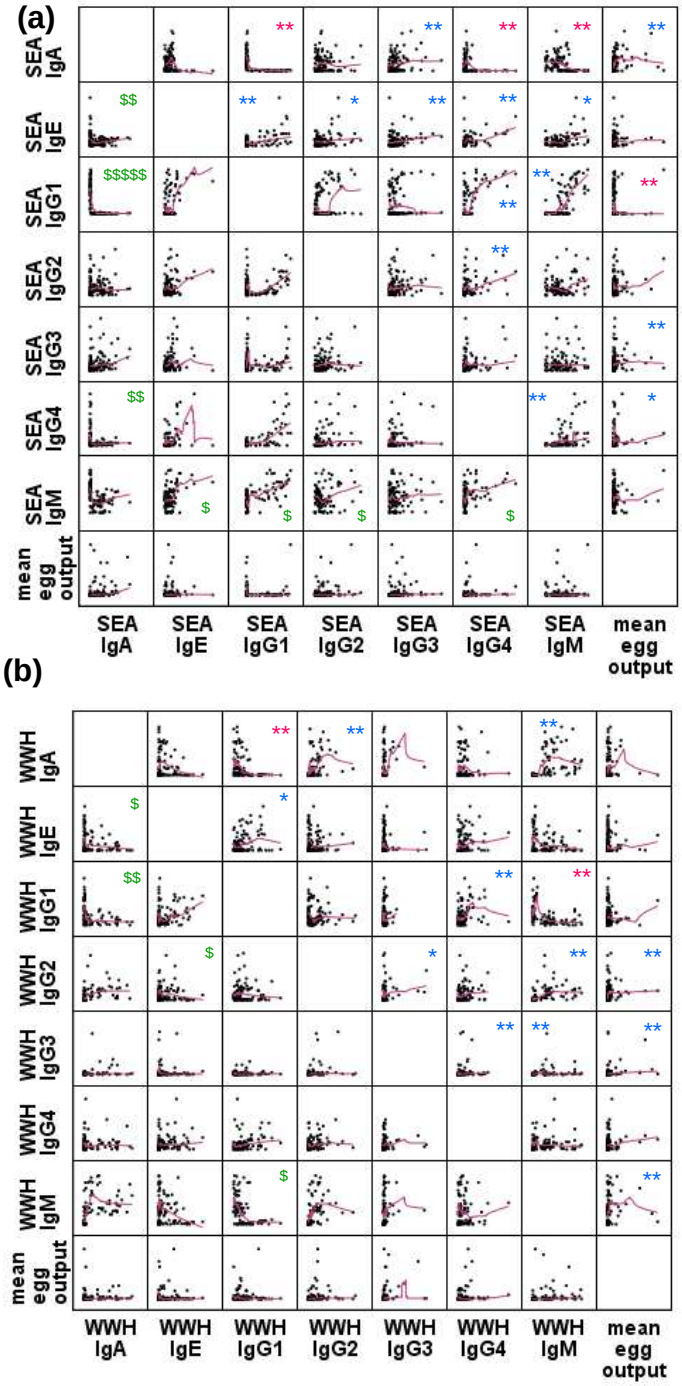

Figure 2.6: Co-distributions between different antibody isotypes directed against (a) SEA antigen (b) WWH antigen for Valhalla. Co-distribution of each antibody response with mean *S. haematobium* egg output is also shown. Upper-right half of graph: significant correlations marked. * $p < 0.05$, ** $p < 0.01$; red = negative correlation, blue = positive correlation. Lower-left half of graph: percentile cutoffs marked. Percentile: \$\$\$\$\$ = 65th, \$\$\$\$ = 70th, \$\$\$ = 75th, \$\$ = 80th, \$ = 85th. Pink lines are Loess lines fitted in SPSS, using 50% of points and an Epanechnikov kernel.

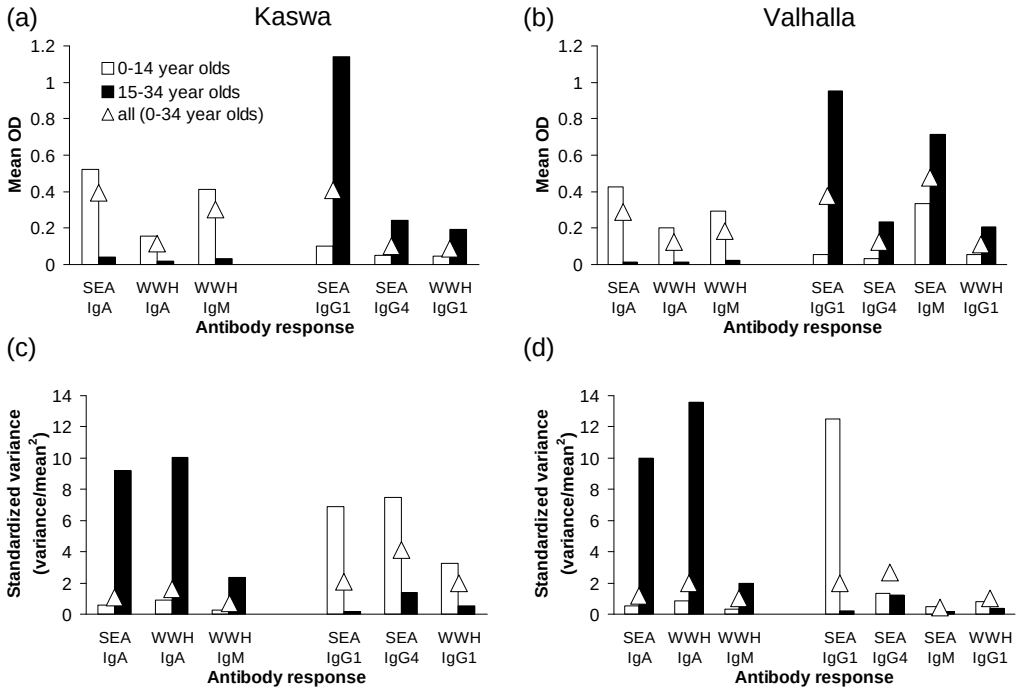

Figure 2.7: Changes in mean levels and standardized variances for antibodies which are negatively correlated with other isotypes, by two age groups in (a,c) Kaswa and (b,d) Valhalla. The left hand group of antibodies in each graph are those that decline with host age; the right hand group increase with host age.

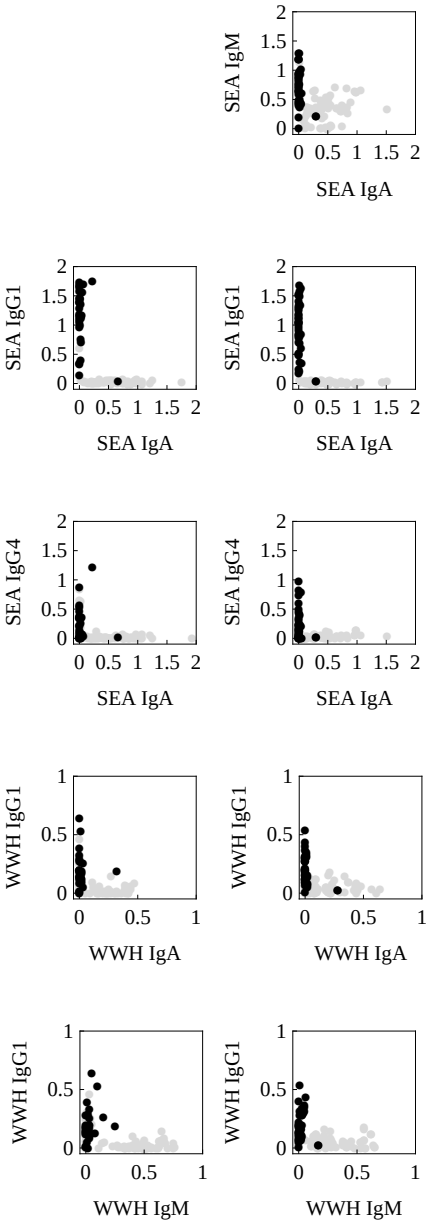

(a) Kaswa (b) Valhalla

Figure 2.8: Changes in co-distributions between antibodies for which a switch is seen by two age groups and altogether for (a) Kaswa and (b) Valhalla. Grey circles: 0–14 year olds, black circles: 15–34 year olds.

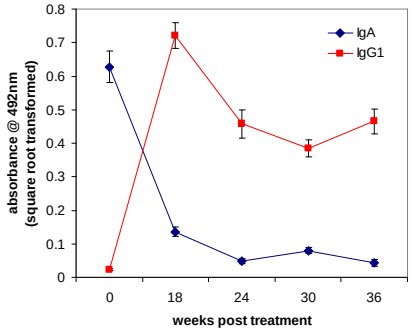

Figure 2.9: Changes in antibody levels after treatment. Levels of SEA IgA and IgG1 in a cohort of 6–15 year olds from Valhalla and Kaswa before treatment, and 18, 24, 30 and 36 weeks post treatment with praziquantel. Sample sizes were 73, 66, 61, 52 and 48 at 0, 18, 24, 30 and 36 weeks respectively. Data previously published in Mutapi *et al.* (1998).

2.4 Discussion

The analysis of infection curves for *S. haematobium* from original data sets and extracted from the literature gave a good estimate for the age range over which the infection peak is likely to occur. Although the use of different types of mean (arithmetic, geometric, including all individuals or only those positive for infection) can affect the apparent timing of the peak (Mutapi *et al.* 2003*a*), this was not expected to have a very dramatic effect, and estimates from studies using geometric means fell within the range of peak ages from studies using arithmetic means. Estimates for the ratio between adult and peak levels of infection were affected by the different means used, and these could not be combined across different types of mean as they gave substantially different answers. No clear pattern could be determined between this ratio and the age or height of the peak infection level, perhaps partly because of the noted instability of this ratio or because of the small number of datasets available for comparison. Earlier models of schistosome infection suggest that comparisons of adult infection levels between populations with different infection rates could give insight into the type of immunity that is acting (Woolhouse 1994*a*), and the ratios of infection level were expected to give similar information, but it was not possible to draw such conclusions from this limited dataset.

The different populations in this analysis showed different directions of change for standardized variance with age – previous studies of other parasite species have suggested that aggregation tends to decrease in older people (Quinnell *et al.* 1995), although earlier analyses of the Burma Valley data set and other data suggest a more complex pattern of aggregation with age for the schistosomes (Chan *et al.* 2000; Quinnell *et al.* 1995; Woolhouse *et al.* 1994). The small number of populations analysed here, and the limited sample sizes (meaning that more age groups could not be used), prevented a definitive conclusion from being drawn as to how infection aggregation varies with host age.

The antibody 'switch', previously reported from some of this data for IgA:IgG1 responses, was found between several other isotypes in the same dataset. A separate study from Zimbabwe (Ndhlovu *et al.* 1996*b*) reports correlations between isotypes which increase or decrease with age which closely match the patterns seen here (although different isotypes are involved). Unfortunately, we do not have access to the raw data for this study, but the patterns reported back up the idea that age-related antibody switches occur in different populations. Little

Table 2.2: Summary of quantitative model criteria drawn up on the basis of the data analysis described in this chapter

Criteria	**minimum level**	**maximum level**
Age of infection peak (years)	6	20
Level of infection in adults relative to the peak level (%)	0	40
Infection prevalence (%)	5	80
Infection intensity standardized variance	2	60
Antibody standardized variance	0.1	14
Spearman's correlation coefficient for antibody switch	-1.0	-0.2
Fold change in antibody responses at 18 and 36 weeks post-treatment compared with pre-treatment	2	∞

analysis of the distribution of schistosome-specific antibody responses has been previously published, beyond correlation analyses, and the observation that they are frequently aggregated (Mutapi & Roddam 2002; Ndhlovu *et al.* 1996*b*). The analyses here have confirmed that most antibody responses against schistosome antigen preparations are aggregated. A clear directional pattern in age-related changes in standardized variance was seen for antibodies involved in switching in the Burma Valley datasets (SV moving in the opposite direction to mean levels with age). No evidence of an antibody switch was seen in the data from Mutoko-Rusike; this may be because relatively few adults were included in this dataset, although it may point to limited robustness of this pattern in different infection settings.

Our attempt to find an alternative metric to characterize the antibody 'switch' met with limited success. While correlation analysis was not ideally suited to picking out what is really a dichotomous relationship, it performed better than the percentile cutoffs which had to be raised to very high levels (70-85%) to detect antibody switches. The drawback of using high percentile levels was that, for some of the populations, the probability of observing no exceptions by chance became unacceptably high. While it did give an alternative method of picking out strong dichotomies in the antibody data, correlation levels were used in subsequent analysis to choose model outputs which reproduced the antibody switch.

The analysis described in this chapter enabled me to draw up a list of quantitative criteria against which to test model outputs, with ranges or limits identified for the age of the infection peak, the ratio between adult and peak levels of infection, infection prevalence and standardized variance, standardized variance for antibody distributions and the correlation coefficient between isotypes involved in the antibody switch. These are all summarised in table 2.2.

Chapter 3

Explaining the slow development of protective antibody responses and observed infection profiles

Part of this work has been published (Mitchell *et al.* 2008), and a copy of the publication is included in appendix F.

3.1 Introduction

In human populations with endemic schistosomiasis, a characteristic age-intensity pattern is seen, with infection intensity (measured by egg output in faeces or urine) rising rapidly through the childhood years to peak in older children or teenagers (peaks have been recorded between 6–20 years of age for *S. haematobium* and between 12–25 years of age for *S. mansoni*), then falling again in adulthood (Clarke 1966; Fisher 1934; Fulford *et al.* 1992). The peak level of intensity is higher and occurs at a younger age in populations with a higher overall infection intensity when compared with areas of lower infection intensity, a phenomenon termed the 'peak shift' (Woolhouse 1998). It has also been observed that these peaks tend to be more convex (more sharply peaked) at higher levels of overall population infection intensity (Anderson & May 1991*a*; Fisher 1934). The peak shift is reproduced by simple mathematical models of acquired immunity, which assume that partial protective immunity develops as a function of infection level (Woolhouse 1992*b*). Protective immunity seems to develop slowly, as individuals endure chronic infection by long-lived adult worms, with frequent superinfection (Woolhouse & Hagan 1999).

I explored three hypotheses for the slow development of protective immunity: (1) immunosuppression by parasites (adult worms or cercariae); (2) that dying worms are the main source of protective antigen; and (3) an antigen threshold requirement for antibody production. The rationale and supporting evidence for these hypotheses is set out in more detail below. The aim of this study was to determine the effects of each of these mechanisms upon population-level patterns of infection and immunity, in particular whether they could significantly delay the development of protective immunity and delay the age at which infection intensity peaks. More quantitatively, I determined whether these models could reproduce age-intensity curves

falling within the limits set out in chapter 2, with a peak between the ages of 6 and 20 and levels of infection in adults being less than 40% of peak intensity levels. Additionally, I verified that the models were still able to reproduce the peak shift when infection rates were varied. Simple mathematical models of immunity were used building upon previous work by Woolhouse (1992*b*, 1993). I focussed upon representing antibody responses in the models, since these have frequently been associated with protection in schistosomiasis (Butterworth *et al.* 1996; Dunne *et al.* 1992*a*; Grzych *et al.* 1993; Hagan *et al.* 1991; Rihet *et al.* 1991) and have clearly defined cellular pathways leading to their production (Gray 2002). As in earlier models, a variety of potential antigen sources were considered: cercariae, live worms, and eggs, with dying worms also being considered as a distinct source of antigen. Protective antibody was assumed to mediate protection through either reducing reinfection, killing adult worms or reducing worm fecundity (Agnew *et al.* 1993; Smithers & Terry 1967). The proposed mechanisms were then introduced as detailed below.

3.1.1 Immunosuppression

As detailed in chapter 1 (section 1.7.1), there is substantial evidence that schistosomes are able to modulate the host immune response, suppressing specific immune responses (Maizels & Yazdanbakhsh 2003). Antigen-specific proliferation and cytokine production are reduced in chronic human infection (Grogan *et al.* 1998*a*; King *et al.* 1996), and the extent of this suppression is related to infection intensity (de Jesus *et al.* 1993; Grogan *et al.* 1998*a*). These responses are restored by praziquantel treatment (Grogan *et al.* 1996; van den Biggelaar *et al.* 2004), suggesting that suppression may be related to worm burden. Murine studies have also demonstrated that cercariae can downregulate local host immune responses (Jenkins *et al.* 2005), and recently it has been suggested that cercariae can also modulate systemic responses to schistosomes (A.M. Mountford pers. comm.)

Suppression was included in the model alongside protective antibody responses, acting to reduce these responses, so having the effect of increasing the rate of superinfection, increasing worm survival or increasing worm fecundity, up to the levels seen in the absence of protective immunity. Suppression was incorporated as a function of cercarial exposure or alternatively as a function of current worm burden, which reflects the correlation seen between suppression and infection intensity. In contrast to protective responses, suppression was assumed to have no immune memory, as it is lifted by chemotherapy (Colley *et al.* 1986; Grogan *et al.* 1996).

3.1.2 Dying worms

As discussed more fully in section 1.7.2, this hypothesis arises from the observation that antibody changes that occur naturally in older children can be speeded up by praziquantel treatment (Mutapi *et al.* 1998, 1997). Praziquantel kills adult worms, exposing the immune system to previously hidden antigens. It is hypothesised that in natural infection, this exposure is delayed for a number of years by the long worm life span (Woolhouse & Hagan 1999). Responses generated by these adult antigens are expected to act against shared epitopes on invading cercariae, or expressed at low levels on the worm surface. It is proposed that the immune system has insufficient exposure to these antigens, either due to reduced expression level (on cercariae or adult worms) or short exposure time (to cercariae), to form a protective response prior to worm death (Fitzsimmons *et al.* 2007; Woolhouse & Hagan 1999).

The life span of adult schistosomes in their human hosts has been estimated at between 3 and 10 years from studies with interrupted transmission (Goddard & Jordan 1980; Vermund *et al.* 1983; Warren *et al.* 1974; Wilkins *et al.* 1984). The distribution of worm survival times, as well as the mean survival time, is expected to affect the timing of exposure to antigen from dying worms, but the distribution of schistosome survival times has not yet been characterised.

Dying worms were incorporated into the model as an additional source of antigen, assumed to be proportional to the instantaneous number of worms killed, since the released antigens are not expected to stay in the body for a long period of time after worm death. Different worm survival curves were used to test their impact upon the timing of the peak and the peak shift.

3.1.3 Antigen threshold

It has been proposed that individuals must be exposed to a certain threshold level of schistosome antigen before they begin to mount a protective immune response (Mutapi *et al.* 2008; Woolhouse & Hagan 1999). This is supported by evidence from a cross-sectional survey in a population with endemic *S. haematobium* infection that increased numbers of worm antigens are recognised by sera from groups with greater experience of infection (Mutapi *et al.* 2008). The basis for this hypothesis is discussed in section 1.7.3. This antigen threshold might be supposed to rely upon current levels of antigen or cumulative exposure to antigen. B and T cells both need minimum threshold levels of receptor binding in order to be activated (Carter & Fearon 1992; Viola & Lanzavecchia 1996), which could be a mechanism for how a threshold based upon current levels of antigen might work. A requirement for a threshold level of cumulative antigen exposure could represent a succession of repeated T cell activation and expansion events, with T cell polarisation leading to an eventual change in the cytokine environment, which can alter the antibody isotypes which are made.

Antigen thresholds were included in the model as levels of either current or cumulative antigen exposure which needed to be exceeded in order for an antibody response to be initiated.

Analysis framework for chapter 3

- The aim of the analysis in this chapter is to explore different hypotheses to explain the delay seen in the development of protective antibody against schistosome infection:
  - Immunosuppression
  - Dying worms
  - Antigen threshold
- Models are tested for their ability to pass the infection intensity criteria:
  - Peaked age infection curve (peaking in the right age range) with sufficient reduction of infection in adults relative to the peak
  - Peak shift between areas with different rates of infection
- Deterministic models are used which describe mean population infection intensity and a single protective antibody response, enabling the model to be tested against all of the above criteria, and to look at the timing of the antibody response.
- The level of suppression is assumed to be proportional to either the current number of live worms, or current exposure to cercariae. This may represent either parasite-derived homologues of immune mediators or host-derived mediators produced in response to the parasite. (Suppression at a constant level irrespective of infection level is considered but is indistinguishable from a weaker antibody response in this framework). An alternative approach which was not taken here would be to explicitly model the cells and cytokines involved in suppression.
- As part of the dying worms hypothesis
  - Different stages of the lifecycle are compared as the source of protective antigen (cercariae, live worms, dying worms, eggs) - the timing of exposure to each stage is expected to differ, with possible effects upon the timing of the immune response.
  - Different worm survival distributions are explored (as these will affect the timing of exposure to dying worms): for fixed worm survival, a delay differential equation is used; for non-exponential worm survival, multiple identical adult worm compartments are used
- Additionally, different structures for the immune mechanisms are included, to check whether they affect the results:
  - Plasma cell populations only, without an explicit memory cell population
  - Plasma cells and a memory cell population (under the assumption that memory cells must be antigenically stimulated to maintain the plasma cell population)
  - An upper limit is placed on the number of memory cells, as the model includes direct antigen-driven (exponential) expansion of the memory cell population, which can lead to an infinite population of memory cells; no limit is placed upon the size of the plasma cell population, since their expansion is independent of the plasma cell population size in these models.

3.2 Methods

A mathematical model consisting of a set of differential equations was developed, building upon previous models of schistosome immunity (Woolhouse 1992*b*, 1993) and of immune memory development (Wilson & Nokes 1999; Wilson *et al.* 2007). Two main immune model structures were explored: one including a single population of plasma cells, and the other including both

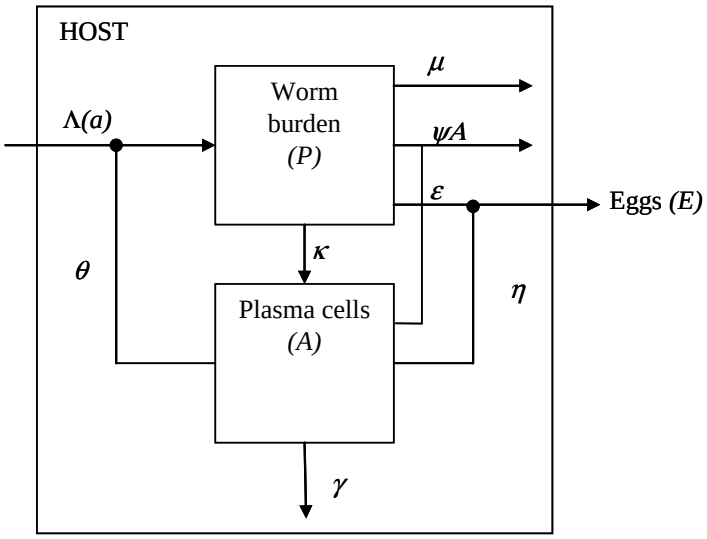

Figure 3.1: Schematic diagram of the baseline model, showing the main state variables, worm burden (P) and plasma cells (A), with production of eggs (E). The model is shown with a single worm compartment (n = 1), which gives exponential worm survival, for clarity. Multiple worm compartments are shown in figure 3.2. The antibody response shown here is triggered by live adult worms, but can also be triggered by cercariae, dying worms or eggs. All three possible antibody targets are shown, although only one will be active at a time. θ and η determine the strength of the anti-reinfection and anti-fecundity responses via an exponential function, and ψ governs the rate of immune-induced death of adult worms. All parameters are defined in table 3.1, with parameter values given.

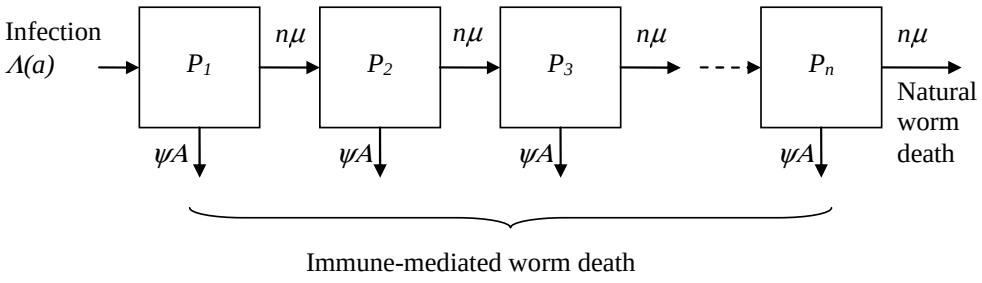

Figure 3.2: Schematic diagram of the multi-compartment worm model, used to alter the natural worm survival curve. n individual compartments are shown, with worms moving through these at a constant rate, $n\mu$, and dying as they leave the last compartment. When the immune response increases the rate of worm death, worms leave each compartment at a rate ψA. All parameters are defined in table 3.1, with parameter values given.

plasma and memory B cell populations. The main antigenic stimulus for an immune response was assumed to be provided by one of four different stages of the worm life cycle: cercariae, live worms, dying worms or eggs. The antibody response was assumed to target a single part of the worm life cycle: reducing re-infection, increasing worm death rate or reducing worm fecundity. The full baseline model is presented first, with modifications for explicit memory responses, fixed worm survival, suppression and antigen thresholds described in subsequent sections. The models are shown schematically in figures 3.1, 3.2 and 3.3 and the equations describing the model are given in the following text. Parameters are defined in detail in table 3.1.

3.2.1 Baseline model

The structure of the baseline model is shown schematically in figure 3.1. The model describes a homogeneous endemic population all experiencing the same age-related rate of infection, which changes with age according to equation 3.1. Contact rates are assumed to increase linearly from zero at birth up to a maximum level (Λ_m), reached at age a_c. Above this age, contact rates remain constant. Individual worm burden (P) is modelled using n compartments (equation 3.2), where i is the compartment number ($i = 1, ..., n$), shown in figure 3.2. Worm burden changes with host age according to an immigration-death process, with age-related infection rate, $\Lambda(a)$, and worm death rate, μ, modified by the immune response. Worms enter the first worm compartment at a rate $\Lambda(a)$, which is reduced if an anti-larval antibody response is present. The level of protection against re-infection is modelled as a decreasing exponential function of the number of plasma cells. It is assumed that antibody levels are directly proportional to the size of the plasma cell population, and that the level of protection is determined by the antibody titre. The strength of the anti-larval response is determined by the parameter θ, and this response reduces the rate of infection by a factor of $e^{-\theta A(a)}$, which scales between 0 and 1 (equation 3.2). Models with exponential worm life span have a single worm compartment ($n = 1$), and have a constant per-capita rate of natural worm death, μ, following the equation for $i = 1$ (equation 3.2). Where multiple worm compartments are used to model non-exponential worm life span ($n > 1$), the first part of equation 3.2, for $i = 1$, describes the first worm compartment and the second part of the equation (for $1 < i \leq n$) describes all subsequent worm compartments. Worms are assumed to pass through the compartments at a constant rate, $n\mu$, dying naturally (in the absence of an immune response) when they leave the final (n^{th}) compartment, so that the rate of natural death is given by $n\mu P_n(a)$. Anti-worm immunity is modelled here as a separate additional worm per-capita death rate, directly proportional to the number of plasma cells, scaled by a factor ψ, which applies equally to all worm compartments (equation 3.2). The number of eggs exiting the body in urine (E) is assumed to be directly proportional to the total worm burden (equation 3.3). Anti-fecundity immunity is modelled as a decreasing exponential function of the number of plasma cells, with strength η, and reduces the number of eggs produced by the total worm population by a factor of $e^{-\eta A(a)}$ (equation 3.3). The effector response is modelled as a single compartment (A) representing a population of plasma cells, which secrete antibody at a constant rate (equivalently this compartment may represent a memory B cell population with constant antigen-independent production of very short-lived plasma cells)(equation 3.4). This population is assumed to increase at a rate directly proportional to antigen exposure (G), with relative strength of increase κ, and is assumed to decay at a constant per-cell rate γ. Antigen (G) comes from cercariae, live adult worms,

dying adult worms or eggs (equation 3.5). Note that, in the case where dying worms stimulate protective antibody and this antibody increases worm death, there is a direct positive feedback term (equation 3.5). The antibody response is assumed to have a single antigen and a single target in this model.

$$\Lambda(a) = \begin{cases} \Lambda_m \frac{a}{a_c} & \text{if } a < a_c, \\ \Lambda_m & \text{if } a \geq a_c. \end{cases} \tag{3.1}$$

$$dP_i(a)/da = \begin{cases} \Lambda(a)e^{-\theta A(a)} - (n\mu + \psi A(a))P_i(a) & \text{for } i = 1, \\ n\mu P_{i-1}(a) - (n\mu + \psi A(a))P_i(a) & \text{for } 1 < i \leq n. \end{cases} \tag{3.2}$$

$$E(a) = \sum_{i=1}^{n} P_i(a)e^{-\eta A(a)} \tag{3.3}$$

$$dA(a)/da = \kappa G(a) - \gamma A(a) \tag{3.4}$$

$$G(a) = \begin{cases} \Lambda(a) & \text{for cercarial antigen,} \\ \sum_{i=1}^{n} P_i(a) & \text{for live adult worm antigen,} \\ n\mu P_n(a) + \sum_{i=1}^{n} P_i(a)\psi A(a) & \text{for dying adult worm antigen,} \\ E(a) & \text{for egg antigen.} \end{cases} \tag{3.5}$$

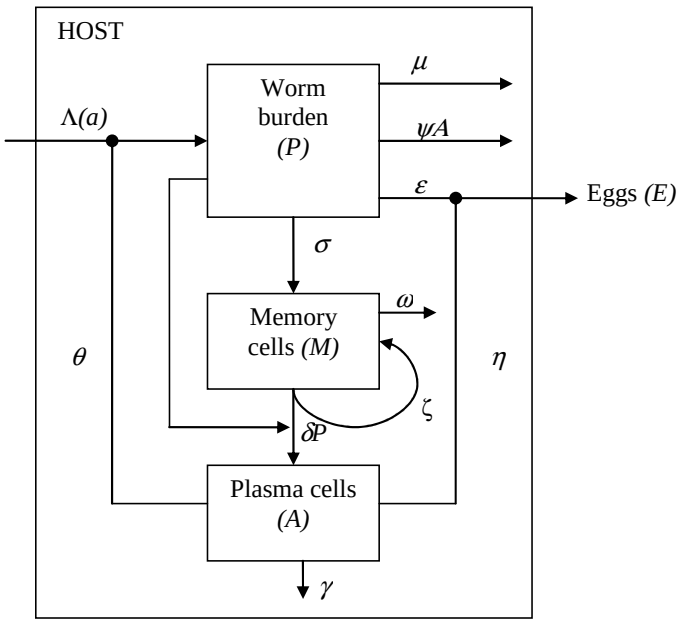

Figure 3.3: Schematic diagram of the memory model, showing the main state variables, worm burden (P), memory cell population (M) and plasma cells (A), with production of eggs (E). The memory and antibody responses shown here are triggered by live adult worms, but can also be triggered by cercariae, dying worms or eggs (with the same antigen triggering both memory and antibody). Plasma cells are produced by activation of memory cells by antigen, at a rate governed by the parameter δ. Antigen-driven memory expansion occurs at a rate ζ. Other details are as in figure 3.1. All parameters are defined in table 3.1, with parameter values given.

3.2.2 Memory model

The structure of the memory model is shown schematically in figure 3.3. For models with an explicit memory response, the memory cell population (M) changes with age as described by equation 3.6 and the plasma cell population (A) now changes with age as described in equation 3.7. The memory cell population is assumed to grow in two ways, firstly through antigen-dependent activation of naïve cells (at a rate directly proportional to antigen exposure, with relative strength σ), and secondly through antigen-dependent proliferation of the memory compartment (at a rate proportional to both the level of antigen and the current level of memory, with relative strength ζ). As before, antigen exposure refers to one single antigen source, with the same source for both the memory and antibody responses (equation 3.5). A maximum limit (K_M) is placed upon the size of the memory cell population, with the overall rate of memory cell expansion through either route limited via the density dependent function $(1 - M(a)/K_M)$. The memory cell population decays at a constant per-cell rate ω. The plasma cell population is now assumed to grow principally through antigen-dependent activation of the memory cell population, and decays at a rate proportional to the plasma cell population size (equation 3.7). As before, the effects of immunity on the infection process are directly mediated by the plasma cell population (with no direct effect of memory), and the equations describing the infection processes are the same as for the earlier model (equations 3.1, 3.2, 3.3 and 3.5).

$$dM(a)/da = (\sigma G(a) + \zeta M(a)G(a))\frac{1 - M(a)}{K_M} - \omega M(a) \tag{3.6}$$

$$dA(a)/da = \delta G(a)M(a) - \gamma A(a) \tag{3.7}$$

3.2.3 Fixed worm survival

An alternative model with fixed worm survival was developed. This model uses a single compartment for worms, with worms leaving this compartment a fixed time interval $(1/\mu)$ – equivalent to the worm life span – after they enter (equation 3.8). The number of dying worms is now calculated as the death rate under this new formulation (equation 3.9). Infection rates, egg output, exposure to other antigens and the development of antibody are all calculated as before (3.1, 3.3, 3.4 and 3.5). Note that with fixed worm survival represented in this way there is no straightforward way to include immune-mediated worm death, and so only anti-larval and anti-fecundity responses are considered in this version of the model.

$$dP(a)/da = \Lambda(a)e^{-\theta A(a)} - \Lambda(a-(1/\mu))e^{-\theta A(a-(1/\mu))}H(a-(1/\mu)) \tag{3.8}$$

$$G(a) = \Lambda(a-(1/\mu))e^{-\theta A(a-(1/\mu))}H(a-(1/\mu)) \quad \text{for dying worm antigen} \tag{3.9}$$

where H is the Heaviside step function (H = 0 when $(a-(1/\mu)) < 0$, H = 1 when $(a-(1/\mu) \geq 0)$.

3.2.4 Suppression

The level of suppression is assumed to be directly proportional to either current worm burden or cercarial exposure (equation 3.10), and is then assumed to reduce the rate at which a protective antibody response is made through an exponential function which scales the effect of suppression to between 0 and 1, with strength ν (equation 3.11). The equations describing infection levels and the different antigens remain the same (3.1, 3.2, 3.3 and 3.5). Alternative versions of the suppression model are also considered, allowing suppression to reduce the effects of protective antibody (rather than reducing its production), and using alternative functions to the exponential to scale both the strength of the antibody response and the strength of suppression (Mitchell *et al.* 2008). In order to assess the likely outcomes if worms only suppress anti-worm responses (enhancing their own survival but not suppressing responses to incoming larvae), the antibody response is allowed to have two simultaneous targets (anti-reinfection and increased worm death), with suppression of only the anti-worm activity (Mitchell *et al.* 2008).

$$S(a) = \begin{cases} \Lambda(a) & \text{for cercarial-related suppression} \\ \sum_{i=1}^{n} P_i(a) & \text{for adult worm-related suppression} \end{cases} \tag{3.10}$$

$$dA(a)/da = \kappa G(a)e^{-\nu S(a)} - \gamma A(a) \tag{3.11}$$

3.2.5 Antigen thresholds

Antigen thresholds are introduced as levels of antigen exposure (either current or cumulative) which must be exceeded before an antibody response can be mounted. Antigen thresholds are included in three different ways. Firstly, a 'fixed current' antigen threshold based upon the current level of antigen exposure and remaining at a constant level (T_1) is introduced (3.12 and 3.13). For this version of the antigen threshold model, any antigen experienced over and above the antigen threshold level (T_1) is able to stimulate a protective antibody response, as before. Secondly a 'dropping current' antigen threshold (T_2) is used, for which again the antigen threshold is based upon the current level of antigen exposure (equation 3.12), but as soon as an antibody response has been stimulated, the antigen threshold is removed (set to 0), so that any antigen encountered subsequently can stimulate a protective response (equation 3.14).

$$dA(a)/da = \begin{cases} \kappa(G(a) - T) - \gamma A(a) & \text{if } G(a) \geq T, \\ -\gamma A(a) & \text{if } G(a) < T. \end{cases} \tag{3.12}$$

$$\text{For a fixed current antigen threshold } T = T_1 \tag{3.13}$$

$$\text{For a dropping current antigen threshold } T = \begin{cases} T_2 & \text{if } A(a) = 0, \\ 0 & \text{if } A(a) > 0. \end{cases} \tag{3.14}$$

where T_1 and T_2 are constants.

Finally, a cumulative antigen threshold is used, where a separate equation is added to the model to record cumulative exposure to antigen (C), with this cumulative exposure building up at a rate directly proportional to the level of antigen, with relative strength β (equation 3.15). If the level of cumulative exposure exceeds the antigen threshold, antibody is made at a rate proportional to current antigen levels (equation 3.16).

$$C(a) = \beta G(a) \tag{3.15}$$

$$dA(a)/da = \begin{cases} \kappa G(a) - \gamma A(a) & \text{if } C(a) \geq T_3, \\ -\gamma A(a) & \text{if } C(a) < T_3. \end{cases} \tag{3.16}$$

where T_3 is a constant.

3.2.6 Model analysis

For all models, all of the possible pairwise combinations of antigen stimulus (cercariae, live worms, dying worms or eggs) and target (reduced re-infection, increased worm death or reduced fecundity) were used in turn. Worm survival was varied (varying the number of worm compartments or using the fixed survival equation) to assess its effects on the age-intensity curve and the level of protective antibody, and the rate of infection was varied to assess the robustness of the peak shift in these models. Parameters governing the strength and decay rates of the immune responses and worm survival were varied to see whether the infection criteria identified in chapter 2 could be met (with the peak occurring between ages 6 and 20, and the level of infection in adults aged 34 being less than 40% of the peak level). For the memory models,

Table 3.1: Parameters used in the models, with initial values, ranges explored, units and sources from the literature where relevant. Antigen units = number of cercariae/live worms/dying worms/eggs as appropriate. 'Cell' refers to units of the plasma cell or memory cell populations.

Parameter	Meaning	Initial value	Range explored	Units	Source/rationale
Λ_m	Maximum rate of infection	50	12.5–200	worms year $^{-1}$person^{-1}	Chan *et al.* (2000)
a_c	Age above which contact rates stay constant	7.8	-	years of age	Chan *et al.* (2000)
n	Number of worm compartments in model	9	1–100	compartments	worm survival distribution exponential for $n = 1$, approximately Gaussian for $n = 9$, approaches fixed for $n = 100$.
$1/\mu$	Natural average worm life span	6.5	3-10	years	Fulford *et al.* (1995); Wilkins *et al.* (1984)
θ	Strength of protection against reinfection	0.016	0.00025–1.024	cell^{-1}	broad range used to find values giving realistic peaked infection curve
ψ	Strength of immune-mediated worm killing	0.016	0.00025–1.024	cell^{-1}	broad range used to find values giving realistic peaked infection curve
η	Strength of anti-fecundity response	0.016	0.00025–1.024	cell^{-1}	broad range used to find values giving realistic peaked infection curve
κ	Rate of production of plasma cells	1	-	cells year^{-1} unit antigen^{-1}	variation accounted for in varying immune strength
γ	Rate of loss of plasma cells	0.08	0.008–80	year^{-1}cell^{-1}	Amanna *et al.* (2007); Ochsenbein *et al.* (2000)
σ	Rate of production of memory B cells	1	-	cells year^{-1} unit antigen^{-1}	variation accounted for in varying immune strength
ζ	Rate of antigen-driven expansion of memory cells	0.01	0.01–0.1	cells year^{-1} unit antigen^{-1} memory cell^{-1}	set to give significant expansion
K_m	Maximum size of memory population	1000	-	cells	set to limit memory cell growth
ω	Rate of loss of memory B cells	0.08	0.008–80	year^{-1}cell^{-1}	Amanna *et al.* (2007); Macallan *et al.* (2005)
δ	Rate of production of plasma cells from antigen-driven memory cell activation	1	-	cells year^{-1} unit antigen^{-1} memory cell^{-1}	variation accounted for in varying immune strength
ν	Strength of suppression	0.1	0.01–1.0	unit antigen^{-1}	set to give significant suppressive effect
T_1	Antigen threshold level for fixed current antigen threshold model	200	100–400	antigen units	set to give significant effect on age-intensity curve
T_2	Initial antigen threshold level for dropping current antigen threshold model	200	100–400	antigen units	set to give significant effect on age-intensity curve
T_3	Antigen threshold level for cumulative antigen threshold model	2000	1000-4000	antigen units	set to give significant effect on age-intensity curve
β	Rate of production of 'cumulative' response	1	-	arbitrary units year^{-1} unit antigen^{-1}	arbitrary constant

simulations were first run using variable memory survival and short-lived plasma cells (with a mean life span of 5 days), without antigen-driven memory expansion, then also allowing variable plasma cell survival, with and without antigen-driven memory expansion. For the suppression models, the strength of suppression was varied to assess the effects upon the age-intensity curve, and in antigen threshold models, the level of the antigen threshold was varied. For models with immune-mediated worm death, the impact of immunity upon average worm life span was also assessed, where the average worm life span (L) is calculated according to equation 3.17.

$$L(a) = \left(\frac{1}{n\mu + \psi A(a)}\right) \sum_{i=1}^{n} \left(\frac{n\mu}{n\mu + \psi A(a)}\right)^{i-1} \tag{3.17}$$

Equations were solved numerically using a variable time step embedded fifth-order Runge-Kutta algorithm with Cash-Karp parameters (Press *et al.* 2002), using either Berkeley Madonna version 8.3.14 © or an adapted version of the rkqs routine from Press *et al.* (2002), implemented in C++.

3.3 Results

3.3.1 Baseline model

For the baseline model (without explicit memory responses, suppression or antigen threshold included), the peaked infection curve and the peak shift could both be reproduced for every combination of antigen and antibody target. Examples are shown for two combinations in figure 3.4. The curves shown fit within all of the infection criteria identified in field data in chapter 2: the age of peak infection intensity was between 6 and 20 years, the level of infection in adults (aged 34) was less than 40% of the peak level of infection, and a peak shift was seen when the rate of infection was changed – as the rate of infection increased, the level of peak intensity was raised and occured at an earlier age. These patterns could all be replicated for some parameter values (within the ranges in table 3.1) for all combinations of antigen and target for the antibody response for the baseline model, regardless of which worm survival curve was used.

3.3.2 Memory models

For the memory models, it was found that the peaked infection curve and peak shift could be reproduced for each combination of antigen and antibody target. Using a stricter requirement, that these models reproduce an age-infection curve with the peak occurring between the ages of 6–20 years old and infection level at age 34 $<$ 40% of the peak level, it was found that plasma cell decay rates determined whether or not this was possible for all antigen:antibody target combinations. With memory cell decay rates allowed to vary over their full range (given in table 3.1), but plasma cell decay rates fixed at a rapid rate of 80 year^{-1}, models with cercariae-triggered anti-fecundity, live worms-triggered anti-worm and eggs-triggered anti-fecundity responses were unable to meet this stricter requirement. If plasma cell decay rates were allowed to vary over the full range given in table 3.1 then these models could also meet these criteria.

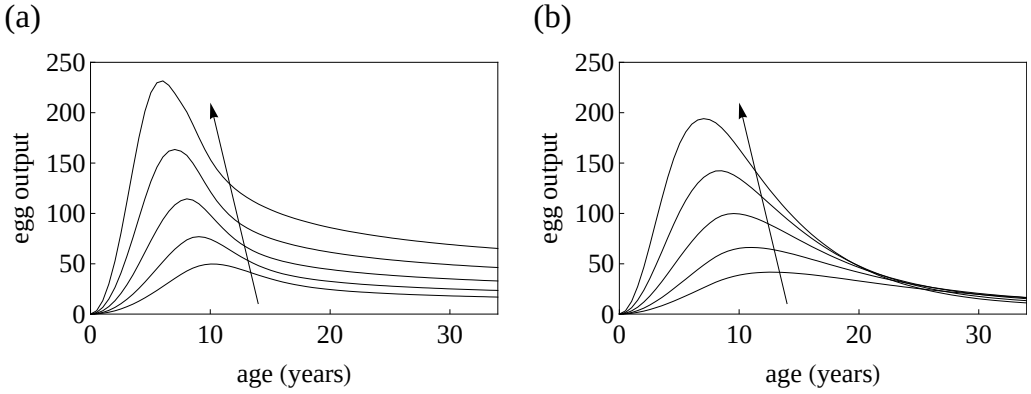

Figure 3.4: Age-infection profiles and peak shift in two permutations of the baseline model without explicit memory cells, suppression or antigen thresholds included. Egg output is shown changing with age for the following values of Λ_m (maximum rate of infection) from bottom to top (with arrow): 12.5, 25, 50, 100, 200. (a) Antigen: live worms; antibody target: increased worm death. $n = 9$, $1/\mu = 10$, $\psi = 0.001$, $\kappa = 1$, $\gamma = 0.008$. (b) Antigen: dying worms; antibody target: reduced re-infection. $n = 1$, $1/\mu = 6.5$, $\theta = 0.016$, $\kappa = 1$, $\gamma = 0.008$. (All parameters fully defined with units in table 3.1.)

3.3.3 Suppression

When suppression was included, then increasing the strength of suppression (by increasing ν) raised the level of the peak parasite burden and delayed the age at which the peak occurred until, when suppression was sufficiently strong, the age-intensity curve tended towards the monotonically increasing immigration-death curve seen when there was no resistance at all (figure 3.5a). The simultaneous effect that increasing suppression had upon the level of protective antibody is shown in figure 3.5b. Increasing suppression delayed the development of a protective antibody response and also reduced the final level of antibody produced. At the higher levels of suppression explored, the protective response did not develop at all. These patterns seen in both infection and antibody profiles with increasing suppression remained the same regardless of the antigen and target of the protective immune response. Suppression also affected the peak shift. For a constant strength of worm-induced suppression, the peak shift could still be observed at the lowest rates of infection, but as the rate of infection increased, the peak shift was reversed, before complete loss of the peaks occurred at the highest infection intensity levels (figure 3.6). Removal of the peak at the highest infection intensity corresponded with almost complete prevention of acquired immunity developing. The same qualitative patterns were seen if suppression was assumed to reduce the effects of protective immunity, rather than reduce its production (Mitchell *et al.* 2008).

If suppression was assumed to be mediated by cercariae rather than adult worms, similar results were seen – suppression delayed the development of protective antibody, but with high strength of suppression or high infection rates, suppression overwhelmed the protective response, removing the infection peak. If the antibody response was assumed to have two targets, with suppression of only one part of the response, then increasing the strength of suppression raised the height and delayed the age of the peak, but could not remove it altogether. The peak shift did not always remain if the suppressed response had a much greater strength than the unsuppressed response, but so long as part of the protective response was not suppressed, some degree of infection control was still achieved in adults.

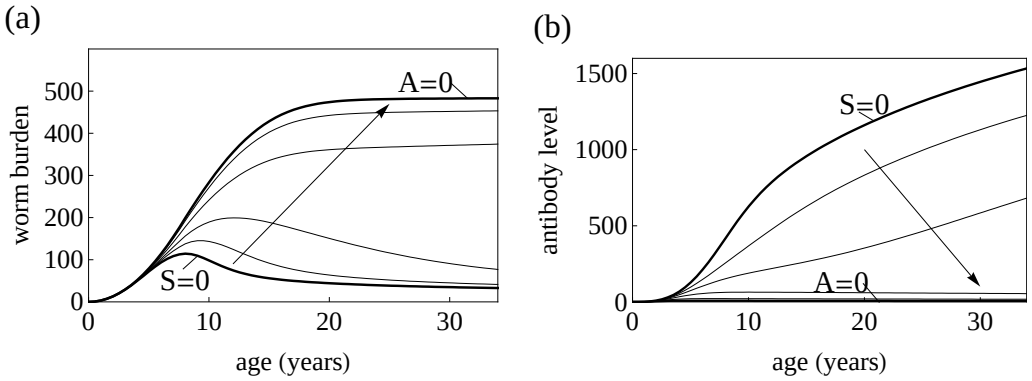

Figure 3.5: The effect of increasingly severe worm-induced suppression upon (a) egg output and (b) levels of protective antibody. Changing levels with age are shown for both. Antigen: live worms; antibody target: increased worm death. n = 9, $\Lambda_m = 50$, $1/\mu = 10$, $\psi = 0.001$, $\kappa = 1$, $\gamma = 0.008$. Bold lines indicate no suppression (S = 0) and no antibody response (A = 0) as marked. Lines in between are for increasing strength of suppression, ν (in direction of arrow): 0.00625, 0.0125, 0.025, 0.05, 0.1. (All parameters fully defined with units in table 3.1.)

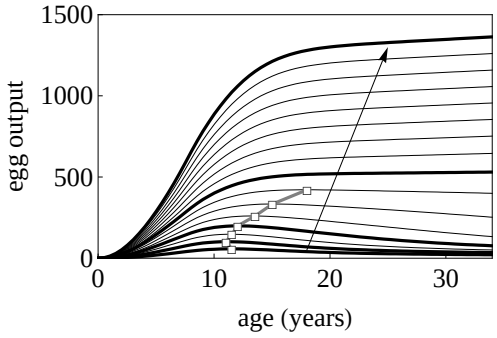

Figure 3.6: The effect of suppression on the peak shift. Egg output is shown changing with age with increasing Λ_m, which increases with the direction of the arrow. Bold infection curves are for Λ_m = 12.5, 25, 50, 100, 200, for comparison with figure 3.4a. Remaining infection curves are for increasing Λ_m from 12.5 to 200 in steps of 12.5. Antigen: live worms; antibody target: increased worm death. n = 9, $1/\mu = 10$, $\psi = 0.001$, $\kappa = 1$, $\gamma = 0.008$, $\nu = 0.0125$. (All parameters fully defined with units in table 3.1.) The trend of the peak shift is highlighted in white squares joined by a grey line.

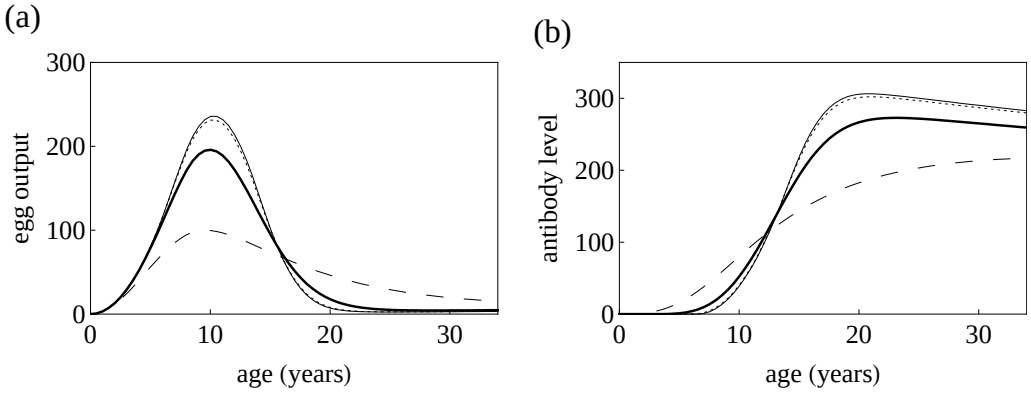

Figure 3.7: The effect of changing the worm survival curve upon (a) egg output and (b) levels of protective antibody. Changing levels with age are shown for both. Antigen: dying worms; antibody target: reduced re-infection, $1/\mu = 6.5$, $\theta = 0.016$, $\kappa = 1$, $\gamma = 0.008$. (All parameters fully defined with units in table 3.1.) Different worm survival curves: dashed line: n = 1 (exponential worm survival), bold line: n = 9 (approximately Gaussian distributed survival), dotted line: n = 100 (approaching fixed worm survival); solid narrow line: fixed worm survival.

Using alternative functions (linear or a Gumbel function) to scale the strength of protective antibody or suppression did not change any of the predicted trends for this model (Mitchell *et al.* 2008).

3.3.4 Dying worms and worm survival

Dying worms were included as one possible source of antigen in the model, to see whether they gave predicted patterns of infection and antibody which were distinct from other potential antigen sources (cercariae, live worms or eggs). Since the antigenic stimulus was assumed to be directly proportional to the current rate of worm death, in the case where worm survival was assumed to be exponentially distributed and there was no immune-mediated worm killing, the rate of worm death was directly proportional to the current number of live worms and there was no mathematical difference between live or dying worms as an antigenic stimulus. However, if other worm survival curves were used, or there was immune-mediated worm death, then worm death was no longer directly proportional to the number of live worms and exposure to dying worms had a different distribution with host age.

Figure 3.7 shows how different worm survival curves altered the age-intensity profiles for both infection and protective antibody when the protective response was assumed to be triggered by dying adult worms. As the survival curve was changed progressively from exponential to fixed (increasing the number of worm compartments and then using the alternative equation for fixed worm survival), the peak occurred at a later age and a higher level, with the final level of infection in adults always settling to the same level regardless of worm survival (note that this level is reached some time after the age of 34 for the curves shown in figure 3.7a). For models with antibody stimulated by dying worm antigen, as the survival curve was changed progressively from exponential to fixed, the development of the protective antibody response was delayed (figure 3.7b), although antibody levels eventually settled at the same stable level regardless of worm survival if the models were run for long enough. Different worm survival curves did not remove the peak shift, but could change its relative 'shape' (figure 3.8). Keeping all other parameters constant, moving from exponential to fixed worm survival increased the

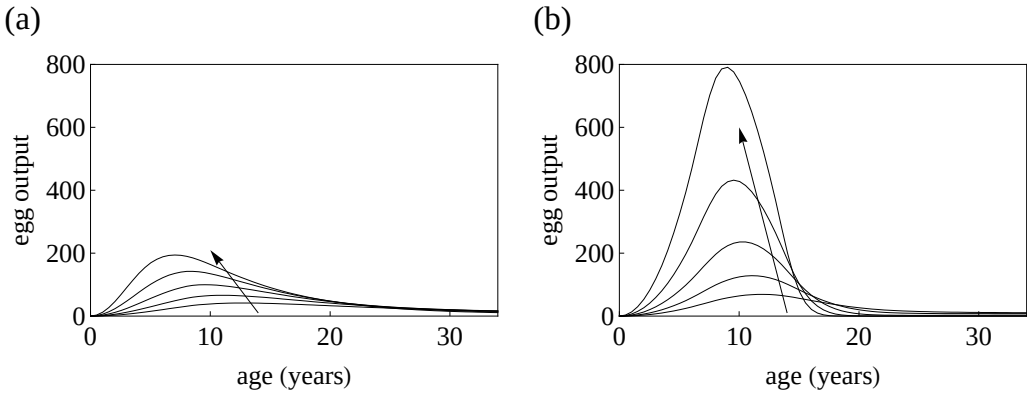

Figure 3.8: The effect of altering the worm survival curve upon the peak shift. (a) Exponential worm survival (n = 1) (same data as in figure 3.4b), (b) fixed worm survival. For both panels, antigen: dying worms; antibody target: reduced re-infection, $1/\mu = 6.5$, $\theta = 0.016$, $\kappa = 1$, $\gamma = 0.008$. Egg output is shown changing with age for the following values of Λ_m (maximum rate of infection) from bottom to top (with arrow): 12.5, 25, 50, 100, 200. (All parameters fully defined with units in table 3.1.)

range of peak infection levels seen over the same range of infection rates, but reduced the range of ages over which peaks occurred.

Changing the worm survival curve could also affect the age-infection curve for models with antigen sources other than dying worms. In particular, models in which protective antibody reduced re-infection (with either cercarial or live worm antigen) tended to have later and higher infection intensity peaks with increasing numbers of worm compartments. This was not due to a delay in the development of protective antibody, which developed earlier (for live worm antigen) or at the same rate (for cercarial antigen) with increasing numbers of worm compartments (data not shown).

3.3.5 Antigen thresholds

Inclusion of an antigen threshold on the protective antibody response had different effects upon the age-intensity profile depending upon which type of antigen threshold was used (figure 3.9a-c). For all of the types of antigen threshold explored, inclusion of an antigen threshold delayed the development of protective antibody (figure 3.9d-f). For a fixed antigen threshold based upon current antigen exposure level (T_1), increasing the level of this antigen threshold delayed the age at which infection peaked and raised the height of the infection peak, but also raised the level of infection in adults (figure 3.9a). For a sufficiently high antigen threshold level, the antigen threshold could not be passed, an antibody response could not be made, and there was no control of infection. For an antigen threshold based upon current exposure which was removed (set to 0) once an antibody response has been initiated (T_2), increasing the antigen threshold level also delayed the age and raised the height of the peak, but lower levels of infection could be achieved in adults. Once an antibody response had been initiated, infection intensity settled to the same level in adults regardless of the antigen threshold level, provided the antigen threshold was passed (figure 3.9b). Again, at sufficiently high antigen threshold levels, it was sometimes impossible for the antigen threshold to be passed, and there was no control of infection.

For a cumulative antigen threshold without any decay in cumulative exposure (T_3), increasing the antigen threshold level also delayed and raised the height of the infection peak,

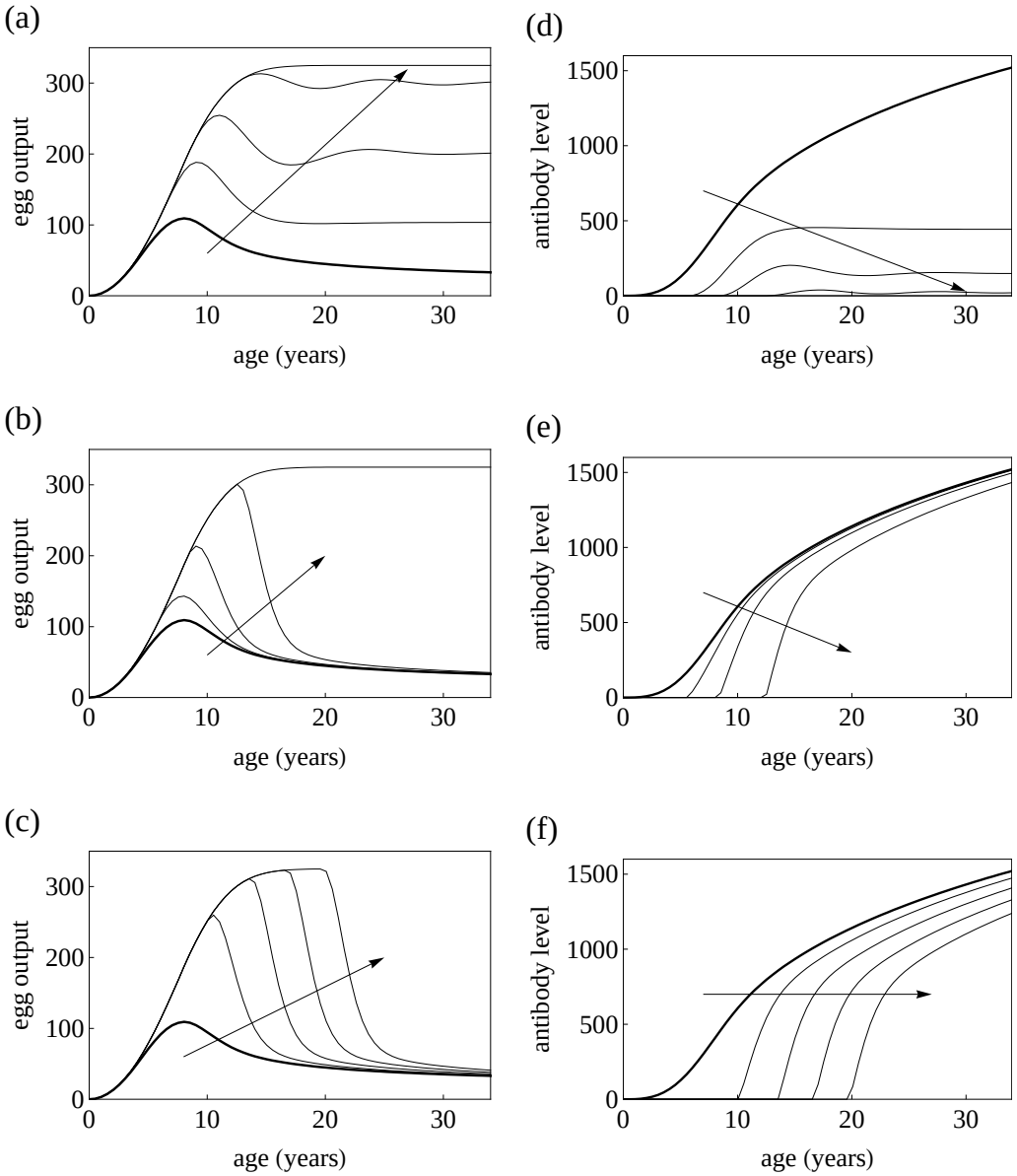

Figure 3.9: The effect of increasing the level of different types of antigen threshold upon egg output (a,b,c) and levels of protective antibody (d,e,f). For all panels, antigen: live worms; antibody target: increased worm death, n = 9, $\Lambda = 50$, $1/\mu = 6.5$, $\psi = 0.001$, $\kappa = 1$, $\gamma = 0.008$. Type of antigen threshold: (a, d) Fixed current; (b, e) dropping current; (c, f) cumulative. Bold lines indicate what happens when there is no antigen threshold (threshold = 0). Other lines show what happens with increasing antigen threshold levels: for (a, d) values for antigen threshold level (T_1) (increasing in direction of arrow) 100, 200, 300, 400; for (b, e) values for T_2 (increasing in direction of arrow) 100, 200, 300, 400; for (c, f) values for T_3 (increasing in direction of arrow) 1000, 2000, 3000, 4000. (All parameters fully defined with units in table 3.1.)

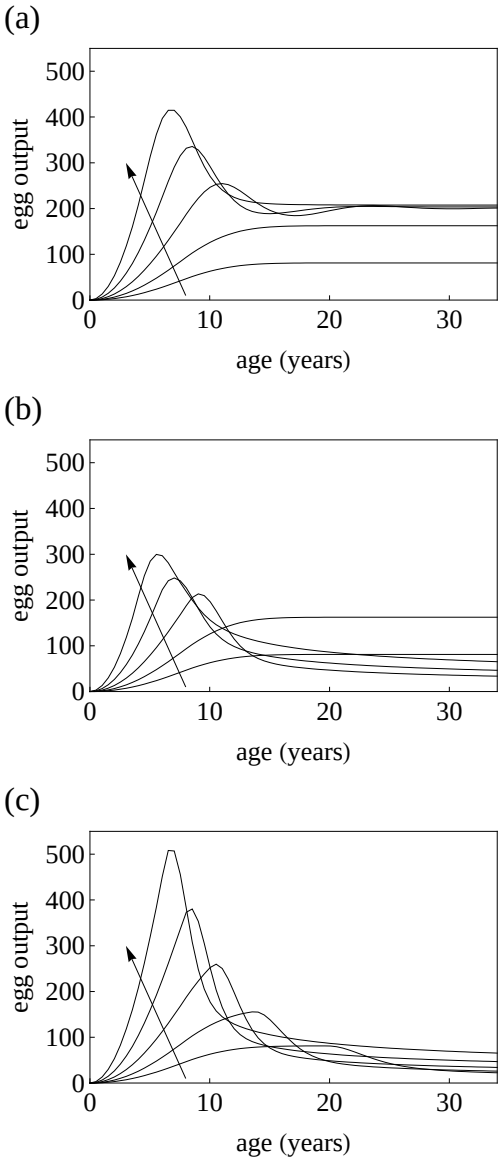

Figure 3.10: The impact of antigen thresholds upon the peak shift. (a) Fixed current antigen threshold, (b) dropping current antigen threshold, (c) cumulative antigen threshold. Egg output is shown changing with age with increasing Λ_m (infection rate) from bottom to top (with the direction of the arrow) 12.5, 25, 50, 100, 200. For all panels, antigen: live worms; antibody target: increased worm death, $n = 9$, $\Lambda_m = 50$, natural mean worm life span $1/\mu = 6.5$, $\psi = 0.001$, $\kappa = 1$, $\gamma = 0.008$. For (a) T_1 (current antigen threshold) = 200, for (b) T_2 (initial antigen threshold) = 200 (with threshold falling to 0 once antibody begins to be made) and for (c) T_3 (cumulative antigen threshold) = 1000. (All parameters fully defined with units in table 3.1.)

but did not affect the level of infection in adults if the antigen threshold was passed. For this model, the peak could be shifted to a later age than with current antigen thresholds, as a cumulative threshold could be exceeded after current antigen exposure has plateaued (figure 3.9c). At a sufficiently high antigen threshold level (T_3), this threshold could not be exceeded within the simulated time period (not shown).

Both types of current antigen threshold failed to replicate the peak shift at low levels of infection (figure 3.10a,b), as at low levels of infection the antigen threshold was never passed and control was never achieved. The cumulative antigen threshold allowed a very strong peak shift to be maintained across populations with varying infection rates (figure 3.10c), although it was possible to find combinations of antigen threshold level (T_3) and infection rate (Λ_m) for which the threshold was not passed during the 34 years simulated and control was not achieved (data not shown).

3.3.6 Average worm life span

For models where the protective immune response increased worm death rate, this could have a large impact upon the average worm life span, which decreased both with host age and with increasing infection rate (figure 3.11). For models which achieved levels of control in line with field estimates (the level of infection in adults is less than 40% of the peak level), worm life span was reduced substantially (as for all of the curves in figure 3.11).

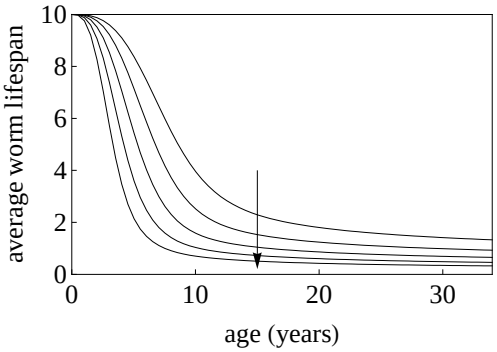

Figure 3.11: Effect of anti-adult worm immune responses on worm life span at different host ages. Results shown for baseline model without explicit memory cells, suppression or antigen thresholds included. The average worm life span is calculated using equation 3.17 and is shown for different values of infection rate (Λ_m) from top to bottom (with the direction of the arrow) 12.5, 25, 50, 100, 200. Antigen: live worms; antibody target: increased worm death, n = 9, $1/\mu$ = 10, $\psi = 0.001$, $\kappa = 1$, $\gamma = 0.008$. (Infection curves for these same populations are shown in figure 3.4a.) (All parameters fully defined with units in table 3.1.)

3.4 Discussion

This analysis showed that a wide range of models were able to reproduce age-intensity curves consistent with field data. These included models with varying representations of the pathways leading to antibody production, different antigens and antibody targets, and different mechanisms for delaying the development of protective antibody responses. Using a mathematical modelling approach to investigate these questions is useful because it allows findings from laboratory and field studies to be applied to a hypothetical population setting

under a set of explicit and verifiable assumptions, producing outputs that can be compared with field data. Previous work by Woolhouse (1992*b*, 1993, 1994*a*), using a simple representation of immunity similar to the baseline model here, showed that the qualitative patterns of a peaked age-intensity curve and a peak shift could be reproduced by all of the possible different combinations of cercariae, live adult worms and eggs as antigen and target for antibody responses. The analysis here was more quantitative, using infection rates which varied with age in accordance with field observations (Chan *et al.* 2000), and testing whether age-intensity profile characteristics fell within ranges identified from field data, in particular the age of the infection peak and the height of the peak relative to adult levels of infection.

Basic models, with the immune response represented as a single population of plasma cells, were able to reproduce these patterns for all possible combinations of antigen and target for the protective response. Most (although not all) of these models required very slow decay rates of the plasma cell population to achieve this – constant per cell decay rates of 0.08–0.008 year^{-1}, equivalent to a half-life of 9–90 years. Antibody-secreting or plasma cells do not divide (Kalia *et al.* 2006), which implies that individual cells would have to have half-lives of 9–90 years if this model were true. Several studies in both mice and humans have suggested that antibody levels can be maintained for months or years by long-lived plasma cells (which constitutively produce antibody)(Ahuja *et al.* 2008; Kalia *et al.* 2006; Radbruch *et al.* 2006). Radbruch *et al.* (2006) suggest that these plasma cells may have a half-life of roughly 23 years, and Amanna *et al.* (2007) demonstrated a half-life of 92 years for the antibody response to vaccinia vaccination (in the absence of re-exposure), which they implied may be maintained by long-lived plasma cells. Others have suggested that antibody can be maintained in an antigen-independent manner through non-specific activation of memory B cells to produce short-lived plasma cells (Bernasconi *et al.* 2002; Kalia *et al.* 2006; Lanzavecchia *et al.* 2006). The baseline model used here could equally represent this mechanism (provided plasma cells have a relatively short half-life), and in this case it would not need to be assumed that individual memory cells can survive for decades, as memory cells can proliferate and maintain their populations (Macallan *et al.* 2005; Wirths & Lanzavecchia 2005).

As some studies suggest that antigen is needed to drive plasma cell production from memory populations (Ochsenbein *et al.* 2000), an alternative model structure was considered including an explicit memory cell population, with antigen-dependent production of plasma cells from this memory population. These memory models were also able to reproduce age-intensity profiles consistent with those seen in the field; for some antigen:target combinations, the plasma cells as well as the memory cell populations needed to have fairly long half-lives (which is not inconsistent with experimental findings, as discussed above).

The models suggested that suppression could delay and reduce the development of protective immune response in humans, but may have complex effects upon population patterns of infection (Mitchell *et al.* 2008). The suppression models showed that very strong immunosuppression of the entire protective response could completely overwhelm it, removing all evidence of acquired immunity and removing the 'peak' in infection intensity altogether, while very weak immunosuppression had little or no effect on the age and intensity of peak infection, as protective immunity was scarcely affected. For a given level of suppression, the impact upon the age-intensity curve was also predicted to vary with the rate of infection, with the peak shift remaining at low rates of infection, but at increasingly high rates of infection the suppressive effect reversed the peak shift and then removed the peaks altogether. Alternatively,

if immunosuppression only acted against part of the immune response, leaving another part intact, then suppression was unable to remove the peaks and had a much more modest effect upon the peak shift.

It has been questioned whether the level of suppression is really likely to be proportional to infection intensity; a recent study of regulatory T cells in a Zimbabwean population with endemic *S. haematobium* found no clear relationship between the percentage of T cells which had a regulatory phenotype and level of infection intensity (N. Nausch, *in prep*). If suppression was assumed in this model to have a constant level regardless of infection level, this was equivalent to assuming that antibody production was induced at a slower rate and did not affect the overall behaviour of the baseline model at all.

Parasite-induced immunosuppression has previously been included in other models of macroparasite infection. Duerr *et al.* (2003*b*) modelled parasite-associated suppression as an increasing rate of parasite establishment (equivalent to infection rate in this model) with increasing parasite burden. Their null model (without suppression) was equivalent to the full suppression model here (in which resistance never developed). Their model predicted sigmoidal age-intensity curves, consistent with onchocerciasis data (Basáñez & Boussinesq 1999; Duerr *et al.* 2003*b*), and their model could not generate peaks or a peak shift, as was seen with very high suppression in our model. Schweitzer & Anderson (1991) included parasite-induced suppression of T cell responses in their more mechanistic models of parasite immunology. Removal of activated T cells by parasites permitted a stable state with high parasite burden and low numbers of activated T cells, with high levels of repeated exposure tending to move the system towards this state. In a more complex model where parasites suppressed IL-2-driven T cell proliferation, progression from an immunosuppressed to an immune state was increasingly delayed at higher infective doses. This is in general agreement with the findings reported here.

In contrast to the predictions from the suppression model, existing field data on *S. mansoni* and *S. haematobium* demonstrates a definite peak in infection intensities in childhood, which is increasingly strongly convex at higher infection intensities (Anderson & May 1991*b*), and a clear peak shift towards younger individuals is seen in more heavily infected populations (Fulford *et al.* 1992). Similar peak shifts have also been demonstrated for filarial and hookworm infections in human populations (Woolhouse 1998). This suggests that significant intensity-related parasite-specific suppression of all immune responses is inconsistent with observed population patterns of schistosome infection intensity.

The models showed that while having dying worms as the principal antigen stimulating a protective antibody response could give rise to age-intensity profiles consistent with field data, other life-cycle stages could also act as the principal antigen. For an individual's exposure to dying worms to have a distinct profile from their exposure to live worms, it was necessary to either have protective antibody increasing worm death, or to have non-exponential worm survival. The models showed that the assumed worm survival curve could make an appreciable difference to the age-intensity profile. If dying worms were the principal antigen, then changing worm survival from an exponential distribution towards distributions with less variation in worm life span (approximately Gaussian-distributed and fixed worm survival) always delayed the timing of initial exposure to dying worms, delaying development of protective antibody, and leading to higher and later infection peaks. The worm survival curve also affected models with other antigenic stimuli, where protective antibody reduced rates of re-infection. Since worm death and egg production were not affected by the immune response in these models, the decline

in infection levels came from natural worm death after the reduction of new worm arrivals. This decline was affected by worm survival, again leading to higher and later infection peaks with reduced worm life span variation, although in this case there was no delay in the generation of protective antibody. In all of these models, the peak shift was maintained regardless of the worm survival curve used. While a fixed worm life span is a deliberate extreme case which is unlikely to occur in reality, using approximately Gaussian distributed worm survival also made a considerable difference to age-intensity patterns. Data from human and animal studies gives limited information about what the true distribution of natural worm survival might be. Maximum life span estimates for schistosomes, based upon finding individuals passing eggs some time after their last possible exposure, go up to 29 years for *S. haematobium* and 33 years for *S. mansoni* (Berberian *et al.* 1953; Christopherson 1924; Fairley 1931; Harris *et al.* 1984), considerably longer than the usual average worm life span estimates of 3–10 years (Goddard & Jordan 1980; Vermund *et al.* 1983; Warren *et al.* 1974; Wilkins *et al.* 1984), which suggests that there is considerable variation but does not support any particular distribution.

The models indicated that the requirement for a threshold level of antigen exposure to be reached before a protective antibody response was mounted could substantially delay the development of a protective response, but the effects upon the age-infection profile varied depending upon the way in which such an antigen threshold was assumed to operate. Problems arose particularly for populations with low levels of infection which never reached the antigen threshold and thus never controlled infection at all. This is not consistent with field studies of populations with endemic *S. haematobium*, which consistently demonstrate lower levels of infection in adults than children, suggestive of protective immunity developing. While this occurred to a certain extent in all of the threshold models, it happened much more frequently in models with antigen thresholds based on current antigen levels. In models with a threshold based upon cumulative antigen exposure, this threshold could be passed over a much broader range of population infection rates.

When the protective immune response was assumed to increase the rate of worm death, worm life span was shortened considerably – for models in which the ratio of infection in adults to the peak level was less than 40% (in line with field estimates; see chapter 2), worm life span in adults was shortened to less than 2 years, and usually less than 1 year, in contrast to the estimates of 3–10 years previously calculated from field data (Goddard & Jordan 1980; Vermund *et al.* 1983; Wilkins *et al.* 1984). The prediction arising from these models that if there is significant immune attrition of adult worms then worm life expectancy will be shorter in adults than in children, has been previously tested in two field studies of *S. mansoni*. One study using transmission control in St. Lucia, showed some evidence of a longer worm life span in children, although the life span in adults was still estimated to be between 2 and 4 years (Goddard & Jordan 1980). Another study analysing pre- and post-treatment data from Kenya failed to find evidence of a significant difference in worm life span with host age (Fulford *et al.* 1995). Field estimates of worm life span have all used the assumption that worm life span is exponentially distributed, for which the evidence (discussed earlier) is equivocal, and this may bias these estimates. Since the interruption of transmission (often used to estimate worm life span) will also alter the levels of exposure to all of the different schistosome life stages, it may also alter the strength of anti-worm immune responses, so that these life span estimates may not fully take into account the effect of immunity upon worm survival.

The results presented here have shown that different representations of the immune system

can give age-intensity profiles consistent with those seen in endemic communities. They also demonstrated that a variety of combinations of different life cycle stages as the principal source of protective antigen, and as the target of protective antibody, could also reproduce plausible age-intensity profiles. The models indicated that antigen thresholds, worm- or cercariae-induced immunosuppression, or having dying worms as the source of protective antigen (with non-exponential worm survival) were all able to delay the development of protective immunity. However, antigen thresholds, particularly those based upon current antigen exposure, prevented the peaked age-intensity curve and peak shift being replicated across all levels of infection rate. Immunosuppression had effects on population levels of infection intensity which have not been reported in field data, in particular reducing the convexity of the age-intensity curve, and reversing the peak shift. This suggests that intensity-related immunosuppression of the specific protective immune response does not occur to a significant extent during schistosome infection. The other proposed mechanisms (dying worms or a cumulative antigen threshold) were consistent with observed field patterns, as were results from baseline models without any additional mechanisms included. Additional patterns from field data, including age-antibody profiles, and infection and antibody distributions and co-distributions, will be considered as extra filters to further discriminate between these proposed hypotheses for the slow development of protective immunity in human schistosome infection.

Chapter 4

Exploration of factors underlying the antibody switch

4.1 Introduction

Infection intensities in populations with endemic urinary schistosomiasis consistently follow a 'peaked' (or convex) curve with age, with infection levels peaking between the ages of 6–20 years old, and lower infection intensities found in older adults (Clarke 1966). In areas with higher overall levels of infection, the peak in infection intensity tends to be higher and occur at an earlier age than in areas with lower infection levels. This pattern is described as a peak shift (Woolhouse 1998). Previous modelling work has demonstrated that the peak shift is consistent with the development of acquired protective immunity as a function of cumulative exposure to schistosome antigens (Woolhouse 1992*b*). Age-related changes in the nature of the immune response generated against schistosomes have also been reported. Two studies in Zimbabwe have identified different groups of schistosome-specific antibody sub-classes (isotypes) which display contrasting age profiles. One group of isotypes was shown to rise with host age while a second group declined in older individuals (Mutapi *et al.* 1997; Ndhlovu *et al.* 1996*b*). Both studies reported negative correlations between antibodies from the two different groups. The 'switch' between the different antibody responses occurred after the peak in infection intensity for both populations. Some of the isotypes which increased with age in these populations have been associated with protection against re-infection in other studies, particularly IgE specific for adult worm antigen preparations (Hagan *et al.* 1991), but these protective responses tend to develop slowly with age, despite frequent exposure to infection from an early age (Woolhouse *et al.* 2000).

In this chapter, two hypotheses were explored for the slow development of protective immunity. The first hypothesis was that dying worms are the main source of protective antigen. It has been observed that praziquantel treatment, which kills adult worms, induces an antibody switch in young children similar to the switch seen occurring naturally in older children (Mutapi *et al.* 1998). It is hypothesised that the long life span of schistosome worms delays exposure to protective antigens, delaying the development of natural protective immunity (Woolhouse & Hagan 1999). Second, it has been proposed that exposure to a certain threshold level of antigen is needed before protective responses can be stimulated (Mutapi *et al.* 2008; Woolhouse

& Hagan 1999). This is supported by the finding that, in a *S. haematobium* endemic area, older or more heavily infected groups produced detectable antibody against a wider range of schistosome antigens (Mutapi *et al.* 2008). Both of these hypotheses were discussed in more detail in chapters 1 and 3.

These hypotheses were tested using deterministic models which describe changing levels of infection and two separate antibody responses with age in a homogeneously exposed population. These models were tested for their ability to reproduce key patterns in infection and antibody observed in field studies of *S. haematobium*, extending the list of patterns to include the antibody switch as well as the age-infection intensity profile and the peak shift. A pattern-oriented modelling approach was taken. This systematically tested the ability of a range of different model structures and parameter sets to simultaneously reproduce several different patterns identified from population-level field data (Grimm *et al.* 2005; Janssen *et al.* 2009; Rossmanith *et al.* 2007). The models were used to test whether one or more of the following factors was necessary to reproduce these patterns: dying worms as the principal antigen (versus other life cycle stages), non-exponential worm survival distribution (expected to affect the timing of exposure to dying worms), an antigen threshold, or cross-regulation between the two antibody responses. Cross-regulation was included specifically to see whether this was necessary to generate the antibody 'switch', in line with the antagonism known to exist between different cytokine responses, which are involved in determining which antibody isotypes are made (Abbas *et al.* 1996; Jeannin *et al.* 1998). It was found that each of these factors enhanced the ability of the models to reproduce the required patterns, but none of them were necessary for the models to be able to reproduce patterns of infection and antibody consistent with field data. The combination of the stage of the schistosome life cycle which stimulated each antibody response, and the stage of the life cycle targeted by the antibodies, was found to be informative.

Analysis framework for chapter 4

- The aim of the analysis in this chapter is to explore different hypotheses to explain both the switch seen in the antibody response to *S. haematobium* and population-level infection profiles:
  - Dying worms
  - Antigen threshold
  - Cross-regulation (representing antagonism between different branches of the immune response)
- Models are tested for their ability to pass both the infection intensity and the antibody switch criteria:
  - Peaked age infection curve (peaking in the right age range) with sufficient reduction of infection in adults relative to the peak
  - Peak shift between areas with different rates of infection
  - Sufficiently long mean worm life span in adult hosts (in line with field estimates)
  - Antibody switch, after the age of the peak in infection
- Deterministic models are used which describe mean population infection intensity and two independent protective antibody responses, enabling the model to be tested against all of the above criteria
- In this model, it is assumed that the antibody switch occurs when one group of B cell clones supersedes a separate group of B cell clones. The two groups of B cells may have the same or different sources of stimulating antigen, antigen targets and survival times - all possible combinations are considered. An alternative approach which was not followed might be to model a single clone of B cells undergoing a true isotype switch.
- Different worm survival distributions are used, since these can affect the timing of exposure to dying worms and the dynamics of a protective response, as shown in chapter 3. Two distributions are used - exponential and approximately Gaussian, using one and nine adult worm compartments respectively to alter the worm survival curve. Fixed worm survival is not considered, as it gave little additional impact over the Gaussian distribution in chapter 3, and cannot be used in models with immune-mediated worm death.
- A cumulative antigen threshold is used, as the analysis in chapter 3 demonstrated that this could give infection profiles consistent with field data over a wide range of infection rates.
- The threshold is only applied to one of the two antibody responses, since only one response is thought to be delayed in this model of the antibody switch; it is applied to the longer-lived response, as previous work suggests that this is likely to be the late-developing response.
- Cross-regulation between the two antibody responses is included as a reduction in the production rate of each plasma cell population, proportional to the level of antigen stimulating the other response. An alternative approach would be use a more detailed model including the cytokines involved in cross-regulation.

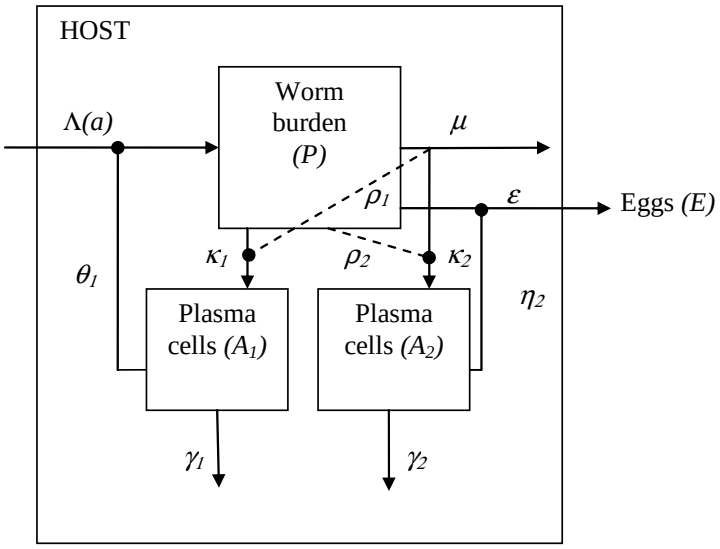

Figure 4.1: Schematic diagram of the plasma cell model. This shows the main state variables, worm burden (P) and two populations of plasma cells (A_1 and A_2), with production of eggs (E). A single worm compartment ($n = 1$), corresponding to exponential worm survival, is shown for clarity. The first antibody response shown here (A_1) receives its antigenic stimulus from the live worm population, and the second (A_2) is stimulated by dying worms, but each response could be stimulated by any one of cercariae, live worms, dying worms or eggs. In the figure, the first antibody response (A_1) is shown reducing re-infection, with relative strength θ_1, and the second antibody response (A_2) is reducing worm fecundity with relative strength η_2, but each response could target any one of re-infection, worm death or fecundity (immune-mediated worm death is shown in figure 2). Cross-regulation between the two responses is shown using dashed lines. All parameters are defined in table 4.1 with parameter values given.

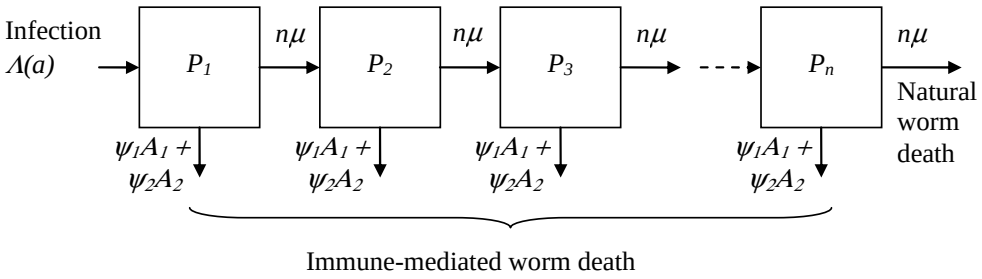

Figure 4.2: Schematic diagram of the multi-compartment worm model, used to alter the natural worm survival curve. The first three and the final (n^{th}) compartments are shown for a model with multiple worm compartments, with worms moving between these compartments at a constant rate, $n\mu$, dying as they leave the final compartment. When either antibody response increases the rate at which worms die, worms additionally leave each compartment at a rate $(\psi_1 A_1 + \psi_2 A_2)$. All parameters are defined in table 4.1 with parameter values given.

4.2 Methods

Age-related development of schistosome infection and antibody responses were modelled using a set of differential equations, using a similar framework to earlier models of helminth immunity (Mitchell *et al.* 2008; Woolhouse 1992*b*, 1993) and immune memory development (Wilson & Nokes 1999; Wilson *et al.* 2007). Two different structures for the immune response were explored: one with only plasma cells, and the other including both plasma cell and memory B cell populations. Different stages of the worm life cycle were allowed to provide the main antigenic stimulus for, and different stages of the life cycle were assumed to be the principle target of, each protective antibody response. The model with plasma cells only is presented first, followed by the memory model and the models including antigen thresholds. The equations are given below, and the model is represented schematically in figures 4.1, 4.2 and 4.3. Parameters are defined, and parameter ranges given, in table 4.1.

4.2.1 Plasma cell model

The plasma cell-only model (figure 4.1) describes the development of infection and two antibody responses (modelled as populations of plasma cells) with age in a homogeneous population with endemic schistosome infection. Each antibody response is stimulated by antigen from a single stage of the schistosome life cycle, and each antibody response targets a single life cycle stage in this model. It is assumed that antibody levels are directly proportional to the size of their respective plasma cell populations. This is reasonable, since plasma cells are constitutive producers of antibody, and antibody has a relatively short plasma half-life in humans, of the order of days to weeks (Morell *et al.* 1970; Waldmann & Strober 1969).

Infection rates are assumed to be the same for all individuals within the population, and to be constant with time, but vary with age as described by equation 4.1. The age-related contact rate (Λ) is zero at birth, increases linearly with age up to age a_c, when it reaches its maximum level (Λ_m), and remains at this maximum level for all subsequent ages. Worm burden (P) is modelled using n compartments (equation 4.2), shown schematically in figure 2. New worms enter the first compartment at a rate $\Lambda(a)$, which can be reduced by anti-reinfection antibody responses as a decreasing exponential function of the number of relevant plasma cells (A_1 or A_2 or both), with relative strength θ_j (θ_1 or θ_2 as appropriate for the 1^{st} or 2^{nd} (j^{th}) antibody response) (equation 4.2). Worms move between compartments at a constant rate $n\mu$, dying naturally when they leave the final (n^{th}) compartment, giving a natural death rate $n\mu P_n(a)$ and an overall mean natural worm life span (in the absence of immunity) of $1/\mu$. Increased immune-induced worm death is included as an additional per-worm death rate, directly proportional to the number of plasma cells and scaled by a factor ψ_j (figure 4.2 and equation 4.2). This additional worm death rate applies equally to all worm compartments (meaning that the ability of the immune response to kill adult worms is not affected by worm age). For exponentially distributed worm life span, a single worm compartment is used ($n = 1$), using the equation for $i = 1$ (where i is the compartment number) (equation 4.2). For an approximately Gaussian distribution of worm life spans, nine worm compartments are used ($n = 9$), with the first compartment described by the first line of equation 4.2, for $i = 1$, and all other compartments described by the second line (for $1 < i \leq n$). The number of eggs measured in urine (E) is assumed to be directly proportional to total worm burden (summed over all worm compartments), and can be reduced by anti-fecundity antibody responses as a decreasing exponential function of the

number of plasma cells, with relative strength η_j (equation 4.3).

The antibody responses are modelled as two separate compartments of plasma cells, A_1 and A_2 (equations 4.4, 4.5). Each plasma cell population grows at a rate directly proportional to the level of antigen (G_j) exposure (with the rate governed by parameter κ_j). The antigen stimulating each cell population (G_j) comes from a single stage of the schistosome life cycle (S_j): cercariae, live adult worms, dying adult worms or eggs (equation 4.6). Each plasma cell population decays at a constant per-cell rate γ_j. Cross-regulation between the two different antibody responses is modelled as a reduction in the production rate of each plasma cell population, proportional to the level of antigen stimulating the other response. This is scaled using a decreasing exponential function, with the strength of cross-regulation governed by the parameter ρ_j.

$$\Lambda(a) = \begin{cases} \Lambda_m \frac{a}{a_c} & \text{if } a < a_c, \\ \Lambda_m & \text{if } a \geq a_c. \end{cases} \tag{4.1}$$

$$dP_i(a)/da = \begin{cases} \Lambda(a)e^{-\theta_1 A_1(a)}e^{-\theta_2 A_2(a)} - (n\mu + \psi_1 A_1(a) + \psi_2 A_2(a))P_i(a) & \text{for } i = 1, \\ n\mu P_{i-1}(a) - (n\mu + \psi_1 A_1(a) + \psi_2 A_2(a))P_i(a) & \text{for } 1 < i \leq n. \end{cases} \tag{4.2}$$

$$E(a) = \sum_{i=1}^{n} P_i(a)e^{-\eta_1 A_1(a)}e^{-\eta_2 A_2(a)} \tag{4.3}$$

$$dA_1(a)/da = \kappa_1 G_1(a)e^{-\rho_1 G_2(a)} - \gamma_1 A_1(a) \tag{4.4}$$

$$dA_2(a)/da = \kappa_2 G_2(a)e^{-\rho_2 G_1(a)} - \gamma_2 A_2(a) \tag{4.5}$$

where $\gamma_1 \geq \gamma_2$

$$G_j(a) = \begin{cases} \Lambda(a) & \text{for } S_j = \text{cercarial antigen}, \\ \sum_{i=1}^{n} P_i(a) & \text{for } S_j = \text{live adult worm antigen}, \\ n\mu P_n(a) + \sum_{i=1}^{n} P_i(a)(\psi_1 A_1(a) + \psi_2 A_2(a)) & \text{for } S_j = \text{dying adult worm antigen}, \\ E(a) & \text{for } S_j = \text{egg antigen}. \end{cases} \tag{4.6}$$

4.2.2 Memory cell model

The memory models include memory B cell populations as well as plasma cells (figure 4.3). The memory cell populations are assumed to grow through antigen-dependent activation of naïve cells, at a rate directly proportional to antigen exposure, with relative strength σ_j (equations 4.7,4.8). The antigenic source comes from a single life cycle stage (equation 4.6), and the same stage stimulates the production of both memory cells and plasma cells for each antibody response. A density dependent function with strength K_M is used to restrict memory cell population growth. The memory cell populations each decay at a constant per cell rate ω_j. In the memory models, the plasma cell populations expand through antigen-dependent activation of their respective memory cell populations, governed by the parameter δ_j, and decay at a constant per-cell rate, γ_j (equations 4.9,4.10). The effects of the immune response upon the

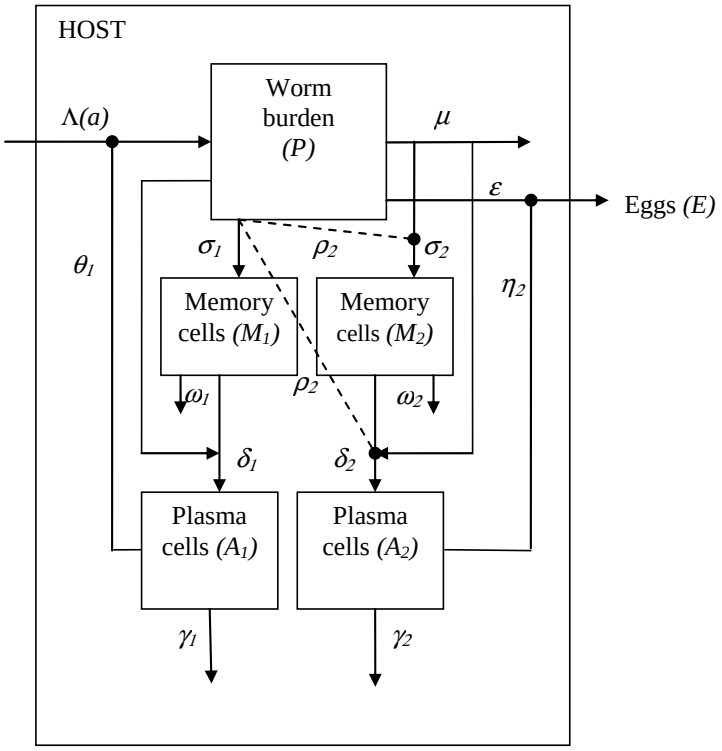

Figure 4.3: Schematic diagram of the memory model. This model has state variables for worm burden (P), two populations of memory cells (M_1 and M_2) and two corresponding populations of plasma cells (A_1 and A_2). Worms produce eggs (E). The first memory response (with associated antibody) shown here (M_1 and A_1) receives its antigenic stimulus from the live worm population, and the second (M_2 and A_2) is stimulated by dying worms, but each response could be stimulated by any one of cercariae, live worms, dying worms or eggs (with the same antigen stimulating both memory cells and plasma cells for each response). Plasma cells are generated through activation of memory cells by antigen, at a rate governed by the parameter δ_j. Protection is mediated by the plasma cell population, as in the plasma cell-only models. Cross-regulation is shown using dashed lines – it is shown acting in one direction (reducing production of M_2 and A_2) for clarity, but may also act to reduce production of M_1 and A_1. Cross-regulation between the two responses affects both memory and plasma cell production. All parameters are defined in table 4.1, with parameter values given.

schistosome life stages are mediated by the plasma cells, with no direct effect of memory cells. The infection processes and the impact of antibody upon the parasite life cycle stages are identical to those in the plasma cell-only model (equations 4.1,4.2,4.3,4.6). Cross-regulation affects the rate of production of both memory and plasma cell populations in these models (with relative strength ρ_j).

$$dM_1(a)/da = \sigma_1 G_1(a) e^{-\rho_1 G_2(a)} \frac{1 - M_1(a)}{K_M} - \omega_1 M_1(a) \tag{4.7}$$

$$dM_2(a)/da = \sigma_2 G_2(a) e^{-\rho_2 G_1(a)} \frac{1 - M_2(a)}{K_M} - \omega_2 M_2(a) \tag{4.8}$$

where $\omega_1 \geq \omega_2$

$$dA_1(a)/da = \delta_1 G_1(a) M_1(a) e^{-\rho_1 G_2(a)} - \gamma_1 A_1(a) \tag{4.9}$$

$$dA_2(a)/da = \delta_2 G_2(a) M_2(a) e^{-\rho_2 G_1(a)} - \gamma_2 A_2(a) \tag{4.10}$$

4.2.3 Antigen threshold

For models which include an antigen threshold, a separate equation records cumulative exposure (C) to one of the antigens (G_2). Cumulative antigen exposure builds up at a rate directly proportional to the level of antigen (with relative strength β), and does not decay over time (equation 4.11).

It is assumed that this cumulative antigenic exposure has to exceed a certain threshold level for one of the two immune responses to be stimulated. As shown in chapter 3, an antigenic threshold can delay the development of an antibody response. In antibody responses which show an age-related 'switch', only one of these responses is delayed, and so an antigen threshold is only applied to one of the responses in this analysis. As different decay rates are used for the two responses (see section 4.2.4), the threshold is applied to the response with less rapid decay (A_2 in this analysis), which is likely to develop later than the more rapidly decaying response (Woolhouse 1994*b*). For the plasma cell-only model, A_2 is not produced if the level of cumulative exposure is below the set threshold. Once this threshold has been exceeded, the plasma cell population grows at a rate proportional to current antigen level (equation 4.12). At all times, these plasma cells decay at a constant per cell rate γ_1. The other antibody response, A_1, is not affected by the antigen threshold, and its production and decay is the same as in the earlier model (equation 4.4).

$$C(a) = \beta G_2(a) \tag{4.11}$$

$$dA_2(a)/da = \begin{cases} -\gamma_2 A_2(a) & \text{if } C(a) < T, \\ \kappa_2 G_2(a) - \gamma_2 A_2(a) & \text{if } C(a) \geq T. \end{cases} \tag{4.12}$$

where T is a constant.

For the memory model, cumulative exposure is calculated in the same way (equation 4.11), but the threshold now applies to the more slowly decaying memory response (M_2 in this analysis). M_2 is only made when the level of cumulative exposure to the relevant antigen exceeds the threshold, and is then made at a rate proportional to current antigen levels (equation 4.13), at all times decaying at a rate ω_2. The equations describing the dynamics of the other memory

response and the two antibody responses are the same as previously (equations 4.7,4.9,4.10).

$$dM_2(a)/da = \begin{cases} -\omega_2 M_2(a) & \text{if } C(a) < T, \\ \sigma_2 G_2(a)\dfrac{1 - M_2(a)}{K_M} - \omega_2 M_2(a) & \text{if } C(a) \geq T. \end{cases} \tag{4.13}$$

where T is a constant.

4.2.4 Model analysis

For both plasma cell-only and memory models, every possible pairwise combination of antigen stimulus (cercariae, live worms, dying worms or eggs) and antibody target (reduced re-infection, increased worm death or reduced fecundity) were used in turn for each of the two antibody responses. All models were run using two different worm survival curves, with worm life spans following exponential or approximately Gaussian distributions (using $n = 1$ or $n = 9$ respectively). Cross-regulation between the two antibody responses was included, operating in one or two directions. An antigen threshold was included in separate models (without cross-regulation). The average worm life span (L), taking into account both natural and immune-mediated death, was calculated using equation (4.14).

$$L(a) = \left(\frac{1}{n\mu + \psi_1 A_1(a) + \psi_2 A_2(a)}\right) \sum_{i=1}^{n} \left(\frac{n\mu}{n\mu + \psi_1 A_1(a) + \psi_2 A_2(a)}\right)^{i-1} \tag{4.14}$$

Models were run for values of age from 0 to 34 years old (in line with field data showing stable contact rates in adults up to the age of 34, see chapter 2). The parameters determining infection rate, antibody strength, antibody and memory decay rates, average worm life span, strength of cross-regulation and threshold level were each varied across plausible ranges, mostly in geometric series (values used are given in table 4.1), and all possible combinations of these parameters were used in turn. For the plasma cell models, the combinations of plasma cell decay rates used were restricted to those in which A_1 decayed at the same or a faster rate than A_2 ($\gamma_1 \geq \gamma_2$). For the memory models, it was assumed that both plasma cell populations decayed very rapidly ($\gamma_1 = \gamma_2 = 80$ year^{-1}), with different combinations of memory cell decay rates, again restricted to combinations where M_1 decayed at the same or a faster rate than M_2 ($\omega_1 \geq \omega_2$). As detailed in chapter 2, published and unpublished data from field studies of endemic *S. haematobium* were analysed and criteria were drawn up for testing whether models could replicate the following patterns: a peaked age intensity curve with control of infection in adults, a peak shift, reasonable mean worm life span and an antibody switch after peak infection intensity. Full details of the criteria and data used are given in table 4.2. For each model, parameter combinations were identified which allowed the model to simultaneously meet all of these criteria over a two-fold change in the infection rate (Λ_m).

The differential equations were solved numerically using a variable time step embedded fifth-order Runge-Kutta algorithm with Cash-Karp parameters, adapted from the rkqs routine in Press *et al.* (2002), implemented in C++.

Table 4.1: Parameters used in the models, with initial values, ranges explored, units and sources from the literature where relevant. Antigen units = number of cercariae/live worms/dying worms/eggs as appropriate. 'Cell' refers to units of the plasma cell or memory cell populations. Subscript j refers to values for the two different antibody responses ($j = 1, 2$)

Parameter	**Meaning**	**Values used**	**Units**	**Source/rationale**
Λ_m	Maximum rate of infection	12.5,25,50,100,200	worms year $^{-1}$person^{-1}	Chan *et al.* (2000)
a_c	Age above which contact rates stay constant	7.8	years of age	fit to data from Chan *et al.* (2000)
n	Number of worm compartments in model	1,9	compartments	$n = 1/n = 9$ for exponential / approximately Gaussian distribution of worm survival respectively
$1/\mu$	Natural mean worm life span	3,6.5,10	years	Fulford *et al.* (1995); Wilkins *et al.* (1984)
κ_j	Rate of production of plasma cells in plasma cell-only model	1	cells year^{-1} unit antigen^{-1}	variation accounted for in varying immune strength
σ_j	Rate of production of memory B cells in memory model	1	cells year^{-1} unit antigen^{-1}	variation accounted for in varying immune strength
δ_j	Rate of production of plasma cells from antigen-driven memory cell activation in memory model	1	plasma cell year^{-1} memory cell^{-1} unit antigen^{-1}	variation accounted for in varying immune strength
K_m	Maximum size of memory population	1000	cells	set to limit memory cell growth rate
γ_j	Rate of loss of plasma cells (all models)	0.008,0.08,0.8,8,80	cells year^{-1} cell^{-1}	Amanna *et al.* (2007); Ochsenbein *et al.* (2000)
ω_j	Rate of loss of memory B cells	0.008,0.08,0.8,8,80	cells year^{-1} cell^{-1}	Amanna *et al.* (2007); Macallan *et al.* (2005)
θ_j	Strength of protection against reinfection	0.00025,0.001,0.004, 0.016,0.064,0.256,1.024	cell^{-1}	broad exploratory range
ψ_j	Strength of immune-mediated worm killing	0.00025,0.001,0.004, 0.016,0.064,0.256,1.024	cell^{-1}	broad exploratory range
η_j	Strength of anti-fecundity response	0.00025,0.001,0.004, 0.016,0.064,0.256,1.024	cell^{-1}	broad exploratory range
ρ_j	Strength of cross-regulation	0.001,0.1,1	unit antigen^{-1}	set to give significant effect on immune development
β	Rate of production of 'cumulative' response (threshold model)	1	arbitrary units year^{-1} unit antigen^{-1}	arbitrary constant
T	Threshold for cumulative antigen exposure	25,250	antigen units	set to give significant effect on age-intensity curve

Table 4.2: Criteria used to judge whether model outputs replicate patterns seen in field data. All criteria must be met over a two-fold change in maximum infection rate (Λ_m) for any parameter set to be deemed successful.

Pattern seen in field data	**Model criterion**	**Justification**
Peaked age intensity curve	maximum level of infection occurs between age 6–20 years old	Bradley & McCullough (1973); Clarke (1966); Mutapi *et al.* (1997); Useh & Ejezie (1999); Wilkins *et al.* (1987, 1984), Mutapi et al. (unpub. data)
Reduction of infection level in adults	infection level at age 34 <40% of peak level	Bradley & McCullough (1973); Clarke (1966); Mutapi *et al.* (1997), Mutapi et al. (unpub. data)
Peak shift	peak infection intensity is lower and occurs at a later age when infection rate is halved (except for lowest value of Λ_m, where infection intensity is higher and occurs at an earlier age when infection rate is doubled)	Woolhouse (1998)
Worm life span	mean worm life span >1 year in 34 year olds	Fulford *et al.* (1995); Wilkins *et al.* (1984)
Antibody switch	the two antibody responses never simultaneously exceed 30% of their respective maximum levels	Mutapi *et al.* (1998, 1997); Ndhlovu *et al.* (1996*b*)
Antibody switch after age of infection peak	initial antibody response falls below 30% of its maximum level after the age at which maximum infection level recorded	Mutapi *et al.* (1997); Ndhlovu *et al.* (1996*b*)

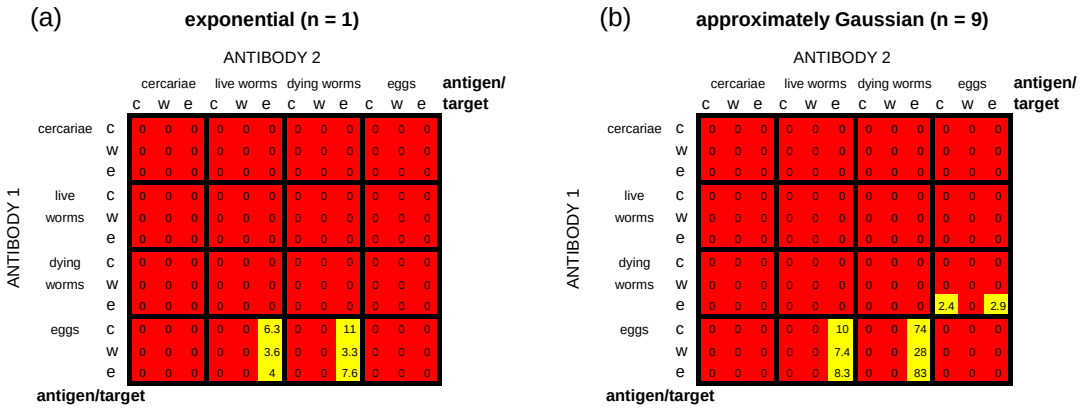

Figure 4.4: Relative success of plasma cell models without cross-regulation or thresholds in reproducing infection and antibody profiles seen in field data. Individual entries give the number of parameter sets per 1000 tested for which all of the criteria (as laid out in table 4.2) are met, for each different antigen:target combination for the two antibody responses. The total number of parameter combinations tested for each antigen:target combination was 11,025. Antigens and targets for A_2 (which has equal or slower decay than A_1) are given along the x-axis of the table, antigens and targets for A_1 are given along the y-axis. Targets: c = cercariae (reduced re-infection); w = worms (increased worm death); e = eggs (reduced fecundity). Red squares indicate that no parameter combinations were ever found for which all criteria were met; orange that fewer than 1 in 1000 parameter combinations were found that could meet all criteria, and yellow that more than 1 in 1000 parameter combinations were able to meet all criteria. No cross-regulation or thresholds are included in these models. In panel (a) models used exponentially-distributed worm survival ($n = 1$). In panel (b) models used approximately Gaussian-distributed worm survival ($n = 9$).

4.3 Results

The combination of both the parasite life cycle stage providing the main antigenic stimulus for each antibody response, and the stage being targeted by the antibody responses ("antigen:target combination"), was critical in determining whether or not the models were able to reproduce all of the patterns identified from field data. For this reason, results are presented and analysed by antigen:target combination within each model structure. For each model structure (described in the subsections below), the main outputs of interest were the number and consistent features of antigen:target combinations for which all of the model criteria could ever be met, and the proportion of total parameter space explored for which all of the criteria were met. Proportions rather than absolute numbers were used because different numbers of parameter sets were explored for each model.

4.3.1 Plasma cell models without cross-regulation or thresholds

Figure 4.4 shows results for the plasma cell-only models without cross-regulation or antigen thresholds. For each of the possible antigen:target combinations of the two antibody responses, the proportion of parameter sets tested over which models were able to simultaneously reproduce all of the required patterns is shown. Results are shown separately for models with exponentially distributed worm life span ($n = 1$; figure 4.4a), and with approximately Gaussian-distributed worm life span ($n = 9$; figure 4.4b). In the absence of either cross-regulation or an antigen threshold, only a small number of antigen:target combinations were able to reproduce all of the

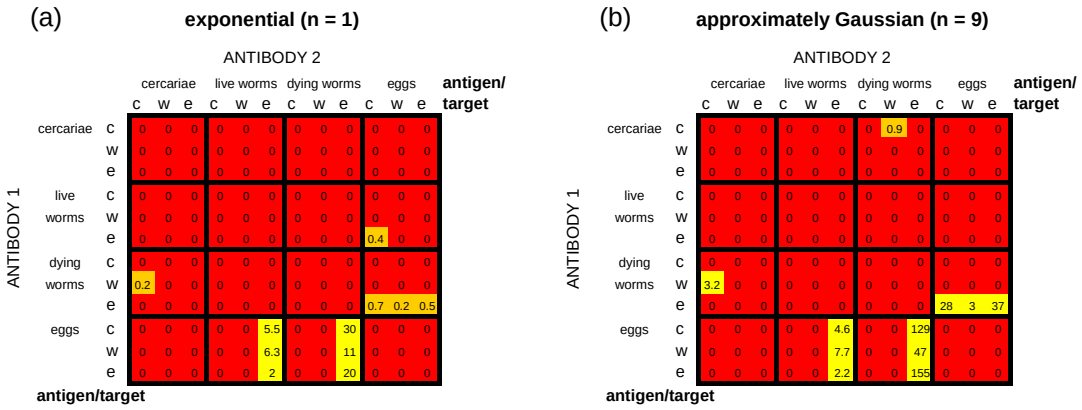

Figure 4.5: Relative success of memory models without cross-regulation or thresholds in reproducing infection and antibody-profiles seen in field data. See legend for figure 4.4. In this model, it is the memory cell populations for each antibody response which differ in their decay rates – M_2 has equal or slower decay than M_1.

patterns for any part of the parameter space tested, 6/144 for $n = 1$ and 8/144 for $n = 9$. These models all had one antibody response stimulated by antigens from live or dying worms, which reduced worm fecundity, with the other antibody response stimulated by egg antigens. In all cases, the antibody response stimulated by eggs peaked early and was replaced by the other, worm-stimulated, response. Usually the egg-stimulated response decayed more rapidly than the worm-stimulated response (models with egg-stimulated A_1 and worm-stimulated A_2), but for some of the models with Gaussian-distributed worm life span and dying worm antigen, this was reversed (models with worm-stimulated A_1 and egg-stimulated A_2). For the antigen:target combinations which were ever able to reproduce the required field patterns, a very restricted part of parameter space ($\leq$8.3% of combinations tested) gave results which passed all of the criteria. Using approximately Gaussian distributed worm survival (figure 4.4b) increased the range of parameters for which it was possible to pass all of the criteria when compared with exponentially distributed worm survival (figure 4.4a). Across the whole parameter space tested, only 0.25 parameter sets per 1000 tested were able to meet all of the criteria for models with exponentially distributed worm survival, compared with 1.5 per 1000 tested for approximately Gaussian distributed worm survival.

4.3.2 Memory models without cross-regulation or thresholds

Figure 4.5 shows the same results for memory models without cross-regulation or an antigen threshold. As in the plasma cell-only models, a small number of antigen:target combinations were able to reproduce all of the field patterns (11/144 for both $n = 1$ and $n = 9$). Most of these, like the plasma cell-only models, had one fecundity-reducing worm-induced antibody response while the other response was stimulated by egg antigen. A small number of models had a different combination of antigens and targets, with one response stimulated by antigens from dying worms, which reduced worm survival, and the other stimulated by cercarial antigens and reducing reinfection.

For the antigen:target combinations which were ever able to reproduce the required field patterns, only a limited range of the parameter space ($\leq$15% of combinations tested) gave results which passed all of the criteria. As with the plasma cell models, using approximately

Gaussian distributed worm survival (figures 4.5b) increased the range of parameters for which it was possible to pass all of the criteria when compared with exponentially distributed worm survival (figures 4.5a). Across the whole parameter space tested, only 0.54 parameter sets per 1000 tested were able to meet all of the criteria for models with exponentially distributed worm survival, compared with 2.9 per 1000 tested for approximately Gaussian distributed worm survival.

4.3.3 Plasma cell models with cross-regulation

Figure 4.6 shows the impact of cross-regulation in plasma cell-only models, acting in one or both directions. Inclusion of cross-regulation increased the number of antigen:target combinations which could meet the criteria. Across all of the cross-regulation models (figure 4.6), 57/144 (40%) of the different antigen:target combinations tested were ever able to reproduce the infection and antibody patterns. For the models that were able to reproduce these field patterns, one of the antibody responses always fell into one of two broad groupings of antigen:target combinations: (i) antigen cercariae/live worms/dying worms, target fecundity; or (ii) antigen cercariae/dying worms, target re-infection. Models with cross-regulation of both responses enabled the greatest number of different antigen and target combinations to reproduce field patterns at least once (figure 4.6e,f). Models with approximately Gaussian-distributed worm survival were able to replicate field patterns for a greater number of antigen:target combinations than equivalent models with exponential worm survival.

Models with cross-regulation of the more rapidly decaying response (A_1) were able to reproduce patterns seen in the field over the greatest proportion of parameter space (figure 4.6c,d), with 0.69 parameter sets per 1000 tested able to meet all of the criteria for models with exponentially distributed worm survival, and 3.6 per 1000 tested for approximately Gaussian distributed worm survival. Similarly, for both models with cross-regulation of the more slowly decaying response (A_2) and models with cross-regulation of both responses, using approximately Gaussian distributed worm survival increased the range of parameters for which it was possible to pass all of the criteria when compared with exponentially distributed worm survival.

4.3.4 Memory models with cross-regulation

Similar overall patterns were seen for memory models with cross-regulation (figure 4.7). Inclusion of cross-regulation increased the number of antigen:target combinations which could meet the criteria. Across all of the cross-regulation models tested, 87/144 (60%) of the different antigen:target combinations tested were ever able to reproduce all of the field patterns. For the models that were able to reproduce these field patterns, one of the antibody responses always fell into one of the three following broad groupings: (i) antigen cercariae/live worms/dying worms, target fecundity; (ii) antigen cercariae/dying worms, target re-infection; or (iii) antigen dying worms; target worm survival (unique to the memory models). Models with cross-regulation of both responses enabled the greatest number of different antigen and target combinations to reproduce field patterns at least once (figure 4.7e,f). Models with approximately Gaussian-distributed worm survival were again able to replicate field patterns for a greater number of antigen:target combinations than equivalent models with exponential worm survival.

Models with cross-regulation of the more rapidly decaying response (M_1) were able to reproduce patterns seen in the field over the greatest proportion of parameter space (figure

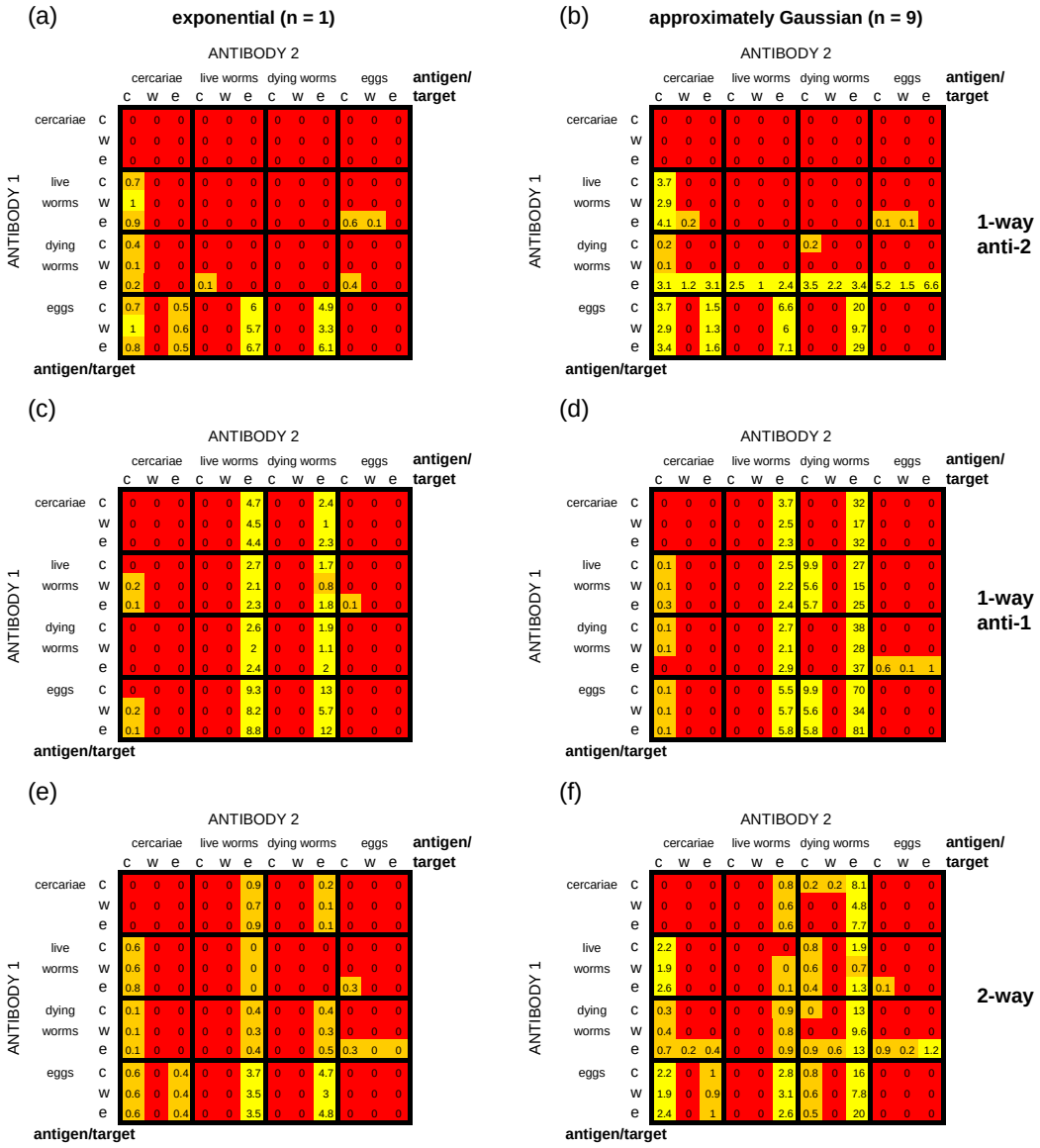

Figure 4.6: Relative success of plasma cell models with cross-regulation in reproducing infection and antibody profiles seen in field data. See legend for figure 4.4. For panels (a) and (b), there is one-way down-regulation of the less rapidly decaying antibody response (A_2), in panels (c) and (d) there is one-way down-regulation of the more rapidly decaying antibody response (A_1) and in panels (e) and (f) there is two-way cross-regulation of both antibody responses. The total number of parameter combinations tested for each antigen:target combination was 33,075 for models with one-way regulation (a,b,c,d) and 99,225 for models with two-way cross-regulation (e,f). The left-hand set of panels are for models with exponentially-distributed worm life span ($n = 1$) (a,c,e), the right-hand set are for models with approximately Gaussian-distributed worm life span ($n = 9$) (b,d,f).

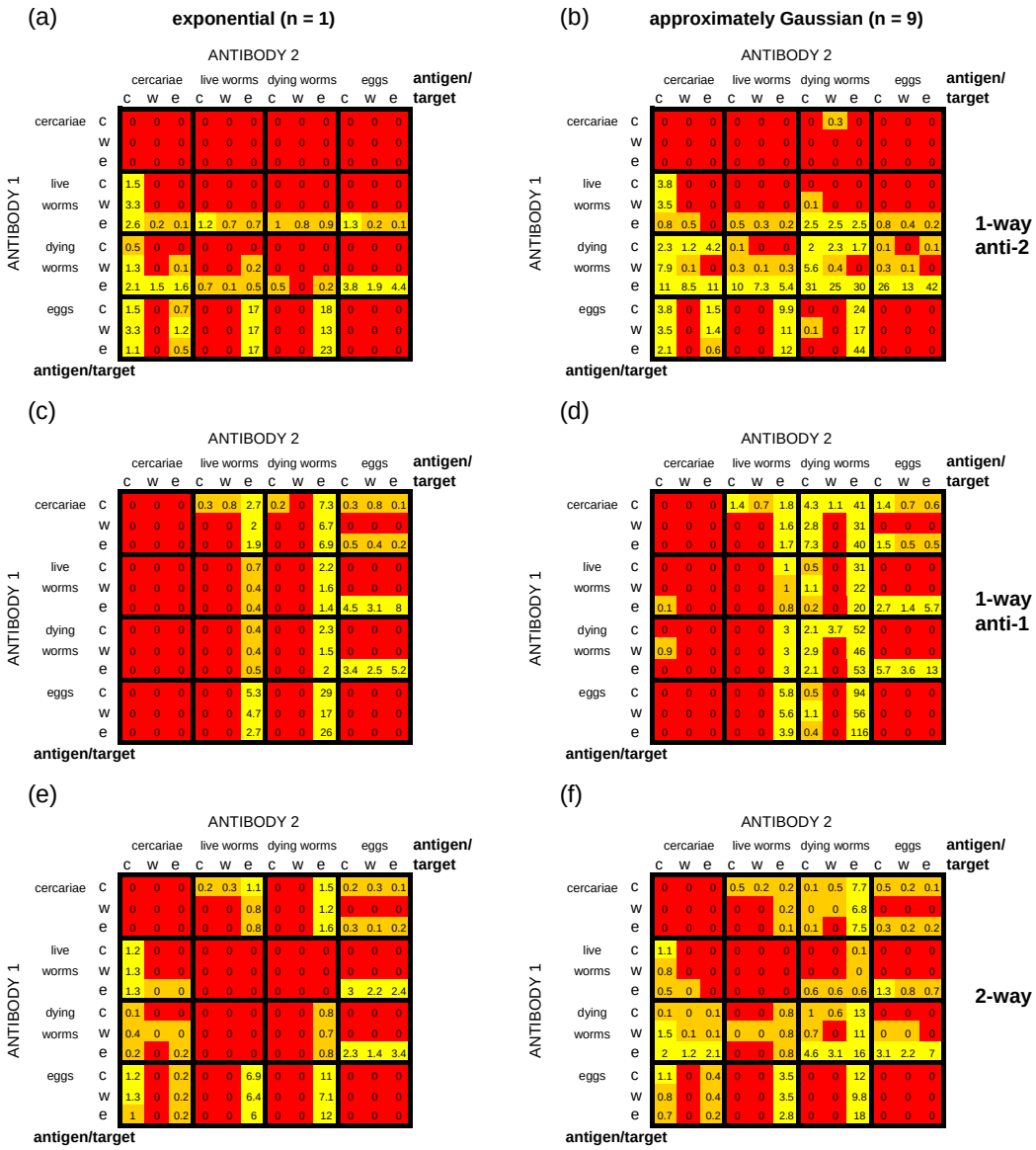

Figure 4.7: Relative success of memory models with cross-regulation in reproducing infection and antibody profiles seen in field data. See legends for figures 4.4 and 4.6. In this model, it is the memory cell populations for each antibody response which differ in their decay rates – M_2 has equal or slower decay than M_1.

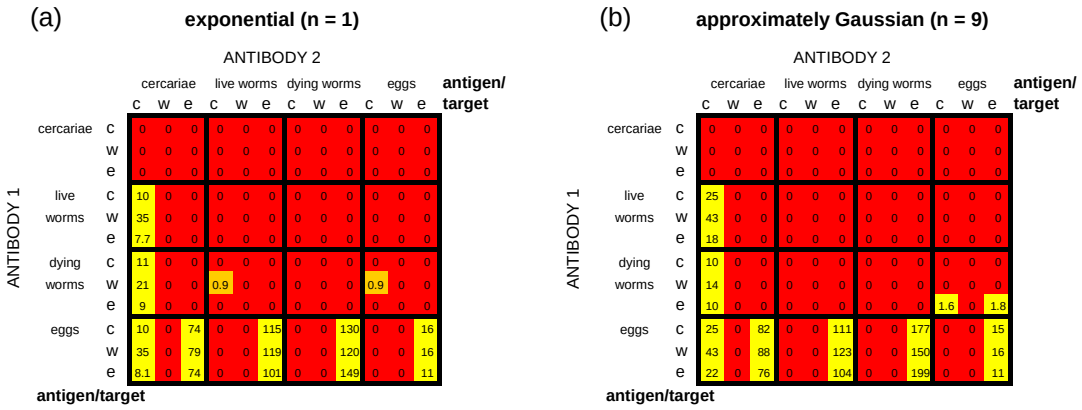

Figure 4.8: Relative success of plasma cell models with an antigen threshold in reproducing infection and antibody profiles seen in field data. See legend for figure 4.4. A threshold is included for the less rapidly decaying antibody response (A_2). The total number of parameter combinations tested for each antigen:target combination was 22,050.

4.7c,d), with 1.1 parameter sets per 1000 tested able to meet all of the criteria for models with exponentially distributed worm survival, and 4.9 per 1000 tested for approximately Gaussian distributed worm survival. Similarly, for both models with cross-regulation of the more slowly decaying response (M_2) and models with cross-regulation of both responses, using approximately Gaussian distributed worm survival increased the range of parameters for which it was possible to pass all of the criteria when compared with exponentially distributed worm survival.

Memory models were able to reproduce field patterns for a greater number of possible antigen:target combinations and over a greater overall portion of parameter space than were equivalent plasma cell models (figure 4.7 cf. figure 4.6).

4.3.5 Plasma cell models with an antigen threshold

The inclusion of an antigen threshold also influenced whether models could reproduce field patterns. For plasma cell models, inclusion of an antigen threshold on the more gradually decaying response (A_2) increased the number of antigen:target combinations which could meet the criteria (figure 4.8). The number of antigen:target combinations which were able to reproduce all of the patterns for any part of the parameter space tested was increased to 23/144 (17%) for both $n = 1$ and $n = 9$. For the models that were able to reproduce these field patterns, one of the antibody responses always fell into one of the two following broad groupings: (i) antigen cercariae/live worms/dying worms/eggs, target fecundity; or (ii) antigen cercariae, target re-infection. Note that the anti-fecundity response stimulated by egg antigens is unique to the threshold models.

For the antigen:target combinations which were ever able to reproduce the required field patterns, up to 20% of combinations tested now gave results which passed all of the criteria. Using approximately Gaussian distributed worm survival (figure 4.8b) slightly increased the range of parameters for which it was possible to pass all of the criteria when compared with exponentially distributed worm survival (figure 4.8a). Across the whole parameter space tested, 8 parameter sets per 1000 tested were able to meet all of the criteria for models with exponentially distributed worm survival, compared with 9.5 per 1000 tested for approximately

Gaussian distributed worm survival.

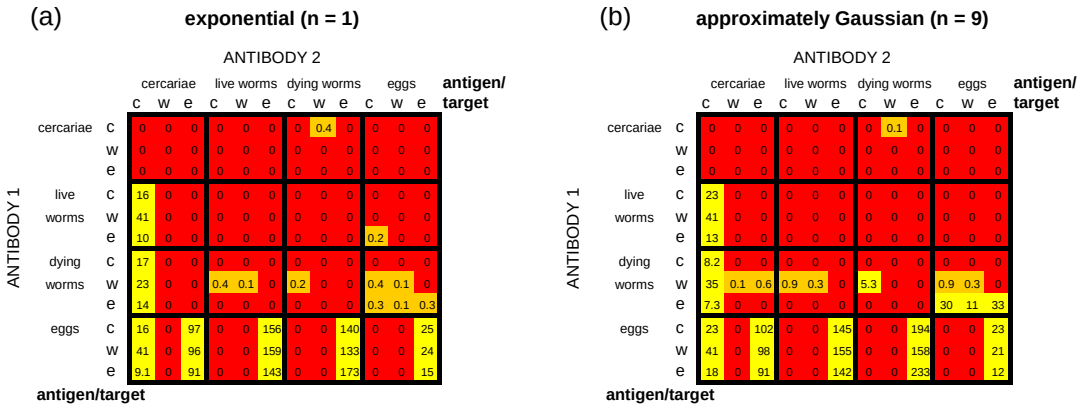

Figure 4.9: Relative success of memory models with an antigen threshold in reproducing infection and antibody profiles seen in field data. See legend for figure 4.8. In this model, it is the memory cell populations for each antibody response which differ in their decay rates – M_2 has equal or slower decay than M_1.

4.3.6 Memory cell models with an antigen threshold

Similar patterns were seen for memory models with an antigen threshold on the more gradually decaying response (M_2) (figure 4.9). The number of antigen:target combinations which were able to reproduce all of the patterns for any part of the parameter space tested was increased to 31/144 (22%) for $n = 1$ and 32/144 (22%) for $n = 9$. For the models that were able to reproduce these field patterns, one of the antibody responses always fell into one of the three following broad groupings: (i) antigen cercariae/live worms/dying worms/eggs, target fecundity; (ii) antigen cercariae, target re-infection; or (iii) antigen dying worms, target worm survival (unique to the memory models). The anti-fecundity response stimulated by egg antigens is unique to the threshold models.

For the antigen:target combinations which were ever able to reproduce the required field patterns, up to 23% of parameter combinations tested now gave results which passed all of the criteria. Using approximately Gaussian distributed worm survival (figure 4.9b) slightly increased the range of parameters for which it was possible to pass all of the criteria when compared with exponentially distributed worm survival (figure 4.9a). Across the whole parameter space tested, 10 parameter sets per 1000 tested were able to meet all of the criteria for models with exponentially distributed worm survival, compared with 11.6 per 1000 tested for approximately Gaussian distributed worm survival.

For models including an antigen threshold, memory models (figure 4.9) were able to reproduce field patterns for a greater number of possible antigen:target combinations and over a greater overall portion of parameter space than were equivalent plasma cell models (figure 4.8).

4.3.7 Models which never meet all criteria

Analysing the results by antigen:target combination, it was found that some of these were never able to reproduce all of the field patterns in any of the different models tested. Altogether,

Table 4.3: Combinations of life cycle stage providing the main source of antigens for, and life cycle stage targeted by, each antibody response, for which the model criteria were never met for any parameter combination

Life cycle stage			
Antigen for A_2	**Targeted by A_2**	**Antigen for A_1**	**Targeted by A_1**
cercariae	cercariae	cercariae	cercariae
cercariae	cercariae	cercariae	worm survival
cercariae	cercariae	cercariae	eggs
cercariae	worm survival	cercariae	cercariae
cercariae	worm survival	cercariae	worm survival
cercariae	worm survival	cercariae	eggs
cercariae	worm survival	live worms	cercariae
cercariae	worm survival	live worms	worm survival
cercariae	worm survival	eggs	cercariae
cercariae	worm survival	eggs	worm survival
cercariae	worm survival	eggs	eggs
cercariae	eggs	cercariae	cercariae
cercariae	eggs	cercariae	worm survival
cercariae	eggs	cercariae	eggs
cercariae	eggs	live worms	cercariae
cercariae	eggs	live worms	worm survival
live worms	cercariae	cercariae	worm survival
live worms	cercariae	cercariae	eggs
live worms	cercariae	live worms	cercariae
live worms	cercariae	live worms	worm survival
live worms	cercariae	eggs	cercariae
live worms	cercariae	eggs	worm survival
live worms	cercariae	eggs	eggs
live worms	worm survival	cercariae	worm survival
live worms	worm survival	cercariae	eggs
live worms	worm survival	live worms	cercariae
live worms	worm survival	live worms	worm survival
live worms	worm survival	dying worms	cercariae
live worms	worm survival	eggs	cercariae
live worms	worm survival	eggs	worm survival
live worms	worm survival	eggs	eggs
dying worms	worm survival	cercariae	eggs
dying worms	worm survival	live worms	cercariae
dying worms	worm survival	live worms	worm survival
dying worms	worm survival	eggs	cercariae
dying worms	worm survival	eggs	worm survival
dying worms	worm survival	eggs	eggs
eggs	cercariae	cercariae	worm survival
eggs	cercariae	live worms	cercariae
eggs	cercariae	live worms	worm survival
eggs	cercariae	eggs	cercariae
eggs	cercariae	eggs	worm survival
eggs	cercariae	eggs	eggs
eggs	worm survival	cercariae	worm survival
eggs	worm survival	live worms	cercariae
eggs	worm survival	live worms	worm survival
eggs	worm survival	dying worms	cercariae
eggs	worm survival	eggs	cercariae
eggs	worm survival	eggs	worm survival
eggs	worm survival	eggs	eggs
eggs	eggs	cercariae	worm survival
eggs	eggs	live worms	cercariae
eggs	eggs	live worms	worm survival
eggs	eggs	dying worms	worm survival

54 of the 144 different antigen:target combinations tested failed to ever pass all of the criteria simultaneously. These combinations are listed in table 4.3. These models are ordered by the A_2 response, which tended to be the stronger determinant of model success. Within this set of antigen:target combinations, dying worms were less likely to be the antigenic stimulus for either response than other stages of the life cycle, and for more than half of them, the target of the longer-lived A_2 response was reduced worm survival.

4.3.8 Immune cell decay rates in successful models

Due to the balanced study design, which used every potential parameter combination, it was possible to identify preferred parameter values from their relative frequencies in models which met all of the criteria. Results are presented for the decay rates for the immune cells (plasma cells and memory B cells), which are estimable (at least in principle). The relative rates of decay for the two antibody responses are of interest as well as absolute values.

For plasma cell-only models with exponential worm life span and without cross-regulation or an antigen threshold, distinct combinations of antibody survival were found to work (figure 4.10a). For these models to meet all of criteria, it was necessary to have one antibody response with very slow decay (A_2 decay of 0.008 or 0.08 year^{-1}, equivalent to a half-life of 9–90 years) with very rapid decay of the other response (A_1 decay of at least 0.8 year^{-1}, or a half-life of 10 months or less), with at least a 100-fold difference between decay rates for the two responses. Inclusion of one or more of Gaussian-distributed worm survival (figure 4.10b,d,f), cross-regulation (figure 4.10c,d) or an antigen threshold (figure 4.10e,f) in the plasma cell-only models increased the range of survival rates which were seen for the 'longer-lived' A_2 response, and allowed field patterns to be reproduced when the two antibody responses had equal decay rates. In all of these models there was still an overall preference for having a disparity between the decay rates of the two plasma cell populations.

For the memory models, plasma cell decay rates were kept constant at 80 year^{-1} (half-life of 3 days) for both responses, and decay rates for memory cell populations were varied. Less clear patterns were seen in memory decay rates (graphs displayed in appendix C). There was a consistent preference for slower decay rates of M_2, but preferred values of M_1 varied widely by model. For all of the models, it was possible to reproduce all of the field patterns when the two memory responses had equal decay rates.

4.3.9 Natural mean worm life span in successful models

The distribution of natural mean worm life span (not taking into account anti-worm immunity) was also investigated in successful models, to see what influence this had upon the ability of the models to reproduce field patterns. These results are shown in appendix C. The preferred worm life span varied with the antigen stimulating A_2, the worm survival distribution and whether or not an antigen threshold was included. For example, in models with cross-regulation, if live or dying worms stimulated A_2, there was a preference for longer-lived worms, but with cercarial antigen, there was a preference for a short worm life span if worm survival was exponentially distributed. Since all of these models were able to pass all of the criteria, it is not possible to conclude from this that any particular value for worm life span is more consistent with patterns seen in field data.

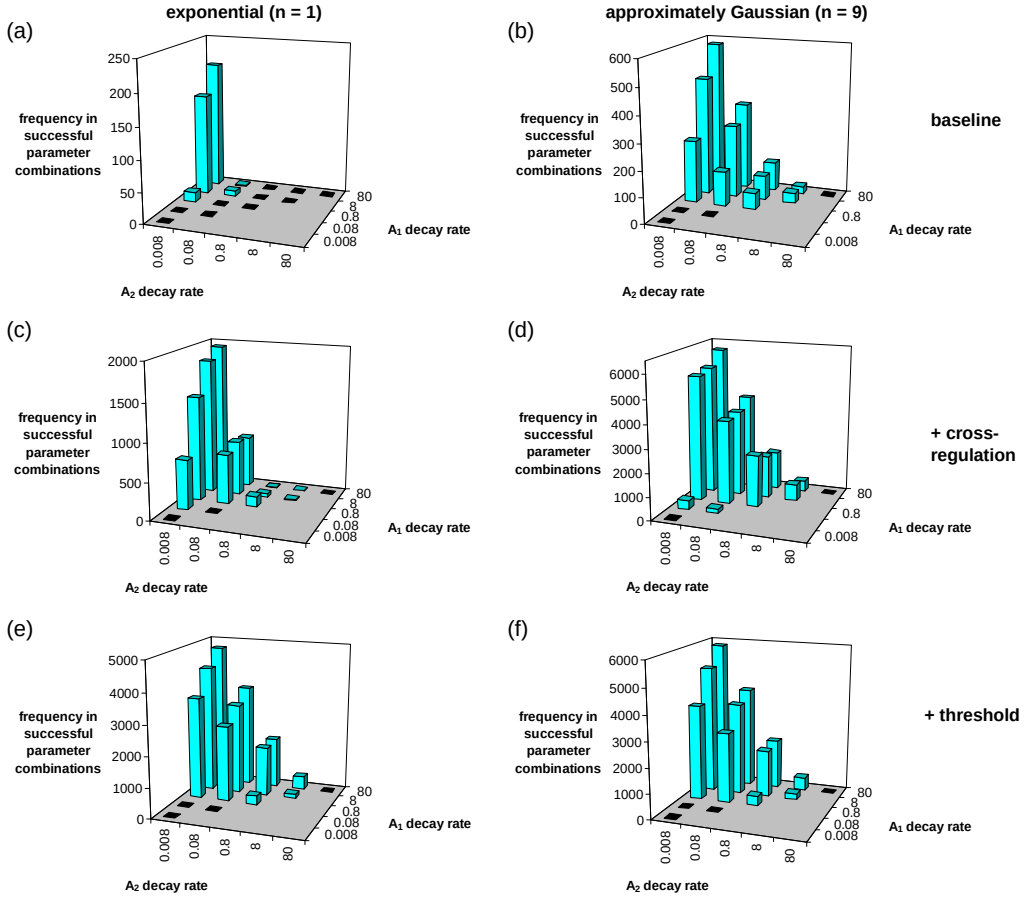

Figure 4.10: Antibody decay rates for plasma cell models which pass all criteria. Plots show the total number of times parameter combinations including the different possible combinations of decay rates for the two plasma cell populations pass all criteria. (a,b) Models without cross-regulation or thresholds, (c,d) cross-regulation models (total frequencies summed over all of them), (e,f) models with a threshold on A_2. The left-hand panels are for models with exponentially-distributed worm life span ($n = 1$) (a, c,e), the right-hand ones are for models with approximately Gaussian-distributed worm life span ($n = 9$) (b,d,f). All of the different combinations of decay rates that were used have a bar on the chart; black bars indicate that no successful parameter combination had this combination of antibody decay rates, blue bars that at least one successful parameter combination had this combination of antibody decay rates. Note that different maximum values are used on the z(frequency)-axis.

4.3.10 Importance of different criteria

The relative importance of the different criteria used was assessed by looking at how frequently they were responsible for excluding parameter combinations. This was done by summing up the number of times each criterion was the only one to be failed by any of the parameter sets tested. It was found that most parameter combinations failed on multiple criteria, with only 6% failing to pass only a single criterion. Each of the six criteria excluded some parameter sets single-handedly, demonstrating that they were all discriminatory in this analysis. Parameter sets that failed only a single criterion were most likely to fail to pass the antibody switch criterion, or the requirement for the age of the infection peak to fall between 6 and 20 years old. They were least likely to fail on either the peak shift criterion or the criterion stipulating the level of infection in adults relative to the peak.

4.4 Discussion

It was shown that testing models for their ability to simultaneously reproduce multiple patterns seen in both infection and antibody data enabled a large number of potential model structures and parameter combinations to be rejected. These results give insight into the likely mechanisms giving rise to these patterns. It was found that both the stage of the life cycle which provided the main antigenic stimuli for each antibody response, and the stage of the life cycle which was targeted by a protective antibody response were critical in determining whether the models could reproduce infection and antibody profiles consistent with field data. Some of the models which had dying worms as the main source of protective antigen were able to reproduce all of the required patterns. However, some models which had other stages of the life cycle acting as the principle antigen source could also meet all of the criteria, suggesting that it is not necessary for dying worms to provide the main source of protective antigen to explain the patterns explored here. Inclusion of cross-regulation, an antigen threshold or using approximately Gaussian-distributed worm survival each increased the number of antibody antigen-target combinations, and the range of parameter space for which it was possible to reproduce patterns seen in the field, but none of these were essential for enabling all of the field patterns to be replicated. From this analysis it is possible to exclude some combinations of life cycle stage providing the main antigenic stimulus for, and life cycle stage targeted by, each antibody response, and these combinations are listed in table 4.3.

The approach used here has similarities to pattern-oriented modelling, testing multiple different model structures and parameter values for their ability to simultaneously reproduce multiple patterns seen in population data (Grimm *et al.* 2005). Previous modelling studies have shown that individual patterns in macroparasite infection data can frequently be reproduced by more than one mechanism or combinations of mechanisms, particularly the peaked age-intensity curve and the peak shift (Duerr *et al.* 2003*a*; Fulford *et al.* 1992; Woolhouse 1992*b*). In this study, 'successful' models had to simultaneously pass six different criteria for infection and antibody profiles, including the peaked age-intensity curve (within limits identified from field data), the peak shift, an antibody 'switch', and realistic mean worm survival, making it much more likely that these models incorporate the 'true' mechanisms determining field patterns. It was shown that all of the criteria used were informative in rejecting particularly parameter sets tested, as they were all able to exclude some parameters single-handedly. Thorough sensitivity analysis,

using a balanced design where all possible combinations of levels of different parameters were investigated, increases confidence that all of the model structures which can possibly reproduce these patterns have been identified here. Although the immune responses are represented in a simplistic fashion in these models, they should capture the important features of the antibody response, being based upon well characterised B cell maturation pathways (Gray 2002), and covering the main alternative theories for the persistence of antibody: (i) antigen-independent mechanisms either through persistence of long-lived plasma cells or continual non-specific activation of memory cells to form short-lived plasma cells (both represented by the plasma cell-only models), and (ii) antigen-dependent mechanisms, with specific antigenic activation of memory cells to form short-lived plasma cells (memory models) (Kalia *et al.* 2006; Ochsenbein *et al.* 2000).

This approach was intended to identify the essential mechanisms underlying universal patterns of schistosome infection and antibody, by selecting models that give outputs consistent with a wide range of studies of endemic *S. haematobium*, rather than trying to accurately replicate patterns seen in individual studies. To this end, patterns were chosen that were seen across multiple different studies. However, some of these patterns are more robust than others; the age of the peak and the peak shift have been well characterised across numerous different studies, but although lower infection levels are always reported in adults for endemic *S. haematobium*, the level relative to the peak can vary considerably in some studies depending upon which age groupings are used. For this reason, a wide range was permitted for this criterion. In this analysis, it was rarely the only criterion on which individual parameter sets were excluded, and so the uncertainty in this pattern will have very little impact upon the results reported here.

The antibody switch has been clearly identified in three Zimbabwean populations (Mutapi *et al.* 1998, 1997; Ndhlovu *et al.* 1996*b*), but was not seen in a fourth study (Mutapi et al., unpub. data; see results for Mutoko-Rusike in chapter 2.). This pattern has not been specifically looked for in other published studies, meaning that it may not be universal. However, it was seen across a number of different isotypes in all three of these populations (see analysis in chapter 2 and Ndhlovu *et al.* (1996*b*)), making it a robust and striking pattern within these populations which deserves exploration.

One potentially important factor which may vary between different populations is the shape of the age-contact profile. The contact data used to define the age-infection rate in these models came from the same area as two of the populations we used to identify the infection and antibody criteria (Chan *et al.* 2000; Mutapi *et al.* 1997), meaning that the models should be able to explain the patterns seen in these particular populations. Additionally, the pattern of increasing water contact with age in young children which was included in this model has been widely reported, but relative contact levels in older children and adults can vary widely between studies (Kabatereine *et al.* 1999). Although the level of infection was varied in these models, no attempt was made to investigate the effect of changing the shape of the age-contact profile, due to sparse data and substantial study-to-study variation where such data is collected.

A potential limitation of these models is that they describe population averages without taking into account distributions of infection or antibody. The assumption that all individuals within a certain population are exposed at the same rate is unlikely to be true, as most studies of water contact (which is the usually best proxy for infection rate) show highly over-dispersed contact patterns between individuals over set periods of time (Chandiwana 1987; Chandiwana

& Woolhouse 1991). Previous models have shown that introducing heterogeneity in contact rates into similar deterministic models gives an earlier and lower infection peak for the same mean contact rate (Woolhouse 1992*b*), and it would also be expected to affect mean antibody profiles. The best way to look at the effects of heterogeneous contact rates for these types of models is through the use of fully stochastic individual based models (Chan *et al.* 2000), but it was not feasible in this study to cover the same breadth of model structures and parameter ranges with stochastic simulation models, which take longer to run and need to be repeated many times to account for stochastic variation in individual simulations.

Previous analyses looking at the age-intensity profiles generated by models with different stages of the life cycle providing the principal antigen source and being targeted by protective antibody found differences in the shapes of these profiles but did not exclude any combinations as being inconsistent with field data (Woolhouse 1992*b*). In this analysis, using more quantitative criteria based on field data, and additionally requiring models to reproduce the antibody switch, a large number of potential antigen:target combinations were excluded. This analysis suggests that the antibody switch may arise when one antibody response, which is stimulated by a life cycle stage that is continually present, reduces the level of antigen inducing another response. In many of the models, one of the antibody responses was stimulated by worms or cercariae and reduced worm fecundity, which reduced host exposure to eggs which were the antigen for the other antibody response. While this process may be enhanced by unequal natural survival of the cells responsible for the two antibody responses, active down-regulation of the second antibody response via responses to the persisting life stage, or an antigen threshold giving a more rapid change between the two responses, none of these were necessary to reproduce a switch under the definition used here. These results suggest that gradual acquisition of exposure to protective antigens is sufficient to explain the slow development of protective immunity, without it being necessary to invoke a major role for dying worms or an antigen threshold, but do suggest that continual exposure to the relevant antigen is most likely to induce such a protective response. These models have suggested that protective immunity may primarily target worm fecundity, which was not routinely considered in earlier immuno-epidemiological models. They have also shown that the assumed worm survival curve can make a considerable difference to the outcome, challenging the usual assumption of exponential worm survival, which is mathematically convenient but has not been empirically demonstrated.

This analysis has confirmed that dying worms or an antigen threshold can both affect the patterns of immune responses to schistosomes, but has not excluded the other alternative explanations explored. To further distinguish between the different potential explanations for the slow development of protective immunity discussed here, additional robust data patterns are considered in the next chapter, including infection and antibody distributions and co-distributions. Using a similar model framework to that used here, stochastic individual-based models are developed, which not only enable the impact of heterogeneity in contact rates to be taken into account, but also allow patterns of aggregation and co-distribution to be simulated and compared with field data. This extra layer of criteria is used to further distinguish some of the key mechanisms underlying the observed dynamics and distributions of both infection and immune responses in human schistosome infection

Chapter 5

Explaining distributions and co-distributions of infection and antibody

5.1 Introduction

Like other helminth infections, schistosomes are highly aggregated among their human hosts, such that many individuals in an endemic population will harbour few or no schistosome worms, whilst a small proportion carry very heavy parasite loads (Guyatt *et al.* 1994; Woolhouse 1994*a*). Previous modelling work has suggested that the level of aggregation observed in human schistosome infection is likely to arise mainly from aggregation between individuals in their relative contact rates, rather than inter-individual differences in immune competence (Chan & Isham 1998). Several observational studies have demonstrated that there is considerable heterogeneity between individuals in the number of water contacts they make over a fixed time period (Chandiwana *et al.* 1991; Etard *et al.* 1995). For practical reasons, these studies have generally been conducted over a fairly short time period, so that the extent to which an individual maintains the same level of contact over their lifetime is unknown. Individuals tend to be predisposed to heavy or light infections (Etard *et al.* 1995), which is likely to be at least partially mediated through contact rates. Mathematical models with varying predisposition have demonstrated that this can have a substantial impact upon the distribution of infection across a population (Quinnell *et al.* 1995). Models have also shown that aggregation in worm burden can occur as a result of 'clumped' infection, with aggregation in the number of worms acquired per contact (Duerr *et al.* 2003*a*; Quinnell *et al.* 1995). Acquired immunity which is generated as a function of infection level is expected to reduce aggregation in worm burden, with modelling work by Galvani (2003) suggesting that parasite aggregation is reduced to a greater extent by immunity affecting susceptibility to re-infection than by immunity which reduces worm fecundity.

Levels of specific antibody against schistosome antigen preparations also tend to be highly aggregated (Mutapi 1997; Mutapi & Roddam 2002), as was discussed in chapter 2, but this has received much less attention in immuno-epidemiological modelling of schistosome infection. Antibody isotypes which demonstrate an age-related 'switch' (Mutapi *et al.* 1997; Ndhlovu

et al. 1996*b*) show a dichotomous relationship with each other (Mutapi *et al.* 1998), which was characterised in chapter 2. As well as occurring naturally with age, this antibody switch has been observed in younger children following praziquantel treatment (Grogan *et al.* 1996; Mutapi *et al.* 1998). Other studies have also reported that praziquantel treatment alters the level of different antibody isotypes (Butterworth *et al.* 1996; Corrêa-Oliveira *et al.* 2000; Gomes *et al.* 2002), with several studies showing that treatment increases levels of isotypes associated with protection against re-infection (Fitzsimmons *et al.* 2007; Satti *et al.* 1996; Webster *et al.* 1997).

In chapter 4, deterministic models describing mean levels of infection and antibody responses in homogeneously exposed populations showed that the age-related antibody switch, as well as peaked age-intensity profiles consistent with field data, could be reproduced by a variety of models. It was shown that the combination of the stage of the life cycle which was assumed to provide the main antigenic stimulus for each antibody response, and the stage of the life cycle which was targeted by each antibody response, was critical in determining whether or not these patterns could be reproduced. Cross-regulation between the two antibody responses and the inclusion of an antigen threshold for one of the responses both enhanced the ability of these models to reproduce these patterns, but neither mechanism was essential for the models to do so. To further distinguish between these mechanisms, and to test the hypothesis that exposure to dying worms is necessary to stimulate a protective antibody response, a different modelling approach was undertaken to see whether these different mechanisms could explain the observed distributions of infection and antibody as well as age-related mean levels. Stochastic individual-based models were used, which made it straightforward to incorporate heterogeneity in individual exposure rates and to measure distributions of simulated infection and antibody levels as well as mean levels. Additionally, these models were tested for their ability to reproduce the observed treatment-induced antibody switch in younger children.

Analysis framework for chapter 5

- The aim of the analysis in this chapter is to further explore different hypotheses to explain both the switch seen in the antibody response to *S. haematobium* and population-level infection profiles, using an increased panel of criteria looking at distributions as well as mean levels of infection and antibody, and post-treatment changes. The hypotheses explored are:
  - Dying worms
  - Antigen threshold
  - Cross-regulation
- Models are tested for their ability to pass an extended list of infection intensity and antibody switch criteria:
  - Peaked age infection curve (peaking in the right age range) with sufficient reduction of infection in adults relative to the peak
  - Peak shift between areas with different rates of infection
  - Aggregated egg output
  - Infection prevalence within criterion range
  - Sufficiently long mean worm life span in adult hosts (in line with field estimates)
  - Antibody switch with age, occurring after the age of the peak in infection
  - Antibody switch occurring after treatment
- Stochastic individual-based models are used which describe infection intensity and levels of two independent antibody responses in a population of individuals, with model outputs being sampled and analysed in the same way as the population data in chapter 2.
- Water contact is assumed to be aggregated, in line with field data, to test whether this is adequate to explain the aggregation seen in infection and antibody responses.
- Worm lifespan is assumed to follow a Gaussian distribution, as this gave the most fits in chapter 4
- Only one antibody response is assumed to be protective, in line with results from chapter 4.
- Cross-regulation is assumed to down-regulate the shorter-lived response, as this gave the most fits in chapter 4.
- The effects of a single round of treatment are modelled as a decline in worm burden (with an increase in exposure to dying worms), with or without a reduction in transmission over the following 36 weeks.
- The following are changed separately to assess their impact upon the results:
  - aggregation of water contacts
  - aggregation of cercariae acquired per contact
  - aggregation of egg output per worm
  - relative number of eggs output per worm

Table 5.1: Model structures used

Immune mechanism	**Life cycle stage**		
	Antigen for A_2	**Targeted by A_2**	**Antigen for A_1**
Cross-regulation	cercariae	cercariae	live worms
	cercariae	cercariae	dying worms
	cercariae	cercariae	eggs
	live worms	eggs	cercariae
	live worms	eggs	live worms
	live worms	eggs	dying worms
	live worms	eggs	eggs
	dying worms	cercariae	live worms
	dying worms	cercariae	eggs
	dying worms	eggs	cercariae
	dying worms	eggs	live worms
	dying worms	eggs	dying worms
	dying worms	eggs	eggs
Antigen threshold	cercariae	cercariae	live worms
	cercariae	cercariae	dying worms
	cercariae	cercariae	eggs
	cercariae	eggs	eggs
	live worms	eggs	eggs
	dying worms	eggs	eggs
	eggs	eggs	eggs

5.2 Methods

An individual-based stochastic discrete-time model was used to describe changes in worm burden and the level of two separate antibody responses with age for people living in an area with stably transmitted endemic schistosome infection. The model was based upon one of the frameworks used for the deterministic population-level models in chapter 4, with the immune response modelled as populations of plasma cells (without memory cell populations) and worm survival assumed to be approximately Gaussian distributed. The model structures used for analysis in this chapter were those that looked most promising (were able to pass all of the criteria over the greatest region of parameter space tested) in the deterministic analysis. The selected models were those with cross-regulation of the short-lived antibody response, and those with an antigen threshold for the longer-lived antibody response. In the deterministic framework, it was found that for the vast majority of successful permutations of these models the shorter-lived antibody response (A_1) had little or no protective effect. Therefore, for the stochastic models it was assumed that only the longer-lived antibody response (A_2) had any protective effect. From now on A_2 is referred to as the 'protective' antibody response, and A_1 as the non-protective response. Only the combinations of life cycle stage providing the main antigenic stimulus for the two antibody responses, and target for the protective antibody response which were successful in the deterministic analysis were explored further in the stochastic models. These combinations are listed in table 5.1.

For each population, separate simulations were run for 161 individuals, with infection and antibody levels recorded at a single age for each individual to give simulated cross-sectional data sets for comparison with field data (chapter 2). Overall infection rates were assumed to stay constant over time. At birth (day 0), the worm burden and antibody levels for each person were

set to 0. For each individual, the simulation started at age (a) = 1 day old and was updated at daily time steps up until the age of sampling. For 136 of these individuals, the sampling ages, which varied between 6–34 years old, were taken from one of the field populations analysed in chapter 2 (Valhalla). An additional group of 25 individuals aged 3–5 years old were simulated to check that the peak of infection did not occur below the age of 6, but were not included in any other part of the analysis. Antibody correlations were calculated for a subset of 101 individuals, chosen to match those with real antibody data available (chapter 2).

Water contact, worm acquisition and death, and measured egg output were all modelled as stochastic processes, with number of contacts, worms and sampled eggs taking only integer values. Antibody development and immune stimulation by egg antigens were modelled as deterministic processes, with antibody level and number of eggs within the host both being continuous variables. The model is described below, with all parameters defined in detail in table 5.2. For consistency with the analysis in chapter 4, parameters in the deterministic models which were yearly rates are kept as yearly rates here, but are converted into probabilities within the model equations, and then converted into daily probabilities by dividing by *dpy* (days per year).

5.2.1 The model

The infection process

Whereas in the deterministic framework the same water contact age-profile is assumed for all individuals in a population, in the stochastic individual-based models individuals are assumed to differ in their contact rates. Each individual in these models has an underlying maximum yearly contact rate Λ_m, drawn from a gamma distribution which has a mean equal to the average population maximum yearly contact rate Λ_{pmax} ($\Lambda_m \sim \text{Gamma}\left(k_1, \frac{\Lambda_{pmax}}{k_1}\right)$ where k_1 is the shape parameter of the gamma distribution). Λ_m is selected in this way at the start of the simulation (when $a = 0$), and is reselected in the same way with a yearly probability ϕ, so at each (daily) time step there is a probability ϕ/dpy that an individual's underlying maximum contact rate will be recalculated (where $dpy = 365$). If ϕ is 0, this assumes perfect predisposition, with individuals maintaining the same relative level of exposure for life. Positive values of ϕ represent individuals making sudden changes in their contact rate, which might happen if they move house or change school or occupation. Here, ϕ is based upon rates at which people reported moving house in a Zimbabwean study population. In this population, a positive correlation was found between infection intensity and distance lived from the nearest water-contact site in young children, suggesting that location of residence is a strong determinant of exposure level (appendix D). A correlation between distance lived from water contact site and infection levels has also been reported in schoolchildren in Tanzania (Rudge *et al.* 2008).

As in chapters 2–4, and based upon field observations from Zimbabwe (Chan *et al.* 2000), an individual's contact rate is assumed to increase linearly with age up to age a_c and then remain constant at a yearly rate Λ_m:

$$\Lambda(a) = \begin{cases} \Lambda_m \frac{a}{a_c} & \text{if } a < a_c, \\ \Lambda_m & \text{if } a \geq a_c. \end{cases} \tag{5.1}$$

On each day, the number of contacts, r, that an individual makes is drawn from a Poisson distribution with mean $\Lambda(a)/dpy$ ($r \sim \text{Pois}(\Lambda(a)/dpy)$). It is assumed that, on average, an individual acquires one schistosome cercariae per contact. To incorporate aggregation in cercarial infection, it is assumed that an individual acquires d cercariae with a probability $1/d$ per contact. t_q is the number of cercariae acquired on the q^{th} contact ($q = 1, ..., r$) on each day such that

$$t_q = \begin{cases} d & \text{if } s < 1/d, \text{ where } s \sim U(0,1) \\ 0 & \text{otherwise.} \end{cases} \tag{5.2}$$

The total number of cercariae, b, acquired during a single day is therefore given by

$$b = \sum_{q=1}^{r} t_q \tag{5.3}$$

New cercariae may be killed upon entry into the host by an anti-reinfection antibody response. It is assumed that cercariae are killed as a decreasing exponential function of antibody level (A_2), in the same way as in the deterministic models, such that the probability of a cercariae surviving is $e^{-\theta A_2(a-1)}$. The number of surviving cercariae acquired on a given day, f, is binomially distributed, $f \sim \text{Binom}(b, e^{-\theta A_2(a-1)})$. The schistosomulum stage is not explicitly represented here; in reality, the larval stages take about 4–6 weeks to reach maturity (becoming adult, egg-laying worms), but this is a relatively short period in comparison with the simulation time for these models (6–34 years), and is not included.

Live worms are modelled passing through nine compartments ($n = 9$) to give approximately Gaussian distributed worm survival (as used in chapters 3 and 4). Newly acquired worms (f) enter the first worm compartment ($i = 1$). The rate at which a worm moves from compartment i to compartment $i+1$ is $n\mu$ per year where $1/\mu$ is the average worm life span in years (see chapters 3 and 4). Therefore the daily probability of a worm moving from compartment i to compartment $i + 1$ is $1 - e^{-n\mu/dpy}$. If compartment i contains $P_i(a - 1)$ worms at age $a - 1$ the number of worms leaving it at age a, m_i, is binomially distributed ($m_i \sim \text{Binom}(P_i(a-1), 1 - e^{-n\mu/dpy})$). Therefore the number of worms in compartment i at age a is given by

$$P_i(a) = \begin{cases} P_i(a-1) + f - m_i & \text{for } i = 1, \\ P_i(a-1) + m_{i-1} - m_i & \text{for } 1 < i \leq n. \end{cases} \tag{5.4}$$

Worms die as they leave the final (n^{th}) compartment. The number of eggs stimulating an immune response (E) is assumed to be proportional to current worm burden, but reduced by anti-fecundity antibody. An anti-fecundity response is assumed to reduce E deterministically via a decreasing exponential function of antibody level (in the same way as in the deterministic models), with relative strength η:

$$E(a) = \sum_{i=1}^{n} P_i(a) e^{-\eta A_2(a-1)} \tag{5.5}$$

Mean egg output (analogous to egg counts measured in urine) is calculated on a single day for each individual (sampling day), as the arithmetic mean of three separate 'samples' (u_y for y = 1,2,3). Each sample is drawn from a negative binomial distribution (implemented as a Poisson distribution with a gamma-distributed mean), with mean $\varepsilon E(a)$ (where ε is the mean number of eggs output in 10ml urine per worm per day) and aggregation parameter k_E:

$$\begin{aligned} &\text{mean egg output} = \sum_{y=1}^{3} u_y \\ &\text{where } u \sim \text{Pois}\left(\text{Gamma}\left(k_E, \frac{\varepsilon E(a)}{k_E}\right)\right) \end{aligned} \tag{5.6}$$

The aggregation parameter for egg output (k_E) is taken from values calculated for *S. mansoni* (de Vlas 1996).

Antibody responses

Two antibody responses (A_1 and A_2) are modelled as separate populations of plasma cells. It is assumed that antibody levels are directly proportional to the number of plasma cells at a given time. Plasma cell population dynamics are modelled deterministically. Each antibody response (the j^{th} antibody response (where j = 1,2)) has a single life stage (S_j) as its principal source of antigen, either cercariae, live worms, dying worms or eggs (within the host). The level of antigen (G_j) stimulating the j^{th} antibody response at age a is calculated as follows:

$$G_j(a) = \begin{cases} b & \text{for } S_j = \text{cercarial antigen,} \\ \left(\sum_{i=1}^{n} P_i(a)\right)/dpy & \text{for } S_j = \text{live adult worm antigen,} \\ m_n & \text{for } S_j = \text{dying adult worm antigen,} \\ E(a)/dpy & \text{for } S_j = \text{internal egg antigen.} \end{cases} \tag{5.7}$$

Levels of live worms and internal eggs are divided by the number of days per year (dpy) to give a direct comparison with the deterministic model output (chapter 4).

Two separate types of models are considered: those with cross-regulation of the non-protective antibody response, and those with an antigen threshold for the protective antibody response. These are described in turn below.

Each plasma cell population (A_j) expands at a rate proportional to the level of antigen stimulating that response (G_j), multiplied by a constant, κ_j. In models with cross-regulation, this rate of growth is down-regulated for the non-protective antibody response, A_1, via a decreasing exponential function of the level of antigen stimulating the protective antibody response (G_2), with relative strength ρ. There is no cross-regulation of the protective antibody response in these models. Each plasma cell population decays with a yearly per cell rate γ_j, giving a daily cell loss of $1 - e^{-\gamma_j/dpy}$.

$$A_1(a) = A_1(a-1) + \kappa_1 G_1(a) e^{-\rho G_2(a)} - A_1(a-1)(1 - e^{-\gamma_1/dpy}) \tag{5.8}$$

$$A_2(a) = A_2(a-1) + \kappa_2 G_2(a) - A_2(a-1)(1 - e^{-\gamma_2/dpy}) \tag{5.9}$$

where $\gamma_1 \geq \gamma_2$

For models with an antigen threshold, a cumulative tally of exposure to antigen is kept (equation 5.10). The non-protective plasma cell compartment (A_1) is unaffected by the threshold and grows at a rate proportional to the level of its antigen, G_1 (equation 5.11). The protective antibody response (A_2) is only made if the antigen cumulative exposure exceeds a threshold level, T (equation 5.12). Once this antigen threshold has been exceeded, the protective plasma cell compartment (A_2) grows at a rate proportional to the level of relevant antigen present (G_2), in the same way as in the cross-regulation model. Both plasma cell populations decay with a yearly per cell rate γ_j, as before.

$$C(a) = C(a-1) + \beta G_1(a) \tag{5.10}$$

$$A_1(a) = A_1(a-1) + \kappa_1 G_1(a) - A_1(a-1)(1 - e^{-\gamma_1/dpy}) \tag{5.11}$$

$$A_2(a) = \begin{cases} A_2(a-1) - A_2(a-1)(1 - e^{-\gamma_2/dpy}) & \text{if } C(a) < T, \\ A_2(a-1) + \kappa_2 G_2(a) - A_2(a-1)(1 - e^{-\gamma_2/dpy}) & \text{if } C(a) \geq T. \end{cases} \tag{5.12}$$

Including treatment

The impact of treatment is assessed in the model by introducing treatment on a single day (the day after sampling) for all individuals aged 6–15 years old. The effects of treatment are assumed to be (i) a decline in worm burden, (ii) a boost to the level of dying worm antigen (equal to the number of worms killed by treatment) and (iii) a reduction in transmission after treatment, modelled as a reduction in the probability of infection per contact on all subsequent days. The simulation is continued for a further 36 weeks after treatment, with egg output and antibody levels recorded at 12, 18, 24, 30 and 36 weeks post-treatment for individuals aged 6–15 years old.

With a given treatment efficacy (probability that a worm is killed by a single round of treatment), x, the number of worms removed from compartment i at age a is binomially distributed ($w_i \sim \text{Binom}(P_i(a-1), x)$). The total number of worms killed across all compartments (z) is given by

$$z = \sum_{i=1}^{n} w_i \tag{5.13}$$

If either antibody response is stimulated by antigens from dying worms, this level is increased by z worms on the day of treatment, such that

$$G_j(a) = z + m_n \qquad \text{for } S_j = \text{dying adult worm antigen} \tag{5.14}$$

The decrease in infection rates after treatment is assumed to apply from the day after

treatment, and to affect all individuals equally. This is included as a reduction in the probability of infection per contact. The number of cercariae acquired on a 'successful' contact, d, is multiplied by a factor φ, such that for any contacts made in the 36 weeks after treatment, the number of new cercariae acquired in a single contact (t_q), is given by

$$t_q = \begin{cases} \varphi d & \text{if } s < 1/d, \text{ where } s \sim U(0,1) \\ 0 & \text{otherwise.} \end{cases} \tag{5.15}$$

5.2.2 Model criteria

Criteria were drawn up to test whether models could reproduce the required patterns of infection and antibody seen in field data. Most of the criteria relate to patterns seen in cross-sectional data, with an additional criterion for the effect of treatment on antibody. As for the deterministic models (chapter 4), there were criteria to test for the following patterns: a peaked age intensity curve with lower levels of infection in adults, a peak shift and an antibody switch occurring after the peak in infection intensity. These were assessed using grouped means for the infection criteria, and Spearman's correlation for the antibody switch (as was used for the original data analysis in chapter 2). Additionally for the stochastic models there were criteria to test whether measured infection prevalence and aggregation in egg output fell within ranges identified from field data, in each of two age groups (6–14 year olds and 15–34 year olds). There was also a criterion for infection aggregation in the whole population, but the equivalent criterion for prevalence was found to be uninformative and was not used. Finally there was a criterion to test whether the antibody switch occurred after treatment. These criteria are listed and defined in full in table 5.3. The peak shift was assessed on the average values of peak age group and peak infection level over all repeat simulations for different values of maximum infection rate; all other criteria were assessed for individual simulations. Initially I had hoped to use formal criteria to test whether the models were able to reproduce observed aggregated distributions of antibody, but it was found that the range of standardized variances for the different antibody isotypes obtained from field data (chapter 2) was too broad to be informative. Antibody aggregation and co-distributions were assessed visually for a subset of the models which passed all of the criteria for qualitative comparison with the field data.

5.2.3 Model analysis

Simulations were run for each of the successful combinations of antigen and antibody target identified from deterministic analysis (listed in table 5.4). In the initial baseline analysis, the parameters governing the stochastic processes were kept constant at the values given in table 5.2. The parameters determining mean population infection rate, worm life span, antibody strength, strength of cross-regulation/antigen threshold level and plasma cell decay rates were each varied across plausible ranges (given in table 5.2). Note that these parameters were the same as those used in the deterministic analysis, with the exception of A_1 strength (assumed to be 0 for all stochastic models), and the inclusion of an additional higher antigen threshold level ($T = 2500$). All possible combinations of these parameters were used in turn, giving 3150 parameter sets for each antigen-target combination. Each simulated cross-sectional data set

Table 5.2: Parameters used in the models, with ranges explored in the baseline analysis, additional values used in the sensitivity analysis, units and sources from the literature where relevant. Antigen units = number of cercariae/live worms/dying worms/eggs as appropriate. 'Cell' refers to units of the antibody-secreting cell or memory cell populations. Subscript j refers to values for the two different antibody responses ($j = 1, 2$)

Parameter	**Meaning**	**Values used in baseline analysis**	**Values used in sensitivity analysis**	**Units**	**Source/rationale**
Λ_{pmax}	Mean population maximum contact rate	12.5,25,50,100,200		worms year^{-1} person^{-1}	Chan *et al.* (2000)
a_c	Age above which contact rates stay constant	7.8		years of age	fit to data from Chan *et al.* (2000)
ϕ	Probability of resampling individual maximum contact rate	0.05	0,0.5	year^{-1}	Appendix D
k_1	Shape parameter for the distribution of individual maximum contact rates	0.5	0.4, ∞	no units	Woolhouse *et al.* (1998)
d	Number of cercariae acquired in a contact with probability $1/d$	1	10,100	contact^{-1}	varied to give different degrees of cercarial aggregation
n	Number of worm compartments in model	9		compartments	approx. Gaussian distributed worm survival
$1/\mu$	Natural mean worm life span	3,6.5,10		years	Fulford *et al.* (1995); Wilkins *et al.* (1984)
ε	Eggs output per worm per 10ml urine	1	0.1,10	eggs worm^{-1}day^{-1}10ml urine^{-1}	Hairston (1965)
k_E	Shape parameter for egg output per worm	1	∞	no units	de Vlas (1996)
κ_j	Rate of production of plasma cells	1		cells year^{-1} unit antigen^{-1}	variation accounted for in varying immune strength
γ_j	Rate of loss of plasma cells	0.008,0.08,0.8,8,80		cells year^{-1} cell^{-1}	Amanna *et al.* (2007); Ochsenbein *et al.* (2000)
θ	Strength of protection against reinfection	0.00025,0.001,0.004, 0.016,0.064,0.256,1.024		cell^{-1}	broad exploratory range
η	Strength of anti-fecundity response	0.00025,0.001,0.004, 0.016,0.064,0.256,1.024		cell^{-1}	broad exploratory range
ρ	Strength of cross-regulation	0.001,0.1,1		unit antigen^{-1}	set to give significant effect on immune development
β	Rate of production of 'cumulative' response	1		arbitrary units year^{-1} unit antigen^{-1}	arbitrary constant
T	Threshold for cumulative antigen exposure	25,250,2500		antigen units	set to give significant effect on age-intensity curve
x	Treatment efficacy	0.8,0.9,1.0		proportion of worms	Danso-Appiah *et al.* (2008)
φ	Post-treatment reduction in infection probability	0,0.5,1		proportion	explored across full possible range

Table 5.3: Criteria used to determine whether models replicated age-related and distributional patterns of infection and antibody seen in cross-sectional and post-treatment field data. Full details of the calculation of quantitative limits for these criteria are given in chapter 2. All criteria except the peak shift were applied to individual simulations, and had to be simultaneously met by at least 50% of repeat simulations. The peak shift was assessed using mean levels across all repeat simulations.

Pattern identified in field data	**Criterion applied to model output**	**Source**
Cross-sectional		
Peaked age intensity curve	maximum level of infection occurs in any age group apart from 3–5 or 24–34 year olds	Bradley & McCullough (1973); Clarke (1966); Mutapi *et al.* (1997); Useh & Ejezie (1999); Wilkins *et al.* (1987, 1984), Mutapi et al. (unpub. data)
Control of infection in adults	infection level in 24–34 year old age group <40% of level in peak age group	Bradley & McCullough (1973); Clarke (1966); Mutapi *et al.* (1997), Mutapi et al. (unpub. data)
Peak shift	peak infection intensity is lower and occurs in the same or older age group when infection rate is halved (except for lowest value of Λ_{pmax}, where infection intensity is higher and occurs in the same or earlier age group when infection rate is doubled)	Woolhouse (1998)
Aggregated egg output	standardized variance (SV) of mean egg output 2–60 for whole population	Mutapi *et al.* (1997) Mutapi et al. (unpub. data)
	SV of mean egg output 2–60 for 6–14 year olds	Mutapi *et al.* (1997) Mutapi et al. (unpub. data)
	SV of mean egg output 2–60 for 15–34 year olds	Mutapi *et al.* (1997) Mutapi et al. (unpub. data)
Prevalence of infection by urine test	prevalence of egg positives 5–80% for 6–14 year olds	Mutapi *et al.* (1997) Mutapi et al. (unpub. data)
	prevalence of egg positives 5–80% for 15–34 year olds	Mutapi *et al.* (1997) Mutapi et al. (unpub. data)
Antibody switch	negative correlation between the two antibody responses across the whole population, Spearman's $\rho <$ -0.2	Mutapi *et al.* (1998, 1997); Ndhlovu *et al.* (1996*b*)
Antibody switch after age of infection peak	initial (non-protective) antibody response first falls below its midpoint value (half way between minimum and maximum levels) in the same or a later age group than the age group with maximum infection	Mutapi *et al.* (1997); Ndhlovu *et al.* (1996*b*)
Post-treatment		
Antibody switch after treatment	A_2 is $\geq$ 200% and A_1 is $\leq$ 50% of respective pre-treatment levels at both 18 and 36 weeks post-treatment	Mutapi *et al.* (1998)

was analysed in the same way as the field data in chapter 2. Mean levels of infection and antibody were calculated for five separate age classes (6–8, 9–10, 11–12, 13–23 and 24–34 year olds) and the prevalence and standardized variance of infection were calculated for two larger age groups (6–14 and 15–34 year olds). The Spearman's correlation coefficient between the two antibody responses was calculated across the whole population. These were used to see whether the model could meet all of the cross-sectional criteria described above. These criteria are set out in full in table 5.3. Successful parameter combinations had to meet these criteria over a two-fold change in contact rate (Λ_{pmax}). Performance curves were drawn for a selection of parameter sets which preliminary analysis indicated were able to meet the model criteria, to determine the optimal number of replicate simulations which needed to be performed for each set of parameter values. Parameter sets for which all of the cross-sectional criteria were met were then tested for their ability to reproduce the treatment-induced antibody switch in the subset of the simulated population aged 6–15 years old. The predicted egg reduction rate (ERR) was calculated by comparing geometric means of infection intensity before and 12 weeks after treatment using the following formula (Saathoff *et al.* 2004):

$$\text{ERR} = \left(1 - \frac{\text{geometric mean egg count after treatment}}{\text{geometric mean egg count before treatment}}\right) \times 100\% \tag{5.16}$$

The ERR is calculated using geometric means in the vast majority of studies which report it for *S. haematobium* (Danso-Appiah *et al.* 2008).

Univariate sensitivity analysis was carried out on models which were able to reproduce both the cross-sectional and post-treatment patterns satisfactorily, varying separately in turn the aggregation of the underlying population contact rate distribution (k_1), the rate at which individual underlying contact rates are re-sampled (ϕ), the aggregation of cercariae acquired per contact (d), the aggregation of eggs per worm (k_E), and the number of eggs excreted in 10ml urine per worm (ε), while varying all other parameters across their full range, as above. The different parameter values used in the sensitivity analysis are given in table 5.2. These models were tested for their ability to reproduce both the cross-sectional and post-treatment patterns.

All simulations were run in C++.

5.3 Results

5.3.1 Identification of successful models

Performance curves were constructed for nine parameter sets which frequently passed all of the criteria. A variable number of repeat simulations, between 20 and 1000, were run ten times for each parameter set to determine how many repeat simulations were needed to give a stable estimate of the proportion of repeat simulations passing all criteria. The performance curves are shown in appendix E. It was found that 400 repeat simulations were sufficient to give a stable estimate of the proportion of repeat simulations passing all criteria. On the basis of these results, which showed quite low proportions of simulations passing all criteria, a threshold of 50% of simulations (i.e. 200 out of 400) passing all criteria was used to identify successful parameter combinations in all subsequent analyses.

5.3.2 Baseline analysis: cross-sectional criteria

The initial analysis used only the baseline parameters for the stochastic processes in the model, but covered the full range of all the other parameters (parameters listed in the 'baseline analysis' column in table 5.2). In the initial analysis, only the cross-sectional criteria were used (all of the criteria listed in table 5.3 apart from the post-treatment antibody switch). In line with field observations and the deterministic analysis in chapter 4, models were assessed for their ability to meet all of the cross-sectional criteria over a two-fold difference in population contact rate. The number of parameter sets which successfully did this are given for each model in table 5.4 (column headed 'cross-sectional'). Only three of the different model structures tested were ever able to meet all of the cross-sectional criteria over a two-fold change in population contact rate (highlighted in bold in table 5.4). These models all had an antigen threshold for the protective antibody response, and all had the protective antibody response reducing worm fecundity. The non-protective antibody response was stimulated by antigens from the egg stage and the protective antibody response could be stimulated by antigen from cercariae, live worms or dying worms.

It was also seen that one of the cross-regulation models (as indicated in table 5.4) was able to meet all of the cross-sectional criteria for some individual parameter sets, although not over a two-fold difference in population contact rate. This model also had the protective antibody response reducing worm fecundity and the non-protective antibody response stimulated by antigens from the egg stage. In this model, the protective antibody response was stimulated by antigen from dying worms.

5.3.3 Importance of different criteria

The criteria used to judge whether model output adequately replicated patterns seen in infection and antibody field data are listed in table 5.3. The relative importance of different criteria in excluding parameter combinations was assessed in detail for the baseline analysis using only the cross-sectional criteria. The number of individual simulations passing each criterion and passing each possible combination of criteria was counted. The criteria which were consistently passed by the fewest number of simulations were the requirement for infection prevalence to lie between 5–80%, particularly in the younger age group (aged 6–14 years old), and the requirement for a negative correlation between the two antibody responses. The majority of simulations failed on multiple criteria, with only 5% failing on a single criterion alone. Simulations that failed on a single criterion were most likely to fail to pass the criteria relating to the age of peak infection intensity, infection prevalence levels in 6–14 year olds or the antibody switch. All of the criteria were at some point the only filter to not be passed, indicating that all of these criteria were informative.

5.3.4 Inclusion of treatment

The parameter sets which were able to meet all of the criteria over a two-fold change in population contact rate (the three antigen threshold models highlighted in table 5.4) were further analysed for their ability to reproduce the observed antibody switch after treatment of children aged 6–15 years old. A range of different treatment efficacies and post-treatment levels of transmission reduction were investigated (listed in table 5.2). These parameters affected the

Table 5.4: Relative success of different model structures in meeting criteria. All criteria had to be met over a two-fold change in population infection rate.

Immune mechanism	**Life cycle stage**			**Number of parameter sets passing following criteria:**	
	Antigen for A_2	**Targeted by A_2**	**Antigen for A_1**	**cross-sectional**	**cross-sectional and post-treatment**
Cross-regulation	cercariae	cercariae	live worms	0	0
	cercariae	cercariae	dying worms	0	0
	cercariae	cercariae	eggs	0	0
	live worms	eggs	cercariae	0	0
	live worms	eggs	live worms	0	0
	live worms	eggs	dying worms	0	0
	live worms	eggs	eggs	0	0
	dying worms	cercariae	live worms	0	0
	dying worms	cercariae	eggs	0	0
	dying worms	eggs	cercariae	0	0
	dying worms	eggs	live worms	0	0
	dying worms	eggs	dying worms	0	0
	dying worms	eggs	eggs	0[a]	0
Antigen threshold	cercariae	cercariae	live worms	0	0
	cercariae	cercariae	dying worms	0	0
	cercariae	cercariae	eggs	0	0
	cercariae	**eggs**	**eggs**	**22**	**0**
	live worms	**eggs**	**eggs**	**254**	**0**
	dying worms	**eggs**	**eggs**	**48**	**32**
	eggs	eggs	eggs	0	0

[a] For this model, 12 individual parameter sets were able to meet all of the criteria, but none of these could meet the criteria over a two-fold change in population infection rate.

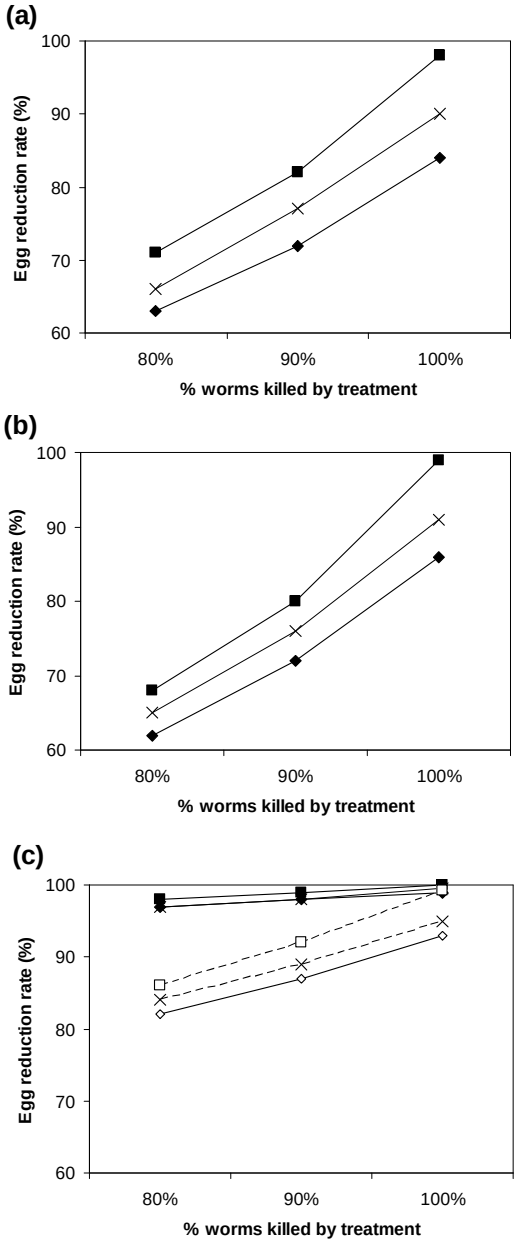

Figure 5.1: Egg reduction rate (ERR) at 12 weeks post treatment in different models. ERR (calculated using the formula given in section 5.2.3) is shown for each of the three antigen threshold models tested. The three panels show results for models with different life cycle stages providing the main antigenic stimulus for the protective antibody response (a) cercariae, (b) live worms, (c) dying worms. For each of these models, A_2 reduces worm fecundity, and A_1 is stimulated by antigen from eggs. The graphs show the mean ERR across all of the parameter sets tested for each value of treatment efficacy and transmission reduction used. For (c) they are additionally split by antigen threshold (T). In all graphs, transmission reduction is shown as squares for 100%, crosses for 50% and diamonds for 0%. In panel (c), open symbols denote antigen threshold (T) = 250, filled symbols denote antigen threshold (T) = 25.

observed egg reduction rate (ERR) at 12 weeks post-treatment (figure 5.1). ERR increased with increased treatment efficacy and with increased reduction of transmission after treatment (figure 5.1), and was also affected by the nature of the immune response. For the two models with antigen from cercariae or live worms stimulating the protective antibody response (A_1), ERR tended to be lower than the actual treatment efficacy, due to new infections acquired during the 12 weeks after treatment (including those acquired on the day of treatment itself) (figure 5.1a,b). For the model with dying worms providing the antigen for the protective antibody response, ERR was often higher than the treatment efficacy, and was affected by the level of the antigen threshold for the protective antibody response, with a greater ERR seen for parameter sets with a lower antigen threshold (figure 5.1c).

Only the models with dying worm antigens stimulating the protective antibody response were able to reproduce the post-treatment antibody switch (table 5.4). This was only possible for a subset of the parameters which reproduced all of the cross-sectional data patterns. The number of parameter sets reproducing the post-treatment antibody switch was robust to the level of treatment efficacy and reduction in transmission post-treatment across all of the levels explored.

Exploratory analysis of the cross-regulation model which was able to reproduce all of the cross-sectional data patterns for individual parameter sets indicated that this model could also reproduce the antibody switch after treatment. This was investigated further in the sensitivity analysis.

5.3.5 Sensitivity analysis

Sensitivity analysis was carried out on the two model structures which were able to reproduce the antibody switch after treatment: one with cross-regulation of the non-protective antibody response, and one with an antigen threshold for the protective antibody response, which both had the protective antibody stimulated by antigens from dying worms, with protective antibody reducing worm fecundity, and the non-protective antibody stimulated by eggs. Each of the parameters governing the stochastic processes in the model was varied separately in turn, using the alternative values given in table 5.2 (column headed 'Values used in sensitivity analysis'), whilst varying all other parameters over the full ranges used in the baseline analysis. These models were assessed for their ability to pass both the cross-sectional and the post-treatment criteria (all criteria listed in table 5.3). Figure 5.2 shows the number of parameter sets which were able to pass all of the criteria for both cross-sectional and post-treatment criteria over a two-fold change in maximum contact rate when each of the stochastic process parameters was varied in turn. For the cross-regulation model (figure 5.2a), this was only possible for models with moderate cercarial aggregation ($d = 10$) or with fewer eggs output in urine per worm ($\varepsilon = 0.1$). In the antigen threshold model, it was found that both the aggregation of the underlying contact rates between individuals and the rate at which this contact level was re-sampled affected whether or not the models were able to meet all of the criteria. Poisson distributed contacts ($k_1 = \infty$) and frequent re-sampling of contact rates ($\phi = 0.5$ year^{-1}) both prevented the models from reproducing field patterns (figure 5.2b). Note that more frequent re-sampling of contact rates reduces the overall aggregation of contact between individuals, so that these results are not independent. Making more modest changes to these parameters – increasing aggregation of the underlying contact rate to the maximum level reported in Woolhouse *et al.*

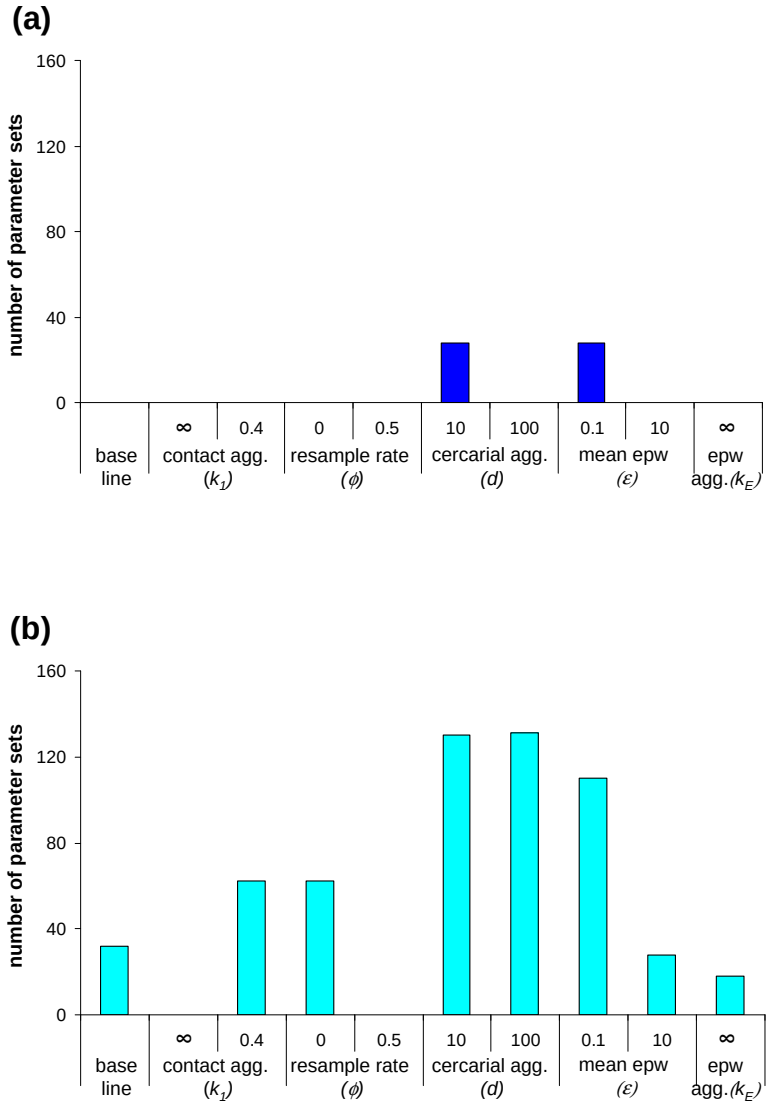

Figure 5.2: Results of univariate sensitivity analysis. Panels show the number of parameter combinations tested which meet all criteria (cross-sectional and post-treatment) over a two-fold change in maximal contact rate when the following parameters are changed individually as shown: the scale parameter for the underlying gamma distribution from which individual maximal contact rates are drawn (k_1), the yearly probability with which the individual maximal contact rate is resampled (ϕ), the parameter governing the aggregation of cercariae acquired per contact (d), the mean number of eggs per worm output in a 10ml urine sample (ε), and the scale parameter for the gamma distribution from which the number of eggs per worm is drawn (k_E). Baseline values for these parameters are: $k_1 = 0.5$, $\phi = 0.05$ year^{-1}, $d = 1$, $\varepsilon = 1$, $k_E = 1$. Results are shown for the two model structures for which cross-sectional and post-treatment criteria were ever met: (a) with cross-regulation of the non-protective antibody response, (b) with an antigen threshold for the protective antibody response. For both of these models, the stage of the schistosome life cycle which provides the main antigenic stimulus for A_2 is dying worms, A_2 reduces worm fecundity, and A_1 is stimulated by antigen from eggs.

(1998) ($k_1 = 0.4$), or using perfect predisposition ($\phi = 0$) – both increased the number of parameter sets which were able to meet all of the criteria. As in the cross-regulation model, varying cercarial aggregation and egg output in urine per worm both made a large difference to the ability of the model to reproduce field patterns. Either level of cercarial aggregation used in this analysis ($d = 10, d = 100$) increased the number of parameter sets meeting all criteria to a similar level, and reducing egg output in urine to 0.1 also greatly increased the area of parameter space over which the criteria were passed. Increasing egg output per worm ($\varepsilon = 10$) made little difference in these models, and reducing the aggregation of eggs per worm found in urine (using a Poisson distribution, $k_E = \infty$) reduced the number of parameter sets able to meet all of the criteria.

5.3.6 Parameter distributions

The ranges of decay rates for the two plasma cell populations in successful parameter sets were plotted for the two different model structures (figure 5.3). These are summed across the baseline and sensitivity analysis results. Similar patterns were seen for both the cross-regulation model (figure 5.3a) and the antigen threshold model (figure 5.3b). For all of the successful parameter sets, there was relatively rapid decay of the initial antibody response (A_1) of 8–80 year^{-1} (half-life 3–30 days), with slower decay of the protective antibody response (A_2) of 0.008–0.8 year^{-1} (half-life of 10 months–90 years) for all except four parameter combinations in the antigen threshold models which had more rapid A_2 decay of 8 year^{-1} (half-life 30 days). Within these ranges there was little apparent preference for particular values or combinations of the two decay rates.

5.3.7 Antibody aggregation and codistributions

The level of antibody aggregation was not used as a criterion in these models since the great majority of simulations gave standardized variances for antibody which fell within the broad range calculated from field data in chapter 2, meaning that this was not an informative criterion. All of the models which passed all of the other criteria gave aggregated distributions for both antibody responses. These are plotted for two randomly selected parameter sets in figure 5.4. Although it was not formally tested for, standardized variance tended to change between the two age groups in the same direction seen in the field data (in the opposite direction to the change in mean level, chapter 2). Visual inspection of antibody codistributions for randomly selected parameter sets (figure 5.4c,f) confirmed that the models had reproduced the dichotomous relationship between the two antibodies which was seen in field data (chapter 2), and that using a negative correlation as a criterion was sufficient to identify this pattern.

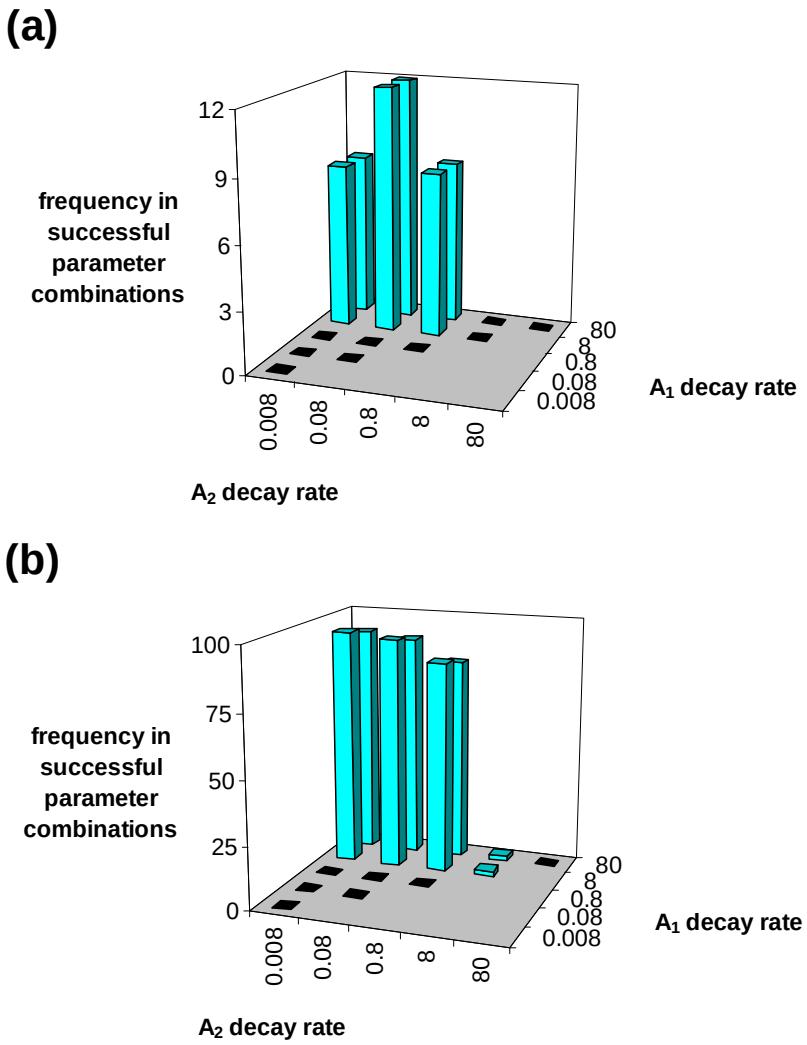

Figure 5.3: Distribution of plasma cell decay rates in successful parameter combinations. The frequency of different combinations of decay rates for the two plasma cell populations are shown for models which were able to meet all of the cross-sectional and post-treatment criteria, in either the baseline or the univariate sensitivity analysis. (a) Models with cross-regulation of the initial antibody response (A_1). (b) Models with an antigen threshold for the protective antibody response (A_2). Bars are drawn for all combinations of plasma cell decay rates which were used. Black bars indicate a frequency of 0, blue bars a frequency > 0.

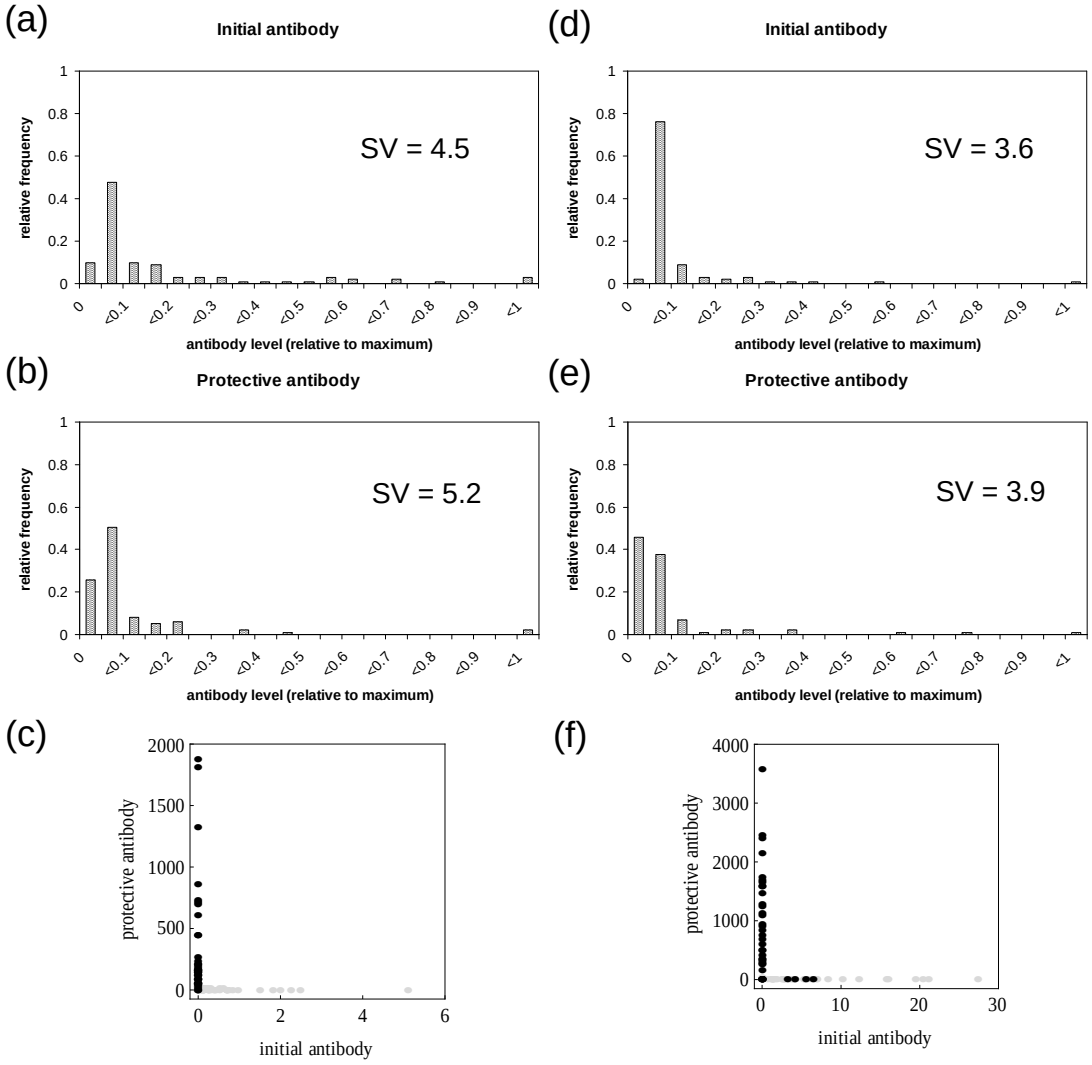

Figure 5.4: Antibody aggregation and co-distributions in the model outputs, shown for two example parameter sets. (a,b,c) Cross-regulation model, parameters used: $\Lambda_{pmax} = 25$, $1/\mu = 10$, $\gamma_1 = 80$, $\gamma_2 = 0.008$, $\eta = 0.256$, $\rho = 0.1$, $k_1 = 0.5$, $\phi = 0.05$, $k_E = 1$, d = 10. (d,e,f) Antigen threshold model, parameters used: $\Lambda_{pmax} = 100$, $1/\mu = 6.5$, $\gamma_1 = 80$, $\gamma_2 = 0.08$, $\eta = 1.024$, $T = 250$, $k_1 = 0.5$, $\phi = 0.05$, $k_E = 1$, d = 100. In (a) and (d) the distribution of the initial antibody response is shown, in (b) and (e) the distribution of the protective antibody response is shown, and in (c) and (f) the co-distribution of the two antibodies is shown. In (c) and (f) data points are coloured by age: grey circles 0–14 years old, black circles 15–34 years old. SV = standardized variance ($\sigma^2/\overline{x}^2$).

5.4 Discussion

Stochastic individual-based models were used to identify model structures that could simultaneously reproduce field patterns of schistosome infection and antibody, including aggregation of infection and age-related and treatment-induced antibody switches. As hypothesised, it was found that dying worms had to provide the main antigenic stimulus for a protective antibody response in order to reproduce these patterns. Additionally, it was found that the protective antibody response had to reduce worm fecundity, and the non-protective antibody response had to be stimulated by eggs. Models including either cross-regulation or an antigen threshold were able to reproduce all of the pre- and post-treatment infection and antibody patterns. The analysis suggested that the plasma cell populations that produce the switching antibody isotypes have different intrinsic decay rates, with the plasma cells producing the initial antibody response decaying more rapidly than those producing protective antibody. It also showed that some aggregation in the number of cercariae acquired per contact or a low number of eggs output in urine per worm both enhanced the ability of the models to reproduce the observed data patterns.

The finding that dying worms provide the main source of protective antigen is in line with several studies showing that praziquantel treatment, which kills adult schistosomes, can boost antibody responses associated with protection against re-infection (Butterworth *et al.* 1996; Fitzsimmons *et al.* 2007; Gomes *et al.* 2002; Grogan *et al.* 1996; Mutapi *et al.* 1998). Models with dying worms providing protective antigen demonstrated immune-enhanced reduction in egg output following treatment, which is known to occur in praziquantel treatment of schistosomes (Nyazema *et al.* 1995; Utzinger *et al.* 2003*b*). The finding that protective immunity is likely to principally target fecundity is supported by the findings of Agnew *et al.* (1996) that for *S. haematobium*, lower levels of egg output were found relative to levels of circulating anodic antigen (CAA, a marker for worm burden) in adults than in children, and that *S. haematobium* fecundity is reduced by the immune response in murine infections (Agnew *et al.* 1992). The models assume that immune stimulation by eggs (found to be the principal source of antigen for the non-protective antibody response) is primarily by very recently laid eggs, since the number of eggs stimulating the immune response is related to current worm burden in these models. This is likely to correspond to secreted egg antigens. If eggs become trapped within the host tissues, secreted antigen has been shown to be sequestered by the granulomatous response within a few days of egg deposition (von Lichtenberg 1964).

For virtually all of the successful models, the plasma cell population producing protective antibody had a slower natural decay rate than the plasma cell population producing the initial (non-protective) response, this being necessary in these simulations to generate and sustain the antibody switch over 36 weeks post treatment. A similar conclusion was reached in a modelling study of the epidemiological patterns of so-called 'blocking' antibodies (Woolhouse 1994*b*), which could be explained by different decay rates of the two supposedly antagonistic antibody responses. The differences in decay rates suggested in the current analysis cannot be attributed to different intrinsic decay rates of the antibody molecules themselves, since natural antibody decay rates in humans are of the order of days to weeks (Morell *et al.* 1970; Waldmann & Strober 1969) which is too rapid to fully explain the differences seen here. One possible explanation is that the different antigens are stimulating different populations of plasma cells belonging to the short- and long-lived subsets, which have differing reported decay rates (Lanzavecchia *et al.*

2006; Ochsenbein *et al.* 2000; Radbruch *et al.* 2006). It is also possible that the cells producing different antibody isotypes have varying dynamics, as different rates of cell turnover have been reported for IgA, IgG and IgM switched memory cell populations (Wirths & Lanzavecchia 2005).

Many of the parameter combinations tested here failed to generate levels of infection prevalence (which is related to parasite aggregation) consistent with field data, frequently giving prevalence levels above 80% in the younger age group. Previous stochastic models of schistosome infection have also given very high prevalence levels (Chan & Isham 1998). It was found that relatively high levels of aggregation of individual contact rates had to be maintained, with fairly high predisposition (infrequent resampling of individual contact rates), in order to reproduce field patterns. The values used in the baseline analysis, of $k_1 = 0.5$ and $\phi = 0.05$ year^{-1}, which were both estimated from field data, were sufficient to reproduce all of the required patterns. Aggregation of cercarial acquisition increased the number of parameter sets for which models met all of the criteria but was not essential, and both reduced mean egg output per worm and increased aggregation of egg output also enhanced the ability of the models to meet the criteria, through the increased occurrence of egg-negative individuals (decreasing the measured prevalence of infection). The level of aggregation of egg output used in most of the models was estimated from *S. mansoni* data, and seems plausible for *S. haematobium*, for which substantial day-to-day variation in urine egg counts is also observed (van Etten *et al.* 1997; Warren *et al.* 1978). The reduced level of mean egg output per worm (0.1 per worm per 10ml urine) which improved model performance is slightly lower than previous estimates (Cheever *et al.* 1977; Woolhouse *et al.* 1996), but plausible given the considerable uncertainty in egg production rates for *S. haematobium* and variation in urine output. Woolhouse *et al.* (1996) assumed that 0.64 eggs were excreted daily per female worm per 10ml urine (assuming 1400ml urine were passed per day and 90 eggs excreted per mated female daily (Hairston 1965)), and Cheever *et al.* (1977) estimated that 1.28 mature eggs were passed per female worm per 10ml urine from autopsy studies. In a small study of live human patients, an average of 200 eggs per mated female were passed in urine per day, but this was highly variable between subjects (range 3–560) (Cheever *et al.* 1975).

Cercarial aggregation is more difficult to measure, with the evidence for aggregated exposure to schistosome infection being sparse and equivocal (discussed by Quinnell *et al.* (1995)).

Although the degree of aggregation of the antibody responses in these models was not formally tested for, due to the wide range in aggregation levels found in field data, the models did give highly aggregated antibody output. This demonstrated that aggregation in individual exposure levels was sufficient to explain antibody aggregation as well as aggregation in infection intensities, without needing to additionally consider other potential sources of antibody aggregation such as variability in individual immune competence.

This analysis used the pattern-oriented modelling (POM) approach which was introduced in chapter 4, requiring models to pass an extended panel of different criteria simultaneously. Other studies using POM have found that some criteria are non-discriminatory (Rossmanith *et al.* 2007). In this study, filters for antibody aggregation and prevalence in the whole population were not used because of their poor discriminatory ability. However, the other ten filters used all had individual discriminatory power, and the fact that successful models were able to pass such a diverse set of filters lends strength to the conclusions drawn.

This analysis considered only models with plasma cell populations (with no explicit memory

response). It would be interesting to extend the analysis to other immune models, starting with the memory models which were successful in the deterministic analysis. Since only models with Gaussian-distributed worm survival were considered here, it is not possible to draw any conclusions about the probable shape of natural worm survival curves - it is possible that some models with exponentially distributed worm life span would also be able to reproduce all of the required patterns, but this would need to be formally tested.

This work has identified a single model structure and a relatively small range of parameter values for which it is possible to reproduce both pre-treatment age-related patterns of infection and antibody, and short-term post-treatment changes in the antibody response. This model can now be used to investigate the longer-term implications of treatment of endemic populations, in terms of its impact upon the development of acquired immunity and consequent effects upon infection. This is important for assessing the overall impact of current large-scale mass-treatment programmes.

Chapter 6

Predicted impact of mass drug administration on the development of protective immunity

6.1 Introduction

Recent attempts at schistosomiasis control have focussed upon mass drug administration (MDA), using the antihelminthic drug praziquantel (Fenwick *et al.* 2009; WHO 2001, 2006). The main aim of these mass treatment programmes has been to reduce morbidity rather than to eliminate infection, although mass treatment can significantly reduce population levels of infection (Kabatereine *et al.* 2007; King *et al.* 1991; Koukounari *et al.* 2007; Tohon *et al.* 2008) and have a demonstrable effect upon transmission rates (French *et al.* 2009; King *et al.* 1991). However, to keep infection levels low, treatments need to be administered repeatedly for an indefinite time period (Chan *et al.* 1998; Utzinger *et al.* 2003*a*).

The main effect of treatment programmes on infection levels is through direct killing of worms, with indirect effects through reduced transmission. Acquired immunity is also expected to have some effect, enhancing the efficacy of treatment during control programmes, and playing a major role in determining the dynamics of infection after treatment programmes cease (Chan 1996; Chan *et al.* 1996). Previous modelling work, in which it was assumed that protective immunity was stimulated by live adult worms, has demonstrated that repeated population-level treatment in this case disrupts the development of acquired immunity, through removal of the antigenic stimulus (Anderson & May 1985; Chan *et al.* 1996). Chan *et al.* (1996) showed that, if treatment was stopped, under some circumstances infection levels could 'overshoot' to exceed pre-treatment levels.

Several studies have demonstrated that praziquantel treatment can induce changes in the antibody response to schistosomes (*S. mansoni* or *S. haematobium*), boosting schistosome-specific antibody responses including IgE and IgG1 (Butterworth *et al.* 1996; Fitzsimmons *et al.* 2007; Gomes *et al.* 2002; Mutapi *et al.* 1998; Satti *et al.* 1996) and bringing about isotypic

changes which occur more gradually with age in the same populations (Grogan *et al.* 1996; Mutapi *et al.* 1998). Praziquantel treatment has also been shown to boost schistosome-specific cytokine responses, including IL-4, IL-5, IL-10, IL-13 and TGF-β (Fitzsimmons *et al.* 2004; Joseph *et al.* 2004*b*; van den Biggelaar *et al.* 2002). Praziquantel kills adult worms, and has been shown to expose a number of antigens on the worm surface of *S. mansoni* in murine and in vitro studies (Redman *et al.* 1996), and to allow or enhance serological recognition of a number of *S. haematobium* antigens in humans (Mutapi *et al.* 2005). It is thought that this increased exposure to antigens released from dying worms is responsible for stimulating the changes seen in the immune responses following praziquantel treatment. Several of the responses which are boosted by praziquantel treatment, including IgE, IgG1, IL-4 and IL-5, have been associated with protection against re-infection in other studies (Dunne *et al.* 1992*a*; Hagan *et al.* 1991; Medhat *et al.* 1998; Roberts *et al.* 1993; Satti *et al.* 1996). This implies that treatment may enhance protective immunity and reduce subsequent re-infection, although this has not yet been directly demonstrated in a field setting.

If protective immunity is assumed to be mainly stimulated by antigens from dying worms, then treatment is expected to increase antigenic exposure and boost protective immune responses in the short term through worm killing. However, since treatment causes worms to die sooner than they would do under natural circumstances, it will result in reduced exposure to dying worms for a period of time after the initial reduction in worm burden. This exposure will be further reduced if population-wide treatment reduces transmission rates, leading to decreased levels of re-infection. The long-term implications of treatment for the development of protective immunity in this case are not fully clear.

The aim of the work described in this chapter was to assess the expected impact of long-term treatment (repeated treatment over several years) upon the development of acquired immunity, and resultant effects on infection, both during and after a mass treatment campaign. Current MDA programmes, such as those carried out by the Schistosomiasis Control Initiative (SCI), aim to implement sustainable long-term control (Fenwick *et al.* 2009). However, it is important to assess the potential consequences of the cessation of these control programmes, given that previous modelling work has shown that infection levels may overshoot and exceed pre-treatment levels if control programmes are stopped (Chan *et al.* 1996).

In this chapter, the model structure and parameter sets that were able to reproduce all of the required cross-sectional and post-treatment patterns in infection and antibody data (chapter 5) were used to predict the longer-term impact of repeated treatment upon the development of protective immunity over a five year treatment period and eleven subsequent years of follow-up. The effects upon infection intensity were also assessed, in particular whether these models, which have dying worms providing the main antigenic stimulus, ever predicted infection levels 'overshooting' pre-treatment levels after treatment ceases, which would imply that cessation of treatment programmes could temporarily impose a greater burden of infection upon populations than they had before treatment started.

Analysis framework for chapter 6

- The aim of the analysis in this chapter is to make predictions about the long-term effects of large-scale mass treatment programmes upon the development of protective antibody responses and the subsequent additional impact upon infection levels, both during the treatment programme and after it stops.
- The same stochastic individual-based models which were used in chapter 5 are used to make these predictions. These models describe infection intensity and levels of two independent antibody responses in a population of individuals.
- Model structures and parameter sets which were able to meet all of the pre- and post-treatment infection and antibody criteria in chapter 5 are used to make these predictions.
- The models are run for a 5-year treatment programme and for a further 10 years after the programme stops, using a constant-sized population with turnover
- Different treatment schedules are compared for their effects upon infection and antibody dynamics:
  - Biannual versus annual treatment
  - 90% versus 75% coverage
  - Treatment of all individuals aged 6-34 years old versus schoolchildren aged 6-34 years old
- Transmission is assumed to either not be affected at all treatment, or to be reduced by 50% or 100% throughout the intervention programme and for one year afterwards. A preferable alternative for assessing the transmission-related effects of treatment would be a full transmission model relating infection rates to egg output. However, there is limited data available to parameterise such a model, as the effects of mass treatment programmes on transmission (as distinct from infection intensity) are rarely measured.

6.2 Methods

6.2.1 The model

The stochastic individual-based model framework described in chapter 5 was also used in this chapter. Treatment was modelled in the same way as in chapter 5, but in this analysis repeated treatments were used, according to the schedules described in section 6.2.3.

6.2.2 Population structure

To maintain a constant size of population aged 6–34 years old over a time period of 15 years, a different population structure from that used in chapter 5 was used here. A population of 175 individuals was simulated, with 5 individuals in each yearly age group from 1 to 34 years old at the time of the baseline survey. Individuals were simulated up to their respective ages before the initial population survey was taken and treatment applied. Individuals were then simulated for a further 15 years after this initial survey, with treatment schedules applied as described in the next section, and individual levels of egg output and antibody were recorded at yearly intervals. When individuals reached the age of 34, they were replaced by 1 day old infants with no infection or antibody responses, to maintain a constant population size. It was

assumed that maternal antibodies play a negligible role in young children, who have very low infection rates in these models.

6.2.3 Treatment schedules

Six different treatment schedules were used (listed in table 6.1). These were used to explore the impact of treatment frequency, target population, coverage and effect of treatment upon transmission. For the standard treatment schedule (schedule 1), treatment was given to school-aged children in the population, defined as those aged 6–15 years old, as recommended by the WHO and implemented by the SCI (Fenwick *et al.* 2009; WHO 2006). Treatment was applied annually for five years (total of five treatments). Annual treatment is advised by the WHO for high-prevalence communities (WHO 2006) and has been used by the SCI in Uganda, Zanzibar and Zambia (Fenwick *et al.* 2009; Kabatereine *et al.* 2006*a*). In the standard treatment schedule, coverage was assumed to be 75%, in line with WHO targets and coverage achieved by SCI programmes in Uganda, Mali and Niger (Fenwick *et al.* 2009; Garba *et al.* 2006; Kabatereine *et al.* 2006*a*; Tohon *et al.* 2008; WHO 2001). In the standard treatment schedule it was assumed that treatment did not affect transmission.

In each of the other treatment schedules, one parameter was changed from the standard schedule (table 6.1). In schedule 2, biannual treatment was given over a five year period (total of three treatments). Biannual treatment is advised by the WHO for areas with moderate prevalence, and has been used in SCI programmes in Burkina Faso and Niger (Fenwick *et al.* 2009; WHO 2006). In schedule 3, a treatment coverage of 90% was used (as achieved in some of the countries targeted by the SCI (Gabrielli *et al.* 2006; Kabatereine *et al.* 2006*b*)). In schedule 4, the whole population over the age of 5 was treated, as recommended and implemented for high risk populations (Fenwick *et al.* 2009; Garba *et al.* 2006; WHO 2006). In schedules 5 and 6, it was assumed that treatment reduced transmission by 100% or 50% respectively. Treatment was assumed to reduce transmission to a fixed level, from the day after the first treatment up until one year after the final treatment. Transmission was then assumed to return to its original level. The changes in transmission were assumed to occur as a step function with no gradual transition between the two levels.

For all of the treatment schedules (1–6), treatment was applied over a five year period (beginning the day after the initial baseline survey), and the population was sampled (infection and antibody levels recorded) yearly throughout the treatment period and for a further 11 years after the final round of treatment. When treatment was applied, this occurred on the day after yearly sampling. Treatment was applied randomly across the eligible population at the required coverage level (75% or 90%) at each round of treatment. It was assumed that an individual's chance of being treated at each treatment round did not depend upon whether or not they had been treated in previous rounds. For all of the schedules, a treatment efficacy of 90% was assumed, in line with field studies reporting egg reduction rates ((1 - geometric mean egg count after treatment/geometric mean egg count before treatment) $\times$ 100%) for *S. haematobium* of 83-99.9% (Danso-Appiah *et al.* 2008; De Clercq *et al.* 2002; King *et al.* 2000; Midzi *et al.* 2008; Saathoff *et al.* 2004; Sissoko *et al.* 2009; Tchuem Tchuente *et al.* 2004). The analysis in chapter 5 showed that the egg reduction rate in the model simulations will also be affected by re-infection rates and the strength of the antibody response, but will fall within this reported range for the model parameters used.

Table 6.1: Treatment schedules used

schedule	description	treatment frequency	target population	treatment coverage	effect on transmission
1	Standard	annual	schoolchildren (6–15 years old)	75%	none
2	Biannual	biannual	schoolchildren (6–15 years old)	75%	none
3	90% coverage	annual	schoolchildren (6–15 years old)	90%	none
4	Treat all aged 6–34 years old	annual	schoolchildren and adults (6–34 years old)	75%	none
5	100% transmission reduction	annual	schoolchildren (6–15 years old)	75%	100% reduction
6	50% transmission reduction	annual	schoolchildren (6–15 years old)	75%	50% reduction

6.2.4 Analysis

The parameter sets identified in chapter 5, all of which were able to reproduce cross-sectional and short-term post-treatment patterns of infection and antibody over a two-fold change in maximum mean population infection rate, were used for simulations of the long-term impact of treatment. For each parameter set, 200 repeat simulations of the whole population were run, and mean levels of infection and antibody for the whole population aged 6–34 years old were calculated pre-treatment and at yearly intervals during and after the simulated treatment regime, for each individual simulation and averaged over the 200 repeats. Averages were calculated over this age range in order to capture the changes in infection and antibody levels in treated individuals as they aged over the long follow-up period. Infection and antibody dynamics were studied to see how quickly they returned to pre-treatment levels. This was studied for the mean values calculated over the 200 repeats, with infection levels analysed for how quickly they returned to within 95% of pre-treatment levels, and antibody levels for when they dropped below 100% of pre-treatment levels. The conditions (particular parameter values or treatment schedules) under which protective antibody levels fell below pre-treatment levels, or infection significantly overshot (exceeded 120% of) pre-treatment levels, were identified.

6.3 Results

6.3.1 Standard treatment schedule

The different factors affecting the speed with which antibody and infection levels returned to pre-treatment levels were assessed first of all for the standard treatment schedule, for which it was assumed that there was no reduction in transmission during or after the period of treatment. Considerable variation was observed between individual simulations for each parameter set, particularly for infection levels but also for antibody (figure 6.1). For all subsequent analyses, the mean values at each time point were calculated over the 200 repeat simulations for each

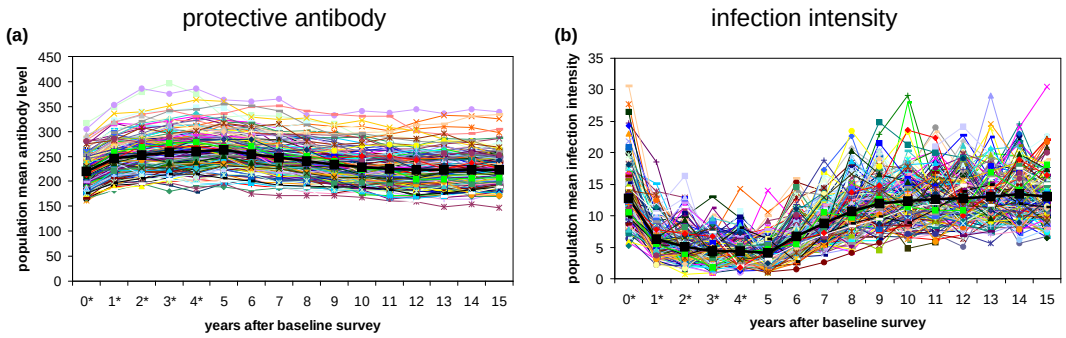

Figure 6.1: The results of 200 separate simulations using a single parameter set from the antigen threshold model. Dynamics of (a) antibody and (b) infection intensity averaged across the whole population are shown for each simulation. The mean level across the 200 simulations is shown by the heavy black line. The standard treatment regime was used, with treatment given at yearly intervals for 5 years to school-aged children (6–15 years old) with 75% coverage. It was assumed that there was no decrease in transmission after treatment. Treatment was applied on the day after surveys marked *. (Parameters used: $\Lambda_{pmax} = 25$, $1/\mu = 6.5$, $\gamma_2 = 0.008$, $\eta = 1.024$, $T = 25$, $k_1 = 0.5$, $\phi = 0.05$, $k_E = 1$, $x = 0.9$, d = 1; all parameters fully defined in chapter 5).

parameter set, and the mean levels were then adjusted relative to the mean level at baseline. For all of the results reported here, levels of the second (non-protective) antibody response closely followed infection dynamics, so that their time-profiles were virtually identical to those shown for infection (non-protective antibody results not shown).

For the 56 parameter sets with cross-regulation of the antibody response, three distinct time-profiles of protective antibody and infection levels were seen, which segregated by the decay rate of the plasma cells producing protective antibody. These are shown in figure 6.2, for the standard treatment schedule (schedule 1), with yearly treatment of schoolchildren with 75% treatment coverage. For all of these models, the level of protective antibody increased after the initial treatment, but the dynamics differed both during and after the five annual rounds of treatment for parameter sets with different rates of plasma cell decay. The maximum relative increase in the level of protective antibody was greatest for models with more rapid decay of the plasma cells producing protective antibody. Models with relatively slow plasma cell decay (0.008 – 0.08 year^{-1}) saw progressive increases in the average population level of protective antibody over the five years of treatment (figure 6.2a,b), whereas in models with more rapid plasma cell decay, antibody levels peaked one year after treatment began and declined during subsequent treatment rounds (figure 6.2c). Both the time at which mean antibody levels fell below pre-treatment levels, and the time at which infection levels returned to 95% of pre-treatment levels varied between models with different rates of plasma cell decay. The level of protective antibody returned to pre-treatment levels around 11 years after treatment ceased for parameter sets with the slowest decay of plasma cells producing protective antibody (0.008 year^{-1}) (figure 6.2a), around 6 years after the final treatment for parameter sets with a medium plasma cell decay rate of 0.08 year^{-1}, with subsequent reduction below pre-treatment levels (figure 6.2b), and within 2 years of the final treatment for models with a rapid plasma cell decay rate of 0.8 year^{-1}, and in every case remained below pre-treatment levels for the remaining 9 years of simulation (figure 6.2c). Levels of infection also followed different trajectories with differing plasma cell

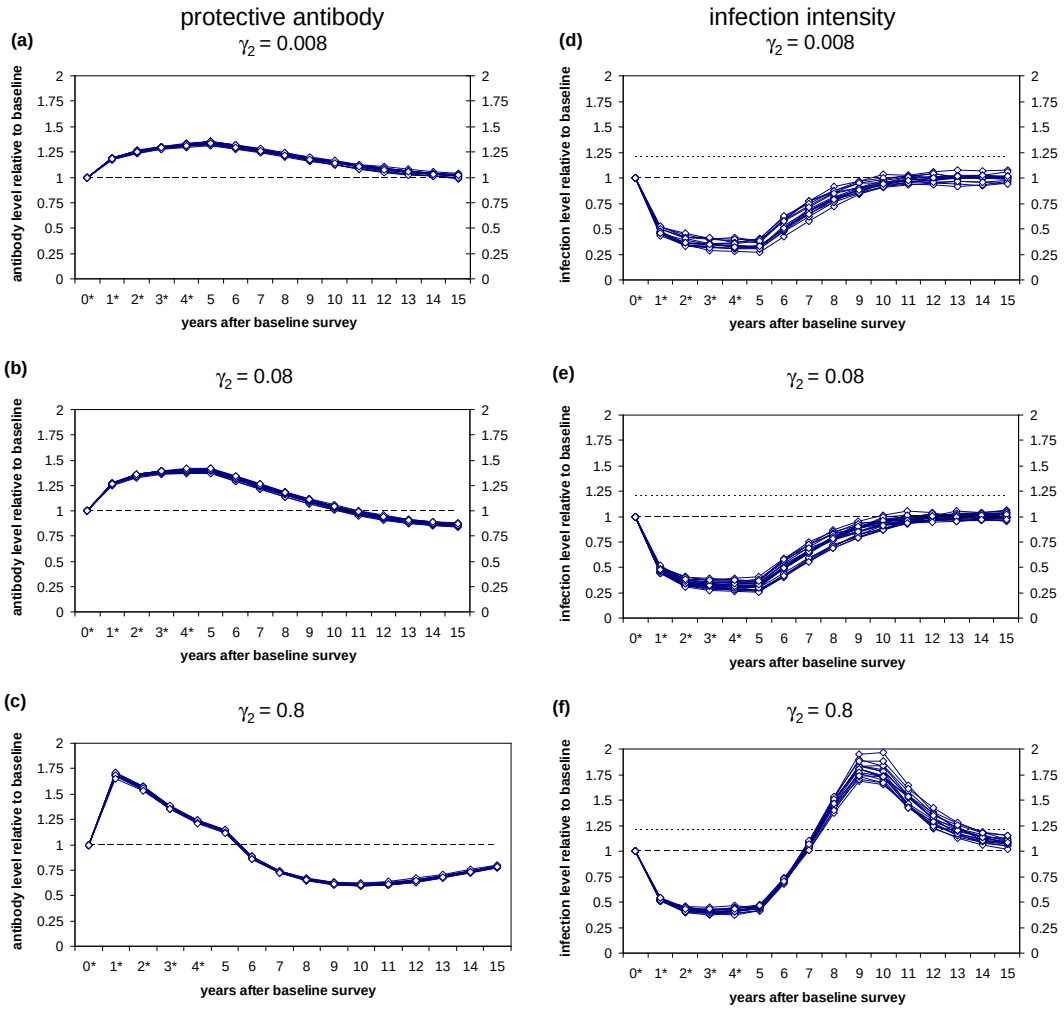

Figure 6.2: Dynamics of protective antibody and infection during and after treatment, without any reduction in transmission, for parameter sets with cross-regulation of the antibody responses. Treatment was applied at yearly intervals for 5 years to school-aged children (6-15 years old) with 75% coverage. Treatment was applied the day after surveys marked *. (a-c) Antibody levels and (d-f) infection levels are shown relative to pre-treatment levels for all of the parameter sets with antibody cross-regulation which reproduced cross-sectional and post-treatment patterns in chapter 5. Results are shown separately for parameter sets with different rates of yearly antibody decay: (a,d) 0.008, (b,e) 0.08 and (c,f) 0.8 year^{-1}. Numbers of parameter sets drawn in each plot: (a,d) 16, (b,e) 24, (c,f) 16. The dashed line on each plot shows the baseline level. The dotted line on the infection intensity plots is at 20% above baseline.

decay rates, particularly after treatment stopped (figure 6.2d-f). With slow plasma cell decay, infection levels returned to within 95% of pre-treatment levels between 5–11 years after the final treatment (figure 6.2d), and 5–9 years after the final treatment for moderate plasma cell decay rates (figure 6.2e), but with more rapid plasma cell decay, infection levels returned to pre-treatment levels 3 years after the final treatment and then overshot pre-treatment levels (by more than 60%) before re-approaching levels of infection seen before control (figure 6.2f). There was no clear order in which infection intensity and protective antibody returned to pre-treatment levels. This was partly obscured by the greater inherent variability in infection levels, but a strong trend for protective antibody to return to pre-treatment levels after or at the same time as infection levels did so for slow plasma cell decay (figure 6.2a,d) was not seen for rapid antibody decay, where protective antibody fell below pre-treatment levels before infection returned to pre-treatment intensities (figure 6.2c,f).

For the 573 parameter sets with a threshold on the protective antibody response, more variable dynamics were observed under the standard treatment regime (figure 6.3). The dynamics of the protective antibody response appeared to be mainly determined by the rate of plasma cell decay and the mean worm life span. (Note that no effect of worm life span was seen in the cross-regulation models, because all of the parameter sets had a mean worm life span of 10 years.) As for the cross-regulation models, a bigger boost in antibody was seen for models with more rapid plasma cell decay, apart from the four parameter sets with very rapid plasma cell decay (8 year^{-1}), where antibody levels had already decreased below pre-treatment levels at one year after the first treatment (figure 6.3d). In these models, antibody was boosted 3 months after treatment, but declined rapidly before the next round of treatment (figure 6.4). For models with slower plasma cell decay, the extent of both the antibody boost during treatment and the decline below pre-treatment levels differed with mean parasite life span. While in most cases levels of protective antibody remained elevated above pre-treatment levels throughout the period of treatment, for models with fairly rapid plasma cell decay (0.8 year^{-1}) and a short mean worm life span of 3 years, levels of protective antibody consistently dropped below pre-treatment levels after only three or four out of five rounds of treatment (figure 6.3c). Over the whole follow-up period, models with a longer parasite life span tended to show both a higher antibody boost and a more substantial drop below pre-treatment levels than models with a shorter parasite life span (figure 6.3a-c). As for the cross-regulation models, antibody levels tended to drop below pre-treatment levels earlier for models with more rapid plasma cell decay. Infection profiles varied, but still segregated by parasite life span (figure 6.3e-g), with infection levels reduced to a lesser extent by treatment and returning to pre-treatment levels earlier with progressively shorter worm life span. It should be noted that parameter sets with a mean worm life span of 3 years had a higher antigen threshold than those with a longer worm life span, as these parameters were not independently distributed among the parameter sets which were successful in chapter 5. Only a few parameter sets, with specific combinations of plasma cell decay rate, antibody strength and antigen threshold level, gave an 'overshoot' in infection levels (figure 6.3g). For mean infection levels to ever exceed 120% of pre-treatment levels after treatment ceased, it was necessary to have fairly rapid plasma cell decay (γ_2) of 0.8 year^{-1}), moderate antibody strength (η) of 0.256 per plasma cell and an antigen threshold (T) of 25 antigen units.

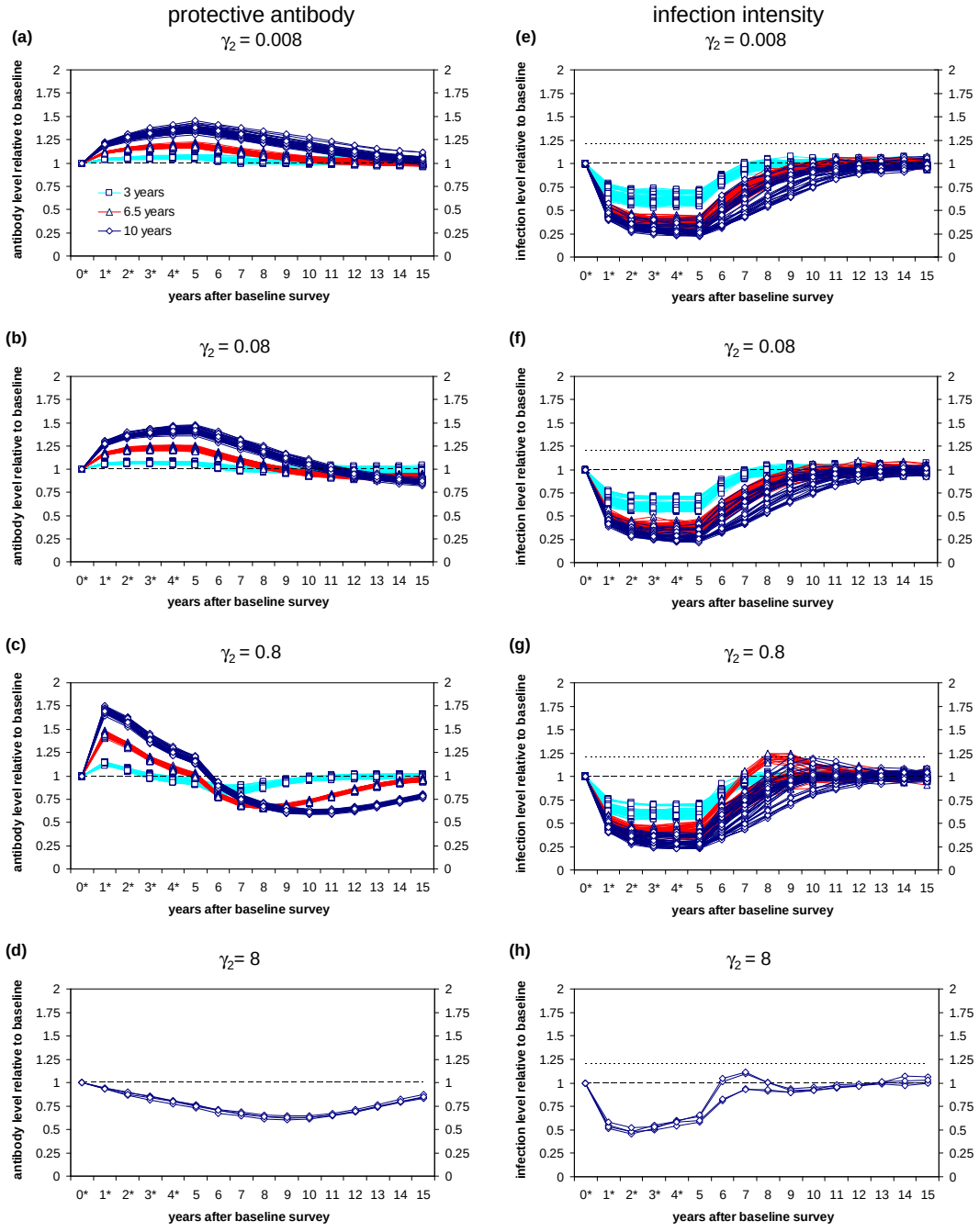

Figure 6.3: Dynamics of protective antibody and infection during and after treatment, without any reduction in transmission, for parameter sets with an antigen threshold. Details as for figure 6.2. An additional rate of plasma cell decay is included in these models, of 8 year^{-1} (d,h). The parameter sets used are those with an antigen threshold which reproduced cross-sectional and post-treatment patterns in chapter 5. Numbers of parameter sets drawn in each plot: (a,e) 195, (b,f) 195, (c,g) 179, (d,h) 4. Within each plot, profiles are distinguished by mean parasite life span: squares, pale blue lines = 3 years; triangles, red lines = 6.5 years; diamonds, dark blue lines = 10 years.

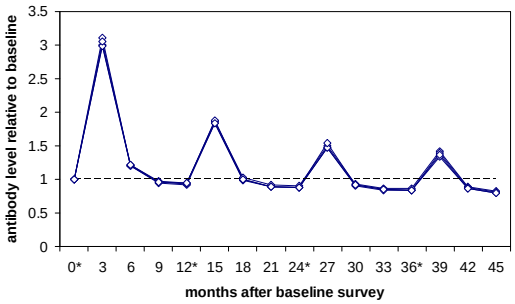

Figure 6.4: Dynamics of protective antibody in models with very rapid plasma cell decay. Antibody levels are shown at 3-monthly intervals for 4 years after the baseline survey. The same parameter sets and treatment regimes are used as in figure 6.3d. Treatment was applied the day after surveys marked *.

6.3.2 Treatment schedules 2–4 – varying treatment frequency, coverage and targeting

The impacts of separately varying the frequency of treatment, coverage of the target population, and age range of the population targeted were assessed by looking at the results of treatment schedules 2–4. Results are shown for four single parameter combinations (figures 6.5 and 6.6), but are qualitatively representative of what was seen across all of the different parameter sets. For each type of model, cross-regulation or threshold, the results are shown for two parameter sets that did or did not give an overshoot in infection in the standard treatment regimes.

For the cross-regulation models, none of the different treatment schedules used (schedules 2–4) made a difference to whether or not particular parameter sets did or did not give an overshoot in infection levels after treatment ceased, but for parameter sets that did, the magnitude of the overshoot was altered by different treatment regimes. With biannual treatment (schedule 2), protective antibody declined and infection increased following non-treatment years during the programmes, but levels of infection and antibody came close to those seen with annual treatment at one year after the biannual treatments (figure 6.5). For parameter sets with an infection overshoot, this overshoot was less pronounced for biannual versus yearly treatment (figure 6.5d).

Changing the level of coverage of the school-aged population (90% coverage (schedule 3) vs. 75% (schedule 1)) made little difference to the dynamics of protective antibody and infection levels during or after treatment; the higher coverage level gave a slightly greater increase in antibody levels and greater reduction in infection during treatment (figure 6.5), with a more pronounced overshoot in infection for the parameter set which had an overshoot with 75% coverage (figure 6.5d).

Treating both adults and children (aged 6–34 years old, schedule 4) rather than just school-aged children (6–15 years old, schedule 1) led to much larger increases in the antibody boost for all parameter combinations (figure 6.5b,d), with a concomitant reduction in infection levels during the treatment programme. In models with treatment of both school-aged children and adults, an increased overshoot in infection levels was seen after treatment ceased for parameter sets with rapid decay of plasma cells, to a greater extent than that seen with increased coverage of the school-age population (figure 6.5d).

For the antigen threshold models, very similar qualitative patterns were seen, which are

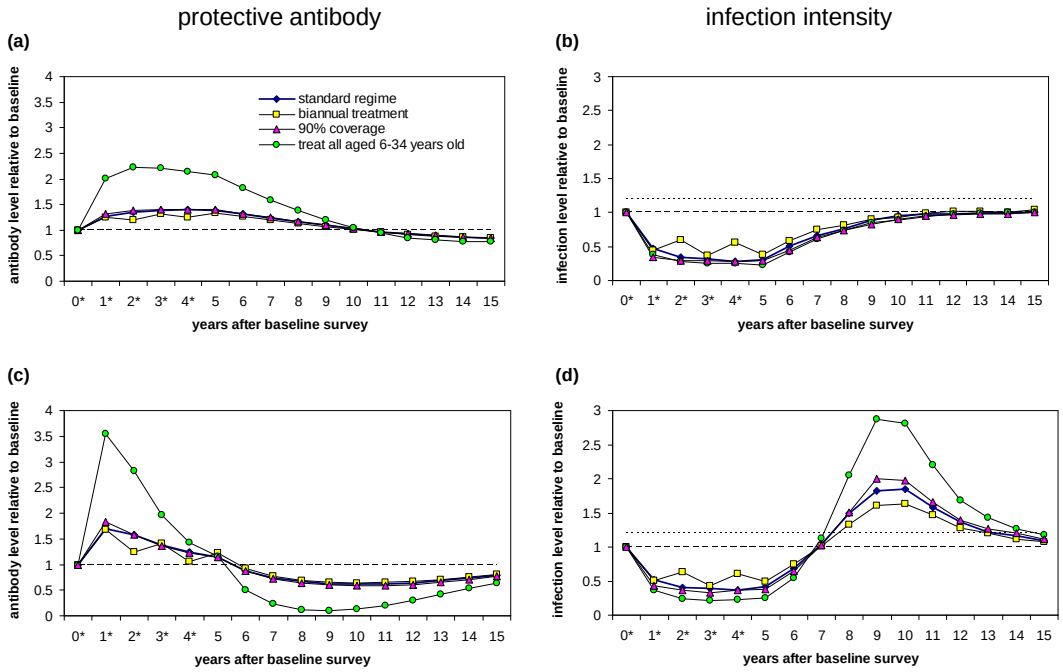

Figure 6.5: Dynamics of protective antibody and infection under different treatment regimes, for parameter sets with cross-regulation. No reduction of transmission occurred after treatment in these models. Results are shown for two different parameter combinations: (a) infection and (b) antibody with $\Lambda_{pmax} = 25, 1/\mu = 10, \gamma_2 = 0.08, \eta = 0.256, k_1 = 0.5, \phi = 0.05, k_E = 1, d = 1, \varepsilon = 0.1$; (c) infection and (d) antibody with $\Lambda_{pmax} = 12.5, 1/\mu = 10, \gamma_2 = 0.8, \eta = 1.024, k_1 = 0.5, \phi = 0.05, k_E = 1, d = 1, \varepsilon = 0.1$ (all parameters fully defined in chapter 5). Treatment was applied over a five-year period, with treatment frequency, coverage and targeting in the following combinations: blue diamonds – standard; yellow squares – biannual treatment; pink triangles – 90% coverage; green circles – treatment of 6–34 year olds. Treatment was applied the day after surveys marked * for all except biannual treatment, where treatment was applied the day after survey 0, 2 and 4. The dashed line on each plot shows the baseline level. The dotted line on the infection intensity plots is at 20% above baseline.

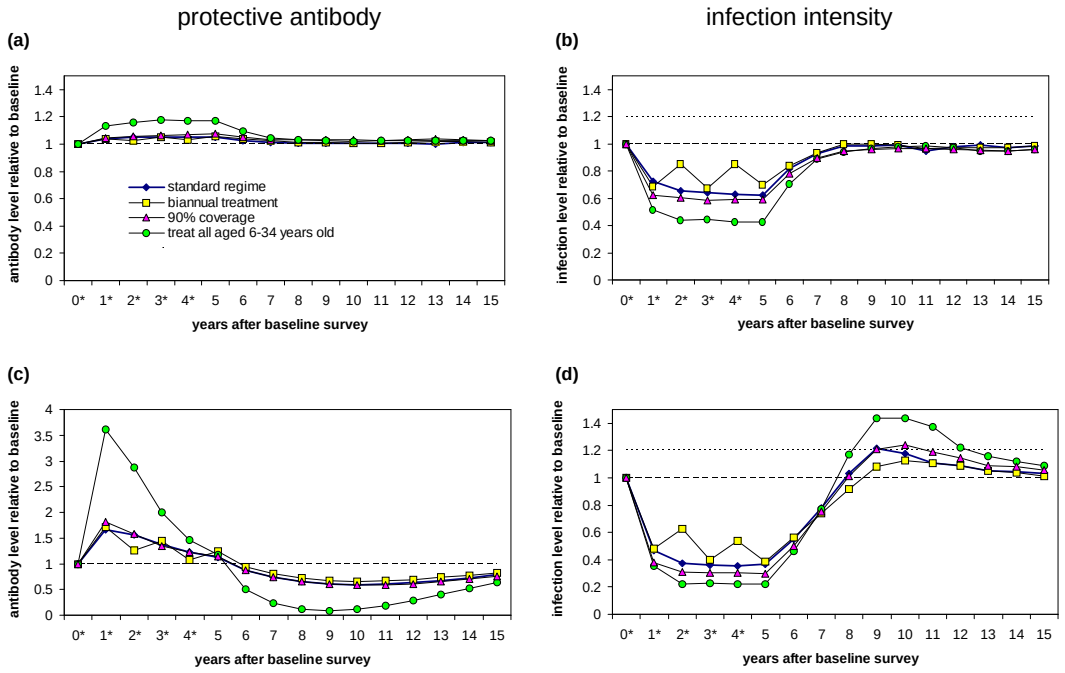

Figure 6.6: Dynamics of protective antibody and infection under different treatment regimes, for parameter sets with an antigen threshold. Details as for figure 6.5, but using the following parameter sets: (a) infection and (b) antibody with $\Lambda_{pmax} = 25, 1/\mu = 3, \gamma_2 = 0.008, \eta = 1.024, T = 250, k_1 = 0.5, \phi = 0.05, k_E = 1, d = 10, \varepsilon = 1$; (c) infection and (d) antibody with $\Lambda_{pmax} = 100, 1/\mu = 10, \gamma_2 = 0.8, \eta = 0.256, T = 25, k_1 = 0.5, \phi = 0.05, k_E = 1, d = 100, \varepsilon = 1$.

illustrated for two different parameter sets (figure 6.6). Because in the antigen threshold models overshoots were more modest than in the cross-regulation models, the different treatment schedules (2–4) did make some difference to how many parameter sets gave infection levels exceeding 120% of pre-treatment levels. In terms of infection reduction and antibody boosting during the period of treatment, and effect on the magnitude of any infection overshoot post-treatment, biannual treatment (schedule 2) had a smaller impact than annual treatment (schedule 1), and led to only one parameter set ever giving an overshoot of 20% over pre-treatment levels. Increased coverage (schedule 3) and treating the whole population (schedule 4) had an increasingly greater impact on the extent of infection reduction, antibody boosting and the magnitude of any infection overshoot for individual parameter sets (figure 6.6). These schedules both increased the number of individual parameter sets for which an overshoot (infection levels exceeding 120% of pre-treatment levels) in infection levels was seen. Treating the whole population also increased the range of possible parameter values for which an overshoot could occur. In addition to parameter sets with fairly rapid plasma cell decay (γ_2) of 0.8 year^{-1}, moderate antibody strength (η) of 0.256 per plasma cell and a threshold (T) of 25 antigen units, other possible parameter combinations now included those with plasma cell decay (γ_2) of 0.8 year^{-1}, antibody strength (η) 0.064 per plasma cell and a threshold (T) of 250 antigen units, and those with plasma cell decay (γ_2) of 8 year^{-1}, antibody strength (η) 1.024 per plasma cell and a threshold (T) of 250 antigen units (data not shown).

6.3.3 Treatment schedules 5 and 6 – reduction of transmission

When treatment was assumed to reduce transmission (treatment schedules 5 and 6), different patterns were predicted. For the cross-regulation models, with 100% reduction of transmission assumed (i.e. no transmission occurring until one year after treatment ceased, schedule 5), infection was reduced to less than 5% of the pre-treatment level after five rounds of treatment. Protective antibody was predicted to fall below pre-treatment levels at some point for all parameter sets, regardless of plasma cell decay rate, but do so more rapidly for faster decaying plasma cells (figure 6.7a-c). For parameter sets with rapid rates of plasma cell decay (0.8 year^{-1}), levels of protective antibody fell below pre-treatment levels after four rounds of treatment (before treatment had ceased). An overshoot in infection level was predicted to occur for all parameter sets regardless of plasma cell decay rate, with the overshoot predicted to be larger and occur earlier for more rapid plasma cell decay (figure 6.7 d-f). The infection profiles also segregated into three distinct groups by infection rate (Λ_{pmax} = 12.5, 25 and 50), as can be seen in figure 6.7. In each panel, the group of parameter sets with the earliest and highest overshoot in infection levels has the highest infection rate (Λ_{pmax} = 50), with the latest and lowest overshoots occurring for the group of parameter sets with the lowest infection rate (Λ_{pmax} = 12.5).

With 50% reduction of transmission up until one year after treatment ceased (schedule 6), the effects on antibody and infection in the cross-regulation models were still substantial, but less severe than with 100% reduction in transmission (figure 6.8). In all cases, antibody levels dropped below pre-treatment levels after treatment ceased, and with rapid plasma cell decay (0.8 year^{-1}) this occurred within a year of the final treatment. Infection levels consistently exceeded pre-treatment levels, but with moderate or slow plasma cell decay (0.008–0.08 year^{-1}), only a quarter of the parameter sets had infection levels ever exceeding 120% of pre-treatment levels. With rapid plasma cell decay (0.8 year^{-1}), an overshoot was consistently seen, as was also seen when there was no reduction in transmission (schedule 1, figure 6.2f).

Results for the antigen threshold models were similar (figures 6.9 and 6.10). With 100% transmission reduction (schedule 5), antibody levels always declined below pre-treatment levels at some point, with the precise timing and extent of this affected by the decay rate of the antibody response and the mean parasite life span. With a short parasite life span of 3 years, antibody levels always declined below pre-treatment levels before treatment ceased, regardless of the plasma cell decay rate, but increasingly earlier in the control programme with increasingly rapid plasma cell decay (figure 6.9a-d). For fairly rapid plasma cell decay (0.8 year^{-1}), levels of protective antibody virtually always declined below pre-treatment during the treatment programme, regardless of parasite life span (only two parameter sets with a long parasite life span of 10 years did not decline below pre-treatment levels until after treatment ceased). Infection levels always overshot after treatment stopped, with considerable variation in when and by how much this occured. The timing and extent of the overshoot were affected by plasma cell decay rates, parasite life span and population infection rates (figure 6.9e-h). With more moderate reduction of transmission, to 50% of pre-treatment levels during and for one year after the control programme (schedule 6), antibody levels still frequently fell below precontrol levels during the treatment programme when parasites had a short life span of 3 years (figure 6.10a-c), or with more rapid plasma cell decay (0.08 year^{-1}) and a parasite life span of 3 or 6.5 years (figure 6.10c). For all of the remaining parameter sets, antibody levels

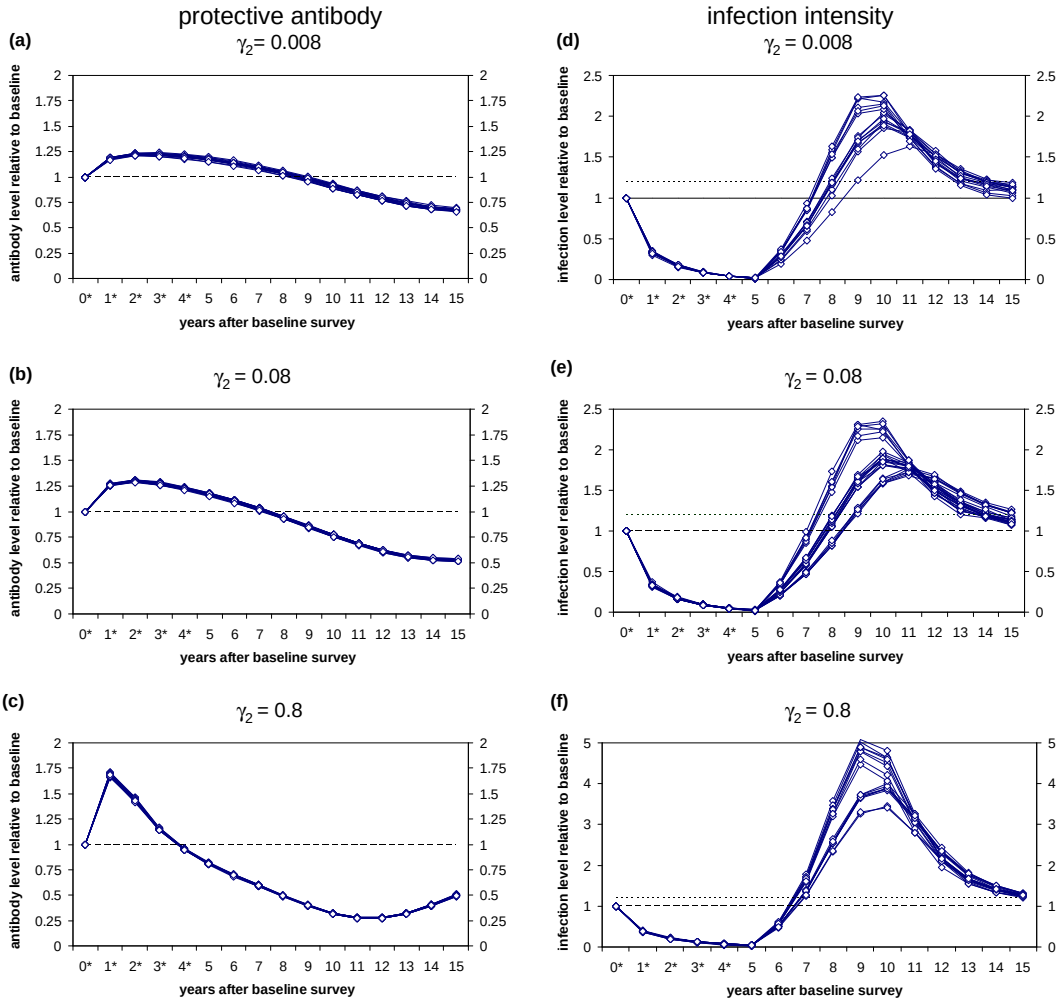

Figure 6.7: Dynamics of protective antibody and infection during and after treatment, with 100% transmission reduction for 1 year post-treatment, for parameter sets with cross-regulation. See legend for figure 6.2. Note that (f) has a different maximum value on the y-axis from (d) and (e).

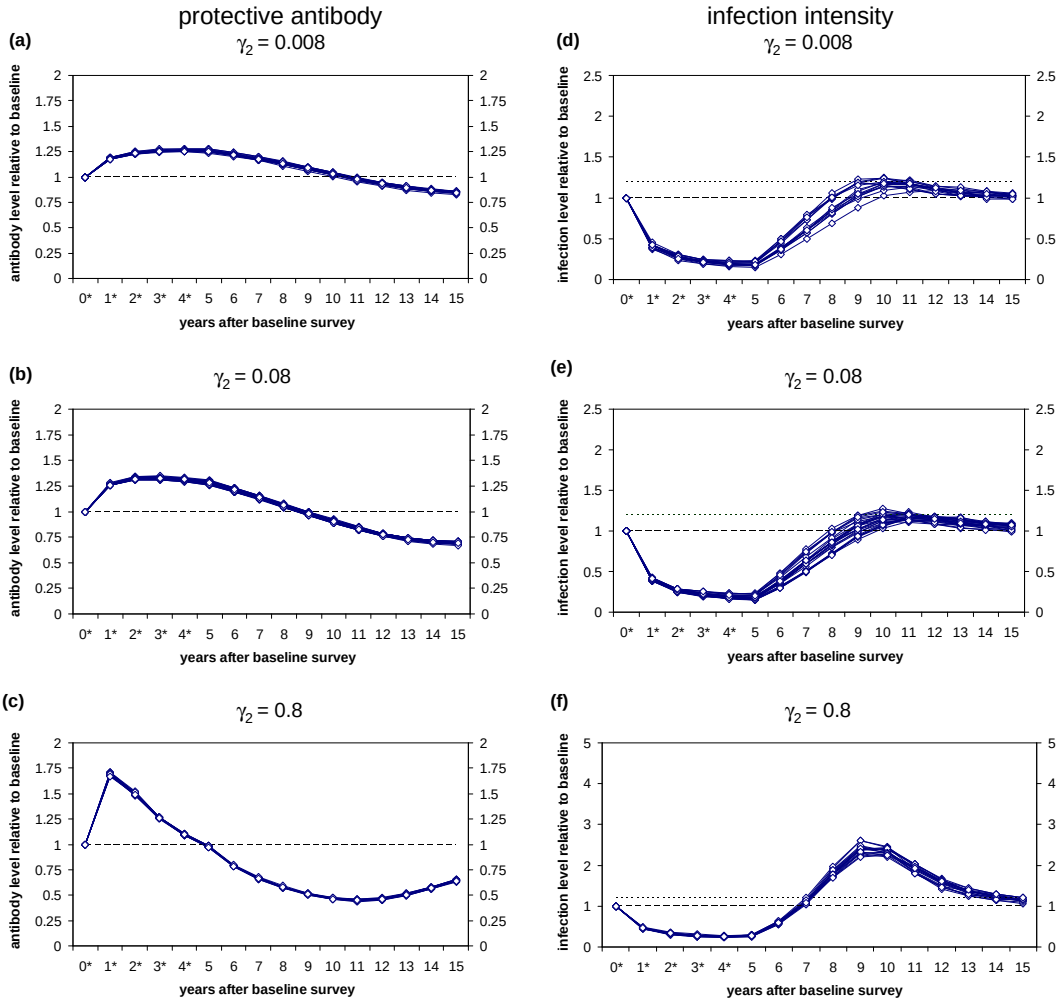

Figure 6.8: Dynamics of protective antibody and infection during and after treatment, with 50% transmission reduction for 1 year post-treatment, for parameter sets with cross-regulation. See legend for figure 6.2. Note that (f) has a different maximum value on the y-axis from (d) and (e).

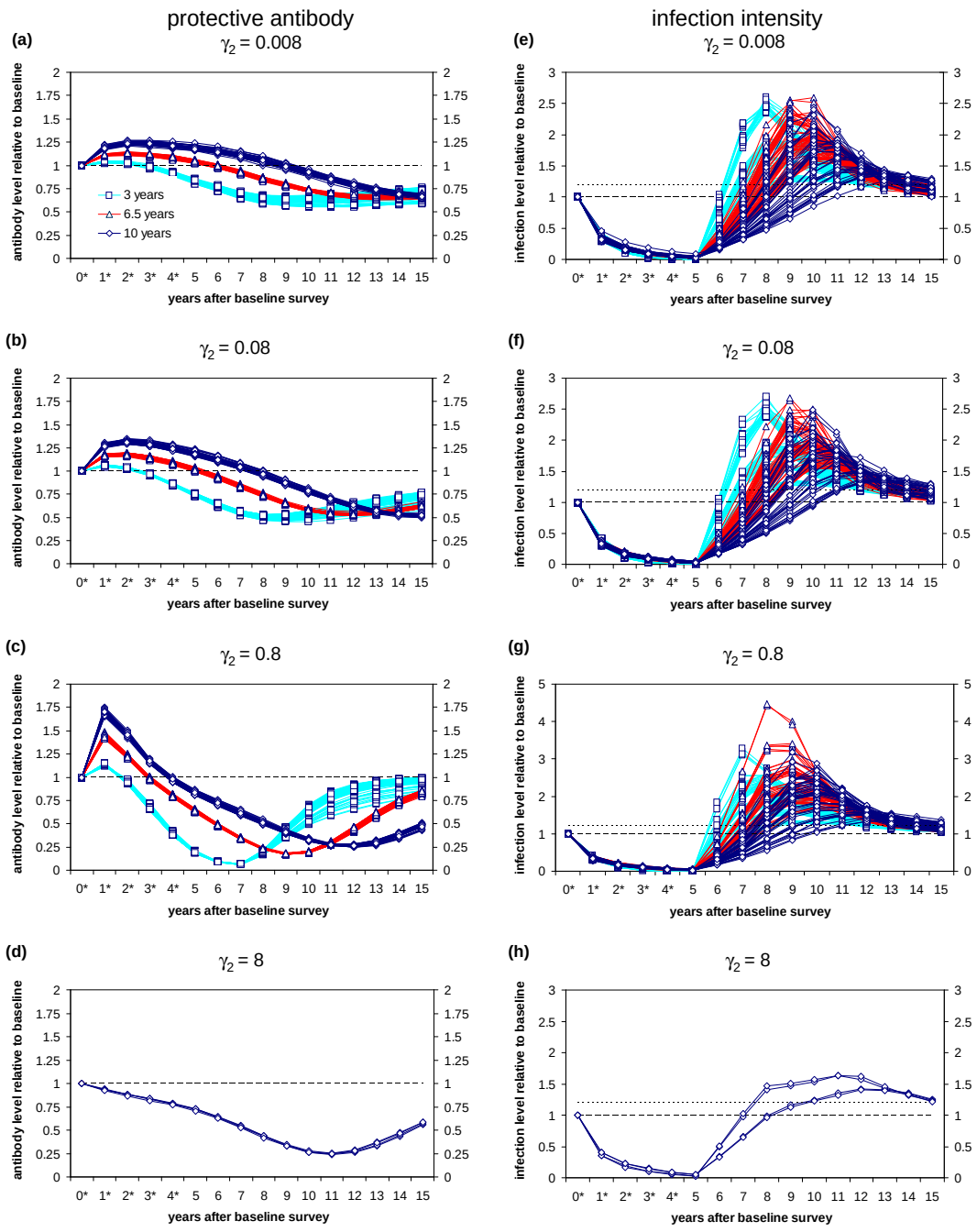

Figure 6.9: Dynamics of protective antibody and infection during and after treatment, with 100% transmission reduction for 1 year post-treatment, for parameter sets with an antigen threshold. See legend for figure 6.3. Note that (g) has a different maximum value on the y-axis from (e),(f) and (h).

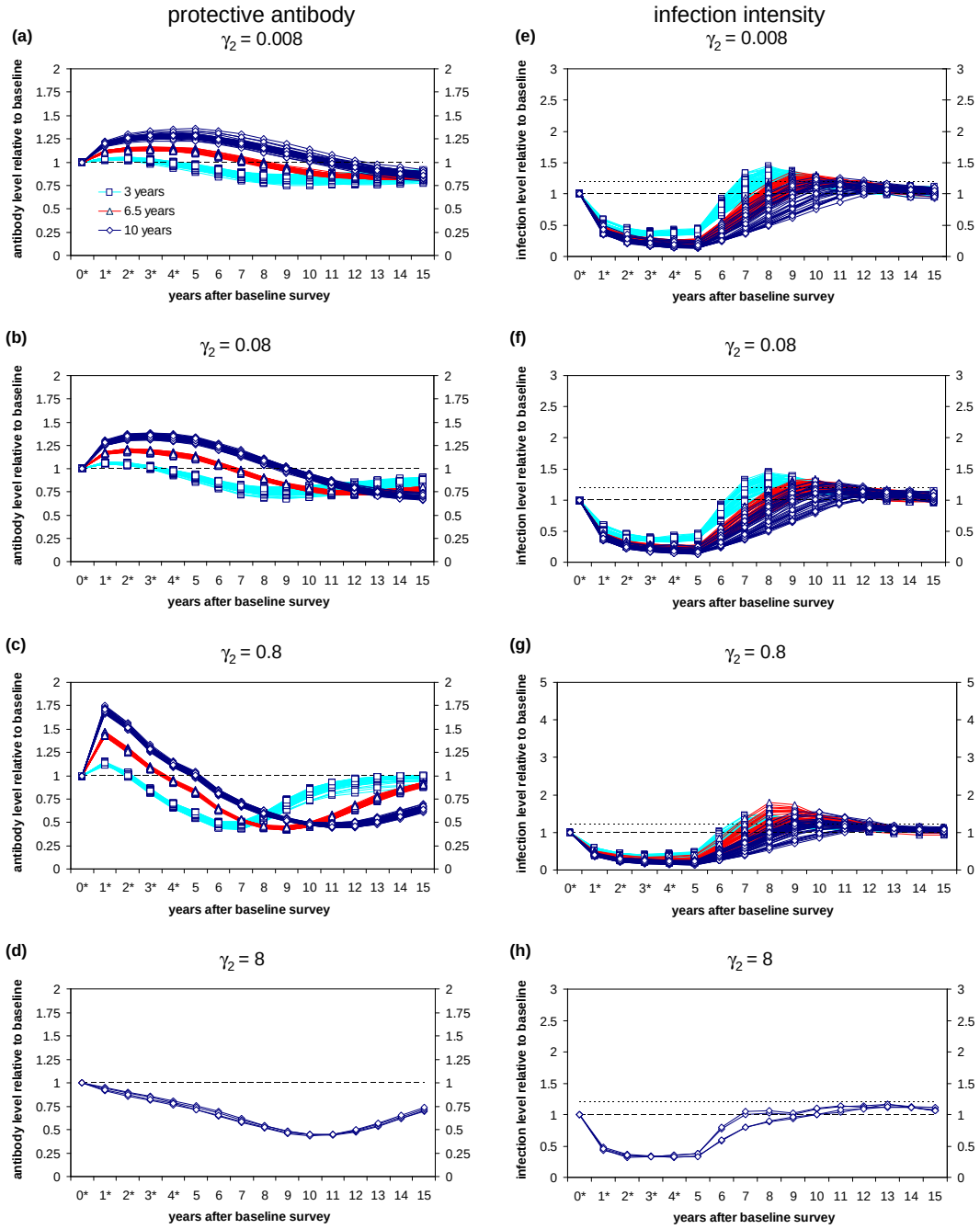

Figure 6.10: Dynamics of protective antibody and infection during and after treatment, with 50% transmission reduction for 1 year post-treatment, for parameter sets with an antigen threshold. See legend for figure 6.3. Note that (g) has a different maximum value on the y-axis from (e),(f) and (h).

were still consistently seen to drop below pre-treatment levels after treatment ceased, although not to the same extent as when transmission was stopped completely (figure 6.10). For models with slow or moderate plasma cell decay rates (0.008–0.08 $year^{-1}$), 58% of parameter sets had an overshoot in infection levels (exceeding 120% of pre-treatment levels), and with more rapid plasma cell decay (0.8 $year^{-1}$), 83% of parameter sets had an overshoot in infection levels after treatment ceased. The occurence, level and timing of the overshoot were also affected by mean parasite life span, as shown in figure 6.10e-h.

6.4 Discussion

In these models, levels of infection were substantially reduced by repeated MDA, and levels of protective antibody, stimulated by dying worms, were boosted by treatment. This replicates patterns seen in the field. It was shown that levels of protective antibody could fall below pre-treatment levels after the control programme ceased, and in some cases even before control stopped. Levels of protective antibody fell below pre-treatment levels earlier in models with increased treatment-related reduction of transmission, more rapid decay of plasma cells or a shorter worm life span. The models showed that if treatment reduced transmission, it reduced subsequent re-infection and therefore reduced antigen exposure, leading to more rapid decline of protective antibody. Even if transmission was unaffected, the models suggested that treatment temporarily reduced exposure to dying worms, as the worm burden was reduced, meaning that plasma cell decay rates strongly influenced the rapidity of antibody decline.

Models with a longer worm life span gave increased antibody boosting after treatment than those with a shorter worm life span, even when all other parameters were identical. This was likely due to the fact that baseline levels of infection were higher in models with longer worm life span than in those with shorter worm life span. Rates of antigenic exposure at baseline are expected to be lower in models with longer worm life span, and so the reduction in antigenic exposure after the initial reduction in worm burden brought about by treatment is likely to have a more rapid relative effect in models with short worm life span, which would explain why antibody levels fell below baseline levels earlier on in these models.

It was also found that infection could rebound to levels exceeding pre-treatment levels after the cessation of MDA. This was relatively rare in the absence of treatment-related transmission reduction, but more likely to occur with rapid plasma cell decay. If treatment substantially reduced transmission, overshooting of infection levels after cessation of treatment became much more likely. The strong impact of reduced transmission on infection levels after cessation of MDA is likely to be due to the substantial effect this has in reducing levels of protective antibody, as discussed above. When infection levels did overshoot pre-treatment levels, this occurred earlier in models with a shorter parasite life span (due to reduced levels of protective antibody), and also occurred earlier in models with higher rates of infection. Although models in which antibody fell below pre-treatment levels earlier on also tended to see infection returning to pre-treatment levels earlier, reduction in antibody levels below pre-treatment levels during MDA did not necessarily correspond with overshooting of infection levels after treatment ceased. This means that protective antibody falling below pre-treatment levels during a treatment programme is neither a necessary nor a sufficient indicator that infection levels will overshoot after treatment ceases.

The different treatment regimes investigated (schedules 2–4) had consistent but relatively

small effects upon the development of protective antibody and on infection dynamics during and after MDA. Increasing the coverage of treatment of school children from 75% to 90% increased antibody levels and decreased infection levels but by a very small amount. The small effect upon antibody levels is probably due to the fact that the mean antibody level across the whole population was dominated by antibody responses in adults, who were not affected by changes in coverage of children. Within the 6–15 year old cohort, much larger antibody boosts were seen (data not shown). The effect of increased coverage on infection levels was smaller than expected. The random allocation of treatment at each round meant that even at 75% coverage, the chances of an individual never being treated over the five rounds of treatment were very small, and this may account for the comparitively small effect of increasing coverage. In reality, there will be individuals who are more likely to be consistently missed in repeat treatment rounds (i.e. treatment is not applied randomly across the population), and so increased coverage is likely to have a greater impact in the field than is suggested by these models.

In this analysis, biannual treatment gave fluctuating dynamics during the treatment programme, with infection and antibody levels approaching those seen with annual treatment a year after each treatment. Slightly less severe overshooting of infection was seen after treatment ceased for biannual compared with annual treatment regimens. The finding that biannual treatment made little difference to long-term infection and antibody dynamics when compared with annual treatment is in agreement with two previous modelling studies – Chan *et al.* (1998) reported that in their model of *S. haematobium* in Ghana, treating after missing a single annual treatment could bring infection down to almost the same level as if two annual treatments had been given, and Williams *et al.* (2002) modelling prevalence of *S. japonicum* in China found little difference of biannual treatment of humans over annual treatment. However, other modelling studies have reported differences in the impact of biannual versus annual treatment (Gurarie & King 2005).

Treating the whole population rather than just school-aged children gave a more pronounced boost to population-level protective antibody and a greater reduction in infection level during MDA, but meant that any overshooting of infection after treatment ceased became more pronounced. This indicated that in these simulated populations, there was significant boosting of antibody in individuals over the age of 15. In general, treatment regimes which caused a more substantial (although transient) increase in infection levels after treatment ceased had caused a greater reduction in infection level during MDA. The reverse did not necessarily hold true, however, as in many cases no such overshoot was ever seen, despite substantial reduction of infection during MDA.

Previous modelling analyses have focussed upon the dynamics of infection during and after MDA, rather than antibody. Modelling studies that have considered the effects of acquired immunity upon infection levels during treatment campaigns have suggested that the strength and duration of protective immune responses play an important role in determining infection dynamics (Chan *et al.* 1996), and this was also found here. Without any reduction in transmission post-treatment, it was found that an overshoot in infection levels was most likely to occur when plasma cell decay rates were relatively rapid (half-life of 10 months); in contrast, Chan *et al.* (1996) reported overshoots occurring only with slow immune decay rates (half-life of 7 years), and not with more rapid decay. This discrepancy may arise because in the study by Chan *et al.* (1996) slow immune decay rates were compensated for with a higher value of R_0 (i.e. increased infection rates). In the current analysis, in models with reduced transmission

after treatment, higher infection rates gave rise to more pronounced infection overshoots after treatment ceased.

It should be noted that the analysis undertaken here was not a formal sensitivity analysis – parameters were not varied systematically, but were chosen in combinations that were able to reproduce all of the patterns of cross-sectional and post-treatment patterns in field data in chapter 5. It was therefore not always possible to fully disentangle the effects of different parameters, as they did not appear independently of one another (for example, antigen threshold level and mean parasite life span). The aim here was rather to make long-term predictions using parameter sets which had already been identified as being consistent with all of the data at my disposal. The analysis was based upon mean yearly levels calculated across multiple replicates of population simulations, rather than looking at the behaviour of individual simulations. Variation was observed between individual simulations, both in terms of whether or not antibody and infection levels returned to pre-treatment levels, and the timing of such returns, so that the reported results do not capture the full possible variation in outcomes for a single village. The advantage of using the mean levels was that it made it possible to assess how the complex time-varying dynamics of infection and antibody varied between different parameter sets and scenarios.

No field studies have yet conclusively demonstrated whether or not praziquantel treatment reduces subsequent reinfection through enhancing protective immune responses. This is difficult to test directly, because reinfection can only be studied after treatment, meaning that untreated controls cannot be used. To overcome this, a different hypothesis has been suggested, that repeated treatment should enhance protection against schistosome infection to a greater extent than single treatment (van den Biggelaar *et al.* 2002). van den Biggelaar *et al.* (2002) demonstrated that repeated treatment over a two-year period could enhance *S. haematobium*-specific cytokine responses to a greater extent than a single treatment in Gabonese school children, but their small sample size precluded any effect upon re-infection rates being detected. In the models and treatment schedules used here, the greatest impact of treatment upon protective immunity was seen after a single treatment rather than after repeated treatment, suggesting that the comparison of the effects of repeated versus single treatments may not allow the full effect of treatment to be evaluated. The models suggest that the extent to which repeated treatment further enhances protective antibody responses will depend upon plasma cell decay rates and subsequent levels of exposure to re-infection (since further parasites must be killed to enhance protective responses). The levels of both existing infection and immunity are also expected to affect the relative impact of treatment. Longitudinal studies of *S. mansoni* infection in occupationally exposed adults in Kenya who were treated with praziquantel whenever they became re-infected have shown resistance to reinfection developing in some individuals after repeated re-infection and treatment (Black *et al.* 2010; Karanja *et al.* 2002). Adults in this study who showed evidence of increasing resistance developing after many repeated rounds of reinfection and treatment had had little exposure to schistosomes before beginning to work as car-washers in Lake Victoria. Another cohort within this study, who worked as sand harvesters but had been exposed to schistosomes from a much earlier age, demonstrated maximum protection against re-infection after only two rounds of re-infection and treatment (Black *et al.* 2010). This suggests that the effects of repeated treatment may be larger in previously unexposed populations. However, these studies do not demonstrate a direct impact of treatment upon the development of protective immunity, since there are no

untreated or singly-treated controls, and there is therefore no way of knowing whether the repeatedly treated individuals would have developed resistance more quickly or more slowly in the absence of treatment. Protection in this study could equally arise from increased exposure to schistosome parasites.

A consistent prediction from the models analysed here is that if treatment significantly reduces transmission, this will have adverse effects on antibody and infection levels after treatment ceases and transmission returns to pre-treatment levels. The results suggest that, if transmission is reduced by 50% or more, infection is very likely to overshoot pre-treatment levels after treatment ceases. Although the effect of treatment on transmission was modelled in a rather simplistic way in this analysis, with an abrupt change in the level of the transmission at the beginning and end of the treatment programme, the overshoots in infection are unlikely to have been caused by this, since they occur over a period of several years after the return to normal transmission levels. While many field studies have assessed infection levels after treatment, few have looked at the effects of treatment upon transmission although some have shown reduced prevalence of infection over time in young children being recruited into their study populaton (King *et al.* 1991). Recent studies of *S. mansoni* infections in Uganda following repeated MDA (French *et al.* 2009) have shown that the force of infection (incorporating both infection rate and the effects of protective immunity) decreases by as much as 70% after one or two rounds of treatment (M. French, pers. comm), falling within the range explored here.

To improve the accuracy of the predictions made here, it would be helpful to include a more realistic description of transmission, such as those used in previous modelling studies (Chan 1996; Chan *et al.* 1996; Woolhouse 1991). This would require a different model structure to be used, with explicit transmission between individuals over time. Several assumptions about transmission between human and snail hosts would need to be made. Formal fitting of predicted levels of infection and antibody from these models to field data, at least for the few years of MDA for which data is available, would also increase the confidence that could be placed in these model predictions. The model has shown that both plasma cell decay rates and worm life span can have distinct effects upon the dynamics of protective antibody and infection. To use this modelling approach to determine likely values for these parameters, further data patterns will be required to test models against, since the ranges used in this chapter were able to reproduce all of the cross-sectional and post-treatment patterns tested in chapter 5. Data on longer-term infection and antibody dynamics during MDA or smaller studies of repeated treatment may be able to generate criteria which narrow down the range of these parameters, although it may not be possible to simultaneously estimate worm life span and plasma cell decay rates, since the models here suggest that they have interacting effects upon antibody and infection dynamics.

Overall, this work has demonstrated that, with protective immune responses stimulated by dying worms, repeated MDA is expected to boost protective immunity, but that during or after cessation of MDA antibody levels could decline below pre-treatment levels, and after MDA ceases infection levels could exceed those seen before MDA commenced. These predictions cannot be directly tested against current field data, as MDA programmes have not routinely measured antibody levels, and other studies of the effects of repeated treatment on *S. haematobium* responses have not yet been carried out on a sufficiently long time scale or large enough population to detect the effects predicted here. However, these predictions have been made using a range of parameter sets which best explain a number of different robust patterns seen in cross-sectional and short-term post-treatment studies of *S. haematobium*

infection, and so represent the most informed prediction that can be made based upon current data. While MDA programmes have had substantial impact upon schistosomiasis infection levels, this analysis highlights the potential negative consequences of ceasing regular repeated treatments.

Chapter 7

Discussion

Urinary schistosomiasis remains a major public health problem, particularly in sub-Saharan Africa. Current control efforts are primarily focussed upon vaccine development and mass drug administration programmes, with the goal of reducing morbidity rather than eliminating infection. Vaccine progress to date has been slow (McManus & Loukas 2008), with only one candidate, the Sh28GST vaccine, having entered Phase III clinical trials (NIH 2009). A greater understanding of how naturally acquired protective immunity develops will be advantageous in furthering vaccine development, for identifying both relevant antigens and the protective immune mediators which need to be stimulated. It is also important to understand how other control measures, including mass chemotherapy, are likely to affect the development of protective immunity, since if infection is not eliminated natural immunity will continue to play a role in determining infection burdens.

In common with other parasitic infections, protective immunity against schistosomes takes a long time to develop (Yazdanbakhsh & Sacks 2010). In endemic areas, increased resistance to re-infection and the development of immune responses associated with protection are seen in older children or adults, but this occurs only after many years of repeated exposure to infection.

In this thesis, I set out to identify some of the important mechanisms underlying the slow development of naturally acquired protective immunity in communities with endemic *S. haematobium* infection, and to investigate the potential impact of mass drug administration programmes upon the development of naturally acquired immunity.

Studies of infection and immune responses in humans are subject to logistical and ethical constraints. It is not possible to follow individuals for the many years that pass between initial schistosome infection and development of protective immunity without being obliged to treat them, which alters the dynamics of both infection and immune responses. Instead, population-based cross-sectional and treatment-reinfection studies are frequently used to study schistosome immunoepidemiology. Age is used as a proxy for length of exposure in these studies, requiring the assumption to be made that transmission has remained stable over a number of years. Mathematical models have an important role to play in interpreting data gathered in this way, and in using such data to test hypotheses about the underlying immune mechanisms (Chan & Isham 1998; Chan *et al.* 2000; Galvani 2005; Woolhouse 1998).

Here, I have used mathematical models to formally test different hypotheses for the slow development of protective immunity against schistosomes. This is the first time that a pattern-oriented modelling approach has been applied to models of helminth immunoepidemiology,

identifying models which can simultaneously reproduce an array of robust patterns identified from field data (Grimm *et al.* 2005). This approach proved to be very useful for excluding particular model structures and parameter combinations, and for discriminating between different hypotheses. This work has also included the first theoretical exploration of the implications of an antigen threshold in helminth-specific immune responses, and to my knowledge is the first time that the role of dying worms as a distinct source of antigen has been considered in models of this nature. While previous population models of helminth immunity have usually focussed upon infection patterns, I have also specifically looked at antibody patterns, in particular antibody aggregation and both the naturally-occurring and treatment-induced antibody switch.

In chapter 2, I set out the criteria which would be used to test the models. The peaked age-intensity curve and aggregated infection have been used previously as patterns to test models of schistosome infection (Chan & Isham 1998; Woolhouse 1992*b*), but I have refined these criteria by identifying quantitative limits for them. The criteria stipulating the age of the peak and the extent of aggregation were found to be highly discriminatory for the models tested against them. Previous individual-based models of infection aggregation have tended to give very high prevalence estimates (Chan & Isham 1998) and the prevalence criteria used here also proved to be very discriminatory. While a concerted effort was made to use as many different data sets as possible to draw up these criteria, information could not be used from a number of published infection studies due to lack of reporting of age-stratified data, the use of different mean calculations (which are not directly comparable) and limited reporting of infection aggregation. Acquisition of the raw data from these studies would enable these criteria to be based upon a wider range of data sets, and increase the general applicability of the findings from these models.

Antibody aggregation and the antibody switch have been reported previously for schistosome specific antibody responses (Mutapi 1997; Mutapi & Roddam 2002; Ndhlovu *et al.* 1996*b*), but this is the first time they have been used as patterns for mathematical modelling. Correlations between different schistosome-specific antibody isotypes are rarely reported in the literature, meaning that the characterisation of the antibody switch relied heavily upon two data sets for three populations from Zimbabwe (Milner *et al.* 2010; Mutapi *et al.* 1997). The antibody switch proved to be a robust phenomenon across several different isotypes in two of these populations, but was not found in the third, possibly because relatively few adults (who will tend to have the highest levels of the late-developing antibody) were included in this study population. Correlation patterns consistent with the antibody switch were also reported across a number of isotypes in a separate published field study (Ndhlovu *et al.* 1996*b*). The antibody switch proved to be a very discriminatory criterion for the models tested in both the deterministic and stochastic modelling frameworks. Given the importance of this criterion in testing these models, it would be of great interest to investigate how wide-spread this pattern is in different study populations from different countries. The antibodies involved in the switch were all highly aggregated across the population, but to varying degrees. The criterion drawn up for antibody aggregation proved to have very little discriminatory ability, and so was not used in the final analysis. Levels of both the initial and protective antibody responses were consistently highly aggregated in the stochastic models (chapter 5), indicating that aggregation in exposure (leading to aggregated infection levels) is sufficient to explain the observed aggregation in antibodies without having to consider additional mechanisms to explain this aggregation, such as variability

in immune competence between individuals.

One pattern which has been modelled several times previously but was not considered here is changing levels of infection aggregation with age (Chan *et al.* 2000; Duerr *et al.* 2003*a*; Fulford *et al.* 1992; Woolhouse 1994*a*). This was not included because there does not seem to be a consensus as to the exact form of this relationship (previous studies have reported it decreasing with age or following a peaked profile), and there was no clear pattern seen in the infection data analysed in chapter 2. Previous simulation modelling has shown that estimates of aggregation can be biassed by small sample sizes, which leads to particular problems when sample sizes decline with age, as frequently occurs in cross-sectional immunoepidemiological studies (Gregory & Woolhouse 1993). If larger data sets were available from which more robust age-related patterns in infection aggregation could be estimated, this could form the basis of a further criterion with which to test the models. The antibody data analysed in chapter 2 suggested that there may be age-related changes in antibody aggregation, although this was not included as a criterion owing to the variation between different isotypes in the magnitude of this effect. If this pattern could be identified consistently across a number of different data sets, it could also form the basis for an additional criterion with which to test these models. The data from the Burma Valley study (Mutapi 1997) show not only a very rapid individual-level antibody switch (evidenced by the dichotomous distribution of the isotypes involved), but also a fairly rapid antibody change at the population level over a narrow age range. Again, if this striking pattern could be demonstrated in multiple settings, it could form the basis of a highly discriminatory criterion with which to test future models.

While the models used in this thesis should be applicable to any of the major human schistosome species, the data used to draw up the criteria were for *S. haematobium*, which means that strictly the conclusions drawn in later chapters apply only to *S. haematobium* infection and antibody responses. The patterns of infection explored here, including the peaked age intensity curve, the peak shift and infection aggregation have all been reported for human *S. mansoni* infections (Fulford *et al.* 1992; Woolhouse 1998), suggesting that such patterns are robust across different schistosome species. However, the quantitative limits for these patterns vary between species, for example, infection intensity has been reported to peak between 10–25 years old for *S. mansoni* (Fulford *et al.* 1992), older than the age range reported for *S. haematobium* of 6–20 years (chapter 2). This could lead to quantitative differences in the parameter distributions of successful models if they were tested against *S. mansoni*-specific criteria, although the qualitative conclusions may not be affected. There is a paucity of published data in *S. mansoni* testing for an antibody switch, but this would be an interesting pattern to test for in *S. mansoni* data, to see how robust the data patterns and model findings in this thesis are across the different schistosome species.

In chapters 3 to 5, different combinations of the criteria were used to test and eliminate candidate hypotheses and model structures. Different models were used in each chapter, with the type and complexity of the model determined by the field patterns which were being used to test them. In chapter 3, where the outcomes of interest were a delay in the protective antibody response, and meeting the criteria for the age-intensity curve and the peak shift, deterministic population-level models with a single antibody response were sufficient. In chapter 4, two antibody responses were included in this deterministic modelling framework in order to test whether the models could reproduce the antibody switch. In chapter 5, where aggregation of infection and antibody were also used as criteria, stochastic individual based models (IBMs)

were used to allow distributions of infection and antibody to be simulated. Introducing the different criteria in separate stages made it easier to determine the relative importance of particular criteria in excluding certain models, and this is an approach I would use again. However, if I were to repeat this analysis, I would use the fully stochastic IBMs throughout for consistency, although it might not be possible to use these to test the same range of model structures and parameter combinations as was done in chapter 4, owing to the greater computational requirements of the stochastic models.

Although parasite-induced immunosuppression was able to delay the development of protective immunity in these models, it was predicted to maintain high levels of infection in older people in highly exposed populations, in clear opposition to field data for endemic schistosome infection. For this reason, immunosuppression was excluded as a potential explanation for the slow development of protective immunity in human schistosome infection. This is not to say that suppression does not occur, since it has been clearly demonstrated in both animal models and human studies (Grogan *et al.* 1998*a*; Maizels & Yazdanbakhsh 2003). It is possible that the principal role of such suppression is to reduce early lethal inflammatory responses, rather than having a substantial impact upon the Th2-type responses which are generally associated with protection in human studies. This analysis suggests that the late development of the Th2-type protective response is not primarily due to immunosuppression, but that a separate mechanism is responsible.

The antigen threshold, which was included in the models in a rather conceptual way, proved to be very effective at delaying the development of protective antibody. Models including a cumulative threshold were favoured over those with an antigen threshold based upon current levels of antigen exposure, which could reproduce the peaked age-intensity profile only over a much reduced range of infection rates (chapter 3). In chapters 3–5, a cumulative antigen threshold was found to greatly enhance the ability of the model to reproduce all of the cross-sectional field patterns tested, including age-intensity profiles and the antibody switch. However, it was not found to be essential in any of these models. It is therefore suggested as a potential mechanism for delaying the development of protective immunity, but not an essential one. The antigen threshold was represented in the models as a plausible immunological phenomenon rather than representation of a specific cellular mechanism. It may be thought of as representing a cascade of different activation and expansion events that need to happen upstream of antibody production, particularly for antibody class switching. This could include repeated T cell activation and accumulation of a polarised T cell response leading to a change in the cytokine environment. Models have shown that with repeated antigen exposure, it is possible to see a delayed but rapid change in the cytokine balance due to the highly nonlinear dynamics of cytokine interactions (Schweitzer & Anderson 1992*a*).

In chapter 5, the only models which were able to meet all of the cross-sectional and post-treatment criteria had dying worms providing the main source of protective antigen, in agreement with the hypothesis that antigen from dying worms is needed to stimulate protective immunity (Woolhouse & Hagan 1999). This study therefore strongly suggests that the main source of antigen stimulating protective responses comes from dying worms. However, this was not necessarily due to delayed antigenic exposure as the original hypothesis suggested (Woolhouse & Hagan 1999). In chapter 3, it was shown that in order to delay the development of protective antibody through delayed antigenic exposure, models with antigen coming from dying worms needed to have non-exponential worm survival. In chapters 3 and 4, models

with exponential worm survival and dying worm antigen were still able to reproduce all of the required patterns. Throughout chapters 3–5, it was demonstrated that models with other stages of the life cycle (cercariae or live worms) stimulating protective antibody could reproduce all of the cross-sectional patterns of infection and antibody required. Dying worms had to be the source of protective antigen in these models only in order to reproduce the post-treatment antibody switch (chapter 5). Together, these findings suggest that delayed antigenic exposure is not necessary to explain patterns associated with naturally acquired protective immunity, and that the particular form of the worm survival curve may not be critical.

The analysis very clearly indicated that protective antibody had to reduce worm fecundity in order for models to reproduce patterns of infection aggregation as well as the antibody switch and age intensity profiles. Models with reduced re-infection were unable to pass all of the criteria used in chapter 5, which included patterns of infection aggregation. This is in agreement with the findings of Galvani (2003), that anti-reinfection immunity reduces infection aggregation to a much greater extent than anti-fecundity responses. The finding that protective antibody responses are likely to target worm fecundity is in agreement with animal and human studies suggesting that *S. haematobium* is susceptible to anti-fecundity responses (Agnew *et al.* 1996, 1992; Webbe *et al.* 1976). It also fits with the observation that the leading vaccine candidate for *S. haematobium*, Sh28GST, induces anti-fecundity responses in primates (Boulanger *et al.* 1999). Praziquantel treatment has been shown to enhance serological recognition of *S. haematobium* GST in people from areas with endemic *S. haematobium* infection (Mutapi *et al.* 2005), making it a putative antigen stimulating the protective immune responses described here.

In models with immune-mediated worm death, it was seen that this mechanism reduced worm life span to very short lengths in models which were able to meet all of the field criteria. The majority of these models were excluded on the grounds that worm life span was reduced below 1 year, much lower than field estimates. The few remaining models with immune-mediated worm death (chapter 4) were not explored further in the stochastic individual based models, but all of these had worm life span estimates of less than 2 years, still well below field estimates of 3-10 years (Goddard & Jordan 1980; Vermund *et al.* 1983; Wilkins *et al.* 1984). One note of caution in dismissing these models is that the estimates of worm life span quoted come from studies in which transmission had stopped and infection levels were decreasing, meaning that immune pressure may have been waning.

Very specific predictions were made about the initial antibody response involved in the antibody switch: it had to be stimulated by antigens from recently laid eggs, have little or no protective capacity, and be relatively short-lived. Woolhouse (1993) demonstrated that the epidemiological patterns associated with 'blocking' antibodies could be best explained if these were neutral antibodies with rapid decay, similar to the initial antibody response described here. It seems most likely that the antigen stimulating this response is a secreted egg antigen, which would be rapidly sequestered from the immune system by granuloma formation around trapped eggs (von Lichtenberg 1964). The combination of a protective anti-fecundity response and a neutral antibody response stimulated by egg antigens was the main driver of the antibody switch in these models, with the protective antibody removing the antigen source for the initial response as it developed.

The models used throughout this thesis assumed that each antibody response was stimulated by a single stage of the schistosome life cycle and targeted a single stage. In reality, overlapping

antigen expression between different stages (Curwen *et al.* 2004) means that antibody responses to a specific antigen could be stimulated by more than one stage of the life cycle and could have damaging effects upon multiple life stages. The models described here could easily be extended to test this, although the number of potential combinations to be tested would vastly increase. A more feasible first step might be to model responses to particular antigens for which the antigen-specific antibody responses have been measured and the stage-specific expression is known, such as Sm22.6 (Fitzsimmons *et al.* 2007).

I have deliberately avoided modelling particular antibody isotype responses in this thesis, choosing instead to model general characteristics of two distinct groups of antibodies seen in three different populations (Mutapi *et al.* 1997; Ndhlovu *et al.* 1996*b*). This is partly because the isotypes included in each group can differ depending upon the antigen preparation used (egg or whole worm) and also differ between populations. In general, but with exceptions, IgG1 or IgE responses best fit the bill for the 'protective' responses modelled here. Several studies have suggested that IgE antibodies specific for egg or adult worm antigen preparations are protective (Dunne *et al.* 1992*a*; Hagan *et al.* 1991), and IgE levels have been reported to be boosted by treatment (Fitzsimmons *et al.* 2007; Mutapi *et al.* 1998). Egg-specific IgE responses were consistently involved in the antibody switch in one of the studies showed switches (Ndhlovu *et al.* 1996*b*) and occasionally in the other (analysis in chapter 2). Worm-specific IgG1 has also been associated with protection against *S. mansoni* re-infection (Satti *et al.* 1996), and in the data analysed here, egg-specific IgG1 was negatively associated with infection intensity in the Valhalla population (chapter 2). In this population, IgG1 was highly and persistently boosted after treatment (Mutapi *et al.* 1998), and both worm- and egg-specific IgG1 were frequently involved in the antibody switch (chapter 2). The initial response in the antibody switch may correspond to egg-specific IgM (Ndhlovu *et al.* 1996*b*), worm-specific IgM (Mutapi *et al.* 1997), or either egg- or worm-specific IgA responses (Mutapi *et al.* 1997).

Having demonstrated that only models with dying worms providing protective antigen were able to reproduce both cross-sectional patterns of infection and antibody and the treatment-induced antibody switch, these models were used to predict the long-term impact of treatment in chapter 6. This is the first time that this has been done using models in which antigens from dying worms provide the main antigenic stimulus, so that treatment can boost protective antibody responses. In previous models with live worms assumed to stimulate the protective response, it was shown that, because treatment removed the antigenic stimulus, overshoots in infection levels were sometimes (although not always) predicted to occur after control programmes ceased (Chan *et al.* 1996). It was found here that overshoots in infection could also occur after the cessation of treatment when dying worms provided the protective antigen, despite boosting of antibody responses during treatment. The treatment models developed here looked at infection and antibody levels in the whole population. In an actual field programme, these are not what would be measured – for example, infection levels are unlikely to be recorded for individuals who do not receive treatment (either because they fall outside the target population or miss one or more rounds of treatment). An advantage of using IBMs like those developed here is that they can be adapted to mimic any real field population, including specific treatment and sampling schedules. Although the analysis of the potential effects of treatment was not a formal sensitivity analysis, some parameters clearly had an independent effect on the development of protective antibody responses during and after treatment, namely the rate of decay of the plasma cells producing the protective antibody, and the mean worm life

span. The very different predicted behaviour of models with different plasma cell decay rates or worm life spans means that additional criteria based upon long-term changes in antibody levels following single or repeated treatments could be used to further discriminate between the successful models identified here. However, since the models also demonstrated that a significant reduction in transmission could alter antibody dynamics, effects of treatment on transmission would need to be either avoided or accurately measured. An independent measure of turnover rates of the B cells involved could be obtained using in vivo labelling with deuterated glucose, which has been successfully used to measure turnover rates of B cells in healthy individuals (Macallan *et al.* 2005), and has already been optimised in tropical field settings (Ghattas *et al.* 2005).

Another hypothesis for the slow development of protective immunity in human schistosomiasis which has not been considered in this work is age-related changes in immune competence. While it seems unlikely that this could fully account for the peak shift in infection intensity, it could be a contributing factor to the delay seen in mounting protective antibody responses (Yazdanbakhsh & Sacks 2010). This could easily be incorporated into the models developed here to investigate whether age-related changes in immune competence are consistent with patterns seen in the field.

In the final analysis of the plasma cell-only models, it was found that the protective antibody response almost always had a slower intrinsic decay rate than the initial response. This could be because the initial response does not form a robust memory response, while the protective response does so; it could reflect differences in the survival of the plasma cell populations stimulated; or it may reflect differences in memory cell turnover rates, which have been shown to differ between B cells expressing different isotypes (Wirths & Lanzavecchia 2005). The differences could be related to the type of antigen stimulating the different responses, since carbohydrate and protein antigens differ in their ability to stimulate effective memory responses (Woolhouse & Hagan 1999).

The representation of protective immune dynamics in these models was fairly simple, although based upon B cell maturation pathways as they are currently understood (Gray 2002). In the final analysis in chapter 5, only models with long-lived plasma cells were considered, although as noted, these could equivalently represent populations of memory B cells with continual antigen-independent activation to short-lived plasma cells. These models do not distinguish between these two alternative proposed mechanisms for antigen-independent antibody maintenance. In chapter 4, models with antigen-dependent activation of explicit memory cell populations to form short-lived plasma cells were also considered. These demonstrated broadly similar results to the simpler plasma cell models, although they did allow some additional combinations of antigen and target for the two different antibody responses to meet all of the criteria, most notably models with antibody responses reducing worm survival. However, these were relatively few in number and had very low worm life span estimates as discussed above. Nonetheless, it would be of interest to explore these models more thoroughly in a stochastic framework, and to extend them to consider models with both memory cells and long-lived plasma cells. More complex models with explicit T cell populations and cytokine dynamics could also be developed, although T cell maturation pathways are still being determined (Gray 2002) and models of current understanding of T cell and cytokine interaction can rapidly become outdated (Schweitzer & Anderson 1992*a*). Models of cytokine interactions could quickly become complex due to the highly non-linear interactions involved (Callard *et al.* 1999), and their

development would need to be closely guided by extensive data sets. The analysis here has demonstrated that by starting with relatively simple models and adding in only as much detail as is necessary to make valid comparisons with field data and reproduce robust patterns in this data, a number of complex patterns can be adequately explained.

The main finding from this work, that protective immune responses against schistosomes are likely to be stimulated by antigens which are released from dying worms, and that these responses reduce worm fecundity, has implications for the development of schistosome vaccines. It suggests that, if the aim of vaccination is to mimic effective protective responses which occur naturally, then the most suitable antigen candidates are those which are highly expressed within adult worms, with low expression on the worm surface or by other stages of the life cycle. It also suggests that initial trials should look for anti-fecundity effects. However, the models also suggest that natural protective immunity receives constant boosting from the continued presence of live worms, while a vaccine would need to induce long-lasting immunity even in the absence of infection. Although an anti-fecundity vaccine would not prevent infection in those who had been vaccinated, it would be expected to reduce infection intensity at the population level by reducing onwards transmission (Chan *et al.* 1997). Similarly, the longevity of the 'immunizing' effect of chemotherapy was shown here to be dependent upon both the duration of protective responses and levels of subsequent antigen exposure.

The work presented here has demonstrated that the pattern-oriented modelling approach is a highly effective one in identifying underlying immune mechanisms from immunoepidemiological studies. A large panel of criteria based upon patterns of both infection and parasite-specific antibody levels proved to be highly discriminatory in excluding possible model structures and parameter combinations, enabling a small group of likely models to be identified that could be used to make long-term predictions. This approach can easily be extended to explore different model structures, or to refine the current models through identification of additional criteria. Individual based models like those developed here are highly versatile and can be tailored to any particular field study, making them a powerful tool in analysing and interpreting field data. As more data on immune markers becomes available, particularly from long-term treatment studies, it is hoped that these models can be refined to provide further insights into the processes underlying the development of protective immunity in human schistosomiasis.

Appendix A

Technical appendix: Pattern-oriented modelling approach taken

1. Identify robust patterns in field data on infection intensity and specific antibody responses, from as many studies as possible. Where relevant, determine quantitative upper and lower bounds for these patterns from available field data.

2. For each of the patterns identified in step (1), draw up one or more criteria which models must meet.

3. Construct mathematical model to test hypotheses. Decide upon which of the criteria drawn up in step (2) will be used to test the compatibility of the model with the data, and ensure that the model includes all of the components necessary to be able to test it against these criteria.

4. Parameterise model. Conduct thorough literature search to identify values and plausible ranges for parameters where possible. Where no data is available, use wide ranges on parameters.

5. For each parameter to be varied, use a geometric series of values covering the full range identified in step (4).

6. Run repeat simulations using the model, performing a grid search of the parameter space, using all possible combinations of the values of each parameter determined in step (5).

7. For each parameter set, test whether the model outputs pass all of the criteria selected in step (3) or not.

8. For each model, record how many of the parameter combinations meet all of the criteria (pass step 7), and retain these parameter sets for further testing or for predictive modelling.

Appendix B

Age-specific antibody distributions

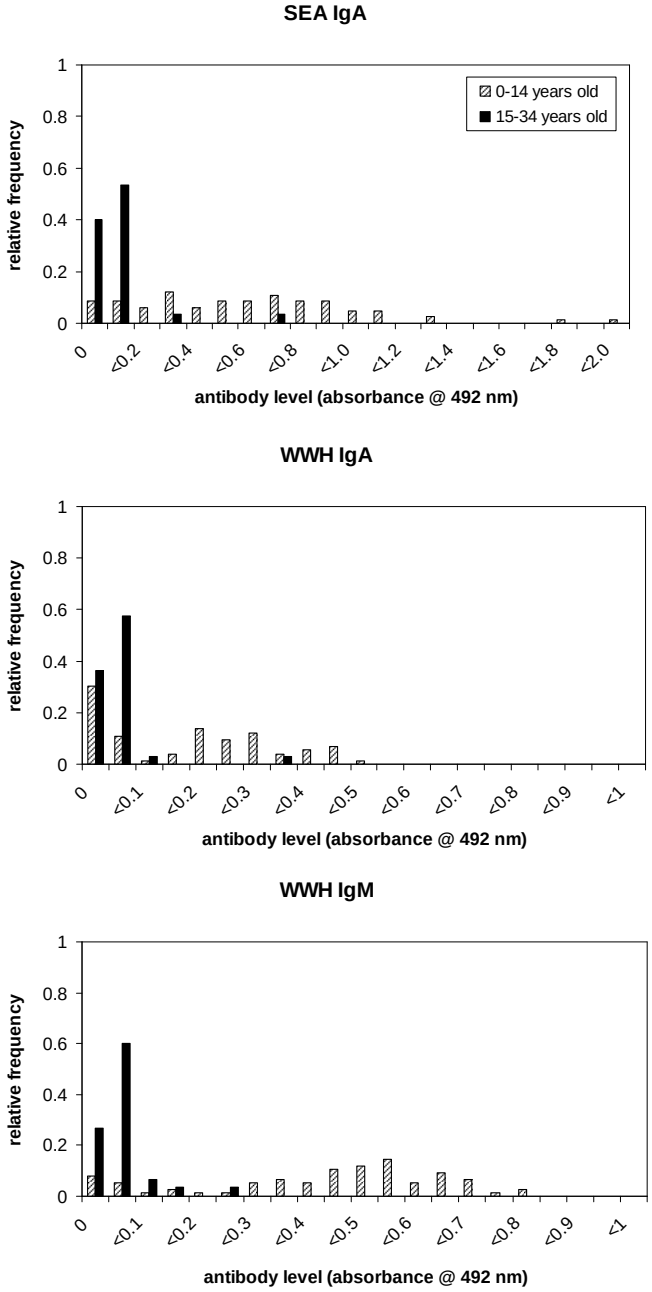

Figure B.1: Kaswa village: antibodies that decrease with age. Antibody distributions are shown in two age groups for antibody responses which are significantly negatively correlated with other responses, and which decrease with host age. Frequencies within each age group are adjusted so that they sum up to 1.

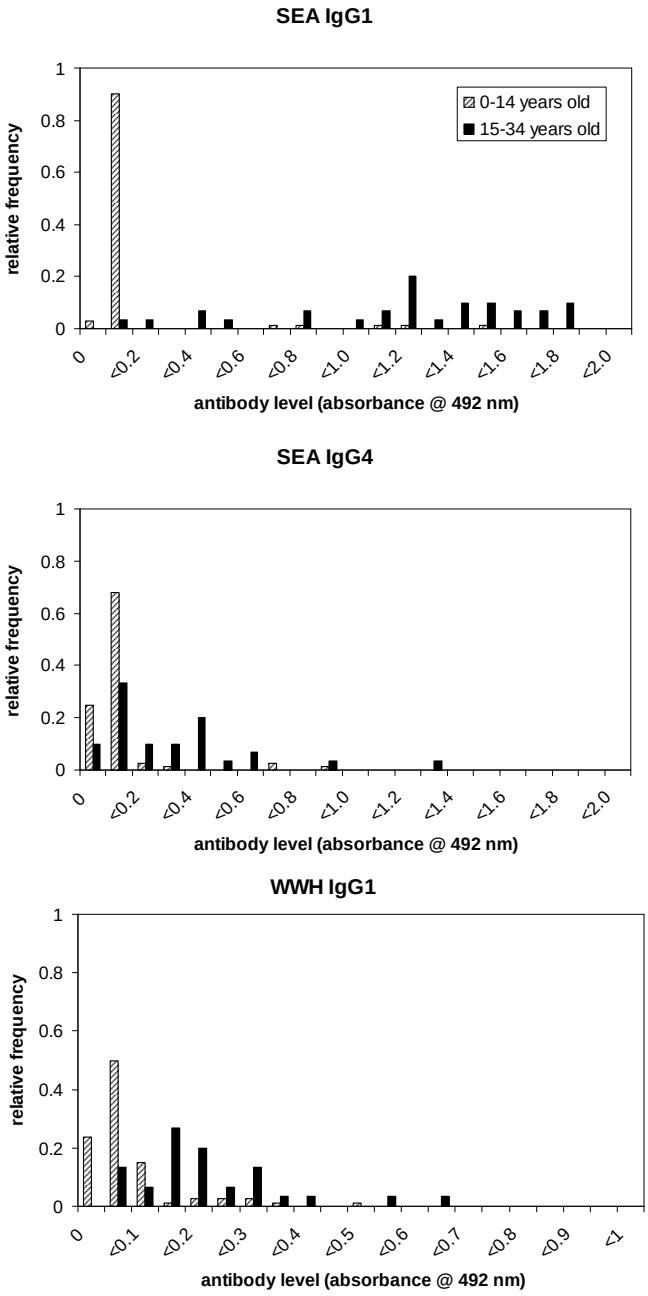

Figure B.2: Kaswa village: antibodies that increase with age. Legend as for figure B.1.

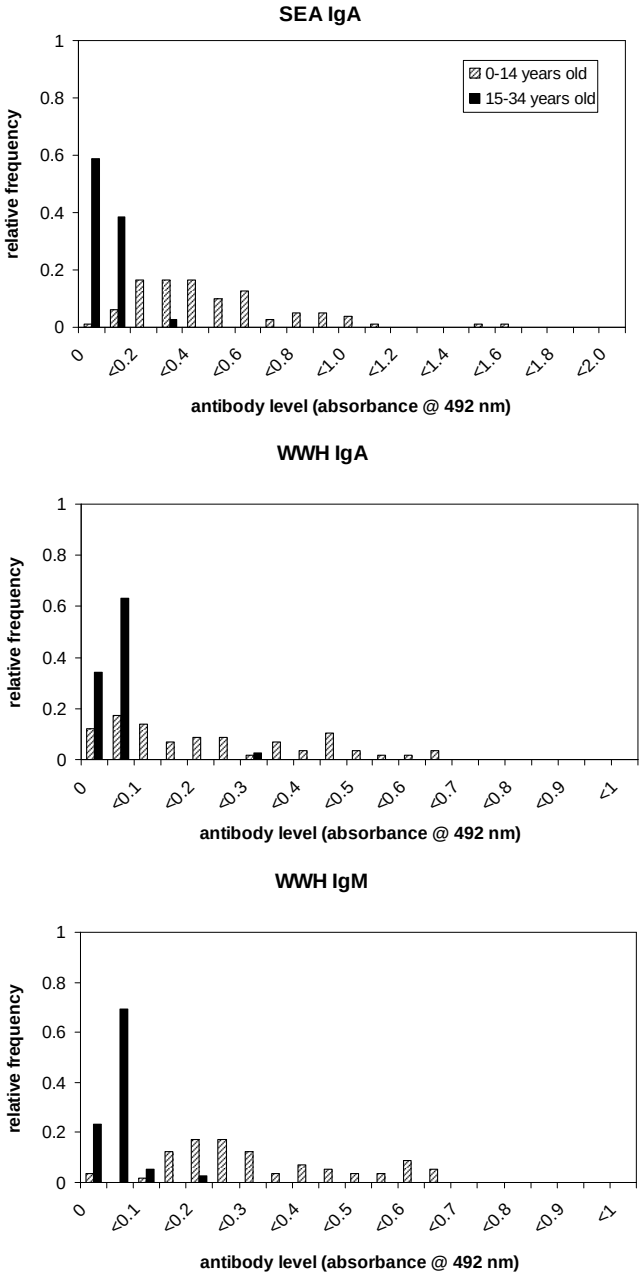

Figure B.3: Valhalla village: antibodies that decrease with age. Legend as for figure B.1

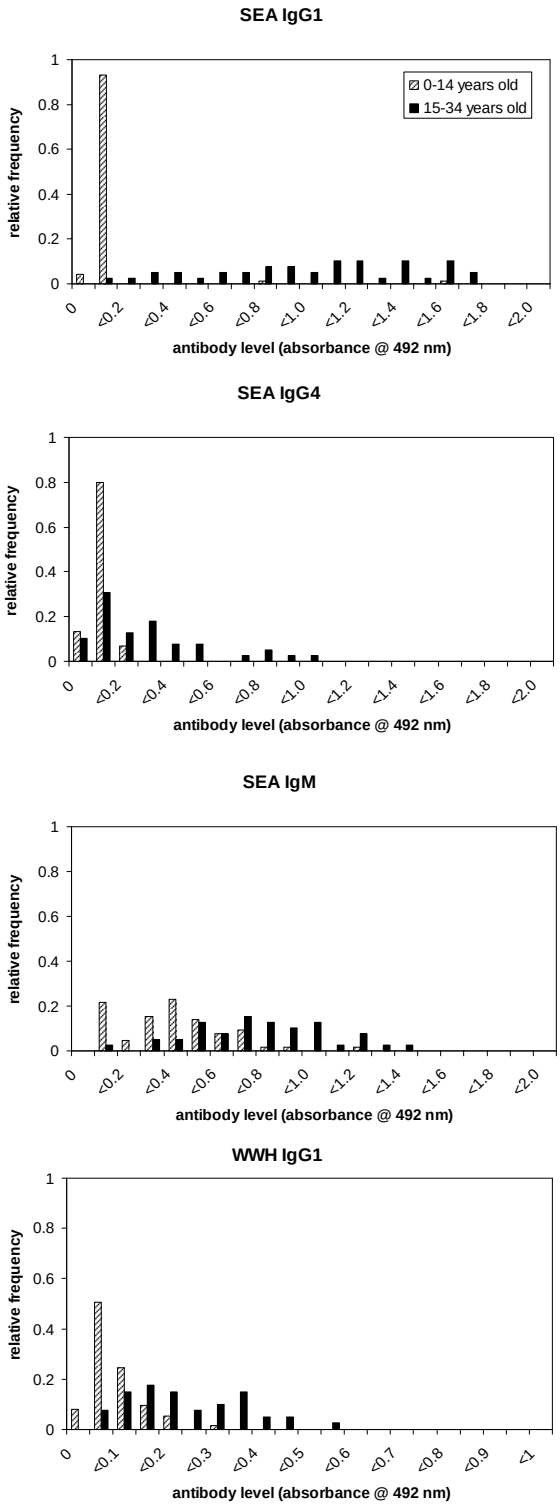

Figure B.4: Valhalla village: antibodies that increase with age. Legend as for figure B.1.

Appendix C

Parameter distributions

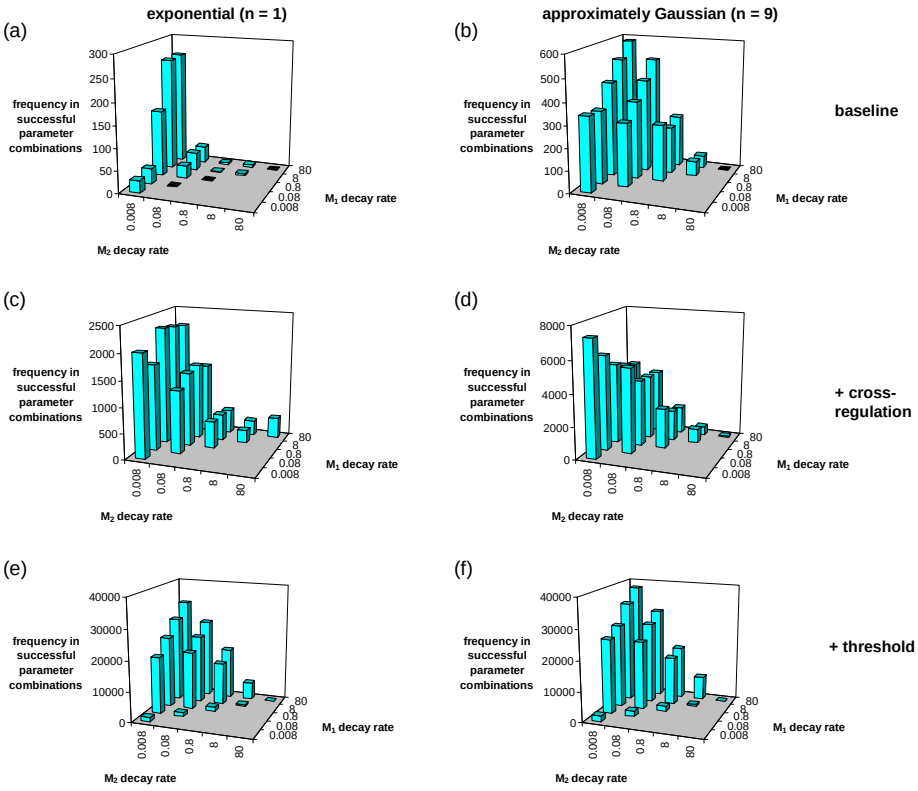

Figure C.1: Memory decay rates for memory models which pass all criteria. Plots show the total number of times parameter combinations including the different possible combinations of decay rates for the two memory cell populations pass all criteria. (a,b) Memory models without cross-regulation or thresholds, (c,d) total frequencies summed over all of the cross-regulation models and (e,f) models with a threshold on M_2. The left-hand panels are for models with exponentially-distributed worm life span ($n = 1$) (a,c,e), the right-hand ones are for models with approximately Gaussian-distributed worm life span ($n = 9$) (b,d,f). All of the different combinations of decay rates that were used have a bar on the chart; black bars indicate that no successful parameter combination had this combination of memory decay rates, blue bars that at least one successful parameter combination had this combination of memory decay rates. Note that different maximum values are used on the z (frequency)-axis.

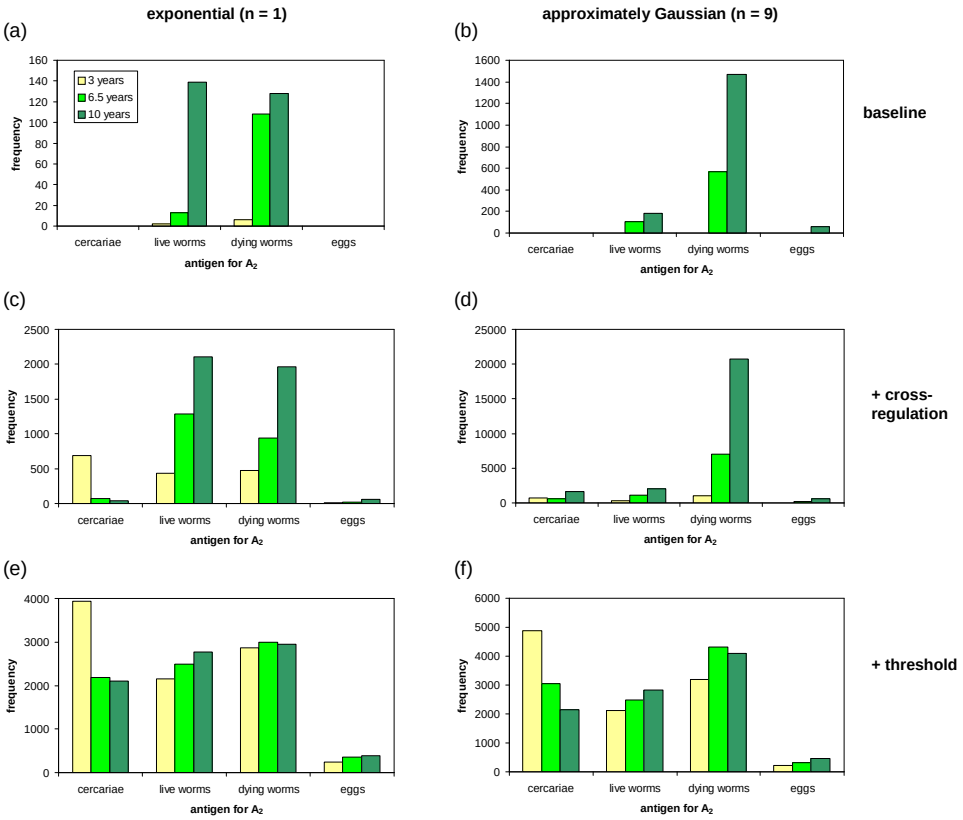

Figure C.2: Mean natural worm life span for plasma cell models which pass all criteria. Plots show the total number of times parameter combinations including the different possible values for natural worm life span are able to meet all criteria for plasma cell models, with results broken down by the life cycle stage providing the antigenic stimulus for A_2. Yellow bars: mean natural life span 3 years; light green bars: mean natural life span 6.5 years; dark green bars: mean natural life span 10 years. (a,b) Plasma cell models without cross-regulation or thresholds, (c,d) total frequencies summed over all of the cross-regulation models and (e,f) models with a threshold on A_2. The left-hand panels are for models with exponentially-distributed worm life span ($n = 1$) (a,c,e), the right-hand ones are for models with approximately Gaussian-distributed worm life span ($n = 9$) (b,d,f). Note that different maximum values are used on the y-axis.

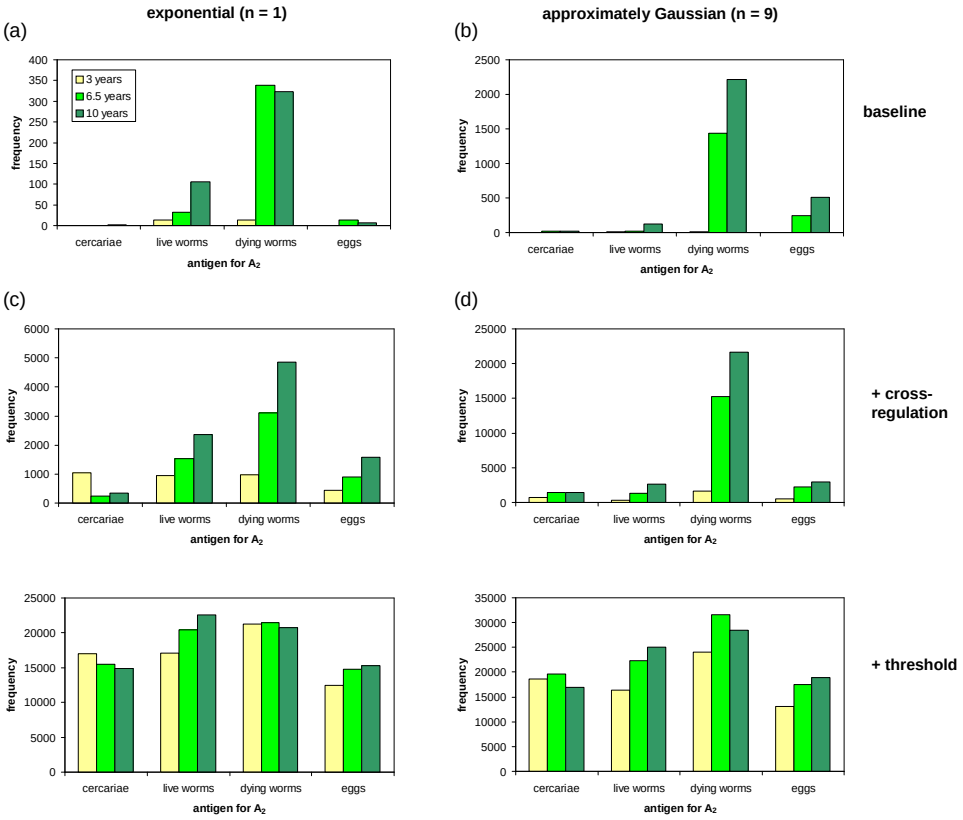

Figure C.3: Mean natural worm life span for memory models which pass all criteria. See legend for figure C.2.

Appendix D

Estimating ϕ

A pilot mapping study was carried out to test whether exposure to *S. haematobium* infection correlated with distance lived from the nearest river water contact site, as was found in a previous study in Zanzibar (Rudge *et al.* 2008). If this was the case, it was expected that infection intensities would be negatively correlated with this distance in young children who had not yet developed protective immunity against infection. After confirming this, I calculated the rates at which individuals in the study population (up to the age of 20) moved house, as a proxy for the rate at which they changed their contact rate (parameter ϕ in chapter 5).

D.1 Data sources

The data presented here were collected as part of a cross-sectional study carried out in the Magaya schools and local community in the Murehwa district of Zimbabwe in September–November 2008. Age and parasitology data were collected as part of the main survey. As part of a pilot mapping study, a GPS receiver was used to record the co-ordinates of active water contact sites used by residents of Magaya village, and the co-ordinates of the households of a number of study participants living in Magaya village. The straight-line distance between each participant's household and the nearest active water contact site was calculated by Eric Fèvre using ArcGIS. When households were mapped, wherever possible information was obtained from adults in the household on the number of years that each study participant had lived in that household. Additional data was obtained from questionnaires given to a subset of the study participants as part of the main study, which included a question asking participants to list the number of previous villages that they had lived in.

D.2 Relationship between infection intensity and distance lived from nearest water contact site

A strong negative correlation was found between individual infection intensity and the distance between household and nearest active water contact site for 29 children in grades 0 or 1 of Magaya primary school, who were aged 4–8 years old (figure D.1, Spearman's ρ = -0.42, p = 0.023). An even stronger negative correlation was found for the 19 children whose parents told us had lived there since they were born (n = 19)(figure D.1, Spearman's ρ = -0.59, p = 0.008).

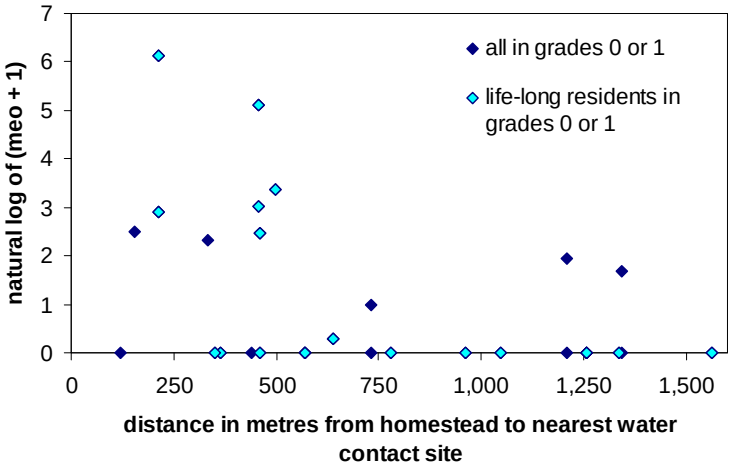

Figure D.1: Relationship between infection intensity (natural log of meo(mean egg output) + 1, where egg counts come from two or three 10ml urine samples collected on consecutive days), and distance lived from water contact site (straight line distance in metres between household and nearest active water contact site on a river) for children in grades 0 or 1 at Magaya primary school. Data shown for all of the children in this group (n = 29, dark blue diamonds) and highlighted for those who were life-long residents at their current household (n = 19, light blue diamonds).

No relationship between infection intensity and distance lived from an active water contact site was found in older individuals (data not shown).

D.3 Rates of moving house

The rate of movement between households was calculated independently from two different data sets. Firstly, information gathered from adults interviewed during the household mapping studies was selected for the eldest child from each household mapped on how long they had lived in that household, and whether they had lived there since birth. Only the eldest child was used to avoid potential biases from siblings moving to households at the same time. Data was available for individuals from 42 different households. The moving rate was calculated as the number of children who had moved to their current household since birth divided by the total length of time that all children had lived in their current household. 21 of the children had moved to their current household since birth, and a total of 367.3 years of residence in current household was reported across all 42 individuals, giving a moving rate of 0.057 per year.

The second method used to estimate moving rates came from questionnaire data for 283 individuals under the age of 20. The number of previous villages which individuals reported living in were added up for each person, and divided by the summed ages for all of these individuals. 179 moves were reported altogether, and the total summed ages came to 3447 years, giving a moving rate of 0.052 per year. Although this method will have missed within-village moves, interviews in the household survey suggested that the majority of local moves occurred between villages.

Both estimates of moving rate (ϕ) were very similar, and so a final value of 0.05 year^{-1} was used in the models in chapter 5.

Appendix E

Performance curves

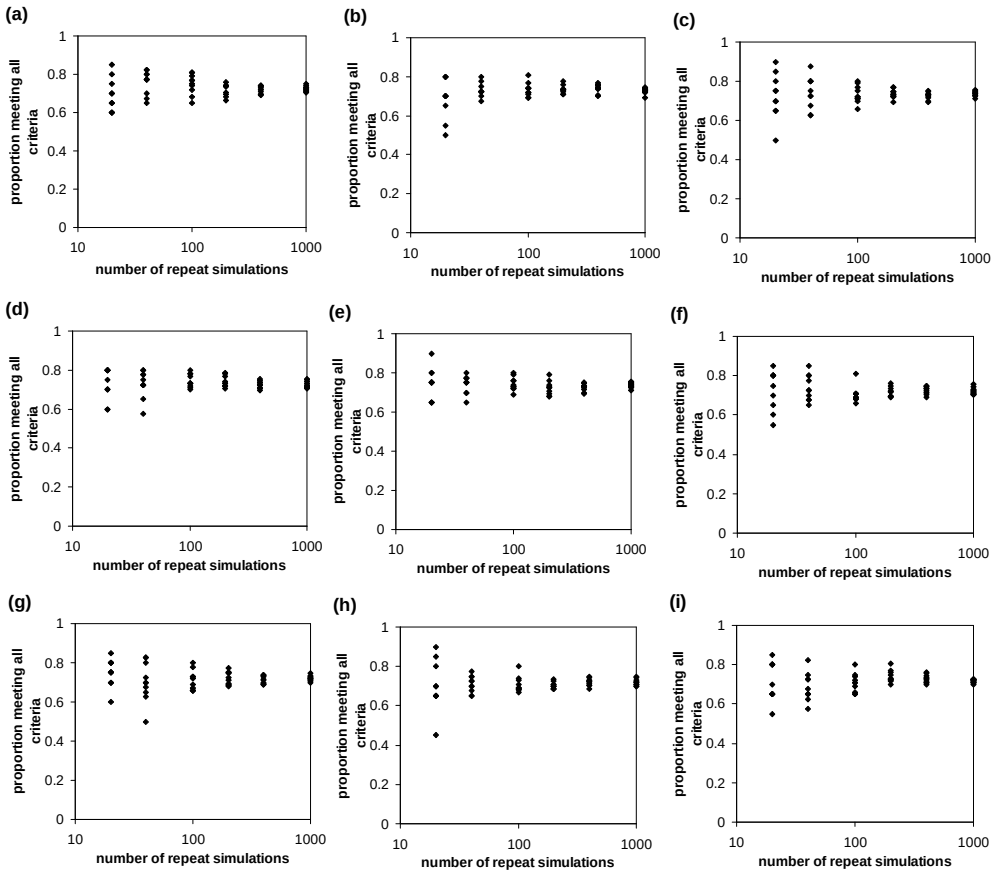

Figure E.1: Performance curves for the nine parameter sets which passed all of the criteria most frequently, for the cross-regulation models which had dying worms stimulating a protective anti-fecundity response, with a second non-protective antibody stimulated by egg antigen. The following numbers of repeat simulations were used ten times each: 20, 40, 100, 200, 400, 1000. The proportion of repeat simulations which passed all criteria is shown for each set of simulations.

Appendix F

Publication

Paper by Mitchell *et al.* (2008) used with permission of Wiley Interscience.

Parasite Immunology, 2008, **30**, 462–470 DOI: 10.1111/j.1365-3024.2008.01043.x

The predicted impact of immunosuppression upon population age–intensity profiles for schistosomiasis

K. M. MITCHELL, F. MUTAPI & M. E. J. WOOLHOUSE

Centre for Infectious Diseases, Institute of Immunology and Infection Research, School of Biological Sciences, University of Edinburgh, Edinburgh, UK

SUMMARY

The slow development of acquired immunity is thought to be responsible for the characteristic convex age–intensity curve seen in human schistosome infection, which peaks earlier in more heavily infected populations (this is described as a peak shift). Schistosomes are able to suppress protective host responses, and it is hypothesized that this suppression is responsible for the delayed development of protective responses. A deterministic mathematical model is used to describe levels of infection and immunity in an endemic population, incorporating protective immune responses which either reduce adult worm burden or reduce superinfection. Suppression, related to current worm burden, is also included and acts against one or both protective responses. If suppression acts against the entire protective response, it is able to delay the development of protective immunity, and the peak shift is predicted to be reversed at higher infection intensities, with removal of the peaks altogether at the highest levels of infection and/or suppression. If only the anti-adult worm protective immune response is vulnerable to suppression, while the anti-reinfection response remains intact, then suppression does not remove the peak in the age–intensity curve. These findings are discussed in the light of existing field and experimental data.

Keywords *acquired resistance, epidemiology, helminth, mathematical models*

Correspondence: Kate M. Mitchell, Ashworth Laboratories, Institute of Immunology and Infection Research, The King's Buildings, University of Edinburgh, West Mains Road, Edinburgh, EH9 3JT, UK (e-mail: k.m.mitchell@sms.ed.ac.uk).
Received: 16 October 2007
Accepted for publication: 30 April 2008

INTRODUCTION

In human populations with endemic schistosomiasis, a characteristic age–intensity pattern is seen, with infection intensity (measured by egg output in faeces or urine) rising rapidly through the childhood years to peak at around 8–15 years of age, then falling again in adulthood (1,2). The peak level of intensity is higher and occurs at a younger age in populations with a higher overall infection intensity when compared with areas of lower infection intensity, a phenomenon termed the 'peak shift' (3). The peaks also become more convex at higher levels of overall population infection intensity (1,4). Both phenomena are reproduced by simple mathematical models of acquired immunity (5). Protective immunity seems to develop slowly, as individuals endure chronic infection by long-lived adult worms, with frequent superinfection (6). There is increasing evidence that schistosomes are able to modulate the host immune response, suppressing both specific responses to schistosomes, and responses to bystander antigens and other pathogens (reviewed by Maizels and Yazdanbakhsh) (7). This active immunosuppression may be able to explain the delayed development of immunity.

In the mouse model of *Schistosoma mansoni* infection, suppression of immunopathological responses to trapped eggs in chronic infection has been clearly shown (8), and suppressor activity can be transferred from chronically to acutely infected mice by adoptive transfer of spleen cells (9).

In humans, experiments using peripheral blood mononuclear cells (PBMCs) from chronically infected individuals have shown that schistosome antigen-specific proliferation and cytokine production are reduced in chronic infection (10–15). This does not appear to be due to tolerance (deletion of antigen-reactive T cells), since antigen-specific responses can be restored *in vitro*, either by neutralization of IL-10 or by culture with dendritic-like cells (which improve antigen presentation by unelucidated contact-dependent and -independent mechanisms) (12,14,16–18). Antigen-specific proliferation and interferon (IFN)-γ production in chronically

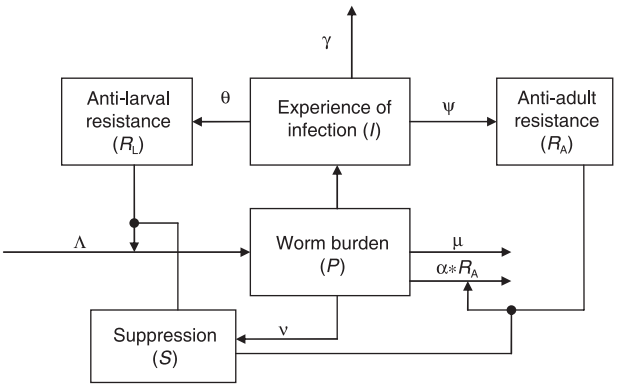

Figure 1 Schematic diagram of the model, showing the main state variables, worm burden (P) and experience of infection (I), and development of anti-larval (R_L) and anti-adult (R_A) resistance and suppressive (S) responses. θ, ψ and ν are indices of responsiveness, used in the Gumbel function to determine the strength of resistance or suppression based upon infection experience (for resistance) or current worm burden (for suppression), respectively. Loss of immune memory occurs at a rate γ. Parameter α, which governs the maximum rate of immune-induced death of adult worms, is set to 1 for all analyses. All parameters are defined in Table 1, with parameter values given. —● indicates suppression of a response.

infected individuals are inversely correlated with infection intensity (10,13), and in one study the percentage increase in cell proliferation upon IL-10 neutralization was shown to be strongly positively correlated with the amount of adult worm-specific IL-10 produced by PBMCs (14). Schistosome antigen-specific IL-10 – a possible marker for suppression – is positively correlated with infection intensity (19,20). Together, these findings suggest that the degree of suppression is related to infection intensity. Proliferative and cytokine responses to schistosome antigens are restored by praziquantel treatment, which kills adult worms (21,22).

The aim of this study was to determine the effects of active immunosuppression by schistosomes on population-level patterns of infection and immunity, in particular to investigate whether it could significantly delay the development of protective immunity and whether it could delay the age at which infection intensity peaks. A simple mathematical model of immunity was used, building on previous work by Woolhouse (5,23). Protective immunity was modelled as a function of cumulative exposure to adult worms, either reducing worm life span (24) or reducing the rate of superinfection by larval stages (concomitant immunity) (25), or both. Suppression was then introduced to reduce the impact of the protective responses, having the effect of increasing worm survival or increasing the rate of superinfection, respectively (up to the levels seen in the absence of immunity). Suppression was incorporated as a function of current worm burden, reflecting the correlation seen with infection intensity. In contrast to protective responses, suppression was assumed to have no immune memory, as it is lifted by chemotherapy (15,21). The model is used to predict the infection intensity curve with age, and the pattern of peak shifts, if suppression is assumed to act upon the entire protective response, or upon only part of it.

METHODS

A mathematical model consisting of a set of differential equations was developed, building upon previous models of schistosome immunity (5,23). Protective immunity was modelled as anti-larval (concomitant) immunity – a response triggered by adult worms but acting against incoming larvae – and direct anti-adult immunity, triggered by and active against adult worms, with these responses acting alone or together. Suppression of either or both of these responses were also included.

The model outline is shown schematically in Figure 1, and the equations describing the model are given below. Parameters are defined in detail in Table 1.

$$dP(a)/da = \Lambda(1 - R_L(1 - S)) - [\mu + \alpha R_A(1 - S)]P(a) \quad (1)$$

Table 1 Parameters used in the model, with initial values, units and source from the literature where relevant. 'Cell' refers to immune memory cell, unit of experience of infection (I)

Parameter	Meaning	Initial value	Units	Source/rationale
Λ	Rate of infection	40	Year^{-1} person^{-1}	(5)
θ	Strength of concomitant immunity	0·0028	Cell^{-1}	Set to give peak worm burden of 110 (5)
ψ	Strength of antiworm immunity	0·0015	Cell^{-1}	Set to give peak worm burden of 110
γ	Rate of immune memory loss	0·1	Year^{-1} cell^{-1}	(5)
μ	Natural death rate of adult worms	0·25	Year^{-1} worm^{-1}	(26,27)
α	Maximum level of additional immune-induced death rate of adult worms	1	Year^{-1} worm^{-1}	Set to give realistic minimum life span
ν	Strength of suppression	0·01	Cell^{-1}	Set to give significant suppressive effect

$$dI(a)/da = P(a) - \gamma I(a) \quad (2)$$

$$R_L(I) = 1 - (\exp(1 - \theta I - \exp(-\theta I))) \quad (3)$$

$$R_A(I) = 1 - (\exp(1 - \psi I - \exp(-\psi I))) \quad (4)$$

$$S(P) = 1 - (\exp(1 - \upsilon P - \exp(-\upsilon P))) \quad (5)$$

The model describes a homogeneous endemic population with a constant rate of infection with respect to both age and time. The individual worm burden (P) changes with age according to an immigration death process, with a constant rate of infection, Λ, and a constant per-capita rate of natural worm death, μ, described by equation (1). Parameter μ is set at 0·25 throughout this analysis, giving an average worm life span of 4 years (26,27). A second differential equation (2) describes the rate of change with age of the state variable 'infection experience' (I). This is roughly equivalent to a pool of memory cells, and increases with cumulative exposure to adult worms, with loss of immune memory at a rate γ, proportional to the memory cell population size (5). Both resistant responses are dependent upon this 'infection experience' and are related to it by a parameter determining the strength and the rapidity of the response (θ and ψ for anti-larval (R_L) and anti-adult responses (R_A), respectively), using a Gumbel function (as in previous models) (5), which scales the response to a value between 0 and 1 (equations 3 and 4). Anti-larval (or concomitant) immunity acts to reduce the rate of infection by a factor of $(1 - R_L)$, so that as resistance increases, the rate of acquisition of new infection decreases. Anti-adult immunity is modelled here as a separate additional worm per-capita death rate, $\alpha \times R_A$ with α set to 1 for this analysis. The model can be altered so that only anti-larval or only anti-adult immunity is acting, or a combination of the two, with the strength of resistance (θ or ψ) scaled to give a peak worm burden of 110 when the infection rate (Λ) is 40 new worms per year.

Suppression is modelled as acting against either or both of the protective responses. This should be regarded as a generic representation of the parasite-specific suppressive response rather than as an accurate representation of any particular immune mediator. Suppression is modelled as a Gumbel function of current worm burden (P), with strength determined by the parameter ν, again scaling the level of suppression between 0 and 1 (equation 5). Suppression may then act upon either resistance response, multiplying R_A or R_L by $(1 - S)$.

Alternatives to the Gumbel function for scaling both resistance and suppression were also investigated to see whether this changed the model output substantially. The functions used were linear ($R_A = \beta I$, $R \leq 1$) and exponential ($R_A = 1 - \exp[-\theta I]$), with equivalent equations for the anti-larval and suppression responses.

The combinations of resistance and suppression that were explored using this model were:

1 Resistance against adult worms only (R_A), with suppression of this response.
2 Resistance against larvae only (R_L), with suppression of this response.
3 Resistance against both adults and larvae (R_{AL}), with suppression of both responses.
4 Resistance against both adults and larvae (R_{AL}), in varying proportions, with suppression of only the anti-adult response.

For each scenario, the magnitude of suppression was varied to assess the effects on the age-intensity curve and the level of overall protective immunity, and the rate of infection was also varied to assess the impact of suppression upon the peak shift.

The expected fractional increase in the protective response if suppression were removed (analogous to IL-10 neutralization) was calculated as $(R_A - R_A(1 - S))/R_A(1 - S)$ for the R_A model, with an equivalent equation for the R_L model.

For the R_{AL} model, the expected impact of anti-adult immunity upon average worm life span was also assessed (with and without suppression) where the average life span $= 1/(\mu + R_A(1 - S))$.

All models were run in Berkeley Madonna version 8·0·1©. Equations were solved numerically using a fourth order Runge-Kutta algorithm with a time step of 0·02 years.

RESULTS

When the immune response is modelled as a single mechanism of resistance without suppression (models R_A and R_L), then the peak shift is reproduced. As the rate of infection (Λ) increases, the level of peak intensity is raised and occurs at an earlier age, with increasing curve convexity (Figure 2a,b). When both mechanisms of resistance are used in the same model (model R_{AL}), then the age–intensity profile is intermediate between that generated with anti-larval or anti-adult immunity alone, and again the peak shift is clearly seen (Figure 2c).

When suppression is included in the single-mechanism models (R_A and R_L), then increasing the strength of suppression (by increasing ν) raises the level of the peak parasite burden and delays the age at which the peak occurs, until, when suppression is sufficiently strong, the age–intensity curve tends towards the monotonically increasing immigration–death curve seen when there is no resistance at all. This is shown for the R_A model (Figure 3a). The trend is similar for

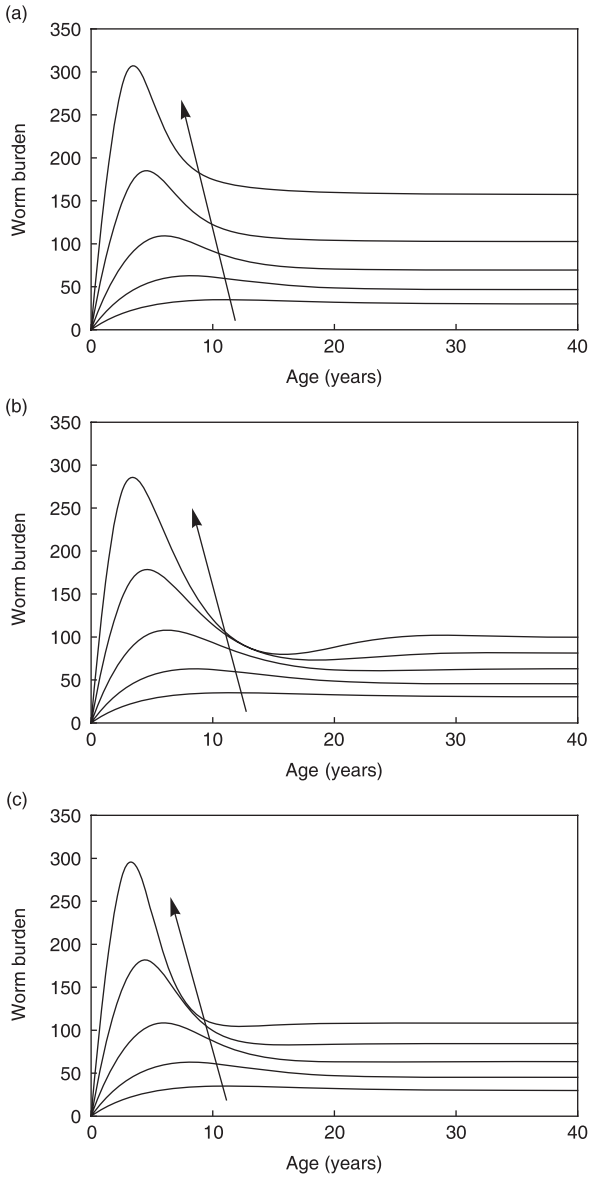

Figure 2 The peak shift in the basic models without suppression. Individual worm burden is shown changing with age for the following values of Λ (rate of infection) from bottom to top (with arrow): 10, 20, 40, 80, 160. For all graphs μ = 0·25, γ = 0·1 and ν = 0. (a) Model R_A: θ = 0, ψ = 0·0015 (b) Model R_L: θ = 0·0028, ψ = 0 (c) Model R_{AL}: θ = 0·0014, ψ = 0·00125.

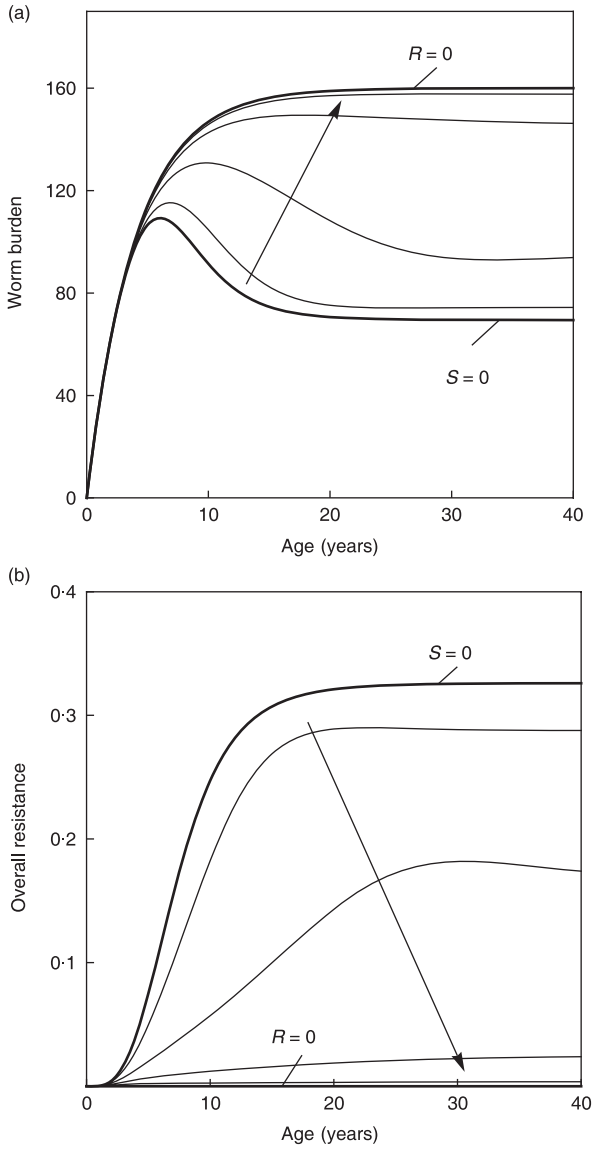

Figure 3 The effect of increasingly severe suppression in the R_A (anti-adult resistance) model upon (a) worm burden and (b) level of overall resistance [$R_A \times (1 - S)$]. Age–intensity profiles are displayed for both. Λ = 40, ψ = 0·0015. Bold lines indicate no suppression and no resistance as marked. Lines in between, increasing strength of suppression ν (in direction of arrow): 0·01, 0·02, 0·03, 0·04.

the R_L model (not shown). Increasing suppression decreases the convexity of the age–intensity curve. The simultaneous effect of increasing suppression on the effective immune response [$R_A \times (1 - S)$] is shown in Figure 3(b) for the R_A model. Increasing suppression delays the development of protective immunity, and also reduces the final level of resistance attained. At the higher levels of suppression explored, the protective response doesn't develop at all. Suppression also delays and reduces the development of protective immunity in the R_L model (data not shown).

Suppression affects the peak shift in both the R_A and the R_L models. For a constant strength of suppression, then at the lowest rates of infection, the peak shift is still observed, but as the rate of infection increases, the peak shift is

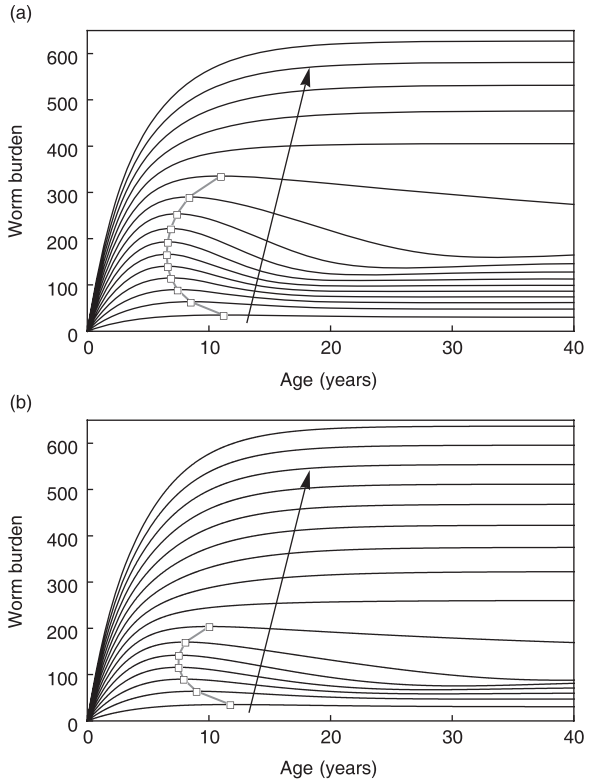

Figure 4 The effect of suppression on the peak shift for the (a) R_A and (b) R_L models. Individual worm burden is shown changing with age with increasing Λ (rate of infection) from 10 to 160 in steps of 10, going in the direction of the arrow. The trend of the peak shift is highlighted. (a) $\theta = 0$, $\psi = 0{\cdot}0015$, $\nu = 0{\cdot}01$. (b) $\theta = 0{\cdot}0028$, $\psi = 0$, $\nu = 0{\cdot}01$. Other parameters are as in Figures 2(a,b).

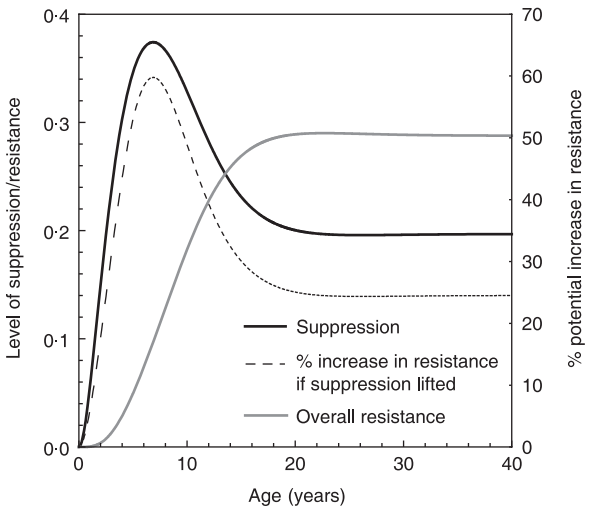

Figure 5 Dynamics of the suppression effect (S), the overall resistance level [$R_A \times (1 - S)$], and the expected rise in resistance level if suppression is removed. This is shown for the R_A model with $\Lambda = 40$, $\psi = 0{\cdot}0015$ and $\nu = 0{\cdot}01$. This corresponds to the second-lowest line in Figure 3(a), which shows the overall effect of this suppression on the population pattern of infection.

reversed, before complete loss of the peaks occurs at the highest infection intensity levels (Figure 4a,b). If an equal level of suppression against both responses is included in the R_{AL} model, then similar effects with increasing suppression and increasing infection rate are seen as for each response modelled separately – suppression can reverse the peak shift and remove the peaks altogether at a sufficiently high level of suppression or infection rate (data not shown). Removal of the peak at the highest infection intensity levels corresponds with almost complete prevention of acquired immunity developing.

The changing levels of the suppressive and protective responses were plotted for the R_A model, when $\Lambda = 40$ and $\nu = 0{\cdot}01$, along with the expected percentage increase in the protective response if suppression were removed (Figure 5). Suppression closely follows the level of worm burden, peaking at an early age, while the effective protective response [$R_A (1 - S)$] rises more slowly, and peaks later on. The percentage increase in protection if suppression were removed (illustrative of what is measured with an IL-10 neutralization assay) follows a similar trend with age to suppression level, peaking at 60%, but averaging out to around 30% over the whole age profile. The small effect that this apparently sizable suppression effect has on the overall age intensity profile can be seen by comparing the bottom two lines in Figure 3(a), with $\nu = 0$ (no suppression) and $\nu = 0{\cdot}01$. This corresponds to a modest delay in the development of anti-adult resistance (top two lines in Figure 3(b), with $\nu = 0$ (no suppression) and $\nu = 0{\cdot}01$).

When both types of immunity are included in the R_{AL} model but suppression acts only against the anti-adult response, different population-level effects are seen. Increasing the strength of suppression raises the height and decreases the convexity of the peak, and makes it occur at a later age, but cannot remove the peak altogether (Figure 6a). Whether or not the peak shift remains depends upon the relative strengths of the initial anti-adult and anti-larval responses. If both responses are quite strong (prior to the effects of suppression) then the magnitude of the peak shift is progressively reduced at higher levels of infection, but the peak shift is not reversed (Figure 6b: AL). However, if the anti-adult response is much stronger than the anti-larval response, then the peak shift may be reversed at intermediate levels of infection rate (Figure 6b: A » L). The peaks are never removed in this model so long as an unsuppressed protective anti-larval response is still acting.

In the R_{AL} model without suppression, the anti-adult immunity component has a large impact upon the average

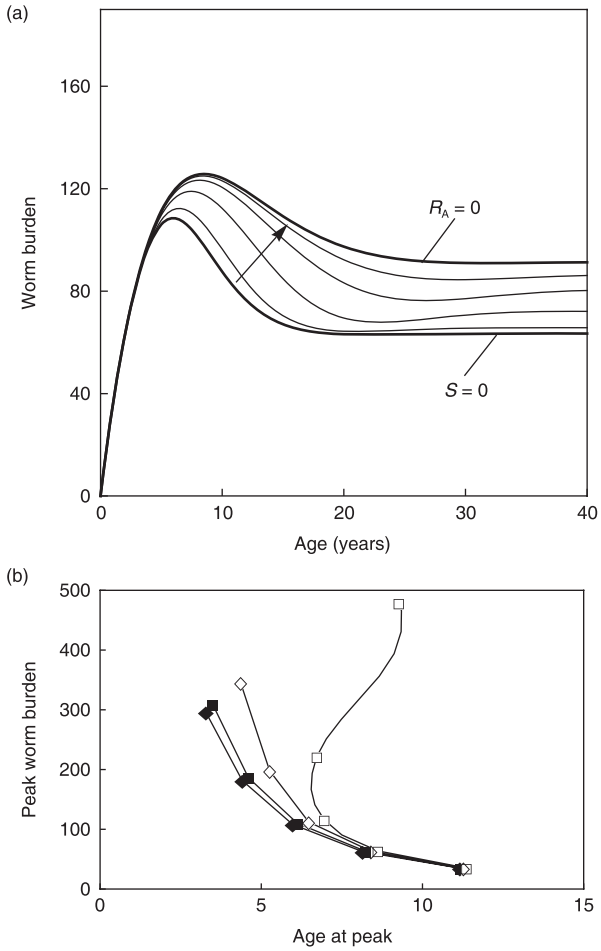

Figure 6 Suppression of R_A alone in the R_{AL} model. (a) Effect of increasing suppression on age–intensity profile. Bold lines indicate no suppression and no anti-adult (R_A) resistance, as marked. Lines in between, increasing strength of suppression ν (in direction of arrow): 0·01, 0·02, 0·03, 0·04. Λ = 40, θ = 0·0014, ψ = 0·00125. (b) Effect of suppression on the peak shift when the two resistant responses are strong (AL) or when the anti-adult response is much stronger (A » L). The trend for age and intensity at peaks is shown with and without suppression acting (ν = 0·01 or 0). Black diamonds: AL, no suppression; white diamonds: AL, with R_A suppressed; black squares: A » L, no suppression; white squares: A » L, with R_A suppressed. AL: θ = 0·0014, ψ = 0·00125. A » L: θ = 0·00028, ψ = 0·00144. Points marked are Λ = 10, 20, 40, 80, 160.

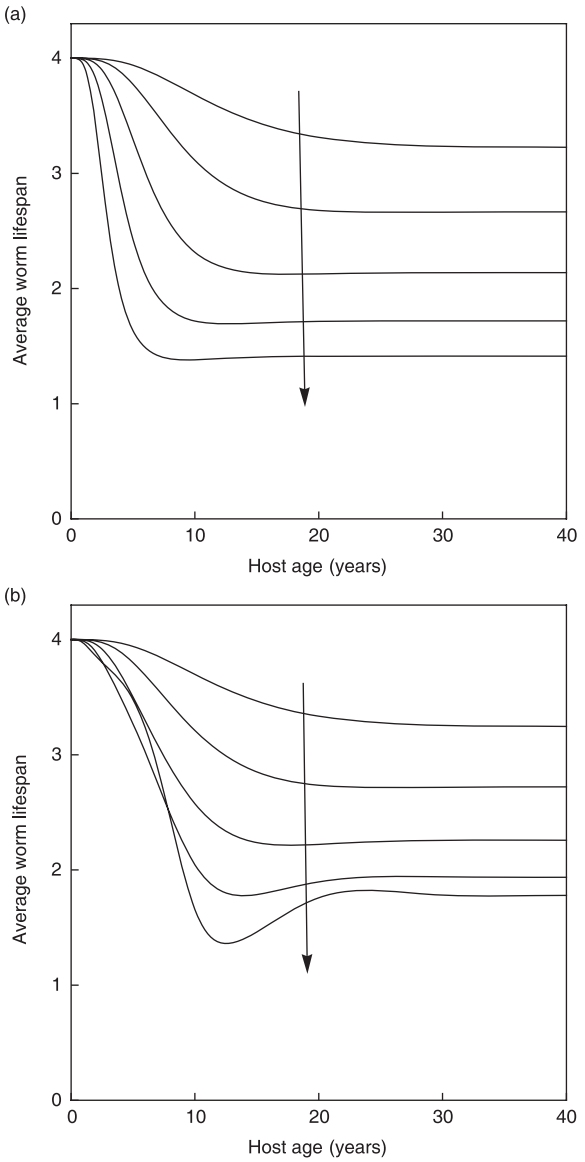

Figure 7 Effect of anti-adult immunity and suppression of anti-adult immunity on worm life span at different host ages (a) R_{AL} model, no suppression. (b) R_{AL} model with suppression of R_A response (ν = 0·01). For both graphs, θ = 0·0014, ψ = 0·00125, Λ (top to bottom, in direction of arrow): 10, 20, 40, 80, 160.

worm life span, which decreases both with host age and with increasing infection rate (Figure 7a). When suppression of anti-adult immunity is included, then at the highest levels of infection rate, the reduction in life span within the host is delayed by a few years, and the final equilibrium life span is slightly increased (Figure 7b).

Using alternative functions (linear or exponential) for the relationship between infection experience and resistance did not change the predicted trends for this model.

DISCUSSION

The model suggests that suppression can delay and reduce the development of protective immunity in humans, but may have complex effects upon population patterns of infection. The model shows that very strong immunosuppression of the entire protective response can completely overwhelm it, removing all evidence of acquired immunity and removing the 'peak' in infection intensity altogether, while very weak

immunosuppression will have little or no effect on the age and intensity of peak infection, as protective immunity is scarcely affected. With the parameter values given in Table 1, and suppression acting against all protective immune responses, then at low rates of infection the peak shift will remain, but at increasingly high rates of infection the suppressive effect should be able to reverse the peak shift and reduce the convexity of peaks, and then remove the peaks altogether.

Alternatively, if immunosuppression only acts against part of the immune response (in this case only the anti-adult response, leaving the anti-larval response intact), then suppression is predicted to be unable to remove the peaks, and have a much more modest effect upon the peak shift. The age at which the peak occurs will be increasingly delayed at higher rates of infection, but the peak shift will only be reversed if the unsuppressed anti-larval response is very weak. Suppression is predicted to extend the worm life span considerably in the youngest hosts, but have very little effect on worm survival in older hosts.

Using a mathematical modelling approach to investigate this question is useful because it allows findings from laboratory studies to be applied to a hypothetical population setting, under a set of explicit and verifiable assumptions, producing outputs that can be compared with field data. The development and action of generic protective and suppressive immune responses were modelled, with protective responses a function of cumulative exposure to adult worms and suppression a function of current worm burden. The relatively simple structure of the model made it ideal for exploratory analyses of the hypothesis that suppression may delay the development of immunity and occurrence of the peak in infection intensity. This framework can be adapted for more detailed models which incorporate more realistic and specific immune responses and age-varying exposure levels, generating model outputs which can be fitted to field data, to allow more quantitative conclusions to be drawn.

Parasite-induced immunosuppression has previously been included in other mathematical models of macroparasite infection (28,29). Duerr and colleagues modelled parasite-associated suppression as an increasing rate of parasite establishment (Λ) with increasing parasite burden (29,30), with their null model (with no suppression) equivalent to our full suppression model (with no resistance). Their model predicted sigmoidal age–intensity curves, consistent with onchocerciasis data (30) (which displays very different patterns to schistosomiasis) (31), and their model could not generate peaks or a peak shift, as was seen with very high suppression in our model. Schweitzer and Anderson included parasite-induced suppression of T cell responses in their more mechanistic models of parasite immunology; removal of activated T cells by parasites permitted a stable state with high parasite burden and low numbers of activated T cells, with high levels of repeated exposure tending to move the system towards this state. In a more complex model where parasites suppressed IL-2-driven T cell proliferation, progression from an immunosuppressed to an immune state was increasingly delayed at higher infective doses (28). This is in general agreement with our model output.

In contrast to the predictions from the suppression model, existing field data on *S. mansoni* and *S. haematobium* demonstrates a definite peak in infection intensities in childhood, which is increasingly strongly convex at higher infection intensities (4), and a clear peak shift towards younger individuals is seen in more heavily infected populations (32). Similar peak shifts have also been demonstrated for filarial and hookworm infections in human populations (3). This suggests that significant intensity-related parasite-specific suppression of all immune responses is inconsistent with observed population patterns of schistosome infection intensity.

A cross-sectional population study of schistosome-specific immune responses has demonstrated a change with age in the cytokine response, from an IL-10 dominated suppressive response in younger children to a (putatively protective) Th2 response in older individuals (19). Blocking of IL-10 led to a 27% increase in parasite-specific IL-5 release by cells in culture (19). While representations of immunity in our model are very generic and cannot be directly attributed to specific cytokines, it is interesting to observe that a switch from a suppressive to a protective response, with a similar level of percentage increase in the protective response if suppression is lifted, can be generated by our model (Figure 5), without having a great impact on the age–intensity curve (Figure 3a). This is not a stable outcome in our model, however, as very different patterns are seen at different levels of infection.

The alternative scenario set forward in this paper, that only part of the immune response is suppressed, requires experimental verification. There is some indication that innate toll-like receptor (TLR)-controlled responses are selectively down-regulated in schistosomiasis (33), and the same may be true for protective adaptive immune responses. In deciding between the complete and partial suppression model, more rigorous demonstration of the biological plausibility of the parameters used will also be necessary, including infection rates and the extent of suppression that occurs. Water contact rates, measured in the field, can be used to estimate infection rates and to parameterize models of immunity (34). In the model, an assumed natural worm life span of 4 years is considerably shortened by anti-adult immunity, to as little as 1·5 years, in contrast to the estimates of 3–6 years previously calculated from field data (26–27, 35); more realistic parameterization of the model will

be necessary to determine whether this is a significant problem. The prediction that, if there is significant immune attrition of adult worms, then worm life expectancy will be shorter in adults than in children (Figure 7a), has been previously tested in two field studies of *S. mansoni*; one study, following transmission control in St. Lucia, showed some evidence of a longer worm life span in children (26), while another study analysing pre- and post-treatment data from Kenya failed to find evidence of a significant difference (36).

In developing these ideas further, it will be informative to explicitly model the egg stage of the schistosome life cycle, since there is evidence that responses to eggs dominate early on in infection, and may be more strongly suppressed than responses to adult worm antigens in chronic infection (15,37). Modelling the egg stage will also allow the model to be fitted to field data on egg output.

While our model indicates that worm-induced immunosuppression may be able to delay the development of protective immunity, it also can have effects on population levels of infection intensity which have not been reported in field data, in particular reducing the convexity of the age–intensity curve, and reversing the peak-shift. This suggests that intensity-related immunosuppression of the specific immune response does not occur to a significant extent during schistosome infection.

ACKNOWLEDGEMENTS

KMM is supported by the Medical Research Council UK. FM is supported by an RCUK Fellowship and the investigation received financial support from the Medical Research Council, UK (Grant no G81/538), the Cunningham Trust, Tenovus Scotland, the Carnegie Trust for the Universities of Scotland and the Wellcome Trust.

REFERENCES

1 Fisher AC. A study of the schistosomiasis of the Stanleyville district of the Belgian Congo. *Trans R Soc Trop Med Hyg* 1934; **28**: 277–306.
2 Clarke VD. The influence of acquired resistance in the epidemiology of bilharziasis. *Cent Afr J Med* 1966; **12**: 1–30.
3 Woolhouse MEJ. Patterns in parasite epidemiology: the peak shift. *Parasitol Today* 1998; **14**: 428–434.
4 Anderson RM & May RM. *Infectious Diseases of Humans: Dynamics and Control*. Oxford, Oxford University Press, 1991.
5 Woolhouse MEJ. A theoretical framework for the immunoepidemiology of helminth infection. *Parasite Immunol* 1992; **14**: 563–578.
6 Woolhouse MEJ & Hagan P. Seeking the ghost of worms past. *Nat Med* 1999; **5**: 1225–1227.
7 Maizels RM & Yazdanbakhsh M. Immune regulation by helminth parasites: cellular and molecular mechanisms. *Nat Rev Immunol* 2003; **3**: 733–744.
8 King CH. Initiation and regulation of disease in schistosomiasis. In Mahmoud AAF (ed.): *Schistosomiasis*. London, Imperial College Press, 2001, 213–264.
9 Weinstock JV & Boros DL. Heterogeneity of the granulomatous response in the liver, colon, ileum, and ileal Peyer's patches to schistosome eggs in murine schistosomiasis mansoni. *J Immunol* 1981; **127**: 1906–1909.
10 de Jesus AMR, Almeida RP, Bacellar O, *et al*. Correlation between cell-mediated immunity and degree of infection in subjects living in an endemic area of schistosomiasis. *Eur J Immunol* 1993; **23**: 152–158.
11 Viana IRC, Sher A, Carvalho OS, *et al*. Interferon-γ production by peripheral blood mononuclear cells from residents of an area endemic for *Schistosoma mansoni*. *Trans R Soc Trop Med Hyg* 1994; **88**: 466–470.
12 Araújo MI, de Jesus AR, Bacellar O, *et al*. Evidence of a T helper type 2 activation in human schistosomiasis. *Eur J Immunol* 1996; **26**: 1399–1403.
13 Grogan JL, Kremsner PG, Deelder AM & Yazdanbakhsh M. Antigen-specific proliferation and interferon-γ and interleukin-5 production are down-regulated during *Schistosoma haematobium* infection. *J Infect Dis* 1998; **177**: 1433–1437.
14 King CL, Medhat A, Malhotra I, *et al*. Cytokine control of parasite-specific anergy in human urinary schistosomiasis. IL-10 modulates lymphocyte reactivity. *J Immunol* 1996; **156**: 4715–4721.
15 Colley DG, Barsoum IS, Dahawi HSS, *et al*. Immune responses and immunoregulation in relation to human schistosomiasis in Egypt. III. Immunity and longitudinal studies of *in vitro* responsiveness after treatment. *Trans R Soc Trop Med Hyg* 1986; **80**: 952–957.
16 Corrêa-Oliveira R, Malaquias LCC, Falcão PL, *et al*. Cytokines as determinants of resistance and pathology in human *Schistosoma mansoni* infection. *Braz J Med Biol Res* 1998; **31**: 171–177.
17 Grogan JL, Kremsner PG, Deelder AM & Yazdanbakhsh M. The effect of anti-IL-10 on proliferation and cytokine production in human schistosomiasis: fresh versus cryopreserved cells. *Parasite Immunol* 1998; **20**: 345–349.
18 van den Biggelaar AHJ, Grogan JL, Filie Y, *et al*. Chronic schistosomiasis: dendritic cells generated from patients can overcome antigen-specific T cell hyporesponsiveness. *J Infect Dis* 2000; **182**: 260–265.
19 Mutapi F, Winborn G, Midzi N, *et al*. Cytokine responses to *Schistosoma haematobium* in a Zimbabwean population: contrasting profiles for IFN-γ, IL-4, IL-5 and IL-10 with age. *BMC Infect Dis* 2007; **7**: 139.
20 Reimert CA, Fitzsimmons CM, Joseph S, *et al*. Eosinophil activity in *Schistosoma mansoni* infections *in vivo* and *in vitro* in relation to plasma cytokine profile pre- and posttreatment with praziquantel. *Clin Vaccine Immunol* 2006; **13**: 584–593.
21 Grogan JL, Kremsner PG, Deelder AM & Yazdanbakhsh M. Elevated proliferation and interleukin-4 release from CD4 (+) cells after chemotherapy in human *Schistosoma haematobium* infection. *Eur J Immunol* 1996; **26**: 1365–1370.
22 van den Biggelaar AHJ, Rodrigues LC, van Ree R, *et al*. Long-term treatment of intestinal helminths increases mite skin-test reactivity in Gabonese schoolchildren. *J Infect Dis* 2004; **189**: 892–900.
23 Woolhouse MEJ. A theoretical framework for immune responses and predisposition to helminth infection. *Parasite Immunol* 1993; **15**: 583–594.
24 Agnew AM, Murare HM & Doenhoff MJ. Immune attrition of adult schistosomes. *Parasite Immunol* 1993; **15**: 261–271.

25 Smithers SR & Terry RJ. Resistance to experimental infection with *Schistosoma mansoni* in rhesus monkeys induced by the transfer of adult worms. *Trans R Soc Trop Med Hyg* 1967; **61**: 517–533.
26 Goddard MJ & Jordan P. On the longevity of *Schistosoma mansoni* in man on St. Lucia, West Indies. *Trans R Soc Trop Med Hyg* 1980; **74**: 185–191.
27 Wilkins HA, de Goll PHC, Marshall TF & Moore PJ. Dynamics of *Schistosoma haematobium* infection in a Gambian community. III. Acquisition and loss of infection. *Trans R Soc Trop Med Hyg* 1984; **78**: 227–232.
28 Schweitzer N & Anderson R. Helminths, immunology and equations. *Immunol Today* 1991; **12**: A76–A81.
29 Duerr HP, Dietz K & Eichner M. On the interpretation of age-intensity profiles and dispersion patterns in parasitological surveys. *Parasitology* 2003; **126**: 87–101.
30 Duerr HP, Dietz K, Schulz-Key H, Buttner DW & Eichner M. Density-dependent parasite establishment suggests infection-associated immunosuppression as an important mechanism for parasite density regulation in onchocerciasis. *Transactions Royal Soc Trop Med Hygiene* 2003; **97**: 242–250.
31 Basáñez MG & Boussinesq M. Population biology of human onchocerciasis. *Philos Trans R Soc Lond B Biol Sci* 1999; **354**: 809–826.
32 Fulford AJC, Butterworth AE, Sturrock RF & Ouma JH. On the use of age-intensity data to detect immunity to parasitic infections, with special reference to *Schistosoma mansoni* in Kenya. *Parasitology* 1992; **105**: 219–227.
33 van der Kleij D, van den Biggelaar AHJ, Kruize YCM, *et al*. Responses to toll-like receptor ligands in children living in areas where schistosome infections are endemic. *J Infect Dis* 2004; **189**: 1044–1051.
34 Woolhouse MEJ, Ndamba J & Bradley DJ. The interpretation of intensity and aggregation data for infections of *Schistosoma haematobium*. *Trans R Soc Trop Med Hyg* 1994; **88**: 520–526.
35 Vermund SH, Bradley DJ & Ruiztiben E. Survival of *Schistosoma mansoni* in the human host – estimates from a community-based prospective study in Puerto Rico. *Am J Trop Med Hyg* 1983; **32**: 1040–1048.
36 Fulford AJC, Butterworth AE, Ouma JH & Sturrock RF. A statistical approach to schistosome population-dynamics and estimation of the life-span of *Schistosoma mansoni* in man. *Parasitology* 1995; **110**: 307–316.
37 Gazzinelli G, Viana IR, Bahia-Oliveira LM, *et al*. Immunological profiles of patients from endemic areas infected with *Schistosoma mansoni*. *Mem Inst Oswaldo Cruz* 1992; **87** (S4): 139–142.

Bibliography

Abbas, A., Murphy, K. & Sher, A. (1996). Functional diversity of helper T lymphocytes. *Nature,* **383**, 787–793.

Agnew, A., Fulford, A. J., Mwanje, M. T., Gachuhi, K., Gutsmann, V., Krijger, F. W., Sturrock, R. F., Vennervald, B. J., Ouma, J. H., Butterworth, A. E. & Deelder, A. M. (1996). Age-dependent reduction of schistosome fecundity in *Schistosoma haematobium* but not *Schistosoma mansoni* infections in humans. *American Journal of Tropical Medicine and Hygiene,* **55** (3), 338–343.

Agnew, A., Murare, H. M. & Doenhoff, M. J. (1993). Immune attrition of adult schistosomes. *Parasite Immunology,* **15**, 261–271.

Agnew, A. M., Fulford, A. J., De Jonge, N., Krijger, F., Rodriguez-Chacon, M., Gutsmann, V. & Deelder, A. M. (1995). The relationship between worm burden and levels of a circulating antigen (CAA) of five species of *Schistosoma* in mice. *Parasitology,* **111**, 67–76.

Agnew, A. M., Murare, H. M., Sandoval, S. N., Dejong, N., Krijer, F. W., Deelder, A. M. & Doenhoff, M. J. (1992). The susceptibility of adult schistosomes to immune attrition. *Memorias Do Instituto Oswaldo Cruz,* **87 (S4)**, 87–93.

Ahmed, S., Oswald, I., Caspar, P., Hieny, S., Keefer, L., Sher, A. & James, S. (1997). Developmental differences determine larval susceptibility to nitric oxide-mediated killing in a murine model of vaccination against *Schistosoma mansoni*. *Infection and Immunity,* **65** (1), 219–226.

Ahuja, A., Anderson, S. M., Khalil, A. & Shlomchik, M. J. (2008). Maintenance of the plasma cell pool is independent of memory B cells. *Proceedings of the National Academy of Sciences of the United States of America,* **105** (12), 4802–4807.

Amanna, I. J., Carlson, N. E. & Slifka, M. K. (2007). Duration of humoral immunity to common viral and vaccine antigens. *New England Journal of Medicine,* **357** (19), 1903–1915.

Anderson, R. M. (1998). Complex dynamic behaviours in the interaction between parasite populations and the host's immune system. *International Journal for Parasitology,* **28** (4), 551–566.

Anderson, R. M. & May, R. M. (1985). Herd-immunity to helminth infection and implications for parasite control. *Nature,* **315** (6019), 493–496.

Anderson, R. M. & May, R. M. (1991*a*). Indirectly transmitted helminths. In *Infectious Diseases of Humans: Dynamics and Control* pp. 550–589. Oxford University Press Oxford.

Anderson, R. M. & May, R. M. (1991*b*). Acquired immunity. In *Infectious Diseases of Humans: Dynamics and Control* pp. 530–540. Oxford University Press Oxford.

Anderson, S., Coulson, P. S., Ljubojevic, S., Mountford, A. P. & Wilson, R. A. (1999). The radiation-attenuated schistosome vaccine induces high levels of protective immunity in the absence of B cells. *Immunology,* **96** (1), 22–28.

Araújo, M. I., de Jesus, A. R., Bacellar, O., Sabin, E., Pearce, E. & Carvalho, E. M. (1996). Evidence of a T helper type 2 activation in human schistosomiasis. *European Journal of Immunology,* **26** (6), 1399–1403.

Asquith, B., Borghans, J. A. M., Ganusov, V. V. & Macallan, D. C. (2009). Lymphocyte kinetics in health and disease. *Trends in Immunology,* **30** (4), 182–189.

Austin, D. J. & Anderson, R. M. (1996). Immunodominance, competition and evolution in immunological responses to helminth parasite antigens. *Parasitology,* **113**, 157–172.

Barbour, A. D. (1996). Modeling the transmission of schistosomiasis: an introductory view. *American Journal of Tropical Medicine and Hygiene,* **55** (S), 135–143.

Basáñez, M. G. & Boussinesq, M. (1999). Population biology of human onchocerciasis. *Philosophical Transactions of the Royal Society B-Biological Sciences,* **354**, 809–826.

Beniguel, L., Diallo, T. O., Remoue, F., Williams, D. L., Cognasse, F., Charrier-Mze, N., N'Diaye, A. A., Perraut, R., Capron, M., Riveau, G. & Garraud, O. (2003). Differential production in vitro of antigen specific IgG1, IgG3 and IgA: a study in *Schistosoma haematobium* infected individuals. *Parasite Immunology,* **25** (1), 39–44.

Bensted-Smith, R., Anderson, R. M., Butterworth, A. E., Dalton, P. R., Kariuki, H. C., Koech, D., Mugambi, M., Ouma, J. H., Siongok, T. K. A. & Sturrock, R. F. (1987). Evidence for predisposition of individual patients to reinfection with *Schistosoma mansoni* after treatment. *Transactions of the Royal Society of Tropical Medicine and Hygiene,* **81** (4), 651–654.

Berberian, D. A., Paquin, H. O. & Fantauzzi, A. (1953). Longevity of *Schistosoma hematobium* and *Schistosoma mansoni* - observations based on a case. *Journal of Parasitology,* **39** (5), 517–519.

Bergquist, N. R., Leonardo, L. R. & Mitchell, G. F. (2005). Vaccine-linked chemotherapy: can schistosomiasis control benefit from an integrated approach? *Trends in Parasitology,* **21** (3), 112–117.

Bergquist, R., Utzinger, J., Chollet, J., Shu-Hua, X., Weiss, N. A. & Tanner, M. (2004). Triggering of high-level resistance against *Schistosoma mansoni* reinfection by artemether in the mouse model. *American Journal of Tropical Medicine and Hygiene,* **71** (6), 774–777.

Bernasconi, N. L., Traggiai, E. & Lanzavecchia, A. (2002). Maintenance of serological memory by polyclonal activation of human memory B cells. *Science,* **298** (5601), 2199–2202.

Black, C. L., Mwinzi, P. N. M., Muok, E. M. O., Abudho, B., Fitzsimmons, C. M., Dunne, D. W., Karanja, D. M. S., Secor, W. E. & Colley, D. G. (2010). Influence of exposure history on the immunology and development of resistance to human schistosomiasis mansoni. *PLoS Neglected Tropical Diseases,* **4** (3), e637.

Boulanger, D., Warter, A., Sellin, B., Lindner, V., Pierce, R. J., Chippaux, J.-P. & Capron, A. (1999). Vaccine potential of a recombinant glutathione S-transferase cloned from *Schistosoma haematobium* in primates experimentally infected with an homologous challenge. *Vaccine,* **17** (4), 319–326.

Bradley, D. J. & McCullough, F. S. (1973). Egg output stability and the epidemiology of *Schistosoma haematobium* Part II. An analysis of the epidemiology of endemic *S. haematobium*. *Transactions of the Royal Society of Tropical Medicine and Hygiene,* **67** (4), 491–500.

Brooker, S., Kabatereine, N. D. B., Clements, A. C. A. & Stothard, J. R. (2004*a*). Schistosomiasis control. *The Lancet,* **363** (9409), 658–659.

Brooker, S., Whawell, S., Kabatereine, N. B., Fenwick, A. & Anderson, R. M. (2004*b*). Evaluating the epidemiological impact of national control programmes for helminths. *Trends in Parasitology,* **20** (11), 537–545.

Brouwer, K., Ndhlovu, P., Munatsi, A. & Shiff, C. (2001). Genetic diversity of a population of *Schistosoma haematobium* derived from schoolchildren in East Central Zimbabwe. *Journal of Parasitology,* **87**, 762–769.

Brouwer, K., Ndhlovu, P. D., Wagatsuma, Y., Munatsi, A. & Shiff, C. (2003). Urinary tract pathology attributed to *Schistosoma haematobium*: does parasite genetics play a role? *American Journal of Tropical Medicine and Hygiene,* **68**, 456–462.

Bundy, D. A. P., Kan, S. P. & Rose, R. (1988). Age-related prevalence, intensity and frequency distribution of gastrointestinal helminth infection in urban slum children from Kuala Lumpur, Malaysia. *Transactions of the Royal Society of Tropical Medicine and Hygiene,* **82** (2), 289–294.

Bushara, H. O., Hussein, M. F., Majid, M. A., Musa, B. E., Taylor, M. G., Bushara, H. O., Hussein, M. F., Majid, M. A., Musa, B. E. & Taylor, M. G. (1983). Observations on cattle schistosomiasis in the Sudan, a study in comparative medicine. IV. Preliminary observations on the mechanism of naturally acquired resistance. *American Journal of Tropical Medicine and Hygiene,* **32** (5), 1065–70.

Bushara, H. O., Majid, A. A., Saad, A. M., Hussein, M. F., Taylor, M. G., Dargie, J. D., Marshall, T. F. & Nelson, G. S. (1980). Observations on cattle schistosomiasis in the Sudan, a study in comparative medicine. II. Experimental demonstration of naturally acquired resistance to *Schistosoma bovis*. *American Journal of Tropical Medicine and Hygiene,* **29** (3), 442–51.

Butterworth, A., Dunne, D., Anthony, F., Capron, M., Khalife, J., Capron, A., Koech, D., Ouma, J. & Sturrock, R. (1988). Immunity in human schistosomiasis mansoni: cross-reactive IgM and IgG2 anti-carbohydrate antibodies block the expression of immunity. *Biochimie,* **70** (8), 1053–1063.

Butterworth, A. E., Dunne, D. W., Fulford, A. J., Ouma, J. H. & Sturrock, R. F. (1996). Immunity and morbidity in *Schistosoma mansoni* infection: quantitative aspects. *American Journal of Tropical Medicine and Hygiene,* **55** (S), 109–115.

Butterworth, A. E., Sturrock, R. F., Houba, V., Mahmoud, A. A. F., Sher, A. & Rees, P. H. (1975). Eosinophils as mediators of antibody-dependent damage to schistosomula. *Nature,* **256** (5520), 727–729.

Butterworth, A. E., Sturrock, R. F., Houba, V. & Rees, P. H. (1974). Antibody-dependent cell-mediated damage to schistosomula in vitro. *Nature,* **252** (5483), 503–505.

Callard, R., George, A. J. T. & Stark, J. (1999). Cytokines, chaos, and complexity. *Immunity,* **11** (5), 507 – 513.

Capron, A., Dessaint, J. P., Capron, M. & Pierce, R. J. (1992). Vaccine strategies against schistosomiasis. *Memorias Do Instituto Oswaldo Cruz,* **87** (S5), 1–9.

Capron, A., Dombrowicz, D. & Capron, M. (1999). Regulation of the immune response in experimental and human schistosomiasis: the limits of an attractive paradigm. *Microbes and Infection,* **1** (7), 485–490.

Capron, A., Riveau, G., Capron, M. & Trottein, F. (2005). Schistosomes: the road from host-parasite interactions to vaccines in clinical trials. *Trends in Parasitology,* **21** (3), 143–149.

Capron, M. & Capron, A. (1986). Rats, mice and men – models for immune effector mechanisms against schistosomiasis. *Parasitology Today,* **2** (3), 69–75.

Carter, R. H. & Fearon, D. T. (1992). CD19: lowering the threshold for antigen receptor stimulation of B lymphocytes. *Science,* **256** (5053), 105–107.

Carvalho-Queiroz, C., Cook, R., Wang, C. C., Correa-Oliveira, R., Bailey, N. A., Egilmez, N. K., Mathiowitz, E. & LoVerde, P. T. (2004). Cross-reactivity of *Schistosoma mansoni* cytosolic superoxide dismutase, a protective vaccine candidate, with host superoxide dismutase and identification of parasite-specific B epitopes. *Infection & Immunity,* **72** (5), 2635–2647.

Chan, M. S. (1996). The consequences of uncertainty for the prediction of the effects of schistosomiasis control programmes. *Epidemiology and Infection,* **117** (3), 537–550.

Chan, M. S., Anderson, R. M., Medley, G. F. & Bundy, D. A. P. (1996). Dynamic aspects of morbidity and acquired immunity in schistosomiasis control. *Acta Tropica,* **62** (2), 105–117.

Chan, M. S. & Isham, V. S. (1998). A stochastic model of schistosomiasis immuno-epidemiology. *Mathematical Biosciences,* **151** (2), 179–198.

Chan, M. S., Montresor, A., Savioli, L. & Bundy, D. A. (1999). Planning chemotherapy based schistosomiasis control: validation of a mathematical model using data on *Schistosoma haematobium* from Pemba, Tanzania. *Epidemiology and Infection,* **123**, 487–497.

Chan, M. S., Mutapi, F., Woolhouse, M. E. J. & Isham, V. S. (2000). Stochastic simulation and the detection of immunity to schistosome infections. *Parasitology,* **120**, 161–169.

Chan, M. S., Nsowah-Nuamah, N. N. N., Adjei, S., Wen, S. T., Hall, A. & Bundy, D. A. P. (1998). Predicting the impact of school-based treatment for urinary schistosomiasis given by the Ghana Partnership for Child Development. *Transactions of the Royal Society of Tropical Medicine and Hygiene,* **92** (4), 386–389.

Chan, M. S., Woolhouse, M. E. J. & Bundy, D. A. P. (1997). Human schistosomiasis: potential long term consequences of vaccination programmes. *Vaccine,* **15** (14), 1545–1550.

Chandiwana, S. K. (1987). Community water-contact patterns and the transmission of *Schistosoma haematobium* in the highveld region of Zimbabwe. *Social Science and Medicine,* **25** (5), 495–505.

Chandiwana, S. K., Taylor, P. & Clarke, V. D. (1988). Prevalence and intensity of schistosomiasis in 2 rural areas in Zimbabwe and their relationship to village location and snail infection rates. *Annals of Tropical Medicine and Parasitology,* **82** (2), 163–173.

Chandiwana, S. K. & Woolhouse, M. E. (1991). Heterogeneities in water contact patterns and the epidemiology of *Schistosoma haematobium*. *Parasitology,* **103** (3), 363–70.

Chandiwana, S. K., Woolhouse, M. E. & Bradley, M. (1991). Factors affecting the intensity of reinfection with *Schistosoma haematobium* following treatment with praziquantel. *Parasitology,* **102**, 73–83.

Cheever, A. W., Kamel, I., Elwi, A. M., Mosimann, J. E. & Danner, R. (1977). *Schistosoma mansoni* and *S. haematobium* infections in Egypt. II. Quantitative parasitological findings at necropsy. *The American Journal of Tropical Medicine and Hygiene,* **26**, 702–716.

Cheever, A. W., Kuntz, R. E., Moore, J. A. & Huang, T. C. (1988). Pathology of *Schistosoma haematobium* infection in the capuchin monkey (*Cebus apella*). *Transactions of the Royal Society of Tropical Medicine and Hygiene,* **82** (1), 107–111.

Cheever, A. W., Kuntz, R. E., Myers, B. J., Moore, J. A. & Huang, T. C. (1974). Schistosomiasis haematobia in African, hamadryas, and gelada baboons. *American Journal of Hygiene and Tropical Medicine,* **23** (3), 429–448.

Cheever, A. W., Torky, A. H. & Shirbiney, M. (1975). The relation of worm burden to passage of *Schistosoma haematobium* eggs in the urine of infected patients. *The American Journal of Tropical Medicine and Hygiene,* **24** (2), 284–288.

Christopherson, J. B. (1924). Longevity of parasitic worms: the term of living existence of *Schistosoma haematobium* in the human body. *Lancet,* **203** (5250), 742–743.

Clarke, V. d. V. (1966). The influence of acquired resistance in the epidemiology of bilharziasis. *Central African Journal of Medicine,* **12** (6), 1–30.

Clennon, J. A., King, C. H., Muchiri, E. M., Kariuki, H. C., Ouma, J. H., Mungai, P. & Kitron, U. (2004). Spatial patterns of urinary schistosomiasis infection in a highly endemic area of coastal Kenya. *American Journal of Tropical Medicine and Hygiene,* **70** (4), 443–448.

Colley, D. G., Barsoum, I. S., Dahawi, H. S. S., Gamil, F., Habib, M. & El Alamy, M. A. (1986). Immune responses and immunoregulation in relation to human schistosomiasis in Egypt. III. Immunity and longitudinal studies of *in vitro* responsiveness after treatment. *Transactions of the Royal Society of Tropical Medicine and Hygiene,* **80** (6), 952–957.

Corrêa-Oliveira, R., Malaquias, L. C. C., Falcão, P. L., Viana, I. R. C., Bahia-Oliveira, L. M. G., Silveira, A. M. S., Fraga, L. A. O., Prata, A., Coffman, R. L., Lambertucci, J. R., Cunha-Melo, J. R., Martins-Filho, O. A., Wilson, R. A. & Gazzinelli, G. (1998). Cytokines as determinants of resistance and pathology in human *Schistosoma mansoni* infection. *Brazilian Journal of Medical and Biological Research,* **31**, 171–177.

Corrêa-Oliveira, R., Rodrigues Caldas, I. & Gazzinelli, G. (2000). Natural versus drug-induced resistance in *Schistosoma mansoni* infection. *Parasitology Today,* **16** (9), 397–399.

Curwen, R. S., Ashton, P. D., Johnston, D. A. & Wilson, R. A. (2004). The *Schistosoma mansoni* soluble proteome: a comparison across four life-cycle stages. *Molecular and Biochemical Parasitology,* **138** (1), 57–66.

Damian, R., Rawlings, C. & Bosshardt, S. (1986). The fecundity of *Schistosoma mansoni* in chronic nonhuman primate infections and after transplantation into naive hosts. *Journal of Parasitology,* **72** (5), 741–747.

Danso-Appiah, A., Utzinger, J., Liu, J. & Olliaro, P. (2008). Drugs for treating urinary schistosomiasis. *Cochrane Database of Systematic Reviews,* **3**, CD000053.

Davies, C., Webster, J., Kruger, O., Munatsi, A., Ndamba, J. & Woolhouse, M. E. J. (1999). Host-parasite population genetics: a cross-sectional comparison of *Bulinus globosus* and *Schistosoma haematobium*. *Parasitology,* **119**, 295–302.

De Clercq, D., Vercruysse, J., Kongs, A., Verl, P., Dompnier, J. P. & Faye, P. C. (2002). Efficacy of artesunate and praziquantel in *Schistosoma haematobium* infected schoolchildren. *Acta Tropica,* **82**, 61–66.

de Jesus, A. M. R., Almeida, R. P., Bacellar, O., Araujo, M. I., Demeure, C., Bina, J. C., Dessein, A. J. & Carvalho, E. M. (1993). Correlation between cell-mediated-immunity and degree of infection in subjects living in an endemic area of schistosomiasis. *European Journal of Immunology,* **23** (1), 152–158.

de Vlas, S. J. (1996). *Modelling human Schistosoma mansoni infection: the art of counting eggs in faeces*. PhD thesis, Erasmus University.

de Vlas, S. J., Gryseels, B., Van Oortmarssen, G. J., Polderman, A. M. & Habbema, J. D. (1992). A model for variations in single and repeated egg counts in *Schistosoma mansoni* infections. *Parasitology,* **104** (3), 451–60.

de Vlas, S. J., Van Oortmarssen, G. J., Gryseels, B., Polderman, A. M., Plaisier, A. P. & Habbema, J. D. (1996). Schistosim: a microsimulation model for the epidemiology and control of schistosomiasis. *American Journal of Tropical Medicine and Hygiene,* **55** (5S), 170–175.

Demeure, C. E., Rihet, P., Abel, L., Ouattara, M., Bourgois, A. & Dessein, A. J. (1993). Resistance to *Schistosoma mansoni* in humans: influence of the IgE/IgG4 balance and IgG2 in immunity to reinfection after chemotherapy. *Journal of Infectious Diseases,* **168** (4), 1000–1008.

Doehring, E., Feldmeier, H. & Daffalla, A. (1983). Day-to-day variation and circadian rhythm of egg excretion in urinary egg excretion in urinary schistosomiasis in the Sudan. *Annals of Tropical Medicine & Parasitology,* **77**, 587–594.

Duerr, H. P., Dietz, K. & Eichner, M. (2003*a*). On the interpretation of age-intensity profiles and dispersion patterns in parasitological surveys. *Parasitology,* **126** (1), 87–101.

Duerr, H. P., Dietz, K., Schulz-Key, H., Buttner, D. W. & Eichner, M. (2003*b*). Density-dependent parasite establishment suggests infection-associated immunosuppression as an important mechanism for parasite density regulation in onchocerciasis. *Transactions of the Royal Society of Tropical Medicine and Hygiene,* **97** (2), 242–250.

Dunne, D. W., Butterworth, A. E., Fulford, A. J., Kariuki, H. C., Langley, J. G., Ouma, J. H., Capron, A., Pierce, R. J. & Sturrock, R. F. (1992*a*). Immunity after treatment of human schistosomiasis: association between IgE antibodies to adult worm antigens and resistance to reinfection. *European Journal of Immunology,* **22** (6), 1483–1494.

Dunne, D. W., Butterworth, A. E., Fulford, A. J., Ouma, J. H. & Sturrock, R. F. (1992*b*). Human IgE responses to *Schistosoma mansoni* and resistance to reinfection. *Memorias do Instituto Oswaldo Cruz,* **87** (S4), 99–103.

Dunne, D. W. & Cooke, A. (2005). A worm's eye view of the immune system: consequences for evolution of human autoimmune disease. *Nature Reviews Immunology,* **5** (5), 420–426.

Earn, D. J. D., Rohani, P., Bolker, B. M. & Grenfell, B. T. (2000). A simple model for complex dynamical transitions in epidemics. *Science,* **287** (5453), 667–670.

Etard, J. F., Audibert, M. & Dabo, A. (1995). Age-acquired resistance and predisposition to reinfection with *Schistosoma haematobium* after treatment with praziquantel in Mali. *American Journal of Tropical Medicine and Hygiene,* **52** (6), 549–558.

Fairley, N. H. (1931). Vesical schistosomiasis complicated by carcinoma. *British Medical Journal,* **1931**, 983–985.

Fallon, P. G. & Doenhoff, M. J. (1994). Drug-resistant schistosomiasis: resistance to praziquantel and oxamniquine induced in *Schistosoma mansoni* in mice is drug specific. *American Journal of Tropical Medicine and Hygiene,* **51**, 83–88.

Fallon, P. G., Teixeira, M. M., Neice, C. M., Williams, T. J., Hellewell, P. G. & Doenhoff, M. J. (1996). Enhancement of *Schistosoma mansoni* infectivity by intradermal injections of larval extracts: a putative role for larval proteases. *Journal of Infectious Diseases,* **173** (6), 1460–1466.

Fenwick, A., Savioli, L., Engels, D., Robert Bergquist, N. & Todd, M. H. (2003). Drugs for the control of parasitic diseases: current status and development in schistosomiasis. *Trends in Parasitology,* **19** (11), 509–515.

Fenwick, A., Webster, J. P., Bosqué-Oliva, E., Blair, L., Fleming, F. M., Zhang, Y., Garba, A., Stothard, J. R., Gabrielli, A. F., Clements, A. C. A., Kabatereine, N. B., Touré, S., Dembelle, R., Nyandindi, U., Mwansa, J. & Koukounari, A. (2009). The Schistosomiasis Control Initiative (SCI): rationale, development and implementation from 2002–2008. *Parasitology,* **136** (13), 1719–1730.

Filipe, J. A. N., Riley, E. M., Drakeley, C. J., Sutherland, C. J. & Ghani, A. C. (2007). Determination of the processes driving the acquisition of immunity to malaria using a mathematical transmission model. *Plos Computational Biology,* **3** (12), 2569–2579.

Fisher, A. C. (1934). A study of the schistosomiasis of the Stanleyville district of the Belgian Congo. *Transactions of the Royal Society of Tropical Medicine and Hygiene,* **28** (3), 277–306.

Fitzsimmons, C. M., Joseph, S., Jones, F. M., Reimert, C. M., Hoffmann, K. F., Kazibwe, F., Kimani, G., Mwatha, J. K., Ouma, J. H., Tukahebwa, E. M., Kariuki, H. C., Vennervald, B. J., Kabatereine, N. B. & Dunne, D. W. (2004). Chemotherapy for schistosomiasis in Ugandan fishermen: treatment can cause a rapid increase in interleukin-5 levels in plasma but decreased levels of eosinophilia and worm-specific immunoglobulin E. *Infection and Immunity,* **72** (7), 4023–4030.

Fitzsimmons, C. M., McBeath, R., Joseph, S., Jones, F. M., Walter, K., Hoffmann, K. F., Kariuki, H. C., Mwatha, J. K., Kimani, G., Kabatereine, N. B., Vennervald, B. J., Ouma, J. H. & Dunne, D. W. (2007). Factors affecting human IgE and IgG responses to allergen-like *Schistosoma mansoni* antigens: molecular structure and patterns of in vivo exposure. *International Archives of Allergy and Immunology,* **142** (1), 40–50.

Fitzsimmons, C. M., Stewart, T. J., Hoffmann, K. F., Grogan, J. L., Yazdanbakhsh, M. & Dunne, D. W. (2004). Human IgE response to the *Schistosoma haematobium* 22.6 kDa antigen. *Parasite Immunology,* **26** (8-9), 371–376.

French, M., Churcher, T., Basáñez, M.-G. & Fenwick, A. (2009). Reductions in environmental transmission observed with a large-scale schistosomiasis control programme in Uganda. *Tropical Medicine and International Health,* **14** (S2), 54–55.

Fulford, A. J. C. (1994). Dispersion and bias: can we trust geometric means? *Parasitology Today,* **10** (11), 446–448.

Fulford, A. J. C., Butterworth, A. E., Ouma, J. H. & Sturrock, R. F. (1995). A statistical approach to schistosome population-dynamics and estimation of the life-span of *Schistosoma mansoni* in man. *Parasitology,* **110**, 307–316.

Fulford, A. J. C., Butterworth, A. E., Sturrock, R. F. & Ouma, J. H. (1992). On the use of age-intensity data to detect immunity to parasitic infections, with special reference to *Schistosoma mansoni* in Kenya. *Parasitology,* **105**, 219–227.

Funk, G. A., Barbour, A. D., Hengartner, H. & Kalinke, U. (1998). Mathematical model of a virus-neutralizing immunoglobulin response. *Journal of Theoretical Biology,* **195** (1), 41–52.

Gabrielli, A.-F., Touré, S., Sellin, B., Sellin, E., Ky, C., Ouedraogo, H., Yaogho, M., Wilson, M. D., Thompson, H., Sanou, S. & Fenwick, A. (2006). A combined school- and community-based campaign targeting all school-age children of Burkina Faso against schistosomiasis and soil-transmitted helminthiasis: performance, financial costs and implications for sustainability. *Acta Tropica,* **99** (2-3), 234 – 242.

Galvani, A. (2003). Immunity, antigenic heterogeneity, and aggregation of helminth parasites. *Journal of Parasitology,* **89** (2), 232–241.

Galvani, A. P. (2005). Age-dependent epidemiological patterns and strain diversity in helminth parasites. *Journal of Parasitology,* **91** (1), 24–30.

Ganley-Leal, L. M., Mwinzi, P., Hightower, A., Karanja, D., Colley, D., Wetzler, L. & Secor, W. E. (2006). Human CD23+ B cells are associated with protection against reinfection by *Schistosoma mansoni*. *American Journal of Tropical Medicine and Hygiene,* **75** (5(S)), 278–278.

Garba, A., Touré, S., Dembelé, R., Bosqué-Oliva, E. & Fenwick, A. (2006). Implementation of national schistosomiasis control programmes in West Africa. *Trends in Parasitology,* **22** (7), 322–326.

Garnett, G. P. (2002). An introduction to mathematical models in sexually transmitted disease epidemiology. *Sexually Transmitted Infections,* **78** (1), 7–12.

Ghattas, H., Darboe, B. M., Wallace, D. L., Griffin, G. E., Prentice, A. M. & Macallan, D. C. (2005). Measuring lymphocyte kinetics in tropical field settings. *Transactions of the Royal Society of Tropical Medicine and Hygiene,* **99** (9), 675–685.

Goddard, M. J. & Jordan, P. (1980). On the longevity of *Schistosoma mansoni* in man on St. Lucia, West Indies. *Transactions of the Royal Society of Tropical Medicine and Hygiene,* **74** (2), 185–191.

Gomes, Y. M., Pereira, V. R. A., Nakazawa, M., Montarroyos, U., Souza, W. V. & Abath, F. G. C. (2002). Antibody isotype responses to egg antigens in human chronic schistosomiasis mansoni before and after treatment. *Memorias Do Instituto Oswaldo Cruz,* **97**, 111–112.

Gounni, A. S., Lamkhioued, B., Ochiai, K., Tanaka, Y., Delaporte, E., Capron, A., Kinet, J. P. & Capron, M. (1994). High-affinity IgE receptor on eosinophils is involved in defence against parasites. *Nature,* **367** (6459), 183–6.

Grassly, N., Fraser, C. & Garnett, G. (2005). Host immunity and synchronized epidemics of syphilis across the United States. *Nature,* **433**, 417–421.

Gray, D. (2002). A role for antigen in the maintenance of immunological memory. *Nature Reviews Immunology,* **2**, 60–65.

Gregory, R. D. & Woolhouse, M. E. J. (1993). Quantification of parasite aggregation: a simulation study. *Acta Tropica,* **54** (2), 131–139.

Grimm, V., Revilla, E., Berger, U., Jeltsch, F., Mooij, W. M., Railsback, S. F., Thulke, H. H., Weiner, J., Wiegand, T. & DeAngelis, D. L. (2005). Pattern-oriented modeling of agent-based complex systems: lessons from ecology. *Science,* **310** (5750), 987–991.

Grogan, J. L., Kremsner, P. G., Deelder, A. M. & Yazdanbakhsh, M. (1996). Elevated proliferation and interleukin-4 release from $CD4^+$ cells after chemotherapy in human *Schistosoma haematobium* infection. *European Journal of Immunology,* **26** (6), 1365–1370.

Grogan, J. L., Kremsner, P. G., Deelder, A. M. & Yazdanbakhsh, M. (1998*a*). Antigen-specific proliferation and interferon-γ and interleukin-5 production are down-regulated during *Schistosoma haematobium* infection. *Journal of Infectious Diseases,* **177** (5), 1433–1437.

Grogan, J. L., Kremsner, P. G., Deelder, A. M. & Yazdanbakhsh, M. (1998*b*). The effect of anti-IL-10 on proliferation and cytokine production in human schistosomiasis: fresh versus cryopreserved cells. *Parasite Immunology,* **20** (7), 345–349.

Grogan, J. L., Kremsner, P. G., van Dam, G. J., Metzger, W., Mordmuller, B., Deelder, A. M. & Yazdanbakhsh, M. (1996). Antischistosome IgG4 and IgE responses are affected differentially by chemotherapy in children versus adults. *Journal of Infectious Diseases,* **173** (5), 1242–1247.

Gryseels, B. (1994). Human resistance to schistosoma infections: age or experience? *Parasitology Today,* **10** (10), 380–384.

Gryseels, B. & Nkulikyinka, L. (1988). The distribution of *Schistosoma mansoni* in the Rusizi plain (Burundi). *Annals of Tropical Medicine & Parasitology,* **82** (6), 581–90.

Gryseels, B., Polman, K., Clerinx, J. & Kestens, L. (2006). Human schistosomiasis. *The Lancet,* **368** (9541), 1106–1118.

Grzych, J. M., Grezel, D., Chuan Bo, X., Neyrinck, J. L., Capron, M., Ouma, J. H., Butterworth, A. E. & Capron, A. (1993). IgA antibodies to a protective antigen in human schistosomiasis mansoni. *Journal of Immunology,* **150** (2), 527–535.

Gurarie, D. & King, C. H. (2005). Heterogeneous model of schistosomiasis transmission and long-term control: the combined influence of spatial variation and age-dependent factors on optimal allocation of drug therapy. *Parasitology,* **130**, 49–65.

Guyatt, H., Smith, T., Gryseels, B., Lengeler, C., Mshinda, H., Siziya, S., Salanave, B., Mohome, N., Makwala, J., Ngimbi, K. & Tanner, M. (1994). Aggregation in schistosomias - comparsion of the relationships between prevalence and intensity in different endemic areas. *Parasitology,* **109**, 45–55.

Habbema, J. D. F., DeVlas, S. J., Plaisier, A. P. & VanOortmarssen, G. J. (1996). The microsimulation approach to epidemiologic modeling of helminthic infections, with special reference to schistosomiasis. *American Journal of Tropical Medicine and Hygiene,* **55** (5S), 165–169.

Hagan, P. (1992). Reinfection, exposure and immunity in human schistosomiasis. *Parasitology Today,* **8** (1), 12–16.

Hagan, P., Blumenthal, U. J., Dunn, D., Simpson, A. J. & Wilkins, H. A. (1991). Human IgE, IgG4 and resistance to reinfection with *Schistosoma haematobium*. *Nature,* **349** (6306), 243–245.

Hagan, P., Wilkins, H. A., Blumenthal, U. J., Hayes, R. J. & Greenwood, B. M. (1985). Eosinophilia and resistance to *Schistosoma haematobium* in man. *Parasite Immunology,* **7** (6), 625–32.

Hairston, N. G. (1965). On the mathematical analysis of schistosome populations. *Bulletin of the World Health Organization,* **33**, 45–62.

Halloran, M. (2001). Concepts of transmission and dynamics. In *Epidemiologic methods for the study of infectious diseases*, (Thomas, J. C. & Weber, D., eds), pp. 56–85. Oxford University Press New York.

Harn, D. A., Cianci, C. M. L. & Caulfield, J. P. (1989). *Schistosoma mansoni*: immunization with cercarial glycocalyx preparation increases the adult worm burden. *Experimental Parasitology,* **68** (1), 108–110.

Harnett, W. (1988). The anthelmintic action of praziquantel. *Parasitology Today,* **4** (5), 144–146.

Harnett, W. & Kusel, J. R. (1986). Increased exposure of parasite antigens at the surface of adult male *Schistosoma mansoni* exposed to praziquantel in vitro. *Parasitology,* **93** (2), 401–405.

Harris, A. R. C., Russell, R. J. & Charters, A. D. (1984). A review of schistosomiasis in immigrants in Western Australia, demonstrating the unusual longevity of *Schistosoma mansoni*. *Transactions of the Royal Society of Tropical Medicine and Hygiene,* **78** (3), 385–388.

He, Y.-X., Chen, L. & Ramaswamy, K. (2002). *Schistosoma mansoni, S. haematobium*, and *S. japonicum*: early events associated with penetration and migration of schistosomula through human skin. *Experimental Parasitology,* **102** (2), 99–108.

Hellriegel, B. (2001). Immunoepidemiology - bridging the gap between immunology and epidemiology. *Trends in Parasitology,* **17** (2), 102–106.

Hsu, S. Y. L., Hsu, H. F. & Burmeister, L. F. (1981). *Schistosoma mansoni* - vaccination of mice with highly X-irradiated cercariae. *Experimental Parasitology,* **52** (1), 91–104.

Janeway, C. A., Travers, P., Walport, M. & Schlomchik, M. (2001). *Immunobiology: the immune system in health and disease.* Churchill Livingstone, New York.

Janssen, M. A., Radtke, N. P. & Lee, A. (2009). Pattern-oriented modeling of commons dilemma experiments. *Adaptive Behavior,* **17** (6), 508–523.

Jeannin, P., Lecoanet, S., Delneste, Y., Gauchat, J.-F. & Bonnefoy, J.-Y. (1998). IgE versus IgG4 production can be differentially regulated by IL-10. *Journal of Immunology,* **160** (7), 3555–3561.

Jenkins, S. J., Hewitson, J. P., Jenkins, G. R. & Mountford, A. P. (2005). Modulation of the host's immune response by schistosome larvae. *Parasite Immunology,* **27** (10-11), 385–393.

Jolly, E. R., Chin, C. S., Miller, S., Bahgat, M. M., Lim, K. C., DeRisi, J. & McKerrow, J. H. (2007). Gene expression patterns during adaptation of a helminth parasite to different environmental niches. *Genome Biology,* **8** (4), R65.

Jordan, P., Webbe, G. & Sturrock, R. (1993). *Human Schistosomiasis.* CAB International, Wallingford.

Joseph, S., Jones, F. M., Kimani, G., Mwatha, J. K., Kamau, T., Kazibwe, F., Kemijumbi, J., Kabatereine, N. B., Booth, M., Kariuki, H. C., Ouma, J. H., Vennervald, B. J. & Dunne, D. W. (2004*a*). Cytokine production in whole blood cultures from a fishing community in an area of high endemicity for *Schistosoma mansoni* in Uganda: the differential effect of parasite worm and egg antigens. *Infection and Immunity,* **72** (2), 728–734.

Joseph, S., Jones, F. M., Walter, K., Fulford, A. J., Kimani, G., Mwatha, J. K., Kamau, T., Kariuki, H. C., Kazibwe, F., Tukahebwa, E., Kabatereine, N. B., Ouma, J. H., Vennervald, B. J. & Dunne, D. W. (2004*b*). Increases in human T helper 2 cytokine responses to *Schistosoma mansoni* worm and worm-tegument antigens are induced by treatment with praziquantel. *Journal of Infectious Diseases,* **190** (4), 835–842.

Kabatereine, N. B., Brooker, S., Koukounari, A., Kazibwe, F., Tukahebwa, E., Fleming, F., Zhang, Y., Webster, J., Stothard, J. R. & Fenwick, A. (2007). Impact of a national helminth control programme on infection and morbidity in Ugandan schoolchildren. *Bulletin of the World Health Organization,* **85** (2), 85–160.

Kabatereine, N. B., Fleming, F. M., Nyandindi, U., Mwanza, J. C. & Blair, L. (2006*a*). The control of schistosomiasis and soil-transmitted helminths in East Africa. *Trends in Parasitology,* **22** (7), 332 – 339.

Kabatereine, N. B., Tukahebwa, E., Kazibwe, F., Namwangye, H., Zaramba, S., Brooker, S., Stothard, J. R., Kamenka, C., Whawell, S., Webster, J. P. & Fenwick, A. (2006*b*). Progress towards countrywide control of schistosomiasis and soil-transmitted helminthiasis in Uganda. *Transactions of the Royal Society of Tropical Medicine and Hygiene,* **100** (3), 208 – 215.

Kabatereine, N. B., Vennervald, B. J., Ouma, J. H., Kemijumbi, J., Butterworth, A. E., Dunne, D. W. & Fulford, A. J. C. (1999). Adult resistance to schistosomiasis mansoni: age-dependence of reinfection remains constant in communities with diverse exposure patterns. *Parasitology,* **118** (1), 101–105.

Kalia, V., Sarkar, S., Gourley, T. S., Rouse, B. T. & Ahmed, R. (2006). Differentiation of memory B and T cells. *Current Opinion in Immunology,* **18** (3), 255–264.

Karanja, D. M. S., Hightower, A. W., Colley, D. G., Mwinzi, P. N. M., Galil, K., Andove, J. & Secor, W. E. (2002). Resistance to reinfection with *Schistosoma mansoni* in occupationally exposed adults and effect of HIV-1 co-infection on susceptibility to schistosomiasis: a longitudinal study. *Lancet,* **360** (9333), 592–596.

Khalife, J., Capron, M., Capron, A., Grzych, J. M., Butterworth, A. E., Dunne, D. W. & Ouma, J. H. (1986). Immunity in human schistosomiasis mansoni. Regulation of protective immune mechanisms by IgM blocking antibodies. *Journal of Experimental Medicine,* **164** (5), 1626–1640.

Khalife, J., Dunne, D. W., Richardson, B. A., Mazza, G., Thorne, K. J. I., Capron, A. & Butterworth, A. E. (1989). Functional role of human IgG subclasses in eosinophil-mediated killing of schistosomula of *Schistosoma mansoni. Journal of Immunology,* **142** (12), 4422–4427.

King, C. (2001*a*). Epidemiology of schistosomiasis: determinants of infection. In *Schistosomiasis*, (Mahmoud, A., ed.), pp. 115–132. Imperial College Press London.

King, C. H. (2001*b*). Disease in schistosomiasis haematobia. In *Schistosomiasis*, (Mahmoud, A., ed.), pp. 265–295. Imperial College Press London.

King, C. H. (2001*c*). Initiation and regulation of disease in schistosomiasis. In *Schistosomiasis*, (Mahmoud, A. A. F., ed.), pp. 213–264. Imperial College Press London.

King, C. H. (2007). Lifting the burden of schistosomiasis–defining elements of infection-associated disease and the benefits of antiparasite treatment. *Journal of Infectious Diseases,* **196** (5), 653–655.

King, C. H., Dickman, K. & Tisch, D. J. (2005). Reassessment of the cost of chronic helminthic infection: a meta-analysis of disability-related outcomes in endemic schistosomiasis. *The Lancet,* **365** (9470), 1561–1569.

King, C. H., Muchiri, E. & Ouma, J. H. (1992). Age-targeted chemotherapy for control of urinary schistosomiasis in endemic populations. *Memorias Do Instituto Oswaldo Cruz,* **87** (S4), 203–210.

King, C. H., Muchiri, E., Ouma, J. H. & Koech, D. (1991). Chemotherapy-based control of schistosomiasis haematobia IV. Impact of repeated annual chemotherapy on prevalence and intensity of *Schistosoma haematobium* infection in an endemic area of Kenya. *American Journal of Tropical Medicine and Hygiene,* **45** (4), 498–508.

King, C. H., Muchiri, E. M. & Ouma, J. H. (2000). Evidence against rapid emergence of praziquantel resistance in *Schistosoma haematobium*, Kenya. *Emerging Infectious Diseases,* **6** (6), 585–594.

King, C. L., Medhat, A., Malhotra, I., Nafeh, M., Helmy, A., Khaudary, J., Ibrahim, S., El-Sherbiny, M., Zaky, S., Stupi, R. J., Brustoski, K., Shehata, M. & Shata, M. T. (1996). Cytokine control of parasite-specific anergy in human urinary schistosomiasis. IL-10 modulates lymphocyte reactivity. *Journal of Immunology,* **156** (12), 4715–4721.

Koukounari, A., Gabrielli, A. F., Touré, S., Bosqué-Oliva, E., Zhang, Y. B., Sellin, B., Donnelly, C. A., Fenwick, A. & Webster, J. P. (2007). *Schistosoma haematobium* infection and morbidity before and after large-scale administration of praziquantel in Burkina Faso. *Journal of Infectious Diseases,* **196** (5), 659–669.

Kumar, P. & Ramaswamy, K. (1999). Vaccination with irradiated cercariae of *Schistosoma mansoni* preferentially induced the accumulation of interferon-γ producing T cells in the skin and skin draining lymph nodes of mice. *Parasitology International,* **48** (2), 109–119.

Lanzavecchia, A., Bernasconi, N., Traggiai, E., Ruprecht, C. R., Corti, D. & Sallusto, F. (2006). Understanding and making use of human memory B cells. *Immunological Reviews,* **211**, 303–309.

Macallan, D. C., Wallace, D. L., Zhang, Y., Ghattas, H., Asquith, B., de Lara, C., Worth, A., Panayiotakopoulos, G., Griffin, G. E., Tough, D. F. & Beverley, P. C. L. (2005). B-cell kinetics in humans: rapid turnover of peripheral blood memory cells. *Blood,* **105** (9), 3633–3640.

MacDonald, G. (1965). The dynamics of helminth infections, with special reference to schistosomes. *Transactions of the Royal Society of Tropical Medicine and Hygiene,* **59** (5), 489–506.

Magnussen, P. (2003). Treatment and re-treatment strategies for schistosomiasis control in different epidemiological settings: a review of 10 years' experiences. *Acta Tropica,* **86** (2-3), 243–254.

Mahmoud, A. (2001). Schistosomiasis: setting the stage. In *Schistosomiasis*, (Mahmoud, A., ed.), pp. 1–5. Imperial College Press London.

Maire, N., Smith, T., Ross, A., Owusu-Agyei, S., Dietz, K. & Molineaux, L. (2006). A model for natural immunity to asexual blood stages of *Plasmodium falciparum* malaria in endemic areas. *The American Journal of Tropical Medicine and Hygiene,* **75** (S2), 19–31.

Maizels, R. M., Bundy, D. A., Selkirk, M. E., Smith, D. F. & Anderson, R. M. (1993). Immunological modulation and evasion by helminth parasites in human populations. *Nature,* **365** (6449), 797–805.

Maizels, R. M. & Yazdanbakhsh, M. (2003). Immune regulation by helminth parasites: cellular and molecular mechanisms. *Nature Reviews Immunology,* **3** (9), 733–744.

Mascie-Taylor, C. G. N. & Karim, E. (2003). The burden of chronic disease. *Science,* **302** (5652), 1921–1922.

McMahon, J. E. & Kolstrup, N. (1979). Praziquantel: a new schistosomicide against *Schistosoma haematobium*. *British Medical Journal,* **2**, 1396–1399.

McManus, D. P. & Loukas, A. (2008). Current status of vaccines for schistosomiasis. *Clinical Microbiology Reviews,* **21** (1), 225–242.

Mduluza, T., Ndhlovu, P. D., Midzi, N., Scott, J. T., Mutapi, F., Mary, C., Couissinier-Paris, P., Turner, C. M. R., Chandiwana, S. K., Woolhouse, M. E. J., Dessein, A. J. & Hagan, P. (2003). Contrasting cellular responses in *Schistosoma haematobium* infected and exposed individuals from areas of high and low transmission in Zimbabwe. *Immunology Letters,* **88** (3), 249–256.

Medhat, A., Shehata, M., Bucci, K., Mohamed, S., Dief, A. D. E., Badary, S., Galal, H., Nafeh, M. & King, C. L. (1998). Increased interleukin-4 and interleukin-5 production in response to *Schistosoma haematobium* adult worm antigens correlates with lack of reinfection after treatment. *Journal of Infectious Diseases,* **178** (2), 512–519.

Mestas, J. & Hughes, C. C. W. (2004). Of mice and not men: differences between mouse and human immunology. *The Journal of Immunology,* **172** (5), 2731–2738.

Midzi, N., Sangweme, D., Zinyowera, S., Mapingure, M. P., Brouwer, K. C., Kumar, N., Mutapi, F., Woelk, G. & Mduluza, T. (2008). Efficacy and side effects of praziquantel treatment against *Schistosoma haematobium* infection among primary school children in Zimbabwe. *Transactions of the Royal Society of Tropical Medicine and Hygiene,* **102** (8), 759–766.

Milner, T., Reilly, L., Nausch, N., Midzi, N., Mduluza, T., Maizels, R. M. & Mutapi, F. (2010). Circulating cytokine levels and antibody responses to human *Schistosoma haematobium*: IL-5 and IL-10 levels depend upon age and infection status. *Parasite Immunology,* **Accepted Article**.

Mitchell, K. M., Mutapi, F. & Woolhouse, M. E. J. (2008). The predicted impact of immunosuppression upon population age-intensity profiles for schistosomiasis. *Parasite Immunology,* **30** (9), 462–470.

Mkoji, G. M., Smith, J. M. & Prichard, R. K. (1988). Antioxidant systems in *Schistosoma mansoni*: correlation between susceptibility to oxidant killing and the levels of scavengers of hydrogen peroxide and oxygen free radicals. *International Journal for Parasitology,* **18** (5), 661–666.

Molineaux, L., Diebner, H., Eichner, M., Collins, W., Jeffery, G. & Dietz, K. (2001). *Plasmodium falciparum* parasitaemia described by a new mathematical model. *Parasitology,* **122** (4), 379–391.

Morell, A., Terry, W. D. & Waldmann, T. A. (1970). Metabolic properties of IgG subclasses in man. *Journal of Clinical Investigation,* **49** (4), 673–680.

Moser, G., Wassom, D. L. & Sher, A. (1980). Studies of the antibody-dependent killing of schistosomula of *Schistosoma mansoni* employing haptenic target antigens. I. Evidence that the loss in susceptibility to immune damage undergone by developing schistosomula involves a change unrelated to the masking of parasite antigens by host molecules. *The Journal of Experimental Medicine,* **152** (1), 41–53.

Mott, K. E. (1983). A reusable polyamide filter for diagnosis of *S. hematobium* infection by urine filtration. *Bulletin De La Societe De Pathologie Exotique,* **76** (1), 101–104.

Mutapi, F. (1997). *Immuno-epidemiology of human schistosomiasis.* PhD thesis, University of Oxford.

Mutapi, F. (2001). Heterogeneities in anti-schistosome humoral responses following chemotherapy. *Trends in Parasitology,* **17** (11), 518–524.

Mutapi, F., Burchmore, R., Mduluza, T., Foucher, A., Harcus, Y., Nicoll, G., Midzi, N., Turner, C. M. & Maizels, R. M. (2005). Praziquantel treatment of individuals exposed to *Schistosoma haematobium* enhances serological recognition of defined parasite antigens. *Journal of Infectious Diseases,* **192** (6), 1108–1118.

Mutapi, F., Burchmore, R., Mduluza, T., Midzi, N., Turner, C. M. R. & Maizels, R. M. (2008). Age-related and infection intensity-related shifts in antibody recognition of defined protein antigens in a schistosome-exposed population. *Journal of Infectious Diseases,* **198** (2), 167–175.

Mutapi, F., Gryseels, B. & Roddam, A. (2003*a*). On the calculation of intestinal schistosome infection intensity. *Acta Tropica,* **87** (2), 225–233.

Mutapi, F., Hagan, P., Woolhouse, M. E. J., Mduluza, T. & Ndhlovu, P. D. (2003*b*). Chemotherapy-induced, age-related changes in antischistosome antibody responses. *Parasite Immunology,* **25** (2), 87–97.

Mutapi, F., Mduluza, T. & Roddam, A. W. (2005). Cluster analysis of schistosome-specific antibody responses partitions the population into distinct epidemiological groups. *Immunology Letters,* **96** (2), 231–240.

Mutapi, F., Ndhlovu, P. D., Hagan, P., Spicer, J. T., Mduluza, T., Turner, C. M. R., Chandiwana, S. K. & Woolhouse, M. E. J. (1998). Chemotherapy accelerates the development of acquired immune responses to *Schistosoma haematobium* infection. *Journal of Infectious Diseases,* **178** (1), 289–293.

Mutapi, F., Ndhlovu, P. D., Hagan, P. & Woolhouse, M. E. J. (1997). A comparison of humoral responses to *Schistosoma haematobium* in areas with low and high levels of infection. *Parasite Immunology,* **19** (6), 255–263.

Mutapi, F., Ndhlovu, P. D., Hagan, P. & Woolhouse, M. E. J. (1998). Changes in specific anti-egg antibody levels following treatment with praziquantel for *Schistosoma haematobium* infection in children. *Parasite Immunology,* **20** (12), 595–600.

Mutapi, F. & Roddam, A. (2002). p values for pathogens: statistical inference from infectious-disease data. *Lancet Infectious Diseases,* **2** (4), 219–230.

Mutapi, F., Winborn, G., Midzi, N., Taylor, M., Mduluza, T. & Maizels, R. M. (2007). Cytokine responses to *Schistosoma haematobium* in a Zimbabwean population: contrasting profiles for IFN-γ, IL-4, IL-5 and IL-10 with age. *BMC Infectious Diseases,* **7**, 139.

Mwinzi, P. N., Ganley-Leal, L., Black, C., Secor, W., Karanja, D. & Colley, D. G. (2009). Circulating CD23+ B cell subset correlates with the development of resistance to *Schistosoma mansoni* reinfection in occupationally exposed adults who have undergone multiple treatments. *Journal of Infectious Diseases,* **199** (2), 272–279.

Naus, C. W. A., Kimani, G., Ouma, J. H., Fulford, A. J. C., Webster, M., van Dam, G. J., Deelder, A. M., Butterworth, A. E. & Dunne, D. W. (1999). Development of antibody isotype responses to *Schistosoma mansoni* in an immunologically naive immigrant population: influence of infection duration, infection intensity, and host age. *Infection and Immunity,* **67** (7), 3444–3451.

Ndamba, J., Makaza, N., Kaondera, K. C., Munjoma, M., Ndamba, J., Makaza, N., Kaondera, K. C. & Munjoma, M. (1991). Morbidity due to *Schistosoma mansoni* among sugar-cane cutters in Zimbabwe. *International Journal of Epidemiology,* **20** (3), 787–95.

Ndhlovu, P., Cadman, H., Gundersen, S., Vennervald, B. J., Friis, H., Christensen, N. O., Mutasa, G., Kaondera, K., Mandaza, G. & Deelder, A. M. (1996*a*). Circulating anodic antigen (CAA) levels in different age groups in a Zimbabwean rural community endemic for *Schistosoma haematobium* determined using the magnetic beads antigen-capture enzyme-linked immunoassay. *American Journal of Tropical Medicine and Hygiene,* **54** (5), 537–42.

Ndhlovu, P., Cadman, H., Vennervald, B. J., Christensen, N. O., Chidimu, M. & Chandiwana, S. K. (1996*b*). Age-related antibody profiles in *Schistosoma haematobium* infections in a rural community in Zimbabwe. *Parasite Immunology,* **18** (4), 181–191.

NIH (2009). Efficacy of vaccine Sh28GST in association with praziquantel (PZQ) for prevention of clinical recurrences of *Schistosoma haematobium* pathology (Bilhvax). Available: http://clinicaltrials.gov/show/NCT00870649. **Accessed 1st July 2010**.

Nyazema, N. Z., Mutamiri, F. F., Mudiwa, I., Chimuka, A. & Ndamba, J. (1995). Immunopharmacological aspects of praziquantel. *Central African Journal of Medicine,* **41** (9), 284–8.

Nyindo, M. & Farah, I. O. (1999). The baboon as a non-human primate model of human schistosome infection. *Parasitology Today,* **15** (12), 478–482.

Ochsenbein, A. F., Pinschewer, D. D., Sierro, S., Horvath, E., Hengartner, H. & Zinkernagel, R. M. (2000). Protective long-term antibody memory by antigen-driven and T help-dependent differentiation of long-lived memory B cells to short-lived plasma cells independent of secondary lymphoid organs. *Proceedings of the National Academy of Sciences of the United States of America,* **97** (24), 13263–13268.

Ouma, J. H., Fulford, A. J. C., Kariuki, H. C., Kimani, G., Sturrock, R. F., Muchemi, G., Butterworth, A. E. & Dunne, D. W. (1998). The development of schistosomiasis mansoni in an immunologically naive immigrant population in Masongaleni, Kenya. *Parasitology,* **117** (2), 123–132.

Paget-McNicol, S., Gatton, M., Hastings, I. & Saul, A. (2002). The *Plasmodium falciparum* var gene switching rate, switching mechanism and patterns of parasite recrudescence described by mathematical modelling. *Parasitology,* **124** (3), 225–235.

Pearce, E. J. (2005). Priming of the immune response by schistosome eggs. *Parasite Immunology,* **27** (7-8), 265–270.

Perelson, A. S. (2002). Modelling viral and immune system dynamics. *Nature Reviews Immunology,* **2** (1), 28–36.

Picquet, M., Vercruysse, J., Shaw, D. J., Diop, M. & Ly, A. (1998). Efficacy of praziquantel against *Schistosoma mansoni* in northern Senegal. *Transactions of the Royal Society of Tropical Medicine and Hygiene,* **92** (1), 90–93.

Polman, K., Engels, D., Fathers, L., Deelder, A. M. & Gryseels, B. (1998). Day-to-day fluctuation of schistosome circulating antigen levels in serum and urine of humans infected with *Schistosoma mansoni* in Burundi. *American Journal of Tropical Medicine and Hygiene,* **59** (1), 150–154.

Press, W., Teukolsky, S., Vetterling, W. & Flannery, B. (2002). *Numerical Recipes in C++: the art of scientific computing.* Cambridge University Press.

Quinnell, R. J. (2003). Genetics of susceptibility to human helminth infection. *International Journal for Parasitology,* **33** (11), 1219–1231.

Quinnell, R. J., Grafen, A. & Woolhouse, M. E. J. (1995). Changes in parasite aggregation with age: a discrete infection model. *Parasitology,* **111** (5), 635–644.

Radbruch, A., Muehlinghaus, G., Luger, E. O., Inamine, A., Smith, K. G. C., Dorner, T. & Hiepe, F. (2006). Competence and competition: the challenge of becoming a long-lived plasma cell. *Nature Reviews Immunology,* **6** (10), 741–750.

Ramaswamy, K., Kumar, P. & He, Y.-X. (2000). A role for parasite-induced PGE2 in IL-10-mediated host immunoregulation by skin stage schistosomula of *Schistosoma mansoni*. *Journal of Immunology,* **165** (8), 4567–4574.

Redman, C. A., Robertson, A., Fallon, P. G., Modha, J., Kusel, J. R., Doenhoff, M. J. & Martin, R. J. (1996). Praziquantel: an urgent and exciting challenge. *Parasitology Today,* **12** (1), 14–20.

Reimert, C. A., Fitzsimmons, C. M., Joseph, S., Mwatha, J. K., Jones, F. M., Kimani, G., Hoffmann, K. F., Booth, M., Kabatereine, N. B., Dunne, D. W. & Vennervald, B. J. (2006). Eosinophil activity in *Schistosoma mansoni* infections *in vivo* and *in vitro* in relation to plasma cytokine profile pre- and posttreatment with praziquantel. *Clinical and Vaccine Immunology,* **13** (5), 584–593.

Remoué, F., To Van, D., Schacht, A. M., Picquet, M., Garraud, O., Vercruysse, J., Ly, A., Capron, A. & Riveau, G. (2001). Gender-dependent specific immune response during chronic human schistosomiasis haematobia. *Clinical and Experimental Immunology,* **124** (1), 62–8.

Ribeiro, R. M. (2007). Dynamics of CD4+ T cells in HIV-1 infection. *Immunology and Cell Biology,* **85**, 287–294.

Rihet, P., Demeure, C. E., Bourgois, A., Prata, A. & Dessein, A. J. (1991). Evidence for an association between human resistance to *Schistosoma mansoni* and high anti-larval IgE levels. *European Journal of Immunology,* **21** (11), 2679–86.

Rihet, P., Demeure, C. E., Dessein, A. J. & Bourgois, A. (1992). Strong serum inhibition of specific IgE correlated to competing IgG4, revealed by a new methodology in subjects from a *S. mansoni* endemic area. *European Journal of Immunology,* **22** (8), 2063–70.

Roberts, M., Butterworth, A. E., Kimani, G., Kamau, T., Fulford, A. J., Dunne, D. W., Ouma, J. H. & Sturrock, R. F. (1993). Immunity after treatment of human schistosomiasis: association between cellular responses and resistance to reinfection. *Infection and Immunity,* **61** (12), 4984–4993.

Roberts, M. G. & Grenfell, B. T. (1991). The population-dynamics of nematode infections of ruminants - periodic perturbations as a model for management. *IMA Journal of Mathematics Applied in Medicine and Biology,* **8** (2), 83–93.

Rossmanith, E., Blaum, N., Grimm, V. & Jeltsch, F. (2007). Pattern-oriented modelling for estimating unknown pre-breeding survival rates: the case of the Lesser Spotted Woodpecker *(Picoides minor)*. *Biological Conservation,* **135** (4), 555–564.

Rudge, J. W., Stothard, J. R., Basáñez, M.-G., Mgeni, A. F., Khamis, I. S., Khamis, A. N. & Rollinson, D. (2008). Micro-epidemiology of urinary schistosomiasis in Zanzibar: local risk factors associated with distribution of infections among schoolchildren and relevance for control. *Acta Tropica,* **105** (1), 45–54.

Saad, A. M., Hussein, M. F., Dargie, J. D., Taylor, M. G. & Nelson, G. S. (1980). *Schistosoma bovis* in calves: the development and clinical pathology of primary infections. *Research in Veterinary Science,* **28** (1), 105–111.

Saathoff, E., Olsen, A., Magnussen, P., Kvalsvig, J., Becker, W. & Appleton, C. (2004). Patterns of *Schistosoma haematobium* infection, impact of praziquantel treatment and re-infection after treatment in a cohort of schoolchildren from rural KwaZulu-Natal/South Africa. *BMC Infectious Diseases,* **4** (1), 40.

Satti, M. Z., Lind, P., Vennervald, B. J., Sulaiman, S. M., Daffalla, A. A. & Ghalib, H. W. (1996). Specific immunoglobulin measurements related to exposure and resistance to *Schistosoma mansoni* infection in Sudanese canal cleaners. *Clinical and Experimental Immunology,* **106** (1), 45–54.

Savioli, L., Hatz, C., Dixon, H., Kisumku, U. & Mott, K. (1990). Control of morbidity due to *Schistosoma haematobium* on Pemba Island: egg excretion and hematuria as indicators of infection. *American Journal of Tropical Medicine and Hygiene,* **43**, 289–295.

Schweitzer, A. N. & Anderson, R. M. (1992*a*). Dynamic interaction between CD4+ T cells and parasitic helminths: mathematical models of heterogeneity in outcome. *Parasitology,* **105** (3), 513–22.

Schweitzer, A. N. & Anderson, R. M. (1992*b*). The regulation of immunological responses to parasitic infections and the development of tolerance. *Proceedings of the Royal Society B: Biological Sciences,* **247** (1319), 107–112.

Schweitzer, N. & Anderson, R. (1991). Helminths, immunology and equations. *Immunology Today,* **12** (3), A76–81.

Scott, J. T., Diakhate, M., Vereecken, K., Fall, A., Diop, M., Ly, A., De Clercq, D., de Vlas, S. J., Berkvens, D., Kestens, L. & Gryseels, B. (2003). Human water contacts patterns in *Schistosoma mansoni* epidemic foci in northern Senegal change according to age, sex and place of residence, but are not related to intensity of infection. *Tropical Medicine & International Health,* **8** (2), 100–108.

Scott, J. T., Turner, C. M. R., Mutapi, F., Woolhouse, M. E. J., Ndhlovu, P. D. & Hagan, P. (2001). Cytokine responses to mitogen and *Schistosoma haematobium* antigens are different in children with distinct infection histories. *Parasite Immunology,* **23** (10), 519–526.

Sher, A. & Moser, G. (1981). Schistosomiasis - immunological properties of developing schistosomula. *American Journal of Pathology,* **102** (1), 121–126.

Sissoko, M. S., Dabo, A., Traoré, H., Diallo, M., Traoré, B., Konaté, D., Niaré, B., Diakité, M., Kamaté, B., Traoré, A., Bathily, A., Tapily, A., Touré, O. B., Cauwenbergh, S., Jansen, H. F. & Doumbo, O. K. (2009). Efficacy of artesunate + sulfamethoxypyrazine/pyrimethamine versus praziquantel in the treatment of *Schistosoma haematobium* in children. *PLoS ONE,* **4** (10), e6732.

Skelly, P. J. & Wilson, R. A. (2006). Making sense of the schistosome surface. *Advances in Parasitology,* **63**, 185–284.

Smithers, S. & Terry, R. (1967). Resistance to experimental infection with *Schistosoma mansoni* in rhesus monkeys induced by the transfer of adult worms. *Transactions of the Royal Society of Tropical Medicine and Hygiene,* **61**, 517–533.

Smithers, S. R., Terry, R. J. & Hockley, D. J. (1969). Host antigens in schistosomiasis. *Proceedings of the Royal Society of London. Series B, Biological Sciences,* **171** (1025), 483–494.

Stelma, F. F., Sall, S., Daff, B., Sow, S., Niang, M. & Gryseels, B. (1997). Oxamniquine cures *Schistosoma mansoni* infection in a focus in which cure rates with praziquantel are unusually low. *Journal of Infectious Diseases,* **176**, 304–307.

Sturrock, R. F., Kimani, R., Cottrell, B. J., Butterworth, A. E., Seitz, H. M., Siongok, T. K. & Houba, V. (1983). Observations on possible immunity to reinfection among Kenyan schoolchildren after treatment for *Schistosoma mansoni*. *Transactions of the Royal Society of Tropical Medicine and Hygiene,* **77** (3), 363–371.

Swanack, T. M., Grant, W. E. & Forstner, M. R. J. (2009). Projecting population trends of endangered amphibian species in the face of uncertainty: a pattern-oriented approach. *Ecological Modelling,* **220** (2), 148–159.

Talla, I., Kongs, A. & Verle, P. (1992). Preliminary study of the prevalence of human schistosomiasis in Richard-Toll (the Senegal river basin). *Transactions of the Royal Society of Tropical Medicine and Hygiene,* **86** (2), 182.

Tchuem Tchuente, L. A., Shaw, D. J., Polla, L., Cioli, D. & Vercruysse, J. (2004). Efficacy of praziquantel against *Schistosoma haematobium* infection in children. *American Journal of Tropical Medicine and Hygiene,* **71** (6), 778–82.

Tchuem Tchuente, L. A., Southgate, V. R., Mbaye, A., Engels, D. & Gryseels, B. (2001). The efficacy of praziquantel against *Schistosoma mansoni* infection in Ndombo, northern Senegal. *Transactions of the Royal Society of Tropical Medicine and Hygiene,* **95** (1), 65–66.

Tingley, G. A., Butterworth, A. E., Anderson, R. M., Kariuki, H. C., Koech, D., Mugambi, M., Ouma, J. H., Siongok, T. K. A. & Sturrock, R. F. (1988). Predisposition of humans to infection with *Schistosoma mansoni*: evidence from the reinfection of individuals following chemotherapy. *Transactions of the Royal Society of Tropical Medicine and Hygiene,* **82** (3), 448 – 452.

Tohon, Z. B., Mainassara, H. B., Garba, A., Mahamane, A. E., Bosqué-Oliva, E., Ibrahim, M.-L., Duchemin, J.-B., Chanteau, S. & Boisier, P. (2008). Controlling schistosomiasis: significant decrease of anaemia prevalence one year after a single dose of praziquantel in Nigerien schoolchildren. *PLoS Neglected Tropical Diseases,* **2** (5), e241.

Tongren, J. E., Drakeley, C. J., McDonald, S. L. R., Reyburn, H. G., Manjurano, A., Nkya, W. M. M., Lemnge, M. M., Gowda, C. D., Todd, J. E., Corran, P. H. & Riley, E. M. (2006). Target antigen, age, and duration of antigen exposure independently regulate immunoglobulin G subclass switching in malaria. *Infection and Immunity,* **74** (1), 257–264.

Uh, H. W., Hartgers, F. C., Yazdanbakhsh, M. & Houwing-Duistermaat, J. J. (2008). Evaluation of regression methods when immunological measurements are constrained by detection limits. *BMC Immunology,* **9**, 59.

Useh, M. F. & Ejezie, G. C. (1999). Modification of behaviour and attitude in the control of schistosomiasis. 1. Observations on water-contact patterns and perception of infection. *Annals of Tropical Medicine and Parasitology,* **93** (7), 711–720.

Utzinger, J., Bergquist, R., Shu-Hua, X., Singer, B. H. & Tanner, M. (2003*a*). Sustainable schistosomiasis control - the way forward. *Lancet,* **362** (9399), 1932–1934.

Utzinger, J., Keiser, J., Shuhua, X., Tanner, M. & Singer, B. H. (2003*b*). Combination chemotherapy of schistosomiasis in laboratory studies and clinical trials. *Antimicrobial Agents and Chemotherapy,* **47** (5), 1487–1495.

van den Biggelaar, A. H. J., Borrmann, S., Kremsner, P. & Yazdanbakhsh, M. (2002). Immune responses induced by repeated treatment do not result in protective immunity to *Schistosoma haematobium*: Interleukin (IL)-5 and IL-10 responses. *Journal of Infectious Diseases,* **186** (10), 1474–1482.

van den Biggelaar, A. H. J., Grogan, J. L., Filie, Y., Jordens, R., Kremsner, P. G., Koning, F. & Yazdanbakhsh, M. (2000). Chronic schistosomiasis: dendritic cells generated from patients can overcome antigen-specific T cell hyporesponsiveness. *Journal of Infectious Diseases,* **182** (1), 260–265.

van den Biggelaar, A. H. J., Rodrigues, L. C., van Ree, R., van der Zee, J. S., Hoeksma-Kruize, Y. C. M., Souverijn, J. H. M., Missinou, M. A., Borrmann, S., Kremsner, P. G. & Yazdanbakhsh, M. (2004). Long-term treatment of intestinal helminths increases mite skin-test reactivity in Gabonese schoolchildren. *Journal of Infectious Diseases,* **189** (5), 892–900.

van den Biggelaar, A. H. J., van Ree, R., Rodrigues, L. C., Lell, B., Deelder, A. M., Kremsner, P. G. & Yazdanbakhsh, M. (2000). Decreased atopy in children infected with *Schistosoma haematobium*: a role for parasite-induced interleukin-10. *Lancet,* **356** (9243), 1723–1727.

van der Werf, M. J., de Vlas, S. J., Brooker, S., Looman, C. W. N., Nagelkerke, N. J. D., Habbema, J. D. F. & Engels, D. (2003). Quantification of clinical morbidity associated with schistosome infection in sub-Saharan Africa. *Acta Tropica,* **86** (2-3), 125–139.

van Etten, L., Kremsner, P. G., Krijger, F. W. & Deelder, A. M. (1997). Day-to-day variation of egg output and schistosome circulating antigens in urine of *Schistosoma haematobium*-infected school children from Gabon and follow-up after chemotherapy. *American Journal of Tropical Medicine and Hygiene,* **57** (3), 337–341.

Vermund, S. H., Bradley, D. J. & Ruiztiben, E. (1983). Survival of *Schistosoma mansoni* in the human host - estimates from a community-based prospective study in Puerto Rico. *American Journal of Hygiene and Tropical Medicine,* **32** (5), 1040–1048.

Viana, I. R. C., Sher, A., Carvalho, O. S., Massara, C. L., Eloi-Santos, S. M., Pearce, E. J., Colley, D. G., Gazzinelli, G. & Corra-Oliveira, R. (1994). Interferon-γ production by peripheral blood mononuclear cells from residents of an area endemic for *Schistosoma mansoni*. *Transactions of the Royal Society of Tropical Medicine and Hygiene,* **88** (4), 466–470.

Viola, A. & Lanzavecchia, A. (1996). T cell activation determined by T cell receptor number and tunable thresholds. *Science,* **273** (5271), 104–106.

von Lichtenberg, F. (1964). Studies on granuloma formation. III. Antigen sequestration and destruction in the schistosome pseudotubercle. *American Journal of Pathology,* **45** (1), 75–93.

Waldmann, T. & Strober, W. (1969). Metabolism of immunoglobulins. *Progress in Allergy,* **13**, 1–110.

Walter, K., Fulford, A. J. C., McBeath, R., Joseph, S., Jones, F. M., Kariuki, H. C., Mwatha, J. K., Kimani, G., Kabatereine, N. B., Vennervald, B. J., Ouma, J. H. & Dunne, D. W. (2006). Increased human IgE induced by killing *Schistosoma mansoni* in vivo is associated with pretreatment Th2 cytokine responsiveness to worm antigens. *The Journal of Immunology,* **177** (8), 5490–5498.

Warren, K., Siongok, T. K., Houser, H., Ouma, J. H. & Peters, P. (1978). Quantification of infection with *Schistosoma haematobium* in relation to epidemiology and selective population chemotherapy. I. Minimal number of daily egg counts in urine necessary to establish intensity of infection. *Journal of Infectious Diseases,* **138**, 849–855.

Warren, K. S., Mahmoud, A. A. F., Cummings, P., Murphy, D. J. & Houser, H. B. (1974). Schistosomiasis mansoni in Yemeni in California: duration of infection, presence of disease, therapeutic management. *American Journal of Tropical Medicine and Hygiene,* **23** (5), 902–909.

Webbe, G., James, C. & Nelson, G. S. (1974). *Schistosoma haematobium* in the baboon (*Papio anubis*). *Annals of Tropical Medicine and Parasitology,* **68** (2), 187–203.

Webbe, G., James, C., Nelson, G. S., Smithers, S. R. & Terry, R. J. (1976). Acquired resistance to *Schistosoma haematobium* in the baboon (*Papio anubis*) after cercarial exposure and adult worm transplantation. *Annals of Tropical Medicine & Parasitology,* **70** (4), 411–424.

Webster, M., Fallon, P. G., Fulford, A. J., Butterworth, A. E., Ouma, J. H., Kimani, G. & Dunne, D. W. (1997). Effect of praziquantel and oxamniquine treatment on human isotype responses to *Schistosoma mansoni*: elevated IgE to adult worm. *Parasite Immunology,* **19** (7), 333–5.

Webster, M., Fulford, A. J., Braun, G., Ouma, J. H., Kariuki, H. C., Havercroft, J. C., Gachuhi, K., Sturrock, R. F., Butterworth, A. E. & Dunne, D. W. (1996). Human immunoglobulin E responses to a recombinant 22.6-kilodalton antigen from *Schistosoma mansoni* adult worms are associated with low intensities of reinfection after treatment. *Infection and Immunity,* **64** (10), 4042–6.

Webster, M., Roberts, M., Fulford, A. J., Marguerite, M., Gallisot, M. C., Diagne, M., Niang, M., Riveau, G., Capron, A. & Dunne, D. W. (1998). Human IgE responses to rSm22.6 are associated with infection intensity rather than age per se, in a recently established focus of schistosomiasis mansoni. *Tropical Medicine & International Health,* **3** (4), 318–26.

Weinstock, J. V. & Boros, D. L. (1981). Heterogeneity of the granulomatous response in the liver, colon, ileum, and ileal Peyer's patches to schistosome eggs in murine schistosomiasis mansoni. *Journal of Immunology,* **127** (5), 1906–1909.

Wertheimer, S. P., Vermund, S. H., Lumey, L. H. & Singer, B. (1987). Lack of demonstrable density-dependent fecundity of shistosomiasis mansoni: analyses of Egyptian quantitative human autopsies. *American Journal of Tropical Medicine and Hygeine,* **37** (1), 79–84.

WHO (2001). Schistosomiasis and soil transmitted helminth infections. Fifty fourth World Health Assembly, resolution WHA54.19. Available: http://www.who.int/wormcontrol/about_us/en/ea54r19.pdf . **Accessed 8 July 2010**.

WHO (2005). *Tropical disease research, progress 2003-2004: 17th Programme Report of the UNICEF/UNDP/World Bank/WHO. Special Programme for Research and Training in Tropical Diseases.* WHO, Geneva.

WHO (2006). *Preventive chemotherapy in human helminthiasis. Coordinated use of anthelminthic drugs in control interventions: a manual for health professionals and programme managers.* WHO, Geneva.

Wiegand, K., Saltz, D., Ward, D. & Levin, S. A. (2008). The role of size inequality in self-thinning: a pattern-oriented simulation model for arid savannas. *Ecological Modelling,* **210** (4), 431–445.

Wilkins, H. A., Blumenthal, U. J., Hagan, P., Hayes, R. J. & Tulloch, S. (1987). Resistance to reinfection after treatment of urinary schistosomiasis. *Transactions of the Royal Society of Tropical Medicine and Hygiene,* **81** (1), 29–35.

Wilkins, H. A., Goll, P. H., de C. Marshall, T. F. & Moore, P. J. (1984). Dynamics of *Schistosoma haematobium* infection in a Gambian community. III. Acquisition and loss of infection. *Transactions of the Royal Society of Tropical Medicine and Hygiene,* **78** (2), 227–232.

Williams, G. M., Sleigh, A. C., Li, Y., Feng, Z., Davis, G. M., Chen, H., Ross, A. G., Bergquist, R. & McManus, D. P. (2002). Mathematical modelling of schistosomiasis japonica: comparison of control strategies in the People's Republic of China. *Acta Tropica,* **82** (2), 253–62.

Wilson, J. N. & Nokes, D. J. (1999). Do we need 3 doses of hepatitis B vaccine? *Vaccine,* **17** (20-21), 2667–2673.

Wilson, J. N., Nokes, D. J., Medley, G. F. & Shouval, D. (2007). Mathematical model of the antibody response to hepatitis B vaccines: implications for reduced schedules. *Vaccine,* **25** (18), 3705–3712.

Wilson, R. A. (1990). Leaky livers, portal shunting and immunity to schistosomes. *Parasitology Today,* **6** (11), 354–358.

Wilson, R. A., Ashton, P. D., Braschi, S., Dillon, G. P., Berriman, M. & Ivens, A. (2007). 'oming in on schistosomes: prospects and limitations for post-genomics. *Trends in Parasitology,* **23** (1), 14–20.

Wilson, R. A. & Coulson, P. S. (2006). Schistosome vaccines: a critical appraisal. *Memorias Do Instituto Oswaldo Cruz,* **101** (S1), 13–20.

Wirths, S. & Lanzavecchia, A. (2005). ABCB1 transporter discriminates human resting naive B cells from cycling transitional and memory B cells. *European Journal of Immunology,* **35**, 3433–3441.

Woolhouse, M. E. J. (1991). On the application of mathematical models of schistosome transmission dynamics. I. Natural transmission. *Acta Tropica,* **49** (4), 241–70.

Woolhouse, M. E. J. (1992*a*). On the application of mathematical models of schistosome transmission dynamics. II. Control. *Acta Tropica,* **50** (3), 189–204.

Woolhouse, M. E. J. (1992*b*). A theoretical framework for the immunoepidemiology of helminth infection. *Parasite Immunology,* **14**, 563–578.

Woolhouse, M. E. J. (1993). A theoretical framework for immune responses and predisposition to helminth infection. *Parasite Immunology,* **15**, 583–594.

Woolhouse, M. E. J. (1994*a*). Immunoepidemiology of human schistosomes: taking the theory into the field. *Parasitology Today,* **10**, 196–202.

Woolhouse, M. E. J. (1994*b*). A theoretical framework for the immunoepidemiology of blocking antibodies to helminth infection. *Parasite Immunology,* **16** (8), 415–24.

Woolhouse, M. E. J. (1995). Human schistosomiasis: potential consequences of vaccination. *Vaccine,* **13** (12), 1045–1050.

Woolhouse, M. E. J. (1998). Patterns in parasite epidemiology: the peak shift. *Parasitology Today,* **14** (10), 428–434.

Woolhouse, M. E. J., Etard, J. F., Dietz, K., Ndhlovu, P. D. & Chandiwana, S. K. (1998). Heterogeneities in schistosome transmission dynamics and control. *Parasitology,* **117** (5), 475–82.

Woolhouse, M. E. J. & Hagan, P. (1999). Seeking the ghost of worms past. *Nature Medicine,* **5** (11), 1225–1227.

Woolhouse, M. E. J., Hasibeder, G. & Chandiwana, S. K. (1996). On estimating the basic reproduction number for *Schistosoma haematobium*. *Tropical Medicine & International Health,* **1** (4), 456–463.

Woolhouse, M. E. J., Mutapi, F., Ndhlovu, P. D., Chandiwana, S. K. & Hagan, P. (2000). Exposure, infection and immune responses to *Schistosoma haematobium* in young children. *Parasitology,* **120**, 37–44.

Woolhouse, M. E. J., Ndamba, J. & Bradley, D. J. (1994). The interpretation of intensity and aggregation data for infections of *Schistosoma haematobium*. *Transactions of the Royal Society of Tropical Medicine and Hygiene,* **88** (5), 520–6.

Woolhouse, M. E. J., Taylor, P., Matanhire, D. & Chandiwana, S. K. (1991). Acquired immunity and epidemiology of *Schistosoma haematobium*. *Nature,* **351** (6329), 757–9.

Yazdanbakhsh, M. & Sacks, D. L. (2010). Why does immunity to parasites take so long to develop? *Nature Reviews Immunology,* **10** (2), 80–81.